Fungal Diversity

Fungal Diversity (2026) 136: 136009
https://doi.org/10.65390/fdiv.2026.136009

Research Article

OPEN ACCESS

One stop shop VI: taxonomic update with molecular phylogeny for important phytopathogenic genera: 126–150

Chitrabhanu S Bhunjun[1,2,3,4], Chayanard Phukhamsakda[3], Kevin D. Hyde[3], Dartanha Jose Soares[5], Ajay Kumar Gautam[6], Shubhi Avasthi[7], Rajnish Kumar Verma[8], Saowaluck Tibpromma[9], Samantha C. Karunarathna[9], Ya-Ru Sun[2,3], Xia Tang[2,3], Deecksha Gomdola[2,3], Niroshini Gunasinghe[10], Danushka S Tennakoon[11], Eric H. C. McKenzie[12], Ahmad Alghamdi[4], Ibrahim F. Halawani[4], Ruvishika S. Jayawardena[2,3,13], Yong Wang[1*] and Feng-Quan Liu[1*]

[1]Department of Plant Pathology, Agriculture College, Guizhou University, Guiyang 550025, China; [2]School of Science, Mae Fah Luang University, Chiang Rai 57100, Thailand; [3]Center of Excellence in Fungal Research, Mae Fah Luang University, Chiang Rai 57100, Thailand; [4]Department of Clinical Laboratory Sciences, College of Applied Medical Sciences, Taif University, P.O. Box 11099, Taif 21944, Saudi Arabia; [5]Empresa Brasileira de Pesquisa Agropecuária (Embrapa Algodão), Rua Osvaldo Cruz, 1143, Campina Grande 58428-095, Brazil; [6]Patanjali Herbal Research Department, Patanjali Research Foundation, Haridwar 249405, India; [7]School of Studies in Botany, Jiwaji University, Gwalior 474011, India; [8]Department of Plant Pathology, Punjab Agricultural University, Ludhiana 141004, India; [9]Center for Yunnan Plateau Biological Resources Protection and Utilization & Yunnan International Joint Laboratory of Fungal Sustainable Utilization in South and Southeast Asia, College of Biology and Food Engineering, Qujing Normal University, Qujing 655099, China; [10]School of Agriculture and Food Sustainability, The University of Queensland, Queensland, Brisbane Qld 4072, Australia; [11]Biology Centre of the Czech Academy of Sciences, Institute of Entomology, České Budějovice 37005, Czech Republic; [12] Bioeconomy Science Institute, Private Mail Bag 92170, Auckland, New Zealand; [13]Kyung Hee University, 26 Kyungheedae-ro, Dongdaemun-gu, Seoul 02447, South Korea

***Corresponding authors:** yongwangbis@aliyun.com (Y. W.); fqliu20011@sina.com (F.-Q. L.)

Received: 26 September 2025 / Accepted: 06 May 2026 / Published: 20 August 2026

Abstract

Pathogenic fungi play pivotal roles in shaping the dynamics of agriculture, and ecosystems. As many fungi are pathogenic on plants and cause significant damage in agriculture and forestry, they pose significant threats to global food security. This is the 6th paper in onestopshop pathogenic genera series. This paper focuses on 25 phytopathogenic genera: *Coleosporium*, *Dichotomophthora*, *Didymella*, *Leptosphaerulina*, *Macrophomina*, *Melampsora*, *Myrothecium*, *Neopseudocercosporella*, *Neopestalotiopsis*, *Neosetophoma*, *Nigrospora*, *Oculimacula*, *Phaeosphaeriopsis*, *Phakopsora*, *Pleiocarpon*, *Pseudopestalotiopsis*, *Pseudogymnoascus*, *Pyrenophora*, *Ramichloridium*, *Ravenelia*, *Seiridium*, *Stenocarpella, Tubakia, Zasmidium* and *Zymoseptoria*. We provide background information, distribution, hosts and disease symptoms for each genus. A table of accepted species and an updated backbone tree is also provided for each entry. We introduce the new species *Dichotomophthora conlutea* and propose the new combinations *Digitiseta chiangmaiensis* and *Myxospora thailandica*.

Key words: 1 new species, 2 new combinations, Classification, Diseases, Pathogens, Phylogeny

Citation: Bhunjun, C.S., Phukhamsakda, C., Hyde, K.D., Soares, D.J., Gautam, A.K., Avasthi, S., Verma, R.K., Tibpromma, S., Karunarathna, S.C., Sun, Y.-R., Tang, X., Gomdola, D., Gunasinghe, N., Tennakoon, D.S., McKenzie, E.H.C., Alghamdi, A., Halawani, I.F., Jayawardena, R.S., Wang, Y., Liu, F.-Q. (2026) One stop shop VI: taxonomic update with molecular phylogeny for important phytopathogenic genera: 126–150. Fungal Diversity 136: 1360079. https://doi.org/10.65390/fdiv.2026.136009

Table of Contents and contributors

144. ***Ramichloridium*** - YR Sun, RS Jayawardena, CS Bhunjun
145. ***Ravenelia*** - AK Gautam, S Avasthi, RK Verma, CS Bhunjun
146. ***Seiridium*** - C Phukhamsakda, CS Bhunjun, IF Halawani
147. ***Stenocarpella*** - X Tang, RS Jayawardena
148. ***Tubakia*** - C Phukhamsakda, CS Bhunjun
149. ***Zasmidium*** - DS Tennakoon, CS Bhunjun
150. ***Zymoseptoria*** - S Tibpromma, CS Bhunjun

Introduction

Fungi are a diverse and heterogeneous group of organisms with an estimated 1.5 to 12 million species (Hawksworth 1991, Wu et al. 2019, Hyde et al. 2024b). There are over 150,000 described species that have been reported with different lifestyles including endophytic, saprotrophic and parasitism (Hyde et al. 2020, Bhunjun et al. 2022, Phukhamsakda et al. 2022, 2025). As pathogens, fungi have profound implications for human health, agriculture, and ecosystems (Hyde et al. 2018, 2019, Fisher et al. 2020). Pathogenic fungi contribute significantly to infectious diseases in humans, ranging from superficial skin infections to life-threatening systemic mycoses (Köhler et al. 2017). In agriculture, pathogens cause devastating diseases in crops, leading to substantial yield losses and threatening food security on a global scale (Fones et al. 2020). The study of pathogens provides a better understanding of the complex interplay between fungi and their hosts, shedding light on mechanisms of infection and virulence factors, thus providing potential avenues for disease management (Zeilinger et al. 2013). There has been a surge in the number of fungal diseases which may have resulted in die-offs and extinction of various wild species (Fisher et al. 2012, Fisher & Denning 2023). A number of these diseases were caused by recently described pathogens, but there has also been a rise in the risks posed by emerging pathogens as a result of climate change (Blehert et al. 2009, Casadevall 2019, Seidel et al. 2024).

This is the sixth paper in the "One Stop Shop series". Previous contributions have been vital in providing a stable platform for the taxonomy of phytopathogenic fungi and fungus-like organisms (Hyde et al. 2014, Jayawardena et al. 2019a, b, 2020, 2025, Table 1). The series has provided clarification on the taxonomy and classification of 125 genera and three families. In this study, we focus on 25 phytopathogenic genera and discuss the background information, distribution, hosts and disease symptoms for each genus.

Materials and methods

Isolates and Molecular analyses

The sequences of ex-type, ex-epitype or reference/voucher strains for all species were retrieved from GenBank. Polymerase chain reaction was used to amplify the partial gene regions of *Dichotomophthora conlutea* with primer pairs as described in Phukhamsakda et al. (2016) and sequenced by Shanghai Sangon Biological Engineering Technology & Services Co. (Shanghai, China). The large subunit ribosomal RNA (LSU) gene, internal transcribed spacer (ITS) region, the small subunit ribosomal RNA (SSU) gene, the translation elongation factor alpha (*tef*) gene, beta-tubulin (*tub2*), calmodulin (*cal*), actin (*act*), the glyceraldehyde-3-phosphate dehydrogenase (*gapdh*) gene, the cytochrome c oxidase (*cox*), histone H3 (*his3*), Minichromosome Maintenance Complex Component 7 gene (*mcm7*), the RNA polymerase II largest (*rpb1*) and second largest subunit (*rpb2*) genes were used in the phylogeny as per related bibliography. The sequences were aligned with MAFFT v. 7 (Katoh et al. 2019), with minimal adjustment using AliView v. 1.26 (Larsson 2014) and BioEdit v. 7.2.5 (Hall 1999). The concatenation of the multi-marker datasets was created by using Sequence Matrix v. 1.8 (Vaidya et al. 2011) and BioEdit v. 7.2.5. Phylogenetic analyses were performed using maximum likelihood, maximum parsimony and Bayesian inference posterior probabilities. Maximum likelihood analyses (ML) were performed on the CIPRES science gateway platform (Miller et al. 2017) using RAxML v. 8.2.12 (Stamatakis 2014). The general time reversible (GTR) model with a discrete gamma distribution plus invariant site (GTR+I+G) was used for nucleotide substitution. The best model for the different gene partitions was determined in JModelTest v. 2.1.10 or MrModeltest v. 2.3 for the Bayesian analysis (Nylander 2004, Darriba et al. 2012). Bayesian inference was conducted using MrBayes v. 3.2.7a on XSEDE (Ronquist and Huelsenbeck 2003).

Case studies

The genera are listed in alphabetical order and the classification follows Hyde et al. (2024b). For all the genera treated herein, we included species published until 30 May 2025 in the phylogenetic analyses (Index Fungorum 2025).

126. *Coleosporium* Lév., Annls Sci. Nat., Bot., sér. 3 8: 373 (1847)

Type species: *Coleosporium campanulae* (Pers.) Tul.

Classification: *Pucciniomycetes*, *Pucciniales*, *Coleosporiaceae*

Background: *Coleosporium* rusts are a group of plant pathogenic fungi belonging to *Coleosporiaceae* (Wijayawardene et al. 2022, Hyde et al. 2024a). Species of *Coleosporium* are obligate plant pathogens, similar to all rust fungi. The rust disease caused by these fungi is commonly known as Coleosporium rust, i.e., commonly referred to either by the genus or the host plant name, followed by the word "rust". These fungi have been studied extensively as they cause diseases on ornamentals grown in gardens (McTaggart & Aime 2018).

Coleosporium was established by Léveille (1847) and comprises about 125 species worldwide (Kirk et al. 2008, Wijayawardene et al. 2020, 2022, Hyde et al. 2024a). These fungi have been documented from a significant number of telial hosts, but only one genus of aecial host, i.e., *Pinus* (Hedgcock 1928). About 12 species of *Coleosporium* infect *Pinus densiflora* as an aecial host (Hedgcock 1928). However, *Coleosporium* on pine trees have rarely been identified to the species level because of their morphological similarities (Suzuki et al. 2018). Scanning electron microscopy has been

Table 1 All entries treated in One stop shop (OSS) series.

OSS1 (Hyde et al. 2014)	OSS2 (Jayawardena et al. 2019a)	OSS3 (Jayawardena et al. 2019b)	OSS4 (Jayawardena et al. 2020)	OSS5 (Jayawardena et al. 2025)	OSS6 (This study)
Bipolaris	*Alternaria*	*Alternaria* (update)	*Armillaria*	*Allophoma*	*Coleosporium*
Botryosphaeriacea e	*Bipolaris* (update)	*Capnodium*	*Barriopsis*	*Alternaria* (update)	*Dichotomophthora*
Botryosphaeria	*Boeremia*	*Chaetothyrina*	*Cercospora*	*Bipolaris* (update)	*Didymella*
Botrytis	*Botryosphaeria* (update)	*Cytospora*	*Cladosporium* (update)	*Boeremia* (update)	*Leptosphaerulina*
Choanephora	*Calonectria*	*Cyphellophora*	*Clinoconidium*	*Calonectria* (update)	*Macrophomina* (update)
Colletotrichum	*Coniella*	*Cyttaria*	*Colletotrichum* (update)	*Calophoma*	*Melampsora*
Curvularia	*Corticiaceae*	*Dactylonectria*	*Cylindricladiella*	*Campylocarpon*	*Myrothecium*
Diaporthe	*Curvularia* (update)	*Diplodia* (update)	*Dothidotthia*	*Clonostachys*	*Neopseudocercosporell a*
Diplodia	*Elsinoë*	*Dothiorella* (update)	*Erysiphaceae*	*Corynespora*	*Neopestalotiopsis* (update)
Dothiorella	*Entyloma*	*Entoleuca*	*Fomitopsis*	*Cryphonectria*	*Neosetophoma*
Fusarium	*Erythricium*	*Eutiarosporella*	*Ganoderma*	*Diaporthe* (update)	*Nigrospora*
Gilbertella	*Fomitiporia*	*Fusarium* (update)	*Golovinomyces*	*Diplocarpon*	*Oculimacula*
Lasiodiplodia	*Fulviformes*	*Ilyonectria*	*Heterobasidium*	*Epicoccum*	*Phaeosphaeriopsis*
Mucor	*Laetisaria*	*Lasiodiplodia* (update)	*Meliola*	*Eutiarosporella* (update)	*Phakopsora*
Neofusicoccum	*Limonomyces*	*Macrophomina*	*Mucor* (update)	*Ganoderma* (update)	*Pleiocarpon*
Pestalotiopsis	*Neofabraea*	*Medeolaria*	*Neoerysiphe*	*Hypomyces*	*Pseudopestalotiopsis* (update)
Phyllosticta	*Neofusicoccum* (update)	*Neonectria*	*Nothophoma*	*Lasiodiplodia* (update)	*Pseudogymnoascus*
Phytophthora	*Phaeoacremoniu m*	*Neopestalotiopsis*	*Phellinus*	*Monilinia*	*Pyrenophora* (update)
Puccinia	*Phellinotus*	*Pestalotiopsis* (update)	*Phytophthora* (update)	*Neocordana*	*Ramichloridium*
Pyrenophora	*Phyllosticta* (update)	*Plasmopara*	*Pseudoseptoria*	*Phragmidium*	*Ravenelia*
Pythium	*Plenodomus*	*Pseudopestalotiopsis*	*Pythium* (update)	*Pileolaria*	*Seiridium*
Rhizopus	*Pseudopyricularia*	*Rosellinia*	*Rhizopus* (update)	*Pseudocercosp ora*	*Stenocarpella*
Stagonosporopsis	*Tilletia*	*Sphaeropsis*	*Stemphylium*	*Rhynchosporiu m*	*Tubakia*
Ustilago	*Venturia*	*Stagonosporopsis* (update)	*Thyrostroma*	*Scytalidium*	*Zasmidium*
Verticillium	*Waitea*	*Verticillium* (update)	*Wojnowiciella*	*Sphaeropsis*	*Zymoseptoria*

used to describe these taxa based on surface sculptures of aeciospores and urediniospores along with different morphologies (Hiratsuka and Kaneko 1975). Two types of basidial development in *Coleosporium* were recognised by Kaneko (1981). In type 1, the entire cell becomes a basidium without change in length while in type two, the cell matures and a septum develops which separates the upper basidial part from the basal stalk-like part. Cummins (1978) and Kaneko (1981) described variations in the shape of the basidiospores. The genus has a wide geographic range, including almost every continent. The fungi primarily damage their telial hosts, which are often ornamentals, including aster, morning glories, and *Plumeria. Plumeria* rust caused by *Coleosporium plumeriae* is perhaps the most important example of a disease caused by the genus. DNA sequence data from the LSU and ITS regions available in GenBank for the species of *Coleosporium* were analysed by Gautam et al. (2021) who provided a taxonomic outline of Indian *Pucciniales*.

Distribution: *Coleosporium* spp. have been observed on almost every continent: North and South America, Asia, islands in the Pacific, Africa and Europe (McMillan 1984, Kolmer et al. 2009). These rust fungi have been reported from many countries including Argentina, Brazil, China, Cuba, Mexico, Georgia, France, India, Japan, Israel, Russia, Malta, Mongolia, Nepal, Philippines, São Tomé and Príncipe, Sierra Leone, Slovenia, Sri Lanka and the USA (Farr & Rossman 2025).

Disease symptoms: *Coleosporium* rust disease symptoms

include chlorosis on leaves, dieback, leaf spotting and defoliation. The yellow-orange uredinia of these rust fungi often appear on the lower leaf surface with corresponding chlorotic spots on the upper surface (Fig. 1). Spermogonia are formed on the aecial host while aecia are formed on the lower surface. These rusts primarily damage their telial hosts, with infected leaves turning yellow to brown with premature leaf fall (Cummins & Hiratsuka 2003, Nelson 2009).

Hosts: species of *Adenocaulon*, *Adenophora*, *Anemone*, *Aposeris*, *Aristolochia*, *Arnica*, *Arundina*, *Aster*, *Begonia*, *Brickellia*, *Cacalia*, *Calendula*, *Campanula*, *Campanumoea*, *Carpesium*, *Carphochaete*, *Choerospondias*, *Cirsium*, *Clematis*, *Clerodendrum*, *Codonopsis*, *Coleosanthus*, *Coleus*, *Convolvulus*, *Dahlia*, *Datisca*, *Erigeron*, *Erythrina*, *Eucommia*, *Euodia*, *Eupatorium*, *Exacum*, *Fauria*, *Heterotheca*, *Ipomoea*, *Knoxia*, *Labiatae*, *Lacinaria*, *Spigelia*, *Liabum*, *Ligularia*, *Lonicera*, *Lycopus*, *Madia*, *Microrhamnus*, *Myriactis*, *Myripnois*, *Orsina*, *Paederia*, *Pedicularis*, *Perezia*, *Perilla*, *Pertya*, *Phlomis*, *Phyllanthus*, *Pinus*, *Plumeria*, *Polymnia*, *Rubia*, *Salvia*, *Satyrium*, *Saussurea*, *Senecio*, *Serratula*, *Sicyos*, *Sida*, *Smilax*, *Stevia*, *Synurus*, *Thunbergia*, *Tylophora*, *Verbesina*, *Vernonia*, *Viburnum*, *Viola* and *Zanthoxylum* (Farr & Rossman 2025).

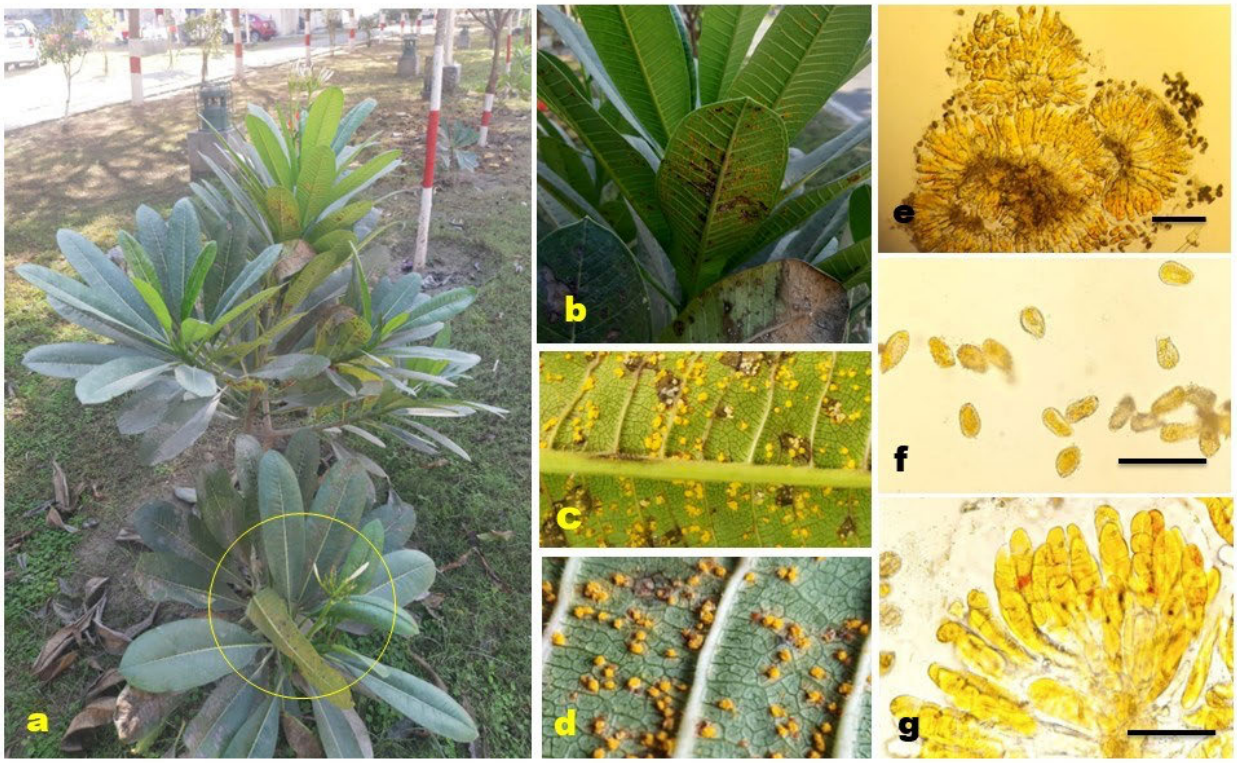

Fig. 1 *Coleosporium plumeriae* on *Plumeria* sp. a-b Host plant with infected and healthy leaves. c-d Sori at various stages of infection. e-f Urediniospores. g Teliospores. Scale bars: 10 µm. This picture is copyright of Ajay Kumar Gautam, Shubhi Avasthi and Rajnish Kumar Verma.

Pathogen biology, disease cycle and epidemiology: *Coleosporium* comprises several species of rust fungi that are obligate biotrophic pathogens. These rust fungi possess a complex life cycle that typically alternates between pines and angiosperms, i.e., two hosts (heteroecious) and consisting of five spore types (macrocyclic), with spermogonia and aecia forming on needles of *Pinus* and uredinia and telia on both monocot and dicot plants (especially *Asteraceae*, but also on *Campanulaceae*, *Orobanchaceae*, *Ranunculaceae*) (Kirk et al. 2008). *Coleosporium* species can infect the same host repeatedly, or more than one host, in a single growing season. A single summer may allow up to 15 disease cycles. The disease cycle begins when basidiospores, produced from germinating teliospores, are wind-dispersed to infect the host plant (Harrington & Wingfield 2000). Upon landing on susceptible tissue, the basidiospores germinate and penetrate the plant's epidermis, initiating infection. The pathogen then forms uredinia, which produce urediniospores that facilitate the spread of the disease. The production of urediniospores continues throughout the summer showing the polycyclic nature of some species of *Coleosporium* (Chapell & Rausher 2016). In the late season, telia develop, producing teliospores that overwinter and serve as the primary inoculum for the next growing season. The epidemiology of *Coleosporium* is influenced by environmental factors such as humidity, temperature, and the presence of susceptible host plants (Chapell & Rausher 2016). Management strategies include removing infected plant material, applying fungicides, and planting resistant cultivars to reduce disease incidence and spread (McTaggart & Aime 2018).

Morphological-based identification: *Coleosporium* is characterised by 1-celled teliospores that are produced in a 1-layered crust under host epidermal cells (Cummins & Hiratsuka 2003). These taxa produce branched, septate mycelium and haustoria for absorption (Kolmer et al. 2009). They produce subepidermal, Group I (Type 2) spermogonia (Zhao et al. 2023). The colour of the spermogonia, the arrangement, size, and shape of the aecia, and the aecial host plant are three important morphological characteristics used

to distinguish species of *Coleosporium* (Hedgcock 1928). Aecia are peridermium-type, subepidermal, erumpent with noticeable peridermium and found on the underside of leaves of the aecial host (abaxial). Aeciospores are catenulate, oblong to round in shape with verrucose spore walls. The aeciospores usually appear a month or two later than the spermogonia. These fungi produce subepidermal, erumpent, caeoma-type uredinia as bright orange pustules initially, fading to whitish later in the disease cycle. The uredinia develop catenuate, echinulate, reticulate, or verrucose urediniospores (with scattered or obscure pores) under the epidermis of the telial host plant. Telia produced by these fungi are often flat and dense, yellow or orange, wax-like, subepidermal, erumpent as low or columnar cushions and gelatinous when wet. Telia are composed of sessile, 1-celled spores, in 1-layered crusts, or pseudocatenuate by the intrusion of young spores among older spores, thick-walled, gelatinizing above teliospores. The teliospores germinate without dormancy and give rise to a phragmobasidium (a 4-celled internal basidium). Each cell of internal basidium produces a sterigma and one ellipsoidal to globoid basidiospore which infects the aecial host (Weir 1925, Hedgcock 1928, Arthur 1934, Cummins & Hiratsuka 2003).

Molecular-based identification: Maier et al. (2003) investigated LSU sequence data for 52 rust fungi of nine families including *Coleosporium* and showed that *Coleosporium* is monophyletic. Molecular data employing LSU sequence was used to characterize *Coleosporium plectranthi* on *Perilla frutescens* var. *japonica* (Yun et al. 2007). Holcomb & Aime (2010) explored *Plumeria* rust from Louisiana and Malaysia and identified the causal organism as *C. plumeriae* based on morpho-taxonomy. By using ITS and LSU sequences, phylogenetic analyses of *Coleosporium* on *Solidago* revealed the first molecular evidence of the North American rust *C. solidaginis* in Europe (Beenken et al. 2017). McTaggart & Aime (2018) carried out a study (ca. 60 collections) of *Coleosporium* infecting species of *Asteraceae* from North America. Based on phylogenetic analyses (ITS and LSU) and morphology of teliospores and basidia, McTaggart & Aime (2018) found that at least three species of *Coleosporium* occur on *Solidago* in North America rather than only one. Based on PCR-RFLP analyses, four species, *C. asterum*, *C. clematidis-apiifoliae*, *C. lycopodis*, and *C. phellodendri were found* to be associated with *Pinus densiflora* (Suzuki et al. 2018). *Coleosporium zanthoxyli* was identified on *Zanthoxylum planispinum* based on the host type, morphological characteristics, and phylogenetic analyses using ITS and LSU sequences (Shin et al. 2019). Both ITS and LSU are suitable loci for the identification of *Coleosporium* species. Aime & McTaggart (2020) resolved the deeper nodes of the rust fungus tree of life and provided an updated higher-rank classification for *Pucciniales* using LSU, SSU, and *cox* sequences from fresh and herbarium material of various species of rust fungi, including species of *Coleosporium.* This study provides an updated phylogeny of *Coleosporium* based on combined LSU and ITS sequence data (Fig. 2, Table 2).

Recommended genetic marker (genus level): ITS, LSU

Recommended genetic marker (species level): ITS, LSU

Accepted number of species: 125

References: Hiratsuka & Kaneko (1975), Cummins (1978), Kaneko (1981), Cummins & Hiratsuka (2003), Maier et al. (2003), Yun et al. (2007), Holcomb & Aime (2010), Beenken et al. (2017), Aime et al. (2018), McTaggart & Aime (2018), Suzuki et al. (2018), Shin et al. (2019), Aime & McTaggart (2020), Sun et al. (2024) (morphology and phylogeny)

127. *Dichotomophthora* Mehrl. & Fitzp. ex M.B. Ellis, Dematiaceous Hyphomycetes (Kew): 388 (1971)

Type species: *Dichotomophthora portulacae* Mehrl. & Fitzp. ex M.B. Ellis

Classification: *Dothideomycetes*, *Pleosporales*, *Pleosporaceae*

Background: *Dichotomophthora* was introduced by Mehrlich & Fitzpatrick (1935) to accommodate the hyphomycetous species *D. portulacae*, causing leaf spots on common purslane (*Portulaca oleracea*) in Hawaii. However, it was not validly published, and Rao (1966) attempted to validate it. Due to misapplications, this attempt was also unsuccessful, and the name was considered invalid until Ellis (1971) validly published it based on the holotype specimen of *D. portulacae* (Marin-Felix et al. 2019b). A second species *D. lutea* was introduced by De Hoog & van Oorschot (1983). The classification of *Dichotomophthora* in *Pleosporaceae*, *Pleosporales* was confirmed by Marin-Felix et al. (2019b) based on multi-gene phylogenetic analysis. Two further species *D. basellae* and *D. brunnea* were introduced, making a total of four accepted species in this genus (Marin-Felix et al. 2019b). *Dichotomophthora* species have been commonly reported as plant pathogens on various hosts (mostly *P. oleracea*), as saprobes and soil-inhabiting fungi and as a causative organism of human keratitis (Mehrlich & Fitzpatrick 1935, Ellis 1971, De Hoog & Oorschot 1983, Klisiewicz et al. 1983, Alfieri et al. 1984, Baudoin 1986, Pfeiffer et al. 1989, De Hoog et al. 2000, Eken 2003, Soares & Nechet 2017, Heidari et al. 2018, Marin-Felix et al. 2019b, Farr & Rossman 2025).

Distribution: worldwide (Farr & Rossman 2025)

Disease symptoms: Disease symptoms caused by *Dichotomophthora* typically manifest as dark, necrotic lesions (Fig. 3). The soil-inhabiting *Dichotomophthora portulacae* is known for causing rot, blight and dieback of the stems and leaf spots in *Portulaca oleracea* (Merhlich & Fitzpatrick 1935, Ellis 1971, Klisiewicz et al. 1983, Baudoin 1986, Mitchell 1986). The disease symptoms are characterised by necrotic, oval to irregular, pale brown spots with darker borders (Kliseiwicz 1985, Heidari et al. 2018, Abdulla 2021). Klisiewicz et al. (1983) observed that the stems of purslane plants, especially at the soil line, showed dark discolouration and constriction. The development of lesions was more frequently observed in parts of the stem that were in contact with the soil and the roots usually were infected by the same pathogen infecting the stems (Klisiewicz et al. 1983). Eken (2003) reported *D. portulacae* to cause crown and root rot of purslane. During experimental studies, symptoms of seed rot and post-emergence damping-off were observed within eight days, when all the seedlings died. In pathogenicity studies, sunken, necrotic lesions became-apparent on leaves and stems within 48 hours of inoculation. Later, the leaves turned yellow and dropped, while dark lesions developed on the stems causing dieback (Eken 2003). *Dichotomophthora portulacae* is more likely to cause the death of its host plants when infected at a young age (Kliseiwicz et al. 1983). *Dichotomophthora lutea* was reported producing brown to black lesions. The infection resulted in a

Table 2 DNA barcodes for accepted species of *Coleosporium*.

Species	Strain	GenBank accession numbers	
		ITS	LSU
Coleosporium abrotanoidis	**HGUP21081**	**OR470522**	**OR462093**
C. asterum	MCA3077	N/A	MG907226
C. begoniae	BPI 910182	KY764061	KY764061
C. bletiae	**BSC1**	**MN108161**	**MN108162**
C. buchananianae	**HGUP21053**	**OR470523**	**N/A**
C. carpesii	ZP-R1302	MK518950	MK518950
C. clematidis	N99	N/A	KX386040
C. clematidis-apiifoliae	TSHR6521	LC333796	LC333796
C. campanulae	N/A	N/A	AF426244
C. dasyandrae	**HGUP21050**	**OR470510**	**OR462089**
C. delicatulum	BPI 871737	MF769638	MF769638
C. eupatorii	MCA 4470	N/A	MF769673
C. inulae	U717	N/A	MG907223
C. ipomoeae	R232	N/A	EU851160
C. julii	**HGUP21048**	**OR470508**	**OR462087**
C. lycopodis	TSHR6560	LC333800	LC333800
C. neocacaliae	HMJAU8098	N/A	KX344990
C. phlomidis	HMAS-76121	KP017553	KP017563
C. plectranthi	CO14	N/A	EF095711
C. plumeriae	**HMJAU8091**	**N/A**	**KX344991**
C. puawhananga	**PDD 101549**	**N/A**	**ON622777**
C. senecionis	PDD 98309	N/A	KJ716348
C. septemberis	**HGUP21046**	**OR470496**	**OR462079**
C. telioevodiae	BJFCQL16	MG561474	MG561474
C. tussilaginis	N/A	N/A	AF426242
C. verbesinae	JRH151	N/A	MG907229

Ex-type/ex-epitype/ex-neotype/ex-lectotype strains and voucher strains are in bold. Sequences that are not available are represented by N/A.

greyish dry rot and the gradual collapse of the tissue (Pfeiffer et al. 1989).

Hosts: *Dichotomophthora portulacae* was reported from Hawaii, USA on *Portulaca oleracea* (Mehrlich & Fitzpatrick 1935). Other hosts include *Basella rubra*, *Nicotiana glauca*, *Portulaca grandiflora* and *P. lutea* (Ellis 1971, Raabe et al. 1981, De Hoog & Oorschot 1983, Richardson 1990, Jing et al. 2008, Camino-Vilaro et al. 2019, Marin-Felix et al. 2019b, Farr & Rossman 2025). *Dichotomophthora lutea* has been isolated from *Beta vulgaris* (Minter et al. 2001), from soil, on seeds, stems, leaves and roots of *Anredera cordifolia*, *Portulaca oleracea*, *Gymnocalycium mihanovichii* var. *friedrichii* and *Myrtillocactus geometrizans* (De Hoog & Oorschot 1983, Miller 1990, Soares & Nechet 2017, Heidari et al. 2018, Camino-Vilaro et al. 2019, Marin-Felix et al. 2019b) in various regions, and from the seedbed of *Pinus radiata* in Italy (Heidari et al. 2018, Marin-Felix et al. 2019b). *Dichotomophthora basellae* was isolated from the leaves of *Basella alba* in Thailand (Marin-Felix et al. 2019b). The location and substrate of *D. brunnea* are unknown (Marin-Felix et al. 2019b).

Pathogen biology, disease cycle and epidemiology: *Dichotomophthora portulacae* is often reported as a major pathogen on purslane (Farr & Rossman 2025). It has been listed as an introduced plant pathogen in the United Kingdom (Jones & Baker 2007). According to Klisiewicz (1985), the fungus produces sclerotia and conidia on both artificial media and dead plant tissues. The sclerotia help the fungus to survive in the soil and act as an inoculum for basal stem infection (Klisiewicz 1985). The plant may become more prone to damage by insects or larvae following the stem infection by *D. portulacae*. *Dichotomophthora portulacae* prefers a temperature range of 27–33 °C and moist, humid conditions for growth and reproduction (in culture media). Thus, the fungus is less likely to infect plants where there is a lack of rain or moisture (Klisiewicz 1985). Once infected, the disease can develop regardless of the environmental conditions, leading to rapid death, especially in seedlings (Klisiewicz 1985, Mitchell 1986). *Dichotomophthora portulacae* can also infect carpetweed (*Mollugo verticillata*), but experimental results showed only mild symptoms (Mitchell 1986). In China, it was reported as an endophyte in Malabar spinach (*Basella rubra*) by Jing et al. (2008). The possibility of using *D. portulacae* as a biological control agent to control weeds, especially in areas with heavy rain and high humidity has been mentioned and investigated to an extent (Rader 1948, Klisiewicz et al. 1983, Klisiewicz 1985, Baudoin 1986, Vink & Elsas 2017). Alves et al. (2020) isolated *Dichotomophthora* as an endophyte from *Jatropha curcas* and two strains showed promising antioxidant activities. Further studies focusing on possible bioactive compounds of *Dichotomophthora* will lead to a better understanding of this genus.

Morphological-based identification: *Dichotomophthora* species are characterised by their macronematous, mononematous, dichotomously branched, irregularly orunbranched conidiophores, and simple, ellipsoidal to

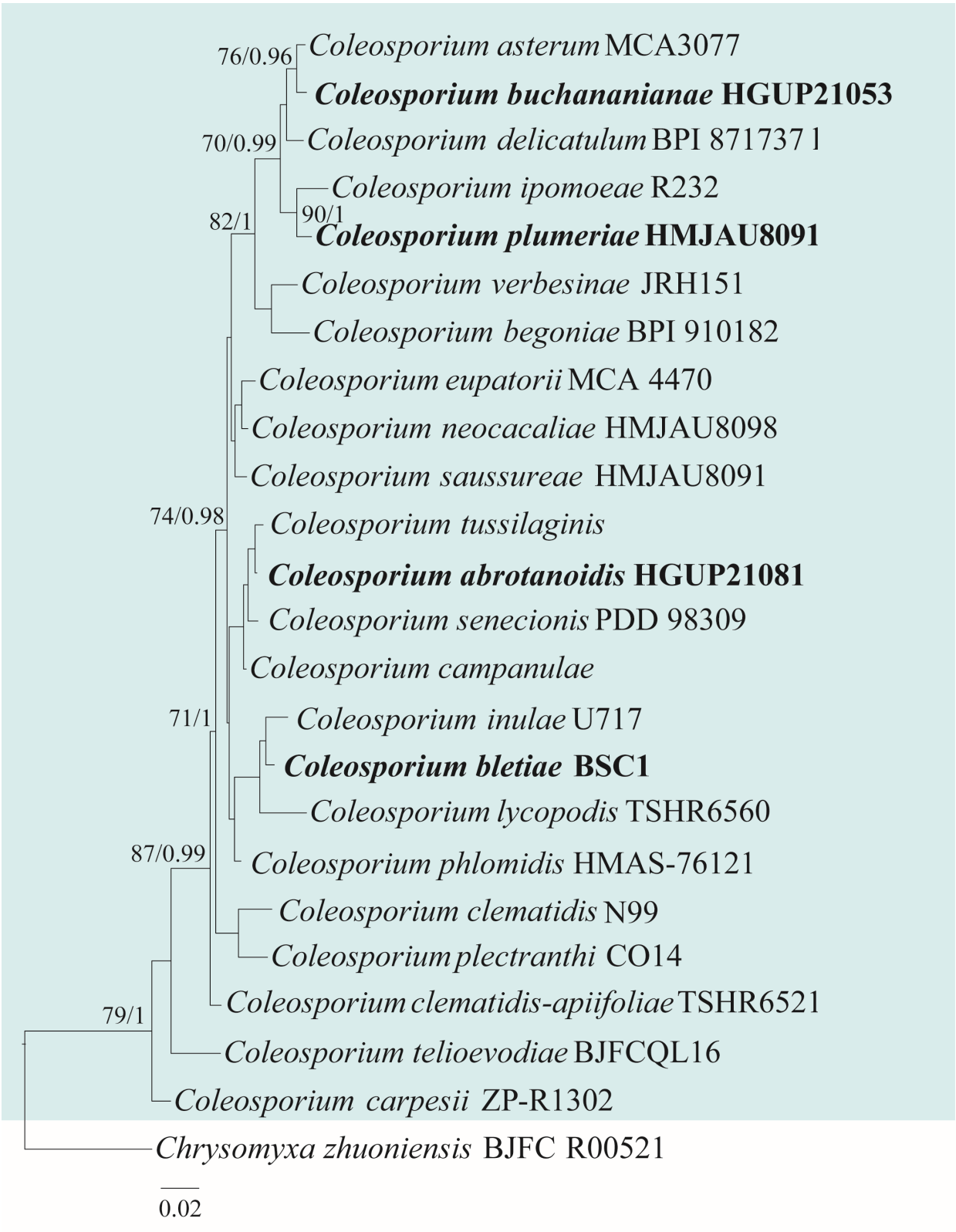

Fig. 2 Maximum likelihood tree of *Coleosporium* species based on the concatenated LSU and ITS sequence data. The best scoring RAxML tree had a final likelihood value of -5967.127022. The tree was rooted to *Chrysomyxa zhuoniensis* (BJFC R00521). Estimated base frequencies were as follows: A = 0.308609, C = 0.152661, G =0.226954, and T = 0.311777; substitution rates AC = 1.138546, AG = 3.032190, AT = 3.398998, CG = 0.509751, CT = 6.693790, and GT = 1.000000. ML bootstrap support values over 70% and Bayesian posterior probabilities (BPP) greater than 0.95 are indicated. Scale bar indicates the number of substitutions per site. Hyphens (-) represent support values less than BS 70%/BPP 0.95.

cylindrical, subhyaline, pale brown to dark brown conidia with 1–5 septa. The sexual morph is not known (Ellis 1971, Marin-Felix 2019b). The colonies of both *D. basellae* and *D. lutea* produce luteous, orange, diffusible pigments in culture (Marin-Felix et al. 2019b). Several reports of *Dichotomophthora* have remained uncertain due to fungal or host misidentifications, such as *D. portulacae* being confused with *D. lutea* in previous studies (De Hoog & van Oorschot 1983, Soares & Nechet 2017, Vink & Elsas 2017, Marin-Felix et al. 2019b). Therefore, more collections are needed to investigate their diversity.

Molecular-based identification: Heidari et al. (2018) used a combination of ITS and *rpb2* sequence data to identify pathogenic strains of *D. lutea* from Iran. Marin-Felix et al. (2019b) included various strains of *Dichotomophthora* isolated from different hosts and regions using ITS, LSU, *gapdh* and *rpb2* molecular data. As a result, four *Dichotomophthora* species (including two new species) were confirmed. In our phylogenetic analysis (Fig. 4), we included two isolates of *Dichotomophthora* (CMAA 1612 and CMAA 1613) from *Anredera cordifolia* (Soares & Nechet 2017). Their identification could not be confirmed in Soares and Nechet (2017) as the isolates (CMAA 1612 and CMAA 1613) only had ITS region. In this study, we provide additional sequence data for the isolate CMAA 1612 and we provide an updated phylogeny of *Dichotomophthora* based on combined ITS, LSU, *gapdh* and *rpb2* sequence data (Fig. 4, Table 3). We also propose the new species *Dichotomophthora conlutea* (Fig. 3 and 4). *Dichotomophthora cactacearum* is excluded from our analysis as there are no description or molecular data for the species.

Table 3 GenBank accession numbers of *Dichotomophthora* species used for phylogenetic analysis.

Species	Strain	GenBank accession numbers			
		ITS	LSU	*gapdh*	*rpb2*
Dichotomophthora basellae	**CPC 33016**	**LT990654**	**LT990626**	**LT990670**	**LT990640**
D. brunnea	**CBS 149.94**	**LT990653**	**N/A**	**LT990669**	**LT990639**
***D. conlutea*#**	**CMAA 1612**	**MF196163**	**PX242776**	**N/A**	**PX251631**
D. conlutea	CMAA 1613	MF196162	N/A	N/A	N/A
D. lutea#	**CBS 145.57**	**LT990647**	**NG_069497**	**LT990663**	**LT990634**
D. lutea	CBS 584.71	LT990648	LT990620	LT990664	LT990635
D. lutea	CBS 585.71	LT990649	LT990621	LT990665	LT990636
D. lutea	CBS 518.78	LT990650	LT990622	LT990666	N/A
D. lutea	CBS 132.81	LT990651	LT990623	LT990667	LT990637
***D. portulacae*#**	**CBS 174.35**	**LT990652**	**MH867137**	**LT990668**	**LT990638**

Ex-type/ex-epitype/ex-neotype/ex-lectotype strains and voucher strains are in bold. Sequences that are not available are represented by N/A. Species confirmed with pathogenicity studies are marked with #.

Dichotomophthora conlutea **D.J. Soares & Bhunjun, sp. nov.**

Index Fungorum number: IF905057; **Facesoffungi number**: FoF 19465; Fig. 3

Etymology: Named based on its close affinity to *Dichotomophthora lutea*.

Conidiophores erect, simple or irregularly branched, sometimes verruculose near the apex, forming a stipe and head; *stipe* up to 900 µm long, 9–12 µm wide, pale brown to brown, smooth; *head* usually divided 3 to 4 times, frequently proliferating to produce additional head. *Conidiogenous cells* polytretic, integrated and terminal. *Conidia* 24–94 × 10–17 µm, solitary, smooth to finely verruculose, 1–6-septate, ellipsoidal to cylindrical, sometimes slightly curved, with rounded ends, initially subhyaline, becoming brown to reddish-brown. *Sclerotia* resembling immature perithecia, immersed in agar, abundant on potato dextrose agar and oatmeal agar, sporadic and scattered on malt extract agar. Sexual morph: unknown.

Culture characteristics: Colonies on PDA, MEA and OA reaching 50–60 mm after 1 week at 25 °C under ultraviolet light (12 h light, 12 h dark), white to grey (PDA and MEA) or dark grey to olivaceous (OA), cottony, velvety, somewhat fluffy, margin regular, effuse; reverse brown or dark-grey to black, periphery white to hazel. Diffusible pigment not observed under the culture conditions and media tested.

Material examined: Brazil, Jaguariúna, São Paulo, on symptomatic leaves of *Anredera cordifolia*, 16 January 2016, DJ Soares, DJS_771 (UB24608, holotype); ex-type CMAA 1612 = CMAA 1613.

Notes: The isolates (CMAA 1612 and CMAA1613) were described based on morphology and ITS sequences (Soares & Nechet 2017). The isolates were not assigned to a specific epithet as they lacked multi-locus data. In the analyses of combined ITS, LSU, *gapdh* and *rpb2* sequence data, *Dichotomophthora conlutea* (CMAA 1612 and CMAA 1613) formed a sister clade to *D. lutea* isolates (Fig. 4). *Dichotomophthora conlutea* morphologically resemble *D. lutea*, however, *D. conlutea* differs by having conidiogenous head that are usually divided 3 to 4 times and frequently proliferating to produce additional heads (De Hoog et al. 1983, Soares & Nechet 2017). The conidia of *D. conlutea* are 1–6-septate while *D. lutea* have 0–4-septate conidia (De Hoog et al. 1983, Marin-Felix et al. 2019b). The two species also differ in the size of their conidia (24–94 × 10–17 µm vs 14–65.5 × 7.5–13 µm in *D. lutea*) (De Hoog et al. 1983, Soares & Nechet 2017, Marin-Felix et al. 2019b). Therefore, we introduce *Dichotomophthora conlutea* as a new species.

Recommended genetic markers (genus level): ITS

Recommended genetic markers (species level): ITS, LSU, *gapdh* and *rpb2*

Accepted number of species: five

References: Mehrlich & Fitzpatrick (1935), Routien (1957), Rao (1966), Ellis (1971), De Hoog & van Oorschot (1983) (morphology); Marin-Felix et al. (2019b) (phylogeny); Klisiewicz et al. (1983), Klisiewicz (1985), Baudoin (1986),

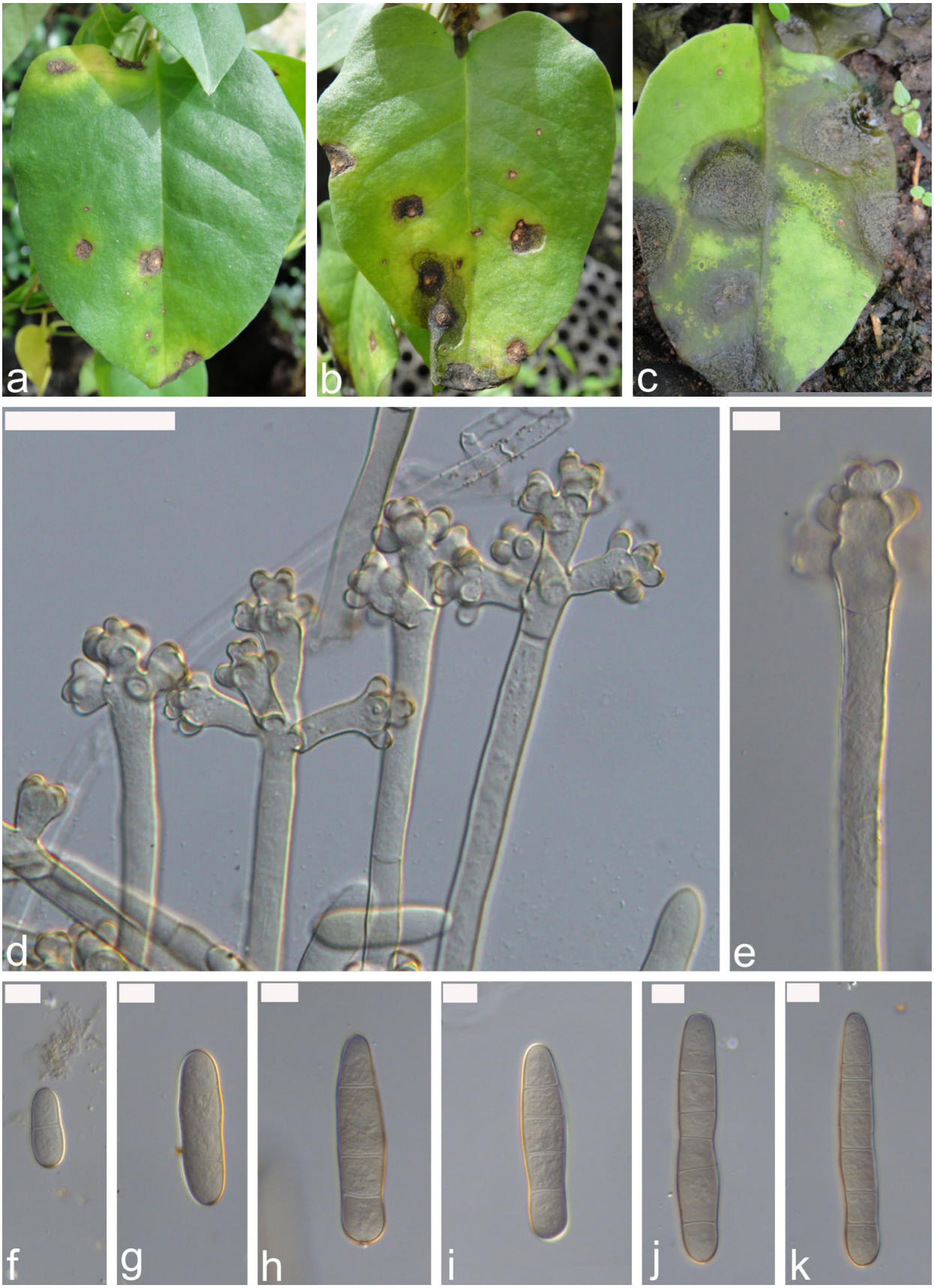

Fig. 3 Symptoms of *Dichotomophthora conlutea* on *Anredera cordifolia* (UB24608, holotype). a Initial symptoms. b Coalescent lesions with leaf yellowing. c Earlier senesced leaves under highly humid conditions showing profuse fungal sporulation. d-e Conidiophores apices showing conidiogenous heads. f-k Conidia. Scale bars: d = 50 µm, e, f, g, h, i, j, k = 10 µm. This picture is copyright of Dartanha Jose Soares.

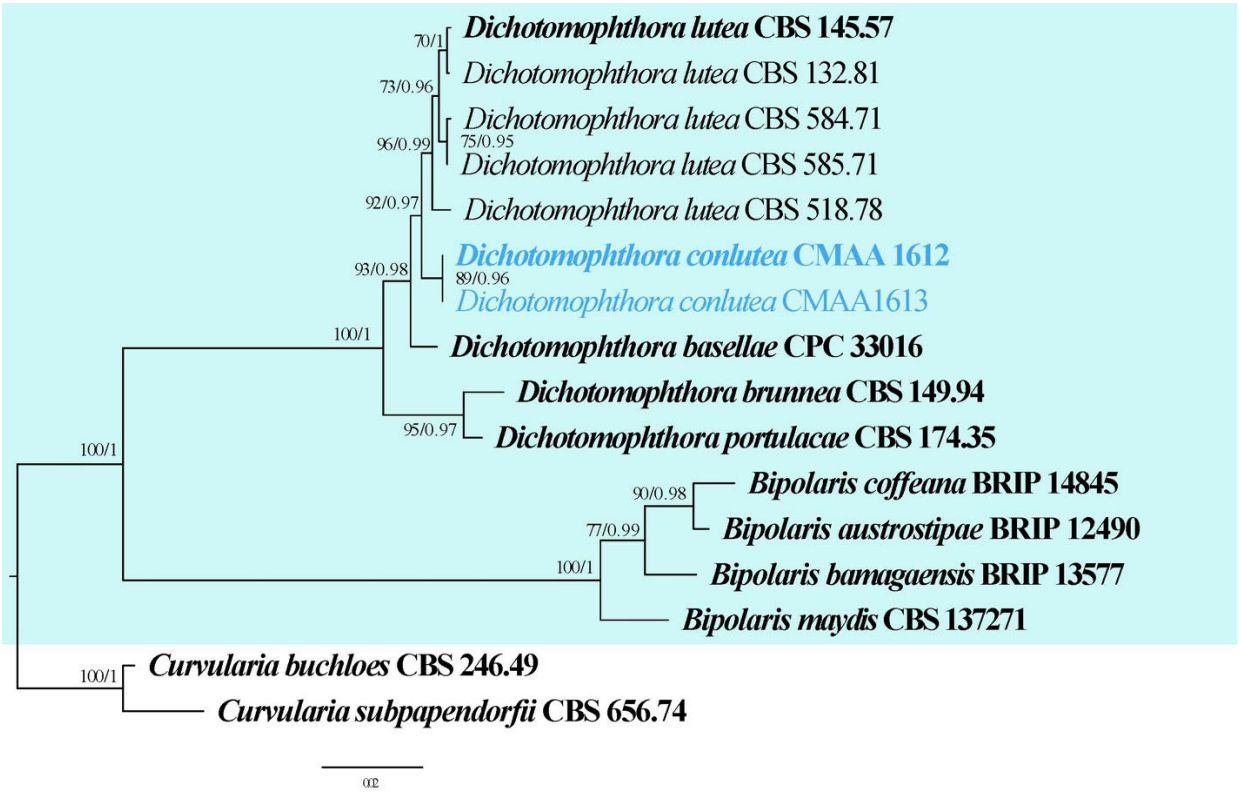

Fig. 4 Maximum likelihood tree of *Dichotomophthora* species based on the concatenated ITS, LSU, *gapdh* and *rpb2* sequence data. The best scoring RAxML tree had a final likelihood value of -6277.820. The tree was rooted to *Curvularia buchloes* (CBS 246.49) and *C. subpapendorfii* (CBS 656.74). Estimated base frequencies were as follows: A = A: 0.250, C = A: 0.250, G = A: 0.250, T = A: 0.250; substitution rates AC = 1.00000, AG = 1.90836, AT = 1.00000, CG = 1.00000, CT = 4.98741, GT = 1.000000. ML bootstrap support values over 70% and Bayesian posterior probabilities (BPP) greater than 0.95 are indicated. Type strains are in bold. The new species is in blue. Scale bar indicates the number of substitutions per site. Hyphens (-) represent support values less than BS 70%/BPP 0.95.

Mitchell (1986), Pfeiffer et al. (1989), Eken (2003), Soares & Nechet (2017) (pathogenicity)

128. *Didymella* Sacc., Michelia 2(6): 57 (1880)

Type species: *Didymella exigua* (Niessl) Sacc.

Classification: *Dothideomycetes*, *Pleosporales, Didymellaceae*

Background: *Didymella* was initially accommodated in *Mycosphaerellaceae* and later placed in *Pleosporaceae*, *Phaeosphaeriaceae* and *Venturiaceae*. Eventually, *Didymellaceae* was introduced to accommodate *Didymella* (De Gruyter et al. 2009). *Didymella exigua* has been accepted as the type or lectotype species of the genus by several authors (Höhnel 1918, Holm 1975, Corlett 1981). *Didymella* is a species-rich genus with a myriad of phytopathogens (Chen et al. 2015, 2017). As *Didymella* appears to be polyphyletic, its taxonomic revision and species delineation might be challenging as several species remain phylogenetically unresolved (Aveskamp et al. 2010, Chen et al. 2015).

Distribution: worldwide (Farr & Rossman 2025)

Disease symptoms: *Didymella* generally causes foliar diseases such as necrotic and tan leaf spots, and leaf blights, bracken blight disease, gummy stem blights, and black rot of fruits (Fig. 5). *Didymella* species cause dark sunken necrotic spots of table beets in New York (Vaghefi et al. 2016). Furthermore, a serious foliar disease was reported from baby lima bean fields in New York, initially exhibiting small necrotic spots that later coalesced and covered the entire leaf area (Gorny et al. 2016). *Didymella glomerata* was found to cause Didymella leaf blight on maize in China (Ma et al. 2022). The infected leaves displayed oval to oblong, grey sunken lesions, scattered over leaf surfaces. However, the stalks and other parts of the plant remained unaffected (Ma et al. 2022).

In addition to foliar diseases, *Didymella* taxa cause gummy stem blight of economically important plants including certain cucurbit crops. Didymella blight initially presents as small, irregularly circular, water-soaked spots. These early lesions may appear as a fading of the fruit color before darkening to shades of gray, brown, or eventually black. As the disease progresses, these spots rapidly enlarge, becoming sunken, often acquiring a firm, leathery texture (Kehinde et al. 2013). Gummy stem blight caused by *Di. bryoniae* has been reported in many countries including China, Tanzania and the United States (Mao et al. 2020). Furthermore, *Di. lycopersici* is an opportunistic pathogen that causes cankerous symptoms on tomato stems (Blancard 2012).

Hosts: *Didymella* taxa have been reported from a wide range of hosts including *Acacia* in Australia, *Araucaria* in Italy, *Berberis* in Netherlands, *Camellia* in China, *Castanea* in New Jersey, *Citrus* in Paraguay, *Cucurbita* in Italy, *Eucalyptus* in Australia, *Fucus* and *Mangifera* in Brazil, *Olea* in Iran, *Pandanus* in Philippines, *Prunus* and *Rosa* in Pakistan, *Rubus* in Australia, Canada and Pakistan, *Vitis* in Germany, and *Zea* in China, among many other hosts (Farr & Rossman 2025).

Pathogen biology, disease cycle and epidemiology: The disease cycle typically starts with the survival of *Didymella* in infected plant debris, seeds, or soil, from which it produces spores that are dispersed by wind or rain splash (Keinath 2008). Upon landing on a susceptible host, the spores germinate and infect through wounds or natural openings, leading to disease symptoms (Babadoost & Zitter 2009, Deb et al. 2020). Under favourable conditions, *Didymella* rapidly develops and sporulates, leading to secondary infections. Several species release their ascospores by an eruptive mechanism. This increases the chance for spores to spread and propagate over long distances. The bitunicate ascus comprises a sensitive inner and rigid outer wall resulting in an explosion of the latter under wet conditions, which causes the release of the ascospores (Ingold 1971, Sadyś & West 2017).

Morphological-based identification: *Didymella* taxa have ostiolate or poroid conidiomata that are pycnidial and subglobose. The conidiogenous cells are generally phialidic, hyaline and ampulliform. The conidia usually display diverse shapes being ellipsoidal to subglobose, oblong to ovoid, or cylindrical. Generally, the conidia are hyaline and aseptate, and become pigmented when mature. The ascomata are mostly pseudothecial, globose to sub-globose and ostiolate. The bitunicate asci are cylindrical, clavate or saccate, usually containing 8 spores. The ascospores are hyaline or brown and can be ellipsoidal to cymbiform, and uni- or multi-septate (Gruyter et al. 2009, Aveskamp et al. 2010, Zhang et al. 2012b, Chen et al. 2015).

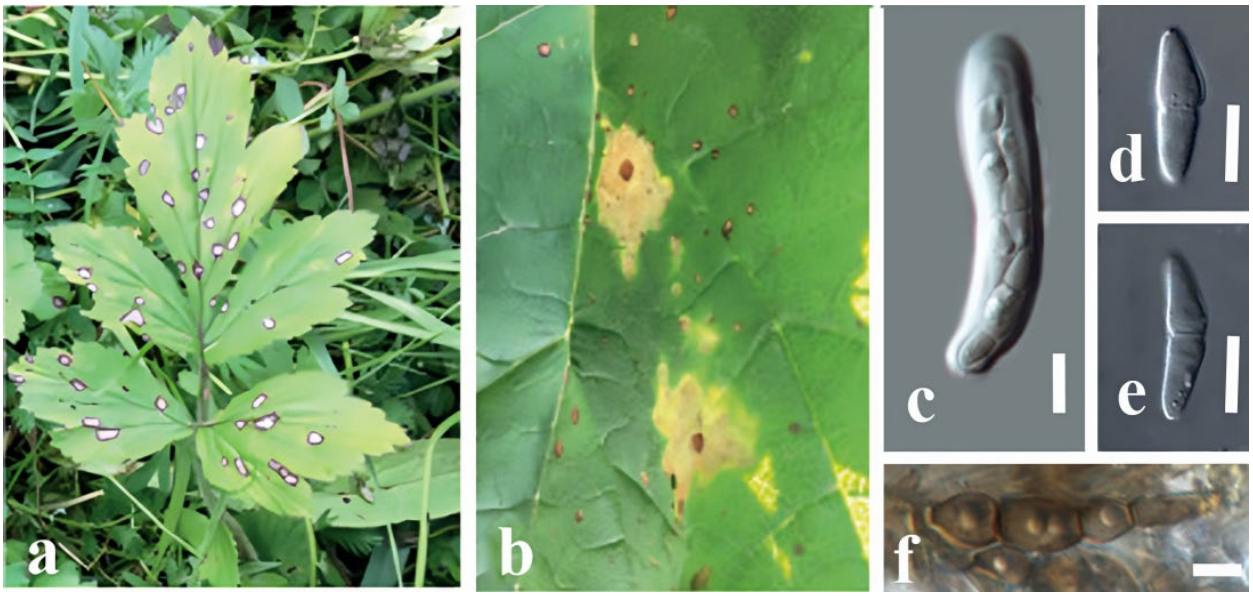

Fig. 5 *Didymella* sp. a Disease symptom of *D. gei* on *Geum* sp. b Disease symptom of *D. qilianensis* on *Rheum officinale.* c Ascus. d-e Ascospores. f Chlamydospores. Scale bars: c-e = 10 μm, f = 5 μm. This picture is copyright of Qian Chen (Chen et al. 2015, 2022).

Molecular-based identification: Studies focusing on the revision of *Didymellaceae* were based on multi-gene phylogenetic analyses of the concatenated ITS, LSU, *tub2*, and *rpb2* sequences (Gruyter et al. 2009, Aveskamp et al. 2010, Chen et al. 2015, Jayasiri et al. 2017, Phukhamsakda et al. 2020). We constructed our phylogenetic tree in accordance with previous studies. Phylogenetic analysis based on the ITS, LSU and *tub2* sequences does not completely resolve the taxonomic placement of certain taxa in *Didymellaceae*. This explains the rationale for including *rpb2* in subsequent phylogenetic analyses (Aveskamp et al. 2010, Chen et al. 2015). This study provides an updated phylogeny of *Didymella* based on combined ITS, LSU, *rpb2* and *tub2* sequence data (Fig. 6, Table 4).

Recommended genetic markers (genus level): LSU

Recommended genetic markers (species level): ITS, LSU, *rpb2* and *tub2*

Accepted number of species: 99

References: Widmer et al. (2002), Ozkilinc et al. (2011), Woudenberg et al. (2012), Khan et al. (2013), Gorny et al. (2016), Pearce et al. (2016), Havenga et al. (2019), Lee et al. (2019), Owati et al. (2019), Ren et al. (2019), Armstrong-Cho et al. (2020), Guo et al. (2020), Scarpari et al. (2020), Jiang et al. (2021), Šišić et al. (2021), Wang et al. (2021), Indermaur et al. (2022), Ma et al. (2022) (pathogenicity data)

129. *Leptosphaerulina* McAlpine, Fungus Diseases of stone-fruit trees in Australia: 103 (1902)

Type species: *Leptosphaerulina australis* McAlpine

Classification: *Dothideomycetes*, *Pleosporales*, *Didymellaceae*

Background: *Leptosphaerulina* was established by McAlpine (1902) with *L. australis* as the type species, which was isolated from the leaves of *Prunus armeniaca* (apricot). Initially, *Leptosphaerulina* was accommodated in *Pseudosphaeriaceae* based on morphological features (Luttrell 1955, Graham & Luttrell 1961, Barr 1982). Later, it was placed in *Pleosporaceae* (Eriksson 1993, 2006, Kirk et al. 2001). Eventually, its placement was confirmed in *Didymellaceae* based on molecular data (Aveskamp et al. 2010, Zhang et al. 2012b, Hyde et al. 2013, Hongsanan et al. 2020a, b). *Didymellaceae* is a species-rich family in *Pleosporales* that includes taxa from a wide range of hosts from different ecosystems (Chen et al. 2017, Thambugala et al. 2018).

Distribution: *Leptosphaerulina* taxa have cosmopolitan distributions and have been recorded from both temperate and tropical countries, including Canada, China, Colombia, Georgia, India, Indonesia, Japan, Kenya, the Netherlands, 2013, Chen et al. 2017, Farr & Rossman 2025).

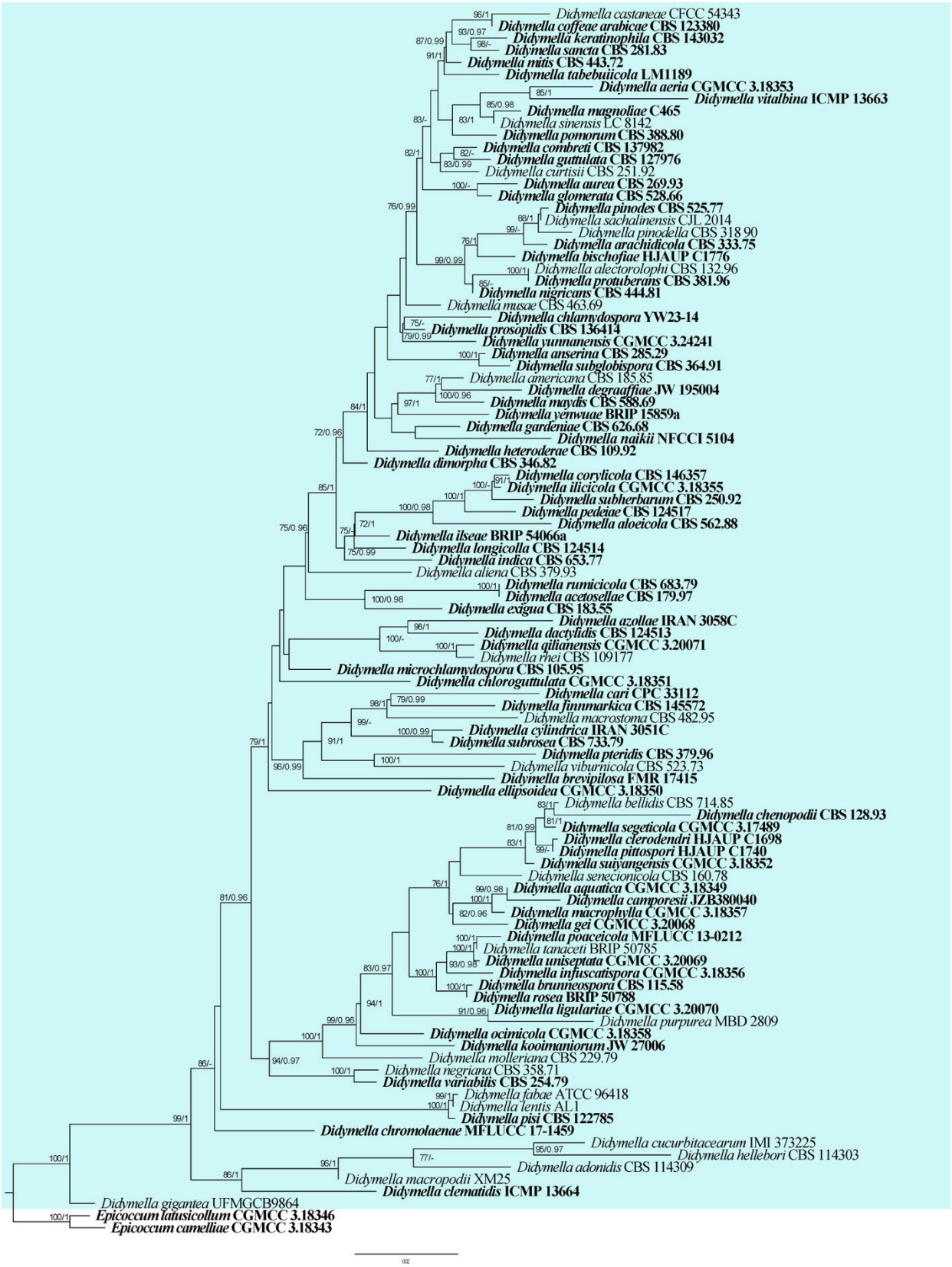

Fig. 6 Maximum likelihood tree of *Didymella* species based on the concatenated ITS, LSU, *rpb2* and *tub2* sequence data. The best scoring RAxML tree had a final likelihood value of -16957.247. The tree was rooted with *Epicoccum camelliae* (CGMCC 3.18343) and *E. latusicollum* (CGMCC 3.18346). Estimated base frequencies were as follows: A = 0.250, C = 0.250, G = 0.250, T = 0.250; substitution rates AC = 1.45908, AG = 6.33861, AT = 1.45908, CG = 1.00000, CT = 11.74000, GT = 1.000000. ML bootstrap support values over 70% and Bayesian posterior probabilities (BPP) greater than 0.95 are indicated. Type strains are in bold. Scale bar indicates the number of substitutions per site. Hyphens (-) represent support values less than BS 70%/BPP 0.95.

Table 4 DNA barcodes for accepted species of *Didymella*.

Species	Strain	GenBank accession numbers			
		ITS	LSU	*rpb2*	*tub2*
Didymella acetosellae#	**CBS 179.97**	**GU237793**	**GU238034**	**KP330415**	**GU237575**
Di. adonidis	CBS 114309	MH862963	MH874526	MT018057	KT389803
Di. aeria	**CGMCC 3.18353**	**KY742051**	**KY742205**	**KY742137**	**KY742293**
Di. alectorolophi	CBS 132.96	GU237778	GU237989	N/A	GU237550
Di. aliena	CBS 379.93	GU237851	GU238037	KP330416	GU237578
Di. aloeicola	**CBS 562.88**	**MN973535**	**MN943742**	**MT018164**	**MT005638**
Di. americana#	CBS 185.85	FJ426972	GU237990	KT389594	FJ427088
Di. anserina	**CBS 285.29**	**KT389499**	**KT389716**	**N/A**	**KT389796**
Di. aquatica	**CGMCC 3.18349**	**KY742055**	**KY742209**	**KY742140**	**KY742297**
Di. arachidicola	**CBS 333.75**	**GU237833**	**GU237996**	**KT389598**	**GU237554**
Di. aurea	**CBS 269.93**	**GU237818**	**GU237999**	**KT389599**	**GU237557**
Di. azollae	**IRAN 3058C**	**MT514913**	**MT514910**	**N/A**	**MT512516**
Di. bellidis#	CBS 714.85	GU237904	GU238046	KP330417	GU237586
Di. bischofiae	**HJAUP C1776**	**OR625712**	**OR625713**	**OR620208**	**OR620206**
Di. brevipilosa	**FMR 17415**	**OU612373**	**N/A**	**OU612359**	**OU612358**
Di. brunneospora	**CBS 115.58**	**KT389505**	**KT389723**	**KT389625**	**KT389802**
Di. camporesii	**JZB380040**	**MN648211**	**MN640406**	**N/A**	**N/A**
Di. cari#	**CPC 33112**	**MH327825**	**MH327861**	**N/A**	**MH327899**
Di. castaneae#	CFCC 54343	MW364357	MW364277	N/A	N/A
Di. chenopodii	CBS 128.93	GU237775	GU238055	KT389602	GU237591
Di. chlamydospora	**YW23-14**	**MK836111**	**MK836109**	**LC480708**	**LC482279**
Di. chloroguttulata	**CGMCC 3.18351**	**KY742057**	**KY742211**	**KY742142**	**KY742299**
Di. chromolaenae	**MFLUCC 17-1459**	**MT214363**	**MT214457**	**N/A**	**N/A**
Di. clematidis#	**ICMP 13664**	**KT309873**	**KT309678**	**N/A**	**KT309460**
Di. clerodendri	**HJAUP C1698**	**OR625709**	**OR625714**	**OR620207**	**OR611942**
Di. coffeae-arabicae#	**CBS 123380**	**FJ426993**	**GU238005**	**KT389603**	**FJ427104**
Di. combreti	**CBS 137982**	**MN973525**	**MN943731**	**MT018139**	**MT005626**
Di. corylicola#	**CBS 146357**	**MN954301**	**MN954290**	**MN958323**	**MN958333**
Di. cucurbitacearum	IMI 373225	AY293804	AY293792	N/A	N/A
Di. curtisii	CBS 251.92	FJ427038	GU238013	N/A	FJ427148
Di. cylindrica	**IRAN 3051C**	**OK257014**	**OK257022**	**OK247736**	**OK247741**
Di. dactylidis	**CBS 124513**	**GU237766**	**GU238061**	**N/A**	**GU237599**
Di. degraaffiae	**JW 195004**	**MN823444**	**MN823295**	**MN824470**	**MN824618**
Di. dimorpha	**CBS 346.82**	**GU237835**	**GU238068**	**N/A**	**GU237606**
Di. ellipsoidea	**CGMCC 3.18350**	**KY742060**	**KY742214**	**KY742145**	**KY742302**
Di. exigua#	**CBS 183.55**	**GU237794**	**EU754155**	**EU874850**	**GU237525**
Di. fabae#	ATCC 96418	DQ383952	N/A	EU874859	N/A
Di. finnmarkica	**CBS 145572**	**MK876388**	**MK876429**	**MK876484**	**N/A**
Di. gardeniae	**CBS 626.68**	**FJ427003**	**GQ387595**	**KT389606**	**FJ427114**
Di. gei	**CGMCC 3.20068**	**MT229698**	**MT229675**	**MT239095**	**MT249266**
Di. gigantea	UFMGCB9864	KU727758	N/A	N/A	N/A
Di. glomerata#	**CBS 528.66**	**FJ427013**	**EU754184**	**GU371781**	**FJ427124**
Di. guttulata	**CBS 127976**	**MN973524**	**MN943730**	**MT018138**	**MT005625**
Di. hellebori	CBS 114303	MH862961	MH874524	N/A	N/A
Di. heteroderae	**CBS 109.92**	**FJ426983**	**GU238002**	**KT389601**	**FJ427098**
Di. ilicicola	**CGMCC 3.18355**	**KY742065**	**KY742219**	**KY742150**	**KY742307**
Di. ilseae	**BRIP 54066a**	**PV425967**	**N/A**	**PV459752**	**N/A**
Di. indica	**CBS 653.77**	**MN973534**	**MN943741**	**MT018159**	**MT005637**
Di. infuscatispora	**CGMCC 3.18356**	**KY742067**	**KY742221**	**KY742152**	**KY742309**
Di. keratinophila	**CBS 143032**	**LT592901**	**LN907343**	**LT593039**	**LT592970**
Di. kooimaniorum	**JW 27006**	**MN823448**	**MN823299**	**MN824474**	**MN824622**
Di. lentis	AL1	DQ383953	N/A	N/A	N/A
Di. ligulariae	**CGMCC 3.20070**	**MT229699**	**MT229676**	**MT239096**	**MT249267**
Di. longicolla	**CBS 124514**	**GU237767**	**GU238095**	**N/A**	**GU237622**
Di. macrophylla	**CGMCC 3.18357**	**KY742070**	**KY742224**	**KY742154**	**KY742312**
Di. macropodii	XM25	MZ292418	MZ298910	N/A	N/A
Di. macrostoma	CBS 482.95	GU237869	GU238099	KT389609	GU237626
Di. magnoliae	**C465**	**MK347814**	**MK348033**	**MK434852**	**N/A**
Di. maydis	**CBS 588.69**	**FJ427086**	**EU754192**	**GU371782**	**FJ427190**

Di. microchlamydospora	**CBS 105.95**	**FJ427028**	**GU238104**	**KP330424**	**FJ427138**
Di. molleriana	CBS 229.79	GU237802	GU238067	KP330418	GU237605
Di. musae	CBS 463.69	FJ427026	GU238011	LT623248	FJ427136
Di. mitis	**CBS 443.72**	**MN973523**	**MN943729**	**MT018137**	**MT005624**
Di. naikii	**NFCCI 5104**	**OM952211**	**OM830704**	**N/A**	**OM858681**
Di. negriana	CBS 358.71	GU237838	GU238116	KT389610	GU237635
Di. nigricans	**CBS 444.81**	**GU237867**	**GU238000**	**N/A**	**GU237558**
Di. ocimicola	**CGMCC 3.18358**	**KY742078**	**KY742232**	**N/A**	**KY742320**
D. pedeiae	**CBS 124517**	**GU237770**	**GU238127**	**KT389612**	**GU237642**
Di. pinodella#	CBS 318.90	FJ427051	GU238016	N/A	FJ427161
Di. pinodes#	**CBS 525.77**	**GU237883**	**GU238023**	**KT389614**	**GU237572**
Di. pisi#	**CBS 122785**	**GU237763**	**GU237969**	**MT018244**	**GU237532**
Di. pittospori	**HJAUP C1740**	**OR625710**	**OR625711**	**N/A**	**OR620205**
Di. poaceicola	**MFLUCC 13-0212**	**KX965726**	**KX954395**	**KX898364**	**N/A**
Di. pomorum#	**CBS 388.80**	**FJ427055**	**GU238027**	**KT389617**	**FJ427165**
Di. prosopidis	**CBS 136414**	**NR_137836**	**NG_069183**	**MT018149**	**MT005631**
Di. protuberans	**CBS 381.96**	**GU237853**	**GU238029**	**KT389620**	**GU237574**
Di. pteridis	**CBS 379.96**	**KT389504**	**KT389722**	**KT389624**	**KT389801**
Di. purpurea	MBD 2809	MK595528	N/A	N/A	N/A
Di. qilianensis	**CGMCC 3.20071**	**MT229701**	**MT229678**	**MT239098**	**MT249269**
Di. rhei#	CBS 109177	GU237743	GU238139	KP330428	GU237653
Di. rosea#	**BRIP 50788**	**KT338640**	**KT287003**	**N/A**	**KT286945**
Di. rumicicola#	**CBS 683.79**	**KT389503**	**KT389721**	**KT389622**	**KT389800**
Di. sachalinensis	CJL 2014	KJ542242	N/A	N/A	N/A
Di. sancta	**CBS 281.83**	**FJ427063**	**GU238030**	**KT389623**	**FJ427170**
Di. segeticola#	**CGMCC 3.17489**	**KP330443**	**KP330455**	**KP330414**	**KP330399**
Di. senecionicola	CBS 160.78	GU237787	GU238143	N/A	GU237657
Di. sinensis	LC 8142	KY742087	KY742241	KY742166	KY742329
Di. subglobispora	**CBS 364.91**	**MN973531**	**MN943737**	**MT018153**	**MT005634**
Di. subherbarum	**CBS 250.92**	**GU237809**	**GU238145**	**N/A**	**GU237659**
Di. subrosea	**CBS 733.79**	**MN973540**	**MN943747**	**MT018174**	**MT005643**
Di. suiyangensis	**CGMCC 3.18352**	**KY742089**	**KY742243**	**KY742168**	**KY742331**
Di. tabebuiicola	**LM1189**	**MZ703618**	**MZ703623**	**MZ712360**	**MZ712364**
Di. tanaceti#	BRIP 50785	KT338641	KT287022	N/A	KT286974
Di. uniseptata	**CGMCC 3.20069**	**MT229702**	**MT229679**	**MT239099**	**MT249270**
Di. variabilis	**CBS 254.79**	**MN973544**	**MN943751**	**MT018182**	**MT005647**
Di. viburnicola	CBS 523.73	GU237879	GU238155	KP330430	GU237667
Di. vitalbina#	**ICMP 13663**	**KT309872**	**KT309677**	**N/A**	**KT309459**
Di. yenwuae	**BRIP 15859a**	**PQ279215**	**N/A**	**PQ299736**	**PQ299737**
Di. yunnanensis#	**CGMCC 3.24241**	**OP647939**	**OP836939**	**OP854286**	**OP854551**

Ex-type/ex-epitype/ex-neotype/ex-lectotype strains and voucher strains are in bold. Sequences that are not available are represented by N/A. Species confirmed with pathogenicity studies are marked with #.

Disease symptoms: Major diseases caused by *Leptosphaerulina* species are leaf spots and blights, as well as scorch spots (Fig. 7). Leaf blight caused by *Leptosphaerulina* spp. is common in humid and damp regions, primarily on grasses such as *Agrostis stolonifera* (creeping bentgrass), *Poa pratensis* (Kentucky bluegrass), and *Lolium perenne* (perennial ryegrass) (Shurtleff et al. 1987, Smiley et al. 1992). The symptoms displayed during the course of leaf blight disease formation are tip dieback often with yellow to brown lesions extending down to the leaf sheaths. Sometimes, the entire leaf or sheath may develop water-soaked spots and quickly become chlorotic (Couch 1962, Smiley et al. 1992).

Hosts: *Leptosphaerulina* taxa have been reported worldwide from a wide range of hosts. These include *Acacia mearnsii* in South Africa, *Arachis hypogaea* in China, *Boerhaavia difusa* in India, *Brassica* spp. in China, *Cannabis sativa* in India, *Crotalaria striata* in India, *Euphorbia geniculata* in India, *Ficus retusa* in India, *Medicago laciniata* in Kenya, *Morus* sp. in Japan, *Oryza sativa* in India, *Terminalia bellerica* in India, *Trifolium pretense* in Georgia, and *Zea mays* in Malaysia, among several others (Farr & Rossman 2025).

Pathogen biology, disease cycle and epidemiology: *Leptosphaerulina* species cause leaf spots and scorch diseases of leguminous plants, including alfalfa, peanut, red and white clover, and soybean (Graham & Luttrell 1961, Anahosur & Fazalnoor 1972). The ascospores of *Leptosphaerulina* are easily dispersed via wind (Graham & Luttrell 1961). The mucilaginous sheath allows them to adhere to leaf surfaces and adsorb water (Tehon & Stout 1928, Furtado & Olive 1971). Following adherence, germ tubes are formed, after which a penetration peg enters the cuticle and epidermal cell walls (Hopskins 1923, Miles 1925, Sundheim & Wilcoxson 1965, Wu & Hanlin 1992). The germ tubes can also enter plant tissues via stomata; however, this process is rather infrequent (Wu & Hanlin 1992).

Morphological-based identification: *Leptosphaerulina* species have ostiolate, papillate and immersed to erumpent ascomata. The asci are bitunicate and saccate while

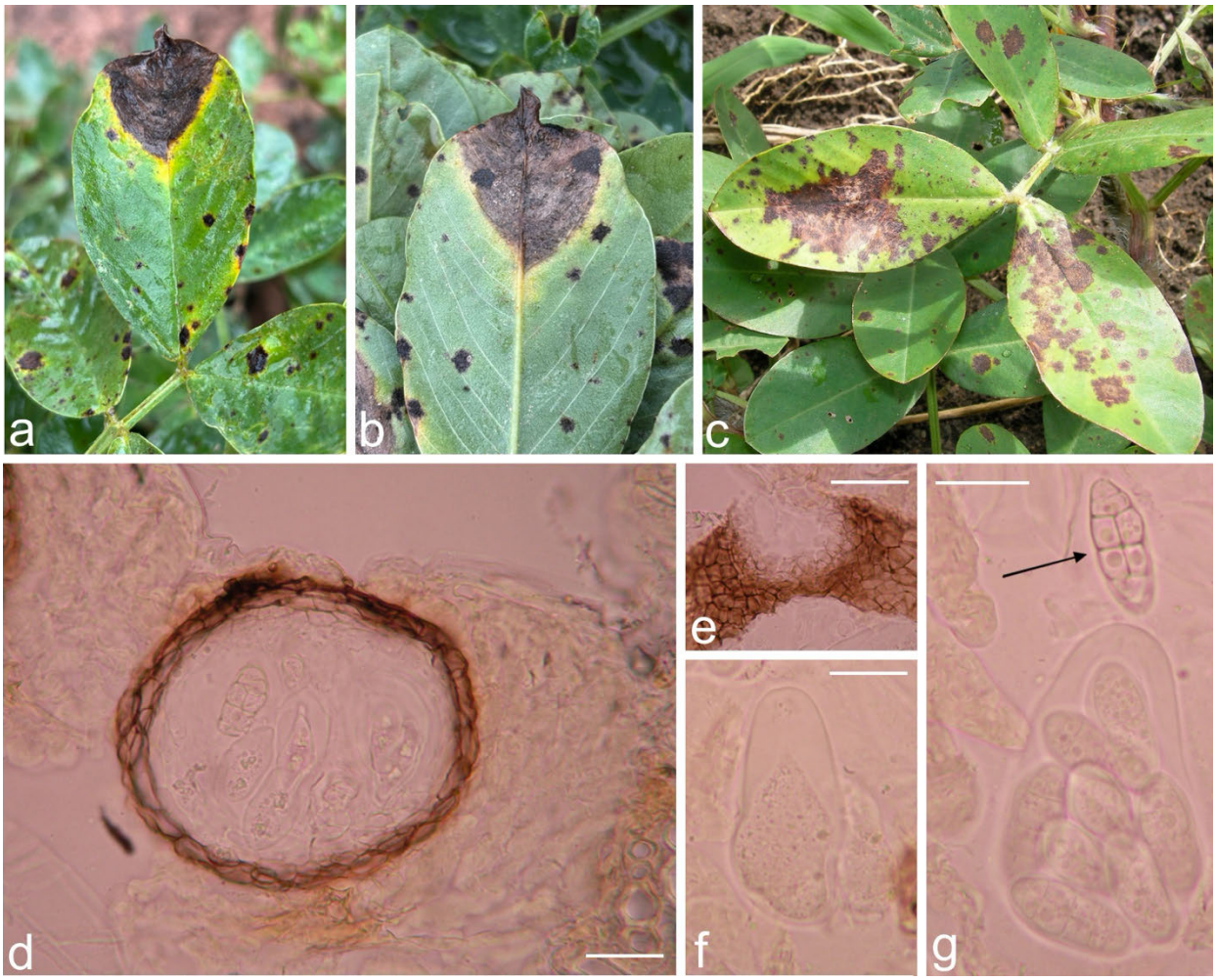

Fig. 7 *Leptosphaerulina crassiasca* on *Arachis hypogaea*. a Adaxial and abaxial b views of the wedge-shaped scorch symptom. c A typical leaf scorch. d Transverse section of perithecium with asci. e Ostiolum. f Immature ascus. g Mature 8-spored ascus and ascospore with longitudinal and transverse septa (indicated with arrow). Scale bars = 25 µm. This picture is copyright of Dartanha Jose Soares.

ascospores are oblong to cylindrical, usually muriform and hyaline, becoming brown when mature (Graham & Luttrell 1961, Abler et al. 2003, Zhang et al. 2012b, Phookamsak et al. 2013). Some phylogenetically distinct *Leptosphaerulina* taxa are cryptic (Phookamsak et al. 2013).

Molecular-based identification: Multi-locus phylogenetic analyses of ITS, LSU, *tub2* and *rpb2* sequences are recommended for species delineation in *Leptosphaerulina* (Chen et al. 2015, Valenzuela-Lopez et al. 2018, Hou et al. 2020). The ITS and LSU markers alone do not provide sufficient phylogenetic resolution (Liang et al. 2021). Phylogenetic analyses of *rpb2* sequences only can yield a phylogenetic tree with a similar topology as that of the concatenated dataset (ITS, LSU, *tub2*, *rpb2* and *tef*) (Liang et al. 2021). Therefore, *rpb2* is the best DNA marker for species delimitation in *Leptosphaerulina* (Liang et al. 2021), however, several species lack *rpb2* sequences. *Leptosphaerulina crassiasca* (XWS02F460) was excluded from the molecular analyses as only the ITS region is available for this taxon. This study provides an updated phylogeny of *Leptosphaerulina* based on combined ITS, LSU, *rpb2*, *tub2* and *tef* sequence data (Fig. 8, Table 5).

Recommended genetic markers (genus level): LSU

Recommended genetic markers (species level): ITS, LSU, *rpb2*, *tub2*, and *tef*

Accepted number of species: 18

References: Liu et al. (2019), Victoria et al. (2020), Zhang & Li (2021), Sheng et al. (2022) (species with pathogenicity data)

130. *Macrophomina* Petr., Annls Mycol. 21(3/4): 314 (1923)

Type species: *Macrophomina phaseolina* (Tassi) Goid.

Classification: *Dothideomycetes*, *Botryosphaeriales*, *Botryosphaeriaceae*

Background: *Macrophomina* was introduced by Petrak (1923) with *M. philippinensis* as the type species. However, the correct name for the type species was followed by a lot of confusion, especially with *M. phaseoli* and *M. phaseolina* being used interchangeably during the first half of the 20th century. It was only in the late 1970s that *M. phaseolina* was widely recognized as the correct name and *M. philippinensis* was synonymised with *M. phaseolina* (Ashby 1927, Holliday & Punithalingam 1970, Babu et al. 2010). *Macrophomina* was widely accepted as a monotypic genus, despite several attempts to propose distinct sub-specific ranks based mainly on host-specificity (Phillips et al. 2013, Sarr et al. 2014).

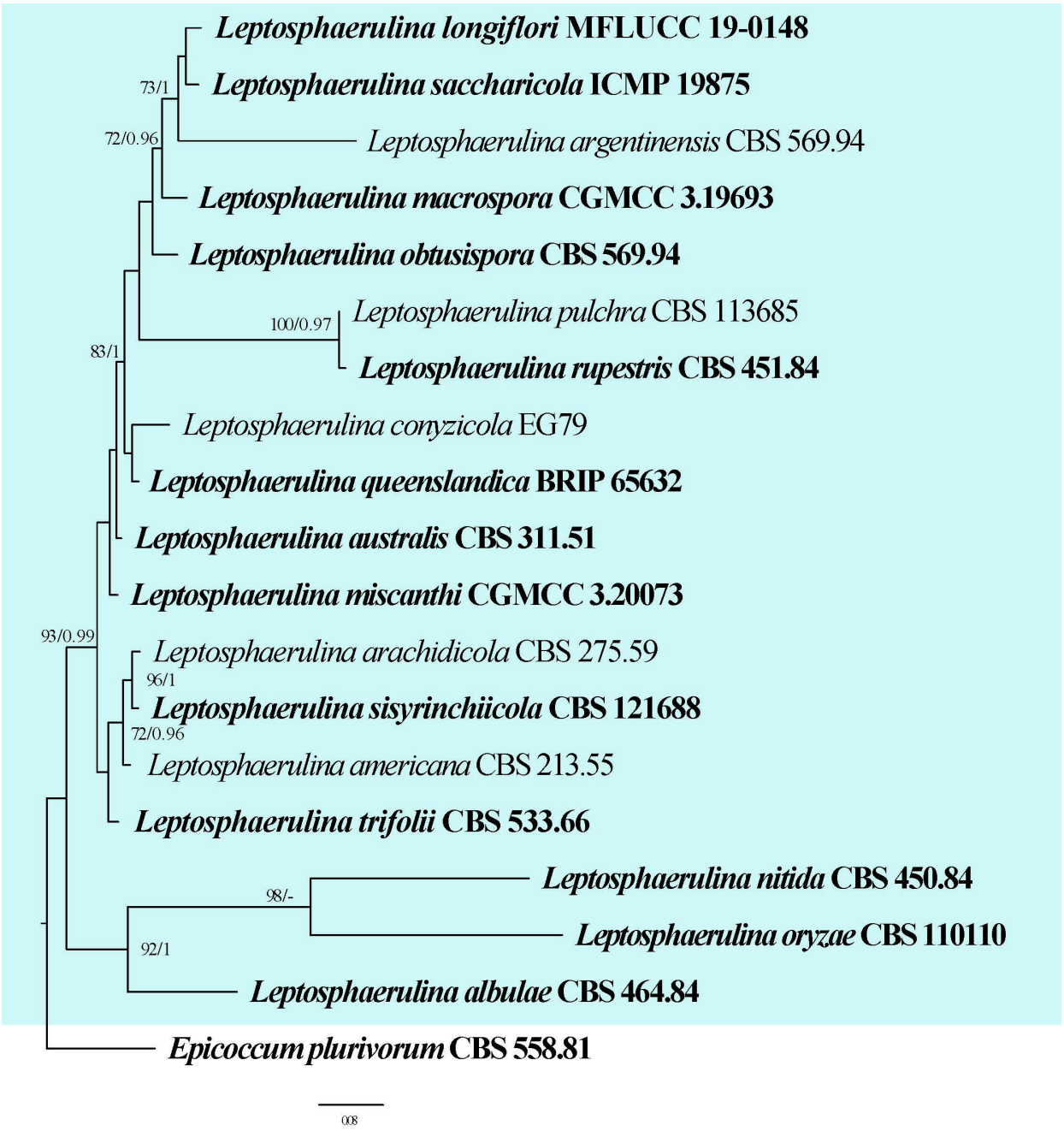

Fig. 8 Maximum likelihood tree of *Leptosphaerulina* species based on the concatenated ITS, LSU, *rpb2*, *tub2* and *tef* sequence data. The best scoring RAxML tree had a final likelihood value of -9591.838. The tree was rooted with *Epicoccum plurivorum* (CBS 558.81). Estimated base frequencies were as follows: A = A: 0.250, C = A: 0.250, G = A: 0.250, T = A: 0.250; substitution rates AC = 1.00000, AG = 3.47926, AT = 1.00000, CG = 1.00000, CT = 9.30598, GT = 1.000000. ML bootstrap support values over 70% and Bayesian posterior probabilities (BPP) greater than 0.95 are indicated. Type strains are in bold. Scale bar indicates the number of substitutions per site. Hyphens (-) represent support values less than BS 70%/BPP 0.95.

Table 5 DNA barcodes for accepted species of *Leptosphaerulina*.

Species	Strain	GenBank accession numbers				
		ITS	LSU	*rpb2*	*tub2*	*tef*
Leptosphaerulina albulae	**CBS 464.84**	**MH861767**	**MH873466**	**N/A**	**N/A**	**N/A**
L. americana	CBS 213.55	MH857452	MH868995	KT389641	GU237539	N/A
L. arachidicola#	CBS 275.59	MH857863	MH869401	MT018278	GU237543	N/A
L. argentinensis	CBS 569.94	MH862490	MH874133	GU357759	N/A	GU349008
L. australis#	**CBS 311.51**	**N/A**	**N/A**	**GU456357**	**N/A**	**GU456272**

L. conyzicola	EG79	N/A	KJ194472	N/A	N/A	N/A
L. longiflori	**MFLUCC 19-0148**	**MK503800**	**MK503811**	**MK503805**	**N/A**	**N/A**
L. macrospora	**CGMCC3 19693**	**MW090232**	**MW090672**	**MW092122**	**MW092141**	**N/A**
L. miscanthi	**CGMCC 3.20073**	**MT229706**	**MT229683**	**MT239103**	**MT249274**	**N/A**
L. nitida	**CBS 450.84**	**MH861755**	**MH873454**	**N/A**	**N/A**	**N/A**
L. obtusispora	**CBS 569.94**	**MN973602**	**MN943811**	**MT018275**	**MT005712**	**N/A**
L. oryzae	**CBS 110110**	**MH862850**	**MH874442**	**KF252193**	**KF252680**	**N/A**
L. pulchra	CBS 113685	MH862938	MH874505	N/A	N/A	N/A
L. queenslandica	**BRIP 65632**	**MW481667**	**MW481664**	**MW626889**	**N/A**	**N/A**
L. rupestris	**CBS 451.84**	**MH861756**	**MH873455**	**N/A**	**N/A**	**N/A**
L. saccharicola	**ICMP 19875**	**KF670717**	**KF670716**	**KF670714**	**N/A**	**KF670715**
L. sisyrinchiicola	**CBS 121688**	**MN973605**	**MN943814**	**MT018279**	**MT005715**	**N/A**
L. trifolii#	**CBS 533.66**	**N/A**	**MN943804**	**MT018266**	**MT005704**	**N/A**

Ex-type/ex-epitype/ex-neotype/ex-lectotype strains and voucher strains are in bold. Sequences that are not available are represented by N/A. Species confirmed with pathogenicity studies are marked with #.

Macrophomina is a diverse, soil- or seed-borne plant pathogen occurring worldwide. *Macrophomina* species commonly cause diseases such as stem and root rot, charcoal rot, seedling blight and stem blight (Agarwal 2010, Ndiaye et al. 2015, Marquez et al. 2021). *Macrophomina* has been reported on approximately 600 cultivated and wild plant species, belonging to over 100 families in more than 80 countries (Khan 2007, Agarwal 2010, Ndiaye et al. 2015, Zhao et al. 2019, Farr & Rossman 2025).

Distribution: worldwide, but mostly in tropical, subtropical and warm-temperate areas (Cohen et al. 2022a, Farr & Rossman 2025)

Disease symptoms: *Macrophomina* species generally cause charcoal-rot or ashy stem blight in various host species (Fig. 9). *Macrophomina* symptoms may vary depending on host and weather conditions. The main disease symptoms are dry or wet dark rot of the root and lower stem (Agarwal 2010, Poudel et al. 2021). Roots and soft-tissue plants, such as melon and strawberry, exhibit early tissue rot due to cell-wall-degrading enzymes, whereas plants with lignified stems, such as cotton, sesame, soybean, and castor bean, usually start exhibiting yellowing and wilt symptoms without visible external stem rot, due to the disruption of water and nutrient flow to aerial parts. Lower stem and taproot cortical tissue become slough. Under heat or drought stress, the symptoms are exacerbated usually inducing premature death of branches or of the whole plant. Symptoms occasionally remain mild until plants start flowering or fruiting, when, under favourable conditions, the plant can quickly die (Dhingra & Sinclair 1978, Cohen et al. 2022b). *Macrophomina* exhibits a strong capacity for rapid colonization of host tissues, eventually leading to their death in a short timeframe. During colonization, it forms microsclerotia and pycnidia on hosts (Dhingra & Sinclair 1978, Khan 2007, Su et al. 2021). On seedling stage, wet root rot followed by damping-off predominates. Aboveground symptoms on adult plants usually appear as foliar yellowing and wilt of either some branches or the entire plant. Eventually symptoms progress to light-brown, grey, or black lesions, due to fungal colonization of plant tissues and production of numerous microsclerotia, characterizing the classical charcoal rot/ashy stem symptoms. At this stage, pycnidia can sometimes, be found on aboveground colonized tissues. As the fungus colonization spreads up the stem during the seasons, it may eventually reach the pods, capsules or grains (Gupta et al. 2012). Underground organs, such as tubers and rhizomes, can also be partially or completely colonized (Mello et al. 2021).

Hosts: *Macrophomina* affects a wide range of hosts, including field crops, vegetables, ornamentals, shrubs and trees (Poudel et al. 2021, Cohen et al. 2022a, Bhunjun et al. 2024, Farr & Rossman 2025). *Macrophomina* species have been recorded worldwide on a broad range of economically important hosts including soybean (*Glycine max*), maize (*Zea mays*), common bean (*Phaseolus vulgaris*), black gram (*Vigna mungo*), chickpea (*Cicer arietinum*), cotton (*Gossypium* spp.), pigeon pea (*Cajanus cajan*), sorghum (*Sorghum bicolor*), sunflower (*Helianthus annuus*), and sesame (*Sesamum indicum*) (Dhingra & Sinclair 1978, Root 1986, Reyes-Franco et al. 2006, Khan 2007, Agarwal 2010, Ndiaye et al. 2015, Santos et al. 2020, Poudel et al. 2021, Cohen et al. 2022b). *Macrophomina phaseolina* is the most common and widespread species causing stem and root rot, charcoal rot and seedling blight in hundreds of plant species (Islam et al. 2012, Farr & Rossman 2024). *Macrophomina pseudo-phaseolina* has been recorded on cowpea (*Vigna unguiculata*), peanut (*Arachis hypogaea*), sorrel (*Hibiscus sabdarifa*), okra (*Abelmoschus esculentus*), cotton (*G. hirsutum*), castor bean (*Ricinus communis*), cassava (*Manihot esculenta*), sweet potato (*Ipomoea batatas*), lentil (*Lens culinaris*), common bean, and few other weeds (Sarr et al. 2014, Ndiaye et al. 2015, Brito et al. 2019, Machado et al. 2019, Mello et al. 2021, Viejobueno et al. 2022, Kouadri et al. 2023). *Macrophomina euphorbiicola* was originally reported on castor bean and bellyache bush (*Jatropha gossypifolia*), and later on *Stevia rebaudiana*, *Amaranthus retroflexus*, and *Convolvulus arvensis* (Machado et al. 2019, Mello et al. 2021, Sanabria-Velazquez et al. 2022, Moslemi et al. 2023). *Macrophomina tecta* was first reported on sorghum and mung bean (*Vigna radiata*), and later on corn (Poudel et al. 2021, Viejobueno et al. 2022). On the other hand, *M. vaccinii* is known only through its original reports on blueberries (*Vaccinium* spp.) (Zhao et al. 2019).

Pathogen biology, disease cycle and epidemiology: Microsclerotia are the primary inoculum source of *Macrophomina* species (Fig. 10). Pycnidia and conidia production has been occasionally observed in different host plants, however, their role in disease development and epidemiology is yet to be understood (Dhingra & Sinclair 1978, Romero Luna et al. 2017). Early infection stages demonstrate that *Macrophomina* should be regarded as hemibiotrophic, instead of a truly necrotrophic fungus (Shirai & Eulgem 2023). Although *Macrophomina* is considered a poor soil competitor, its microsclerotia in infected roots and plant residues play an

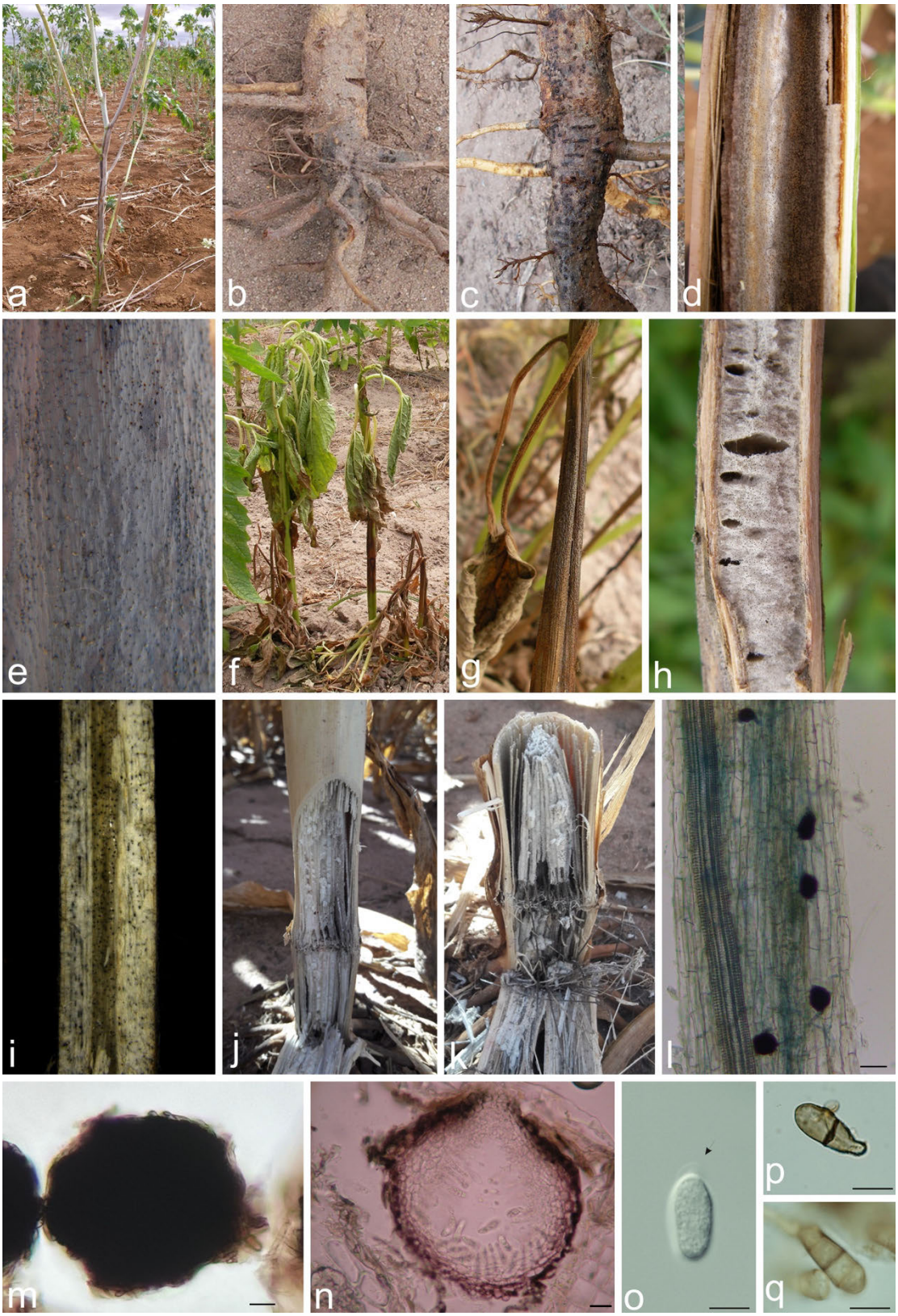

Fig. 9 *Macrophomina phaseolina* on various hosts. a Castor bean plant showing stem blight and branch death. b-c Roots of castor bean with extensive black lesions. d Longitudinal section of castor bean stem showing profuse microsclerotia formation. e Castor bean stem with presence of pycnidia and conidia cirrus. f Wilted and dead sesame plants. g-h Profuse formation of microsclerotia externally and internally (h) on sesame stem. i Longitudinal section of soybean stem with microsclerotia. j-k Corn stem with microsclerotia. l Microsclerotia formed on sesame root tissue. m Microsclerotium. n Transversal section of a pycnidium with conidia. o-q Immature *M. pseudophaseolina* conidium with apical mucous appendage and (p-q) mature pigmented conidia. Scale bars: l = 100 µm, m-q = 10 µm. This picture is copyright of Dartanha Jose Soares (except i by HK da Silva, j-k by R Veras and o-q by AR Machado).

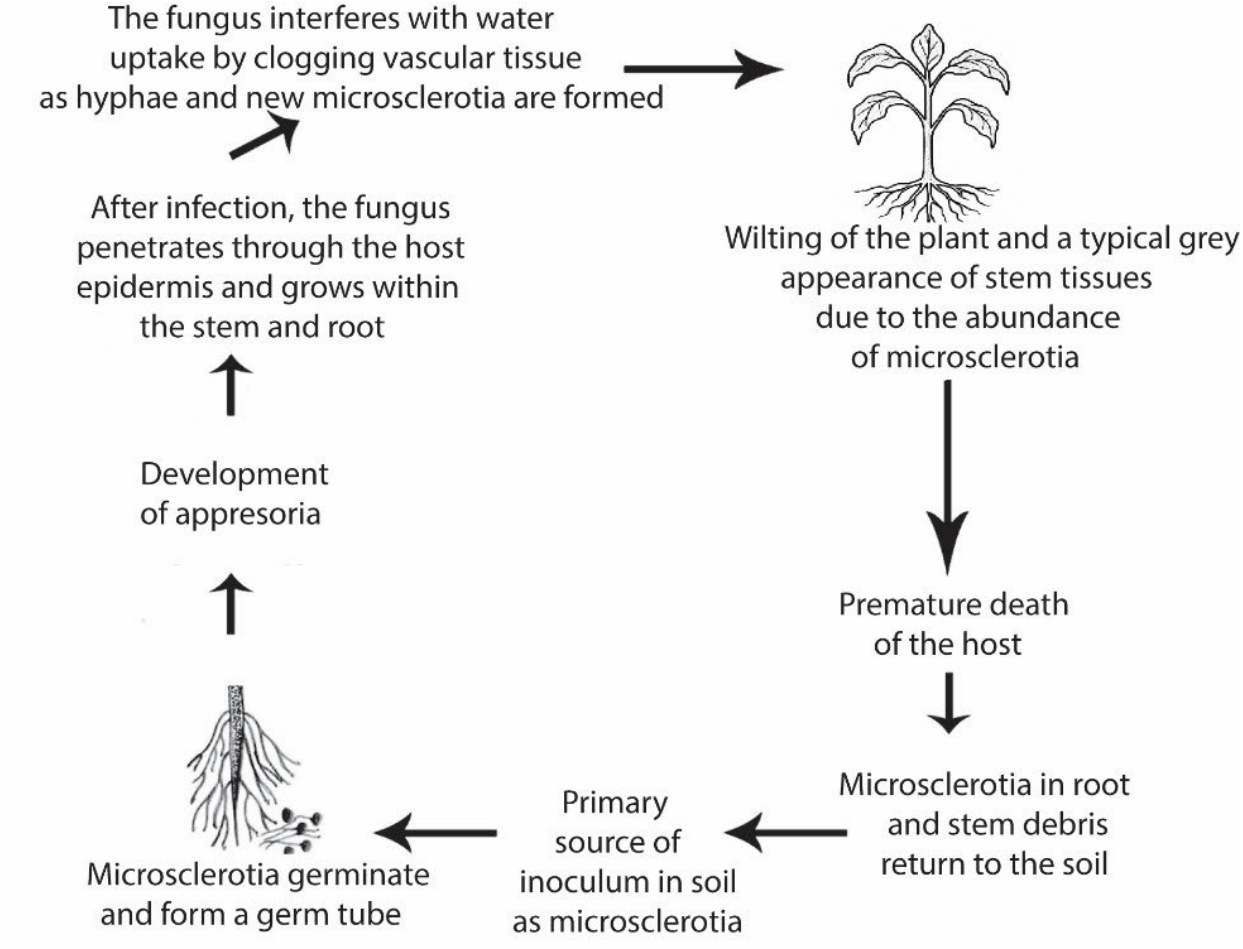

Fig. 10 Charcoal rot lifecycle of *Macrophomina phaseolina*. Redrawn from Smith et al. (2014).

important role in its survival (Dhingra & Sinclair 1978, Gupta et al. 2012, Romero Luna et al. 2017). Depending on the environmental conditions and on the constitution of the host tissues, the microsclerotia can survive for several years in the soil (Gupta et al. 2012). Temperatures between 25 and 35 °C are favourable to microsclerotia germination and disease development. The microsclerotia can infect seedlings and roots of both young and mature plants. During colonization, *Macrophomina* produces enzymes and toxins that degrade root tissue, and with the onset of infection, the root and stem tissue is colonized within 2-3 weeks, with abundant microsclerotia being produced in the colonized tissues (Romero Luna et a. 2017). *Macrophomina* species can survive not only in soil and crop debris for long periods (mostly through microsclerotia), but also in asymptomatic seeds as mycelium and in symptomatic seeds as microsclerotia (Dhingra & Sinclair, 1978, Machado et al. 2019).

Morphological-based identification: *Macrophomina* is readily recognized based on the presence of microsclerotia (Petrak 1923). Conidiomata are pycnidial, globose, thick-walled, variable in size, dark brown, mostly immersed to erumpent. Ostiole is central, unilocular and papillate. Conidiophores are absent. Conidiogenous cells are hyaline, lageniform to cylindrical, proliferating percurrently near the apex and covered with a mucous layer when young. Conidia are hyaline, ellipsoid to obovoid, truncate at base, rounded at apex and covered with a thin outer mucous sheath when young (type C according to Nag Raj (1993)). Mature conidia become septate, medium to dark-brown, without mucoid appendages. Sclerotia are composed of dark-brown to black thick-walled cells that are irregular in shape and variable in size (Sutton, 1980, Saar et al. 2014, Zhao et al. 2019, Machado et al. 2019, Poudel et al. 2021, Moslemi et al. 2023).

Molecular-based identification: The identification of *Macrophomina* species based on morphology is difficult due to the largely overlapping of morphological features between the species (Machado et al. 2019). However, only the ITS region should not be used due to its low resolution to distinguish *Macrophomina* species (Machado et al. 2019, Poudel et al. 2021). The concatenation of multiple loci has been widely used for recent taxonomic studies of *Macrophomina* species. Most studies were based on *act*, *cal*, ITS, *tef*, and *tub2* loci (Sarr et al. 2014, Machado et al. 2019, Zhao et al. 2019, Poudel et al. 2021). This study provides an updated phylogeny of *Macrophomina* based on combined ITS, *tef*, *tub2*, *act* and *cal* sequence data (Fig. 11, Table 6).

Recommended genetic markers (genus level): ITS

Recommended genetic markers (species level): ITS, *tef*, *tub2*, *act* and *cal*

Accepted number of species: five

References: Huda-Shakirah et al. (2019), Zhao et al. (2019), Machado et al. (2019), Nouri et al. (2020), Poudel et al. (2021) (morphology, phylogeny and accepted species numbers).

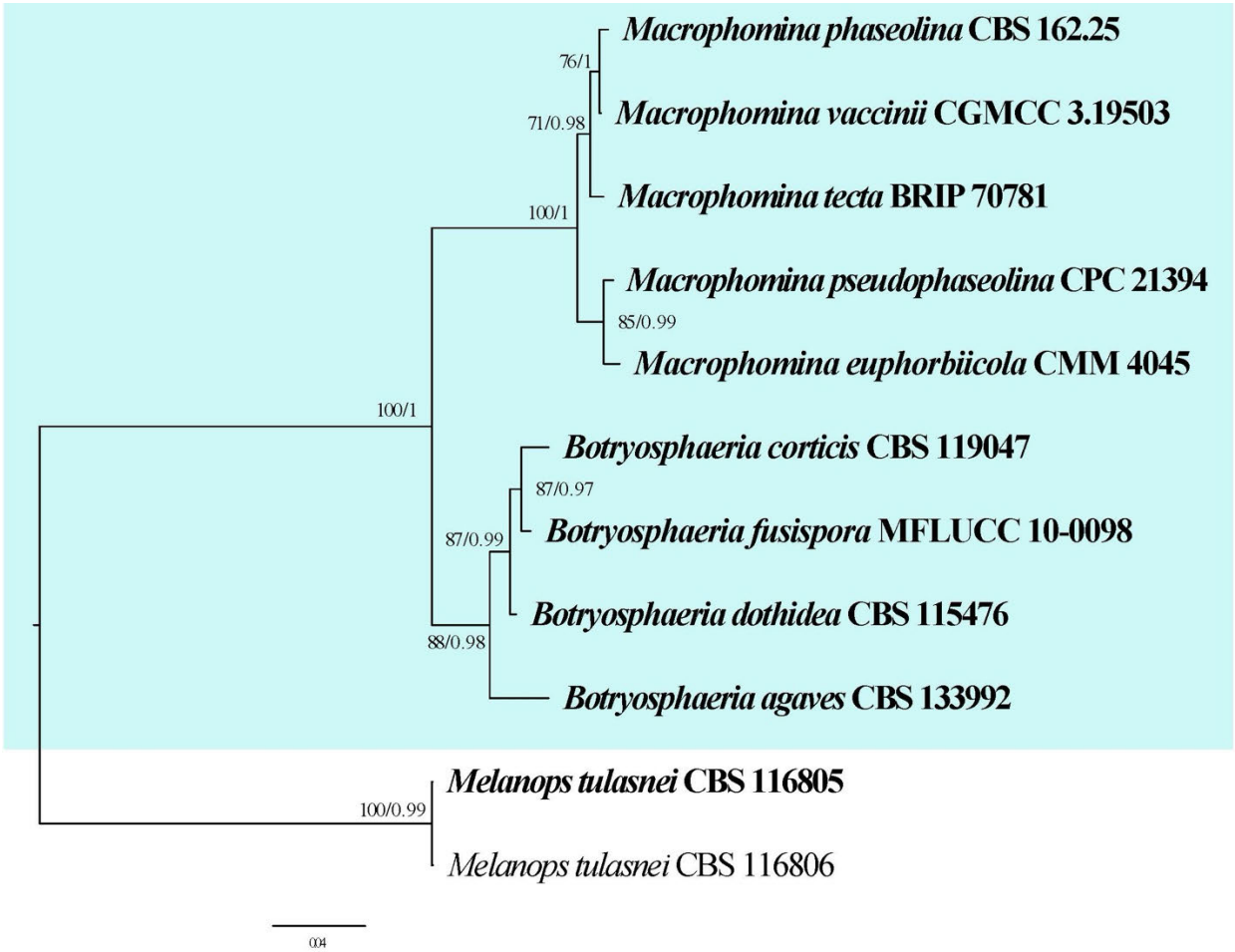

Fig. 11 Maximum likelihood tree of *Macrophomina* species based on the concatenated ITS, *tef*, *tub2*, *act* and *cal* sequence data. The best scoring RAxML tree had a final likelihood value of -4916.432. The tree was rooted with *Melanops tulasnei* (CBS 116805 and CBS 116806). Estimated base frequencies were as follows: A = 0.202, C = 0.317, G = 0.255, T = 0.225; substitution rates AC = 1.00000, AG = 3.15050, AT = 1.00000, CG = 1.00000, CT = 5.38755, GT = 1.000000. ML bootstrap support values over 70% and Bayesian posterior probabilities (BPP) greater than 0.95 are indicated. Type strains are in bold. Scale bar indicates the number of substitutions per site. Hyphens (-) represent support values less than BS 70%/BPP 0.95.

Table 6 DNA barcodes for accepted species of *Macrophomina*.

Species	Strain	GenBank accession numbers				
		ITS	*tef*	*tub2*	*act*	*cal*
Macrophomina euphorbiicola#	**CMM 4045**	**KU058928**	**KU058898**	**MF457657**	**MF457654**	**MF457660**
M. phaseolina#	**CBS 162.25**	**KF531826**	**KF951996**	**KF531805**	**KF951803**	**N/A**
M. pseudophaseolina#	**CPC 21394**	**KF951786**	**KF952148**	**KF952228**	**KF951913**	**N/A**
M. tecta	**BRIP 70781**	**MW591684**	**MW592271**	**MW592300**	**MW592058**	**MW592138**
M. vaccinii#	**CGMCC 3.19503**	**MK687450**	**MK687426**	**MK687434**	**MK687442**	**N/A**

Ex-type/ex-epitype/ex-neotype/ex-lectotype strains and voucher strains are in bold. Sequences that are not available are represented by N/A. Species confirmed with pathogenicity studies are marked with #.

131. *Melampsora* Castagne, Observ. Uréd. 2: 18 (1843)

Type species: *Melampsora euphorbiae* (Ficinus & C. Schub.) Castagne

Classification: *Pucciniomycetes*, *Pucciniales*, *Melampsoraceae*

Background: *Melampsora* is a genus of plant pathogenic rust fungi belonging to *Basidiomycota*. The genus was established by Castagne (1843) with *Me. euphorbiae* as the type species causing rust on *Euphorbia* sp. *Melampsora* is characterised by the formation of sessile and unicellular teliospores which are united laterally and form crusts or columns on the host. The genus is an obligate biotrophic parasite that contains about 100 species with most of them

being heteroecious. Members of this genus infect a variety of host plants including agricultural and non-agricultural crops. Poplar leaf rusts caused by various species of *Melampsora* including *Me. larcici-populina*, *Me. medusa* and *Me. occidentalis* are important tree diseases. Linin flax rust, *Melampsora lini* (Ehrenb.) Lév., is the most important pathogen of cultivated *Linum usitatissimum*.

Distribution: Algeria, Argentina, Canada, China, Colorado, France, Germany, Greenland, India, Iran, Japan, Mongolia, Morocco, Mozambique, Nepal, New Zealand, Pakistan, Russia, Shanxi, Siberia, Spain, Sri Lanka, Tibet, USA, Uzbekistan and Venezuela (Farr & Rossman 2025).

Hosts: *Abies, Acalypha, Aleurites, Chelidonium*, *Chosenia, Corydalis, Euphorbia, Hypericum, Hypericum, Larix, Lobelia, Mercurialis, Pinus, Piscaria, Polygala, Populus, Ribes, Salix, Saxifraga, Serissa, Stellera, Stereospermum, Vernonia* and *Wikstroemia* (Farr & Rossman 2025).

Disease symptoms: *Melampsora* species produce yellow leaf spots, which eventually become necrotic (Fig. 12). The common rust symptoms appear as orange spore-producing structures (uredinia) on the underside of host leaves. On alternate hosts (conifers), after sporulation *Melampsora* species cause shrinkage and finally death of infected needles. Yellow aecia of these rust fungi are sometimes visible on cones of the alternate hosts (Cummins1959, Cummins & Hiratsuka 2003).

Fig. 12 *Melampsora* on *Euphorbia* sp. a Infection of rust on leaves. b Uredinia. c Telia (tiny black dots). This picture is copyright of Ajay Kumar Gautam, Shubhi Avasthi and Rajnish Kumar Verma.

Pathogen biology, disease cycle and epidemiology: *Melampsora* species enter the host surface either through stomatal openings or by direct penetration through epidermal cells. After entry, the pathogen forms primary and secondary mycelium intercellularly for the establishment and giving rise to haustoria. *Melampsora* spp. often form a crust-like brown membrane compacted into flat, dark-coloured groups of single-celled sessile teliospores below the cuticle or epidermis of the host plant. *Melampsora* species are often heteroecious requiring two unrelated host plants or complete their life cycle on the one host (autoecious). They may produce five different spore types (macrocyclic) which reflects the complexity of these fungi. In several *Melampsora* species, however, only uredinial and telial stages have been described. Over half of the described species of *Melampsora* are known on *Salix* (willow) and *Populus* (poplar). None of the species of *Salix* in the world are entirely free of rust infection. For heteroecious species, the alternate hosts include conifers (*Tsuga, Abies, Larix* and *Ribes* spp.) (Sinclair 1987, Pei et al. 1993).

Morphological-based identification: The identification of *Melampsora* rust fungi is mainly based on their morphology, alternate hosts, and telial host range. The identification is also based on the position of uredinia and telia on leaves of host plants, the thickness of spore walls along with morphology of uredinial paraphyses. *Melampsora* produces intercellular, septate, branched, dikaryotic, and subepidermal mycelium within the parenchymatous tissues of the host. Spermogonia

are of Group I (type 3 subcuticular; or type 2, subepidermal), flask-shaped, pale yellow, containing paraphyses and minute, oval to globose spermatia. Aecia are orange-yellow, scattered on the undersurface of the leaves or sometimes on the stem, subepidermal, erumpent, and of *Caeoma*–type (some species have peridial cells adherent to the host epidermis). Aeciospores are polygonal in shape, echinulate, or verrucose with rod-like columns or blocks. Uredinia are subepidermal, erumpent and *Uredo*-type occur on both surfaces of leaves. They are bright yellow or orange initially and fade to nearly colourless with the progress of the disease. Capitate paraphyses are found abundantly in uredinia. Urediniospores are orange in colour, echinulate, with colourless walls, borne singly on pedicels and intermixed with capitate paraphyses. The pores of these spores may be scattered or bizonate, and obscure. Telia are reddish brown, elongated, subepidermal or relatively subcuticular, and remain covered, forming adherent crusts of 1 spore deep on the stem. The 1-celled sessile teliospores have a single germ pore and a brown wall. *Melampsora* species form external basidia (Cummins & Hiratsuka 2003, Ebinghaus et al. 2020).

Molecular-based identification: Maier et al. (2003) analysed LSU sequence data of *Melampsora* and placed it in a basal position of the *Pucciniales* (*Uredinales*). This DNA sequence-based systematic placement of this genus also supported its proposal to be ancestral (Durrieu 1980). However, based on SSU sequence data, Wingfield et al. (2004) proposed *Racospermyces* (*Endoraecium*) in the basal-most position and *Melampsora* in a derived lineage. Pei et al. (2005) generated LSU and ITS sequences of 11 species of *Melampsora* from *Salix* sp. and *Populus* sp. and Aime et al. (2006) examined two nuclear rDNA genes (18S and 28S) from field or herbarium specimens and DNA sequences from GenBank. They included two *Melampsora* species (*Me. epitea* Thüm. and *Me. euphorbiae* Castagne) in their study along with other rust fungi. Similarly, based on morphological characteristics and the ITS sequence data, a new species of *Melampsora* (*Me. iranica*) was reported on *Salix elbursensis* in the northwest of Iran (Damadi et al. 2011). Using ITS-2 and large ribosomal subunit RNA gene (LSU) regions, Busby et al. (2012) identified *Me. columbiana* on two species of *Populus* from North America. The molecular analyses using rDNA sequence information of two heteroecious rust species, *Me. chelidonii-pierotii* and *Me. yezoensis,* which parasitize *Salix* spp. and members of *Papaveraceae* revealed their phylogenetic similarity, although they have different survival strategies (Shinyama and Yamaoka 2012). Fifteen *Melampsora* spp. were examined phylogenetically using six nuclear and mitochondrial loci by Vialle et al. (2013). They observed that only three lineages fitted exactly defined morphological species, whereas, 12 were concordant with host specialization. Zhao et al. (2015a, b) studied *Melampsora* species on willows in China, and two new species and one new record of *Melampsora* were identified. The internal transcribed spacer (ITS1 and ITS2) region and LSU sequences were used in molecular phylogeny along with morphological characteristics to identify these fungi. In a similar study of *Melampsora* species on willows, one new species (*Melampsora salicis-reinii*) and two new records (*Me. ribesii-viminalis* and *Me. ribesii-purpureae*) were identified from Japan based on morphological and molecular phylogenetic studies using ITS region (Zhao et al. 2015c). Ali et al. (2016) re-examined *Melampsora euphorbiae*, *Me. euphorbiae-gerardianae* and *Me. helioscopiae* reported previously on *Euphorbia helioscopia* in Pakistan and described a new species, *Me. pakistanica*. Yun et al. (2016) reported *Me. yezoensis* as a new rust species on *Salix koreensis* based on morphology and molecular data of the ITS region. Based on analysis of sequences of ITS region and LSU (D1/D2) along with morphological characters, Zheng et al. (2019) reported a North American poplar leaf rust species, *Me. medusae*, in China. Aime & McTaggart (2020) included two species of *Melampsora* (*Me. euphorbiae* and *Me. laricis-populina*) in their study to provide a higher-rank classification for *Pucciniales*. Based on a combined LSU and ITS dataset for 25 rust genera, including 12 species of *Melampsora,* a phylogenetic analysis of Indian *Pucciniales* was carried out by Gautam et al. (2021) which provided a better understanding of their phylogeny and evolution. This study provides an updated phylogeny of *Melampsora* based on combined LSU and ITS sequence data (Fig. 13, Table 7).

Recommended genetic marker (genus level): ITS, LSU

Recommended genetic marker (species level): ITS, LSU

Accepted number of species: 100

References: Cummins (1959), Sinclair (1987), Pei et al. (1993), Cummins & Hiratsuka (2003), Pei et al. (2005), Aime (2006), Aime et al. (2006), Feau et al. (2009), Damadi et al. (2011), Busby et al. (2012), Shinyama & Yamaoka (2012), Vialle et al. (2013), Padamsee & McKenzie (2014), Toome & Aime (2015), Ali et al. (2016), Giordano et al. (2019), Aime & McTaggart (2020) (morphology and phylogeny)

Table 7 DNA barcodes for accepted species of *Melampsora*.

Species	Strain	GenBank accession numbers	
		ITS	LSU
Melampsora abietis-populi	**HMAS 247978**	**MK028579**	**MK064529**
Me. allii-populina	DAOM216857	JN881728	JN934902
Me. amygdalinae	N/A	AY444776	AY444782
Me. babylonicae	**HGUP21117**	**OR462100**	**OR462105**
Me. bigelowii	**1268MEB-SAN-SKA.1**	**GQ479205**	**GQ479205**
Me. × columbiana	**sn-35**	**JQ042235**	**JQ042235**
Me. caprearum	N/A	AY444779	AY444781
Me. chelidonii-pierotii	N/A	AB646769	N/A
Me. coleosporioides	N/A	AY652948	AY652951
Me. danbaensis	**HMAS353134**	**PP852474**	**PP852478**
Me. epitea	**TNS-F-121034**	**KX386070**	**KX386097**
Me. euphorbiae	**BPI 863501**	**N/A**	**DQ437504**

Me. ferrinii	PUR N6740	N/A	NG_060305
Me. hypericorum	PDD 97325	N/A	KJ716353
Me. hyperici-pseudohenryi	**HMAS353133**	**PP852476**	**PP852480**
Me. hyperici-sampsonii	**HMAS350001**	**MK518877**	**MK518547**
Me. iranica	SMD-2008 IRANSIF	FJ386431	FJ386431
Me. laricis-pentandrae	N/A	AY444771	AY444783
Me. laricis-populina	HMAS 247976	MK028584	MK028584
Me. laricis-miyabeana	**HMAS 247980**	**N/A**	**MK064532**
Me. × *medusae-populina*	97G13	AY375276	AY375276
Me. microspora	**BA13c**	**N/A**	**KX237556**
Me. paradoxa	**1273MEP-SAY-USA.1**	**GQ479273**	**GQ479273**
Me. populnea	N/A	AY444772	AY444786
Me. pruinosae	HMAS 247982	MK028585	MK064533
Me. salicis-albae	N/A	AY444775	AY444788
Me. salicis-argyraceae	**HMAAC4051**	**N/A**	**MK372204**
Me. salicis-cavaleriei	**HMAAC4044**	**MK277297**	**MK277302**
Me. salicis-michelsonii	**HMAAC4039**	**MK277293**	**MK277298**
Me. salicis-sinicae	HMAAC4085	MK372181	MK372214
Me. yezoensis	**DUCC509**	**KT199021**	**N/A**
Me. yoshinagae	**Am111**	**N/A**	**MT636462**

Ex-type/ex-epitype/ex-neotype/ex-lectotype strains and voucher strains are in bold. Sequences that are not available are represented by N/A.

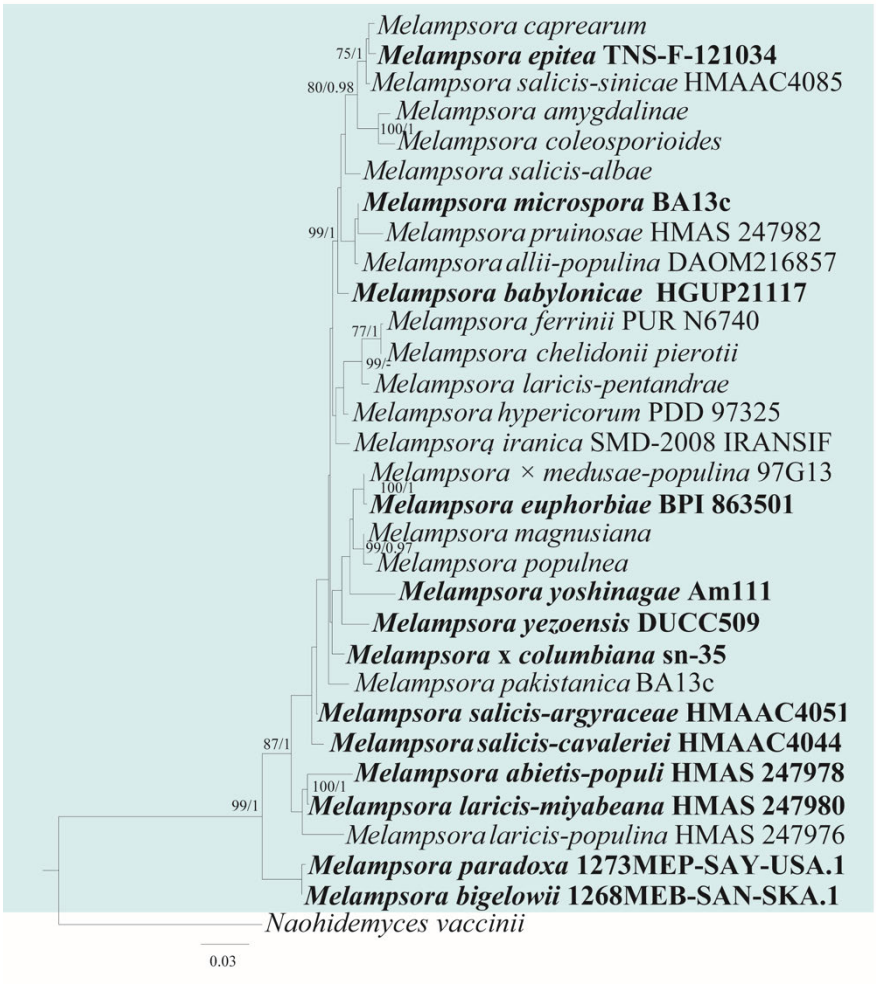

Fig. 13 Maximum likelihood tree of *Melampsora* species based on the concatenated LSU and ITS sequence data. The best scoring RAxML tree had a final likelihood value of -5783.292563. The tree was rooted to *Naohidemyces vaccini.* Estimated base frequencies were as follows: A =0.300219, C =0.176250, G =0.227689, and T =0.295842; substitution rates AC =1.261606, AG =1.929654, AT =0.708137, CG =0.305156, CT =2.230781, and GT = 1.000000. ML bootstrap support values over 70% and Bayesian posterior probabilities (BPP) greater than 0.95 are indicated. Type strains are in bold. Scale bar indicates the number of substitutions per site. Hyphens (-) represent support values less than BS 70%/BPP 0.95.

132. *Myrothecium* Tode, Fungi Mecklenburgenses Selecti 1: 25 (1790)

Type species: *Myrothecium inundatum* Tode.

Classification: *Sordariomycetes*, *Hypocreales*, *Stachybotryaceae*

Background: *Myrothecium* was introduced by Tode (1790). *Myrothecium sensu lato* encompasses approximately 18 genera, all grouped within *Stachybotryaceae* (Lombard et al. 2016, Liang et al. 2019). Many species are recognized for their significant biological activities (Brian et al 1948, Lee et al. 2008, Ruma et al. 2015). Although several *Myrothecium* species are considered weak or opportunistic plant pathogens, species such as *Albifimbria verrucaria* (synonym *Myrothecium verrucaria*) and *Paramyrothecium roridum* (synonym *My. roridum*) have been studied more in depth due to their aggressive pathogenicity on a wide range of plant hosts (Han et al. 2014, Ben et al. 2016, Weaver et al. 2021). *Myrothecium* have also been reported as saprobes and endophytes from different substrates and ecosystems, including soil, decaying plant matter, and living plant tissues (Ahrazem et al. 2000, Quezado Duval et al. 2010, Chen et al. 2016). Despite numerous studies, the taxonomy of many taxa within the genus remains unresolved, and further molecular and morphological studies are necessary to clarify their classification.

Distribution: worldwide (Farr & Rossman 2025)

Disease symptoms: *Myrothecium* species are opportunistic fungal pathogens that infect a wide range of plants, causing leaf spots, stem cankers, fruit rots, and seedling damping-off (Maji 2013, Chen et al. 2016, Fujinawa et al. 2016, Lombard et al. 2016). Infections usually appear as small, circular to irregular brown or tan necrotic spots with dark, well-defined margins on leaves. These lesions may expand, coalesce, and cause extensive blight (Lombard et al. 2016). *Myrothecium* can cause elongated, sunken, dark lesions or cankers on stems and petioles that may crack or become soft and water-soaked. Seedlings infected by *Myrothecium* spp. may suffer from pre- or post-emergence damping-off, showing basal stem rot and eventual seedling collapse (Maji 2013, Chen et al. 2016, Fujinawa et al. 2016).

Hosts: *Chrysanthemum* spp., cotton (*Gossypium hirsutum*), cucumber (*Cucumis sativus*), gerbera (*Gerbera jamesonii*), pepper (*Capsicum spp.*), poinsettia (*Euphorbia pulcherrima*), soybean (*Glycine max*), tomato (*Solanum lycopersicum*), and watermelon (*Citrullus lanatus*) (Farr & Rossman 2025).

Pathogen biology, disease cycle and epidemiology: *Myrothecium* thrives in warm, humid environments and has a broad host range, infecting vegetables, ornamentals, and field crops (Maji 2013, Chen et al. 2016, Fujinawa et al. 2016, Lombard et al. 2016). The disease cycle begins with the overwintering of *Myrothecium* in plant debris, soil, or on infected seeds (Nguyen et al. 1973, van Bruggen et al. 2016). Under favourable environmental conditions, particularly high humidity and warm temperatures, conidia germinate and infect host plants. Initial infection is often localized but can spread rapidly in moist environments. *Myrothecium* penetrates through wounds or weakened tissue, leading to leaf spots, stem lesions, and in severe cases, plant wilting and dieback. Secondary spread occurs via water splash, wind-driven rain, and mechanical transmission (Nguyen et al. 1973, van Bruggen et al. 2016).

Morphological-based identification: The generic concept of *Myrothecium* has undergone several emendations over time (Link 1809, von Höhnel 1905, Pidoplichko & Kirilenko 1971, Lombard et al. 2016). *Myrothecium sensu stricto* includes species with cup-shaped sporodochia, which are often covered with slimy masses of green to black conidia (Tode 1790, Chen et al. 2016, Lombard et al. 2016, Fig. 14). These sporodochia may be scattered or aggregated. The conidiophores are short and often branched, bearing phialidic conidiogenous cells that produce conidia in a slimy matrix. The conidia are usually cylindrical to ellipsoidal, smooth or roughened, and vary from hyaline to dark green or black. These morphological traits were previously used to distinguish *Myrothecium* from morphologically similar genera (Link 1809, von Höhnel 1905, Pidoplichko & Kirilenko 1971). However, due to overlapping morphology, molecular data are needed for species identification.

Molecular-based identification: There have been relatively few comprehensive phylogenetic studies focused on *Myrothecium* due to the lack of multi-loci data for a number of species (Ruiz et al. 2008, Alves et al. 2010, Jiang et al. 2014, 2017, Wu et al. 2014b). This underscores the need for extensive molecular studies incorporating broader taxon sampling, to clarify the evolutionary relationships and classification within this genus. Decock et al. (2008) used ITS sequence data to distinguish *Septomyrothecium* from *Myrothecium*, and their results indicated that *Myrothecium* is paraphyletic. Chen et al. (2015) re-evaluated the phylogeny of *Myrothecium* based on ITS and *tef* sequences, suggesting the polyphyly of *Myrothecium* within *Stachybotryaceae*. Lombard et al. (2016) resolved *Myrothecium sensu lato* to 18 genera and confirmed the placement of two species in *Myrothecium* and excluded 12 species previously identified as *Myrothecium*. This study provides an updated phylogeny of *Myrothecium* and related genera in *Stachybotryaceae* based on multi-loci sequence data (ITS, LSU, *rpb2, tef*, *tub2* and *cal*) (Fig. 15, Table 8). We included *Myrothecium* species that have multi-locus data to determine their phylogenetic placement. We propose the new combinations *Digitiseta chiangmaiensis* and *Myxospora thailandica* (Fig. 15 and S1).

***Digitiseta chiangmaiensis* (D.Q. Dai & K.D. Hyde) Bhunjun, Phukhams. & K.D. Hyde, comb. nov.**

Index Fungorum number: IF905055; **Facesoffungi number:** FoF 19467

Synonym: *Myrothecium chiangmaiense* D.Q. Dai & K.D. Hyde, in Dai et al., Fungal Diversity 82: 49 (2016)

Description: See Dai et al. (2017)

Notes: *Digitiseta chiangmaiensis* was described as *Myrothecium chiangmaiense* from dead culms of bamboo in Thailand (Dai et al. 2017). In the analyses of combined ITS, LSU, *rpb2, tef*, *tub2* and *cal* sequence data of *Stachybotryaceae*, the strain (MFLUCC 11–0506) clustered with *Digitiseta multidigitata* (MUCL 41187). Therefore, we transfer *Myrothecium chiangmaiense* to *Digitiseta* (Fig. 15 and S1).

***Myxospora thailandica* (D.Q. Dai & K.D. Hyde) Bhunjun, Phukhams. & K.D. Hyde, comb. nov.**

Index Fungorum number: IF905056; **Facesoffungi number:** FoF 19466

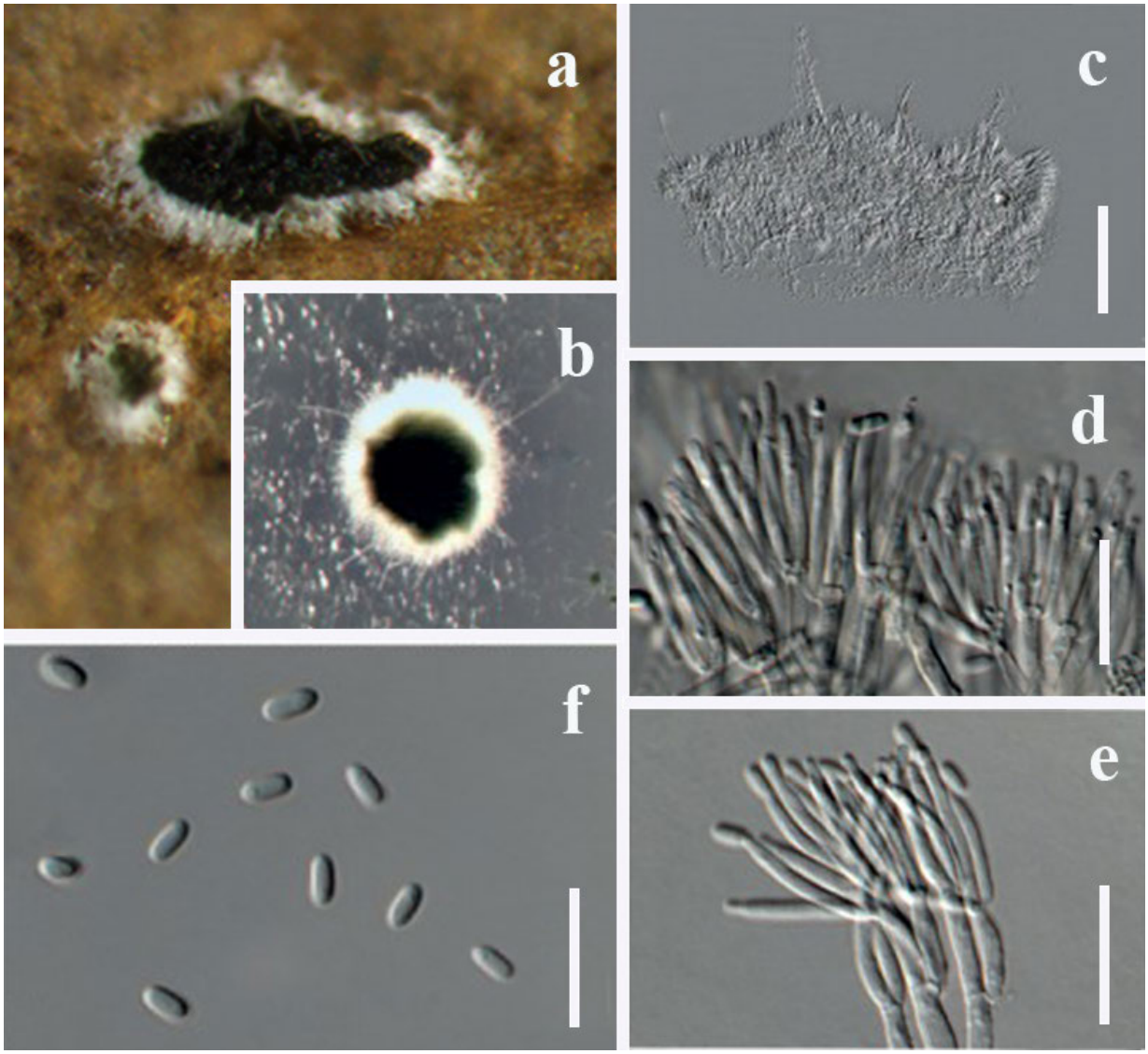

Fig. 14 *Myrothecium* sp. a-b Conidiomata. c Sporodochia. d-e Conidiogenous cells. f Conidia. Scale bar: c = 100 µm, d-f = 10 µm. This picture is copyright of Pedro Crous (Lombard et al. 2016).

Table 8 DNA barcodes for accepted species of *Myrothecium*.

Species	Strain	GenBank accession number					
		ITS	LSU	*rpb2*	*tef*	*tub2*	*cal*
Myrothecium inundatum	**CBS 275.48**	**KU846452**	**KU846474**	**N/A**	**KU846514**	**KU846533**	**KU846435**
My. inundatum	CBS 196.74	KU846451	KU846473	N/A	KU846513	KU846532	KU846434
My. inundatum	CBS 120646	KU846455	KU846477	N/A	KU846516	KU846536	KU846438
My. simplex	**CBS 582.93**	**KU846456**	**KU846478**	**N/A**	**KU846517**	**KU846537**	**KU846439**

Ex-type/ex-epitype/ex-neotype/ex-lectotype strains and voucher strains are in bold. Sequences that are not available are represented by N/A.

Synonym: *Myrothecium thailandicum* D.Q. Dai & K.D. Hyde, in Dai et al., Fungal Diversity 82: 49 (2016)

Description: See Dai et al. (2017)

Notes: *Myxospora thailandica* was described as *Myrothecium thailandicum* from dead culms of bamboo in Thailand (Dai et al. 2017). In the analyses of combined ITS, LSU, *rpb2, tef*, *tub2* and *cal* sequence data of *Stachybotryaceae*, the strain (MFLUCC 11-0395) clustered with *Myxospora crassiseta* (CBS 731.83). Therefore, we transfer *Myrothecium thailandicum* to *Myxospora* (Fig. 15 and S1).

Recommended genetic markers (genus level): ITS

Recommended genetic markers (species level): ITS, LSU, *rpb2, tef*, *tub2* and *cal*

Accepted number of species: two

References: Crous et al (2014), Fujinawa et al. (2016), Lombard et al. (2016) (morphology and phylogeny)

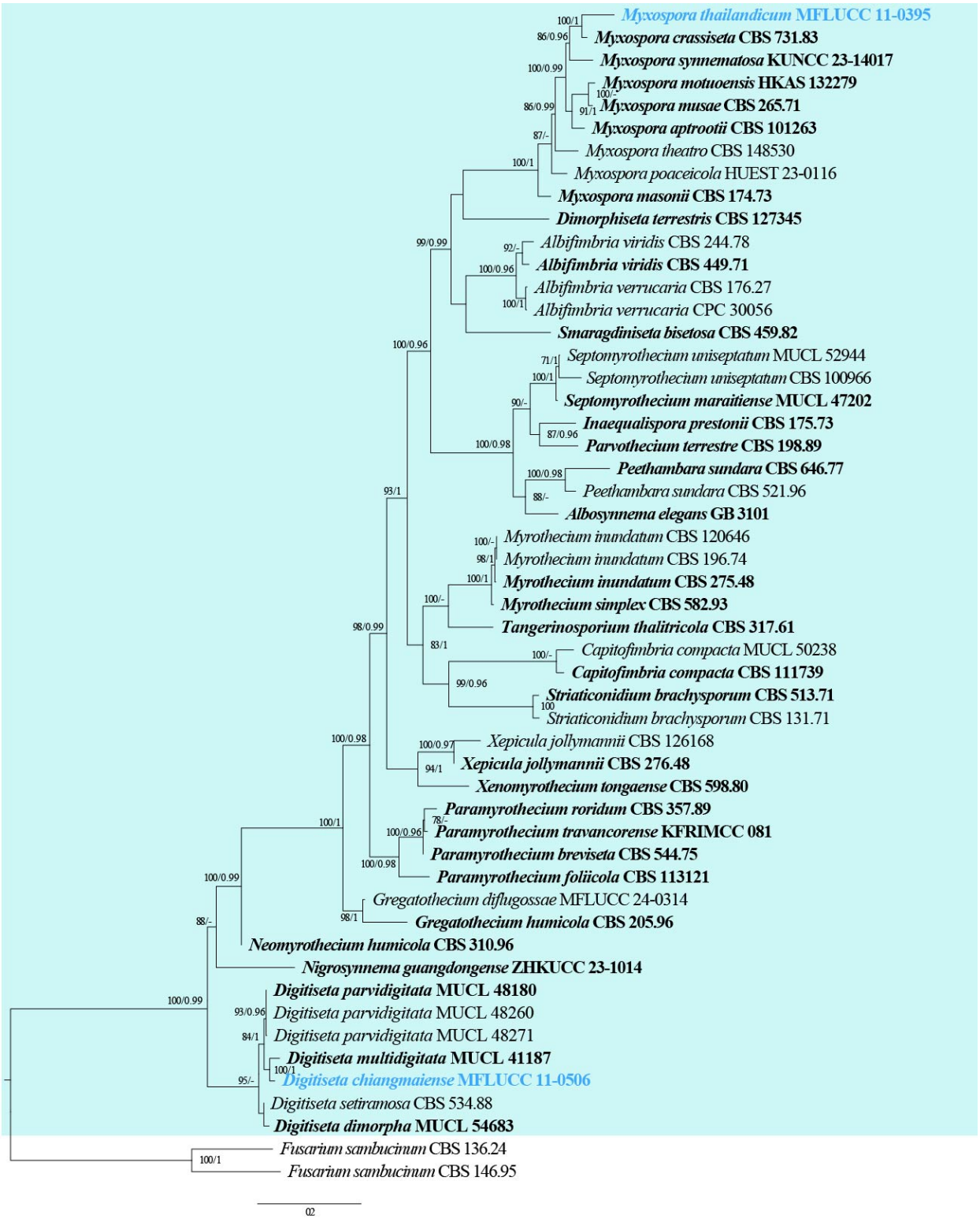

Fig. 15 Maximum likelihood tree of *Myrothecium* and related genera in *Stachybotryaceae* based on the concatenated ITS, LSU, *rpb2, tef*, *tub2* and *cal* sequence data. The best scoring RAxML tree had a final likelihood value of -39144.227. The tree was rooted with *Fusarium sambucinum* (CBS 146.95 and CBS 136.24). Estimated base frequencies were as follows: A = 0.237, C = 0.272, G = 0.269, T = 0.222, with substitution rates AC = 1.24675, AG = 2.95299, AT = 1.24675, CG = 1.00000, CT = 5.51631, GT = 1.000000. ML support values over 70% and Bayesian posterior probabilities (BPP) greater than 0.95 are indicated. Type strains are in bold. The new combinations are in blue. Scale bar indicates the number of substitutions per site. Hyphens (-) represent support values less than BS 70%/BPP 0.95.

133. *Neopseudocercosporella* Videira & Crous, Stud. Mycol. 83:80 (2016)

Type species: *Neopseudocercosporella capsellae* (Ellis & Everh.) Videira & Crous

Classification: *Dothideomycetes*, *Mycosphaerellales*, *Mycosphaerellaceae*

Background*: Neopseudocercosporella* is an important pathogen that affects economic crops worldwide. The genus was established by Videira et al. (2016). Both species *Neopseudocercosporella brassicae* and *N. capsellae* cause white leaf spot disease in plants in the family *Brassicaceae* (Videira et al. 2016, Gunasinghe et al. 2020, 2021). Videira et al. (2016) suggested that the two species could be synonymous despite having distinct disease symptoms, ascospore morphology and culture characteristics.

Distribution*:* worldwide (Farr & Rossman 2025), however, the disease is more destructive in Subtropical, Mediterranean, or Temperate climate regions with cool and wet climates

Disease symptoms: *Neopseudocercosporella* species are generally foliar pathogens that produce leaf lesions with necrosis or chlorosis, but can also produce stem, and pod lesions under favourable weather conditions (Petrie & Vanterpool 1978, Fig. 16). *Neopseudocercosporella capsellae* initially causes numerous brown elongated spots on mature lower leaves that later coalesce to form large irregularly shaped, white or pale beige lesions on *Brassica napus* (rapeseed) (Gunasinghe et al. 2020). As the crop matures, *P. capsellae* spreads to stems and pods to develop grey to black lesions. These lesions can expand rapidly to cover large areas with ash-depressed centres (Carmody 2017) or purple to grey-speckled areas (Petrie & Vanterpool 1978). The leaf disease symptoms can vary among other brassica hosts depending on the degree of waxiness of the leaf surface and may not resemble the white leaf spot lesions on rapeseed (Crossan 1954). For example, the disease symptoms can be round, semi-transparent larger lesions with brownish-grey centres with well-defined brown or tan margins on turnip and wild mustard and ashy black centred, rectangular or rounded lesions with well-defined margins on cabbage (Miller & McWhorter 1948).

Hosts: *Neopseudocercosporella capsellae* infects a range of cultivated crucifers including *Brassica napus* and *B. juncea* (Boerema & Verhoeven 1977, Gudelj et al. 2004, Murtza et al. 2021, Farr & Rossman 2025) with Chinese cabbage (*B. rapa* sub sp. *pekinensis*) and cauliflower (*B. oleracea*) recorded as common hosts (Lancaster 2006). *Neopseudocercosporella* species have also been isolated from the leaf lesions of a number of different 'wild' or 'weedy' crucifers such as *Capsella bursa-pastoris* (shepherd's purse), *Malcolmia africana* (African mustard) and *Raphanus raphanistrum* (white charlock) (Crossan 1954, Deighton 1973, Petrie & Vanterpool 1978, Föller & Paul 2002, Lancaster 2006).

Pathogen biology, disease cycle and epidemiology: *Neopseudocercosporella* is capable of completing its life cycle in an asexual or sexual stage (Petrie & Vanterpool 1978, Inman et al. 1991, Barbetti 2000, Fig. 17). In the sexual stage, the ascomata release ascospores which initiate the new disease cycle (Inman et al. 1991). During the asexual stage, the conidia initiate the new disease cycle and asexual resting structures (stromatic knots) are responsible for the survival of the pathogen between crops (Crossan 1954, Perron & Nourani 1990, Fitt et al. 2006).

Morphological-based identification: *Neopseudocercosporella* differs from the closely related genera *Fusoidiella* and *Filiella* which produce fusiform or acicular-filiform conidia, respectively, compared to the subcylindrical conidia of *Neopseudocercosporella* (Videira et al. 2016). *Apseudocercosporella* can be distinguished from *Neopseudocercosporella* by having slightly thickened and darkened conidial hila and conidiogenous cells (Braun 1995). The two *Neopseudocercosporella* species are distinguishable based on the morphology of ascospores and colony characteristics (Inman et al. 1991).

Molecular-based identification: Videira et al. (2016) established *Neopseudocercosporella* using LSU, ITS*, act, tef*, *his3*, *rpb2*, *cal* and *tub2* sequences. Although the two species have morphologically distinct features, Videira et al. (2016) suggested that these two species could be synonymous, considering the high similarity in molecular data. However, they are currently considered two distinct species, pending recollection of fresh material. As the members share high sequence similarity, a polyphasic approach is recommended for species-level identification (Videira et al. 2016, 2017). This study provides an updated phylogeny of *Neopseudocercosporella* based on combined LSU, ITS, *act*, *tef*, *rpb2*, *cal* and *tub2* sequence data (Fig. 18, Table 9).

Recommended genetic markers (genus level): LSU and ITS

Recommended genetic markers (species level): LSU, ITS, *act*, *tef*, *rpb2*, *cal* and *tub2*

Accepted number of species: two

References: Gunasinghe et al. (2016), Videira et al. (2016), (2017), Murtza et al. (2021) (morphology and phylogeny)

Table 9 DNA barcodes for accepted species of *Neopseudocercosporella.*

Species	Isolate	GenBank accession numbers						
		LSU	ITS	*act*	*tef*	*rpb2*	*cal*	*tub2*
***Neopseudocercosporella brassicae*#**	**CBS 228.32**	**KF251808**	**KF251304**	**KF253613**	**KF253252**	**KX348058**	**KF253967**	**KF252783**
N. brassicae	CBS 173.88	KX286991	KX287293	KX287582	KX287857	KX288447	N/A	N/A
N. brassicae	CBS 267.53	KF251809	KF251305	KF253614	KF253253	KX348059	KF253968	KF252784
***N. capsellae*#**	**CBS 135464**	**KX286992**	**DQ303091**	**KF253616**	**KX287858**	**KX288448**	**KF253970**	**KF252786**
N. capsellae	CPC 12518	KX286994	KX287295	KX287584	KX287860	KX288451	N/A	N/A
N. capsellae	CBS 112033	KF251810	KF251306	KF253615	KF253254	KX348061	KF253969	N/A

Ex-type/ex-epitype/ex-neotype/ex-lectotype strains and voucher strains are in bold. Sequences that are not available are represented by N/A. Species confirmed with pathogenicity studies are marked with #.

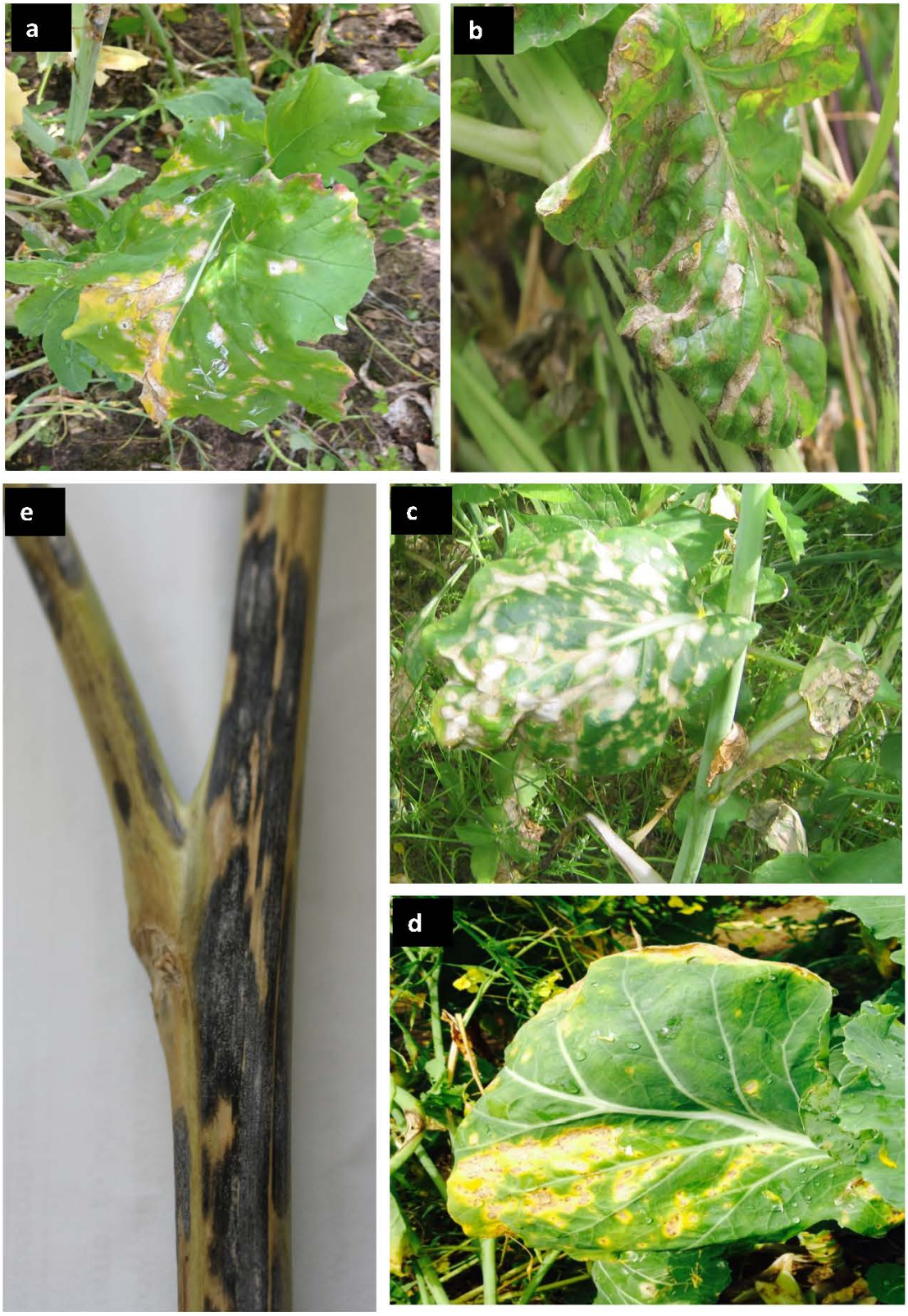

Fig. 16 White leaf spot symptoms caused by *Neopseudocercosporella capsellae* on different hosts: a Leaf lesions on *Brassica napus* (rapeseed), initially brown, elongated spots that later become white with the production of conidia. b Irregular, semi-transparent larger lesions with brownish-grey centres with well-defined brown or tan margins on *Raphanus sativus*. c Initially, brown to elongated spots that later become white cantered on *Brassica campestris* var. *chinensis* (Chinese cabbage). d Rectangular or rounded with well-defined margins with ashy brown or black centre on *Bressica oleracea* var. *capitata* (cabbage). e Stem lesions on *Brassica nigra* appearing as large black lesions with ash depressed centres. This picture is copyright of Niroshini Gunasinghe.

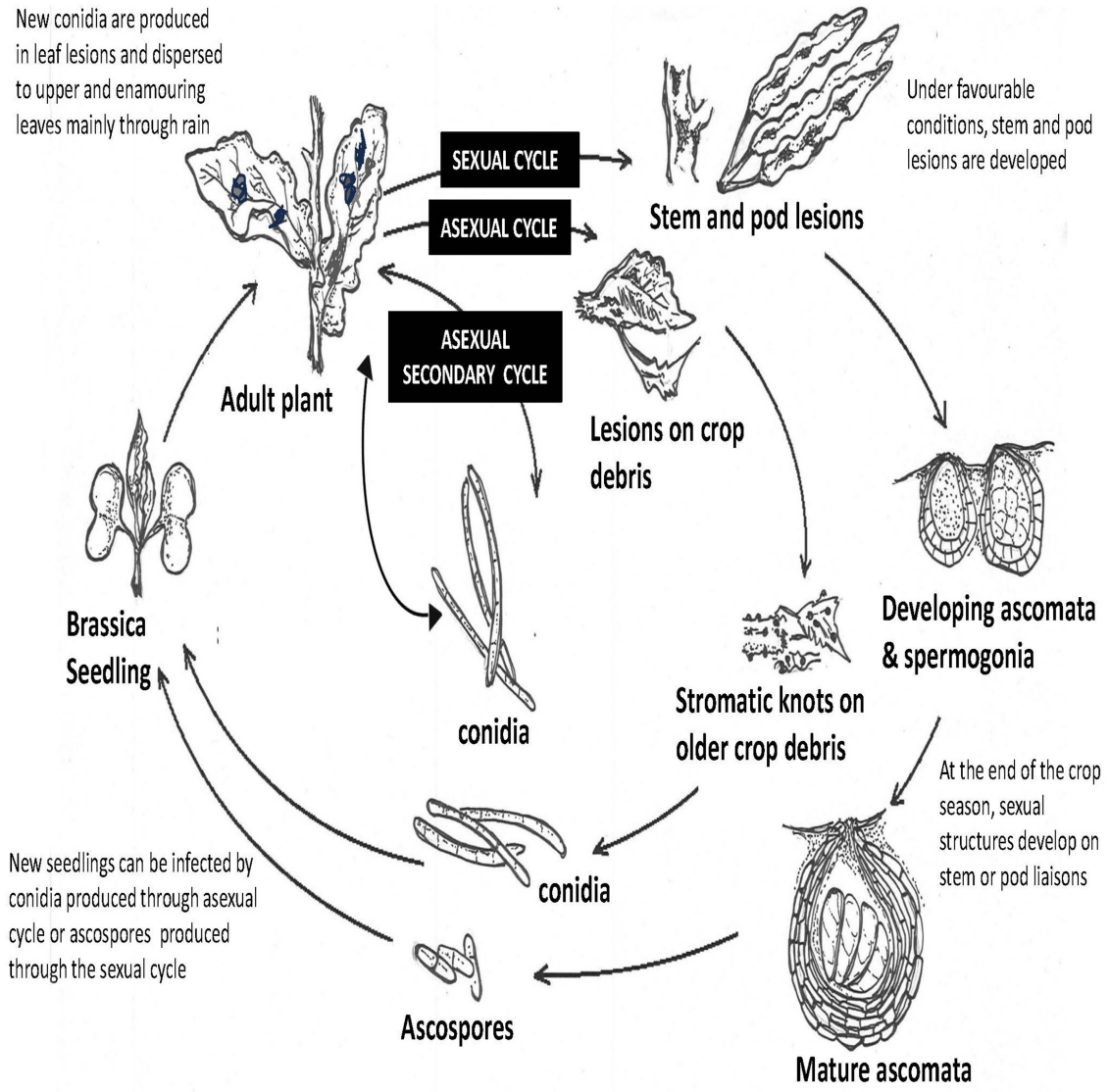

Fig. 17 Disease cycle of *Neopseudocercosporella* species. Redrawn from Gunasinghe et al. (2020).

134. *Neopestalotiopsis* Maharachch., K.D. Hyde & Crous, in Maharachchikumbura et al., Stud. Mycol. 79:135 (2014)

Type species: *Neopestalotiopsis protearum* (Crous & L. Swart) Maharachch.

Classification: *Sordariomycetes, Amphisphaeriales, Sporocadaceae*

Background: *Neopestalotiopsis* was introduced by Maharachchikumbura et al. (2014) to accommodate pestalotiopsis-like taxa that have versicolorous median cells and indistinct conidiophores. *Neopestalotiopsis* are primarily known as plant pathogens but have also been reported as saprobes and endophytes. *Neopestalotiopsis* species can cause leaf spots, fruit rot, and other plant diseases, affecting economically important crops such as tea, strawberry, and avocado (Espinoza et al. 2008, González et al. 2012, Chamorro et al. 2016, Sun et al. 2023). The species have also been associated with a wide variety of host plants across tropical and subtropical regions (Rodríguez-Gálvez et al. 2020, Diogo et al. 2021, Zhang et al. 2024).

Distribution: worldwide (Farr & Rossman 2025)

Disease symptoms: *Neopestalotiopsis* species are known to cause various diseases including canker, blight, dieback, fruit rots and leaf spot (Fig. 19). *Neopestalotiopsis* taxa have been reported as an important pathogen causing dieback, trunk diseases, leaf blights, leaf spot diseases, fruit rot, postharvest disease and severe defoliation of grapevine

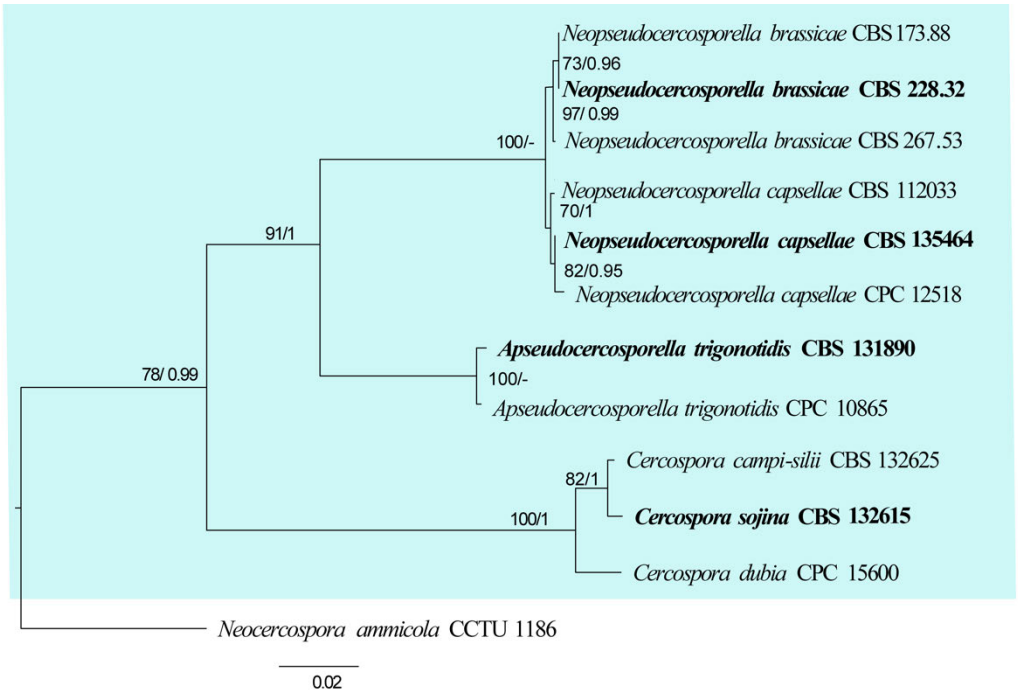

Fig. 18 Maximum likelihood tree of *Neopseudocercosporella* species based on the concatenated LSU, ITS, *act*, *tef*, *rpb2*, *cal* and *tub2* sequence data. The best scoring RAxML tree had a final likelihood value of -6877.382. The tree was rooted with *Neocercospora ammicola* (CCTU 1186). Estimated base frequencies were as follows: A = 0.239, C = 0.255, G = 0.287, and T = 0.219; substitution rates AC = 1.65698, AG = 2.88680, AT = 1.65698, CG = 1.00000, CT = 7.29436, and GT = 1.000000. ML bootstrap support values over 70% and Bayesian posterior probabilities (BPP) greater than 0.95 are indicated. Scale bar indicates the number of substitutions per site. Hyphens (-) represent support values less than BS 70%/BPP 0.95.

Fig. 19 Disease symptoms of: a *Neopestalotiopsis* sp. on *Smilax* sp. b *Neopestalotiopsis* sp. on *Ginkgo biloba.* c *Neopestalotiopsis rhapidis* on *Podocarpus macrophyllus.* d *Neopestalotiopsis* sp. on *Smilax scobinicaulis.* e *Neopestalotiopsis* sp. on *Syzygium samarangense.* f *Neopestalotiopsis amomi* on *Amomum villosum.* This picture is copyright of Yaru Sun.

cultivars (Jayawardena et al. 2015, 2016, Maharachchikumbura et al. 2017, Sun et al. 2023). As a result, they reduce the yield and quality of grapes, leading to the death of individual plants. *Neopestalotiopsis* have also been associated with stem blight, flower blight, twig dieback and fruit rots of a wide range of plants worldwide (Akinsanmi et al. 2016, Borrero et al. 2017, Mahapatra et al. 2018, Rodríguez-Gálvez et al. 2020, Zhang et al. 2024). *Neopestalotiopsis* species cause guava scab (Solarte et al. 2018), leaf spot on sweet potatoes (Maharachchikumbura et al. 2016), crown and root rot of strawberries, as well as canker and dieback on blueberries (Espinoza et al. 2008, González et al. 2012, Chamorro et al. 2016). *Neopestalotiopsis* also infects the leaves and fruits of strawberries, with the infection initially manifesting as circular, black, and slightly sunken spots that expand outwards on the surface (Ayoubi and Soleimani 2016). In fruit rots, the pathogen initially develops small, circular, black and slightly sunken spots on fruits that enlarge rapidly, becoming sunken and resulting in a soft decay of the fruit flesh (Maharachchikumbura et al. 2013a, b).

Hosts: *Neopestalotiopsis* have a wide host range including *Acacia mollissima*, *Achras sapota*, *Acrostichum aureum*, *Alpinia malaccensis*, *Annona squamosa*, *Ardisia crenata*, *Artocarpus heterophyllus*, *Bulbophyllum*, *Calliandra haematocephala*, *Camellia*, *Carya illinoinensis*, *Cinchona*, *Cissus*, *Citrus*, *Cocos nucifera*, *Crotalaria juncea*, *Elaeis guineensis*, *Elettaria cardamomum*, *Eriobotrya japonica*, *Eucalyptus*, *Ficus macrocarpa*, *Fragaria×ananassa*, *Garcinia mangostana*, *Hevea brasiliensis*, *Ilex chinensis*, *Ipomoea*, *Kadsura coccinea*, *Leucospermum cuneiforme*, *Ligustrum lucidum*, *Litsea rotundifolia*, *Macadamia*, *Machilus thunbergia*, *Mangifera indica*, *Magnolia*, *Malus*, *Musa*, *Nopalea cochenillifera*, *Neodypsis decaryi*, *Paeonia suffruticosa*, *Pandanus*, *Paphiopedilum micranthum*, *Phoenix dactylifera*, *Picea*, *Pinus brutia*, *Platanus orientalis*, *Prunus dulcis*, *Psidium*, *Pteridium*, *Punica granatum*, *Rosa*, *Quercus rubra*, *Rhizophora*, *Sonneratia alba*, *Sporobolus elongatus*, *Syzygium*, *Taxus chinensis*, *Telopea*, *Thuja occidentalis*, *Vaccinium* and *Vitis* (Farr & Rossman 2025).

Pathogen biology, disease cycle and epidemiology: *Neopestalotiopsis* species are opportunistic pathogens that primarily infect plants through wounds or natural openings, often under conditions of plant stress or environmental imbalance (Belisário et al. 2020, Diogo et al. 2021). The disease cycle typically begins with conidia landing on the surface of a susceptible host, where they germinate and penetrate plant tissues, leading to symptoms such as leaf spots, fruit rot, stem cankers, or dieback (Belisário et al. 2020). Under favourable conditions, *Neopestalotiopsis* rapidly colonizes plant tissue, producing new conidia on acervuli that emerge on infected surfaces. These spores are then dispersed by wind, rain splash or insects, facilitating secondary infections throughout the growing season (Diogo et al. 2021). The pathogen can persist in plant debris or soil, serving as a source of primary inoculum in subsequent seasons.

Morphological-based identification: *Neopestalotiopsis* species can be differentiated from other pestalotioid taxa by using morphology and molecular data (Maharachchikumbura et al. 2014b). *Neopestalotiopsis* species differ from *Pestalotiopsis* and *Pseudopestalotiopsis* in having versicolorous median cells whereas both *Pestalotiopsis* and *Pseudopestalotiopsis* have concolourous median cells (Maharachchikumbura et al. 2014b). However, using morphological characters to delimitate species is problematic as the morphological characters are plastic and vary between hosts and environments (Maharachchikumbura et al. 2011, 2016). Therefore, molecular data is important to identify different pestalotioid species (Maharachchikumbura et al. 2016, 2021).

Molecular-based identification: *Neopestalotiopsis* is closely related to *Pestalotiopsis* and *Pseudopestalotiopsis*. *Neopestalotiopsis* species can be roughly separated from *Pestalotiopsis* and *Pseudopestalotiopsis* based on base pair difference in the ITS region (Maharachchikumbura et al. 2014b). It is recommended to use ITS, *tub2* and *tef* genes to provide a better resolution in phylogenetic analyses. This study provides an updated phylogeny of *Neopestalotiopsis* based on combined ITS, *tub2* and *tef* sequence data (Fig. 20, Table 10).

Recommended genetic marker (genus level): LSU

Recommended genetic markers (species level): ITS, *tub2* and *tef*

Accepted number of species: 112

References: Maharachchikumbura et al. (2012), (2014b), (2016), Jayawardena et al. (2015), (2016), Mahapatra et al. (2018), Rodríguez-Gálvez et al. (2020), Razaghi et al. (2024) (morphology, phylogeny and pathogenicity)

Table 10. DNA barcodes for accepted species of *Neopestalotiopsis*.

Species	Strain	GenBank accession numbers		
		ITS	*tub2*	*tef*
Neopestalotiopsis acericola	**CFCC 70620**	**PP784733**	**PP842610**	**PP842622**
Neo. acrostichi	**MFLUCC 17-1754**	**MK764272**	**MK764338**	**MK764316**
Neo. ageratinae	**CGMCC 3.23468**	**OR247899**	**OR381006**	**OR361406**
Neo. alpapicalis	**MFLUCC 17-2544**	**MK357772**	**MK463545**	**MK463547**
Neo. amomi	**HKAS 124563**	**OP498012**	**OP752133**	**OP653489**
Neo. aotearoa	**CBS 367.54**	**MH857366**	**KM199454**	**KM199526**
Neo. asiatica	**MFLUCC 12-0286**	**JX398983**	**JX399018**	**JX399049**
Neo. australis	**CBS 114159**	**KM199348**	**KM199432**	**KM199537**
Neo. brachiata	**MFLUCC 17-1555**	**MK764274**	**MK764340**	**MK764318**
Neo. camelliae-oleiferae#	**CSUFTCC81**	**OK493585**	**OK562360**	**OK507955**
Neo. castanopsidis	**CGMCC 3.23478**	**OR247897**	**OR381018**	**OR361418**
Neo. cavernicola	**KUMCC 20-0269**	**MW545802**	**MW557596**	**MW550735**
Neo. celtidis	**CGMCC 3.23513**	**OR247900**	**OR381049**	**OR361449**
Neo. cercidicola	**CFCC 70632**	**PP784737**	**PP842626**	**PP842614**

Neo. chiangmaiensis	**MFLUCC 18-0113**	**N/A**	**MH412725**	**MH388404**
Neo. chrysea	**MFLUCC 12-0261**	**JX398985**	**JX399020**	**JX399051**
Neo. clavispora	**MFLUCC 12-0281**	**JX398979**	**JX399014**	**JX399045**
Neo. cocoes	**MFLUCC 15-0152**	**KX789687**	**N/A**	**KX789689**
Neo. coffee-arabicae	**HGUP4019**	**KF412649**	**KF412643**	**KF412646**
Neo. collariata	**CGMCC 3.23493**	**OR247905**	**OR381026**	**OR361426**
Neo. concentrica	**CFCC 55162**	**OK560707**	**OM117698**	**OM622433**
Neo. cubana	**CBS 600.96**	**KM199347**	**KM199438**	**KM199521**
Neo. dendrobii	**MFLUCC 14-0106**	**MK993571**	**MK975835**	**MK975829**
Neo. dimorphospora	**CGMCC 3.23497**	**OR247903**	**OR381030**	**OR361430**
Neo. dolichoconidiophora	**CGMCC 3.23490**	**OR247911**	**OR381021**	**OR361421**
Neo. drenthii	**BRIP 72264a**	**MZ303787**	**MZ312680**	**MZ344172**
Neo. egyptiaca	**CBS 140162**	**KP943747**	**KP943746**	**KP943748**
Neo. elaeagni	**HGUP10002**	**MW930716**	**MZ683391**	**MZ203452**
Neo. elaeidis	**MFLU 15-1466**	**ON650690**	**N/A**	**ON734012**
Neo. ellipsospora	**MFLUCC 12-0283**	**JX398980**	**JX399016**	**JX399047**
Neo. eucalypticola	**CBS 264.37**	**KM199376**	**KM199431**	**KM199551**
Neo. eucalyptorum	**CBS 147684**	**MW794108**	**MW802841**	**MW805397**
Neo. fijiensis	**CGMCC 3.23465**	**OR247892**	**OR381003**	**OR361403**
Neo. fimbriata	**CGMCC 3.23479**	**OR247869**	**OR381020**	**OR361420**
Neo. foedans	**CGMCC 3.9123**	**JX398987**	**JX399022**	**JX399053**
Neo. formicidarum	**CBS 115.83**	**KM199344**	**KM199444**	**KM199519**
Neo. fragariae#	**ZHKUCC 22-0113**	**ON553410**	**ON569075**	**ON569076**
Neo. fuzhouensis	**CGMCC 3.23509**	**OR247877**	**OR381047**	**OR361447**
Neo. guajavae	**FMBCC 11.1**	**MF783085**	**MH460871**	**MH460868**
Neo. guajavicola	**FMBCC 11.4**	**MH209245**	**MH460873**	**MH460870**
Neo. guangxiensis	**CGMCC 3.23505**	**OR247881**	**OR381040**	**OR361440**
Neo. guizhouensis	**CGMCC 3.23501**	**OR247883**	**OR381036**	**OR361436**
Neo. hadrolaeliae	**VIC 47180**	**MK454709**	**MK465120**	**MK465122**
Neo. haikouensis	**SAUCC212271**	**OK087294**	**OK104870**	**OK104877**
Neo. hispanica	**CBS 147686**	**MW794107**	**MW802840**	**MW805399**
Neo. honoluluana	**CBS 114495**	**KM199364**	**KM199457**	**KM199548**
Neo. hydeana	**MFLUCC 20-0132**	**MW266069**	**MW251119**	**MW251129**
Neo. hyperici	**KUNCC 22-12598**	**OP498009**	**OP737883**	**OP737880**
Neo. iberica	**CBS 147688**	**MW794111**	**MW802844**	**MW805402**
Neo. iranensis	**CBS 137768**	**KM074048**	**KM074057**	**KM074051**
Neo. javaensis	**CBS 257.31**	**KM199357**	**KM199437**	**KM199543**
Neo. jiangxiensis	**CGMCC 3.23492**	**OR247890**	**OR381024**	**OR361424**
Neo. keteleeria	**MFLUCC 13-0915**	**KJ503820**	**KJ503821**	**KJ503822**
Neo. liquidambaris	**CGMCC 3.23508**	**OR247878**	**OR381046**	**OR361446**
Neo. longiappendiculata	**CBS 147690**	**MW794112**	**MW802845**	**MW805404**
Neo. lusitanica	**CBS 147692**	**MW794110**	**MW802843**	**MW805406**
Neo. macadamiae#	**BRIP 63737B**	**KX186604**	**KX186654**	**KX186627**
Neo. machili	**CGMCC 3.23477**	**OR247870**	**OR381016**	**OR361416**
Neo. maddoxii	**BRIP 72266a**	**MZ303782**	**MZ312675**	**MZ344167**
Neo. magna	**MFLUCC 15-0652**	**KF582795**	**KF582793**	**KF582791**
Neo. megabetaspora	**CGMCC 3.23474**	**OR247875**	**OR381010**	**OR361410**
Neo. mesopotamica	**CBS 336.86**	**KM199362**	**KM199441**	**KM199555**
Neo. mianyangensis#	**CGMCC 3.23554**	**OP546681**	**OP672161**	**OP723490**
Neo. moniliformis	**CGMCC 3.23498**	**OR247886**	**OR381031**	**OR361431**
Neo. musae	**MFLUCC 15-0776**	**KX789683**	**KX789686**	**KX789685**
Neo. nanningensis	**CGMCC 3.23475**	**OR247872**	**OR381014**	**OR361414**
Neo. natalensis	**CBS 138.41**	**KM199377**	**KM199466**	**KM199552**
Neo. nebuloides	**BRIP 66617**	**MK966339**	**MK977632**	**MK977633**
Neo. olumideae	**BRIP 72273a**	**MZ303790**	**MZ312683**	**MZ344175**
Neo. paeoniae	**CBS 318.74**	**MH554031**	**MH554707**	**N/A**
Neo. paeoniae-suffruticosae#	**CGMCC 3.23555**	**OP082292**	**OP235980**	**OP204794**
Neo. pandanicola	**KUMCC 17-0175**	**N/A**	**MH412720**	**MH388389**
Neo. pernambucana	RV01	KJ792466	N/A	N/A
Neo. perukae	**FMBCC 11.3**	**MH209077**	**MH460876**	**MH523647**
Neo. petila	**MFLUCC 17-1738**	**MK764275**	**MK764341**	**MK764319**
Neo. phangngaensis	**MFLUCC 18-0119**	**MH388354**	**MH412721**	**MH388390**
Neo. phoenicis	**CFCC 70625**	**PP784730**	**PP842607**	**PP842619**

Neo. photiniae	**GUCC 21-0820**	**OP806524**	**OP896200**	**OP828691**
Neo. phyllostachydis	**CGMCC 3.23491**	**OR247891**	**OR381023**	**OR361423**
Neo. piceana	**CBS 394.48**	**KM199368**	**KM199453**	**KM199527**
Neo. poae	**CGMCC 3.23506**	**OR247880**	**OR381042**	**OR361442**
Neo. protearum	**CBS 114178**	**JN712498**	**KM199463**	**KM199542**
Neo. psidii	**FMBCC 11.2**	**MF783082**	**MH477870**	**MH460874**
Neo. rhapidis	**GUCC 21501**	**MW931620**	**MW980441**	**MW980442**
Neo. rhizophorae	**MFLUCC 17-1550**	**MK764277**	**MK764343**	**MK764321**
Neo. rhododendri	**GUCC 21504**	**MW979577**	**MW980443**	**MW980444**
Neo. rhododendricola	**KUN-HKAS 123204**	**OK283069**	**OK274147**	**OK274148**
Neo. rosae	**CBS 124745**	**KM199360**	**KM199430**	**KM199524**
***Neo. rosicola*#**	**CFCC 51992**	**KY885239**	**KY885245**	**KY885243**
Neo. samarangensis	**CBS 115451**	**KM199365**	**KM199447**	**KM199556**
Neo. saprophytica	**MFLUCC 12-0282**	**KM199345**	**KM199433**	**KM199538**
***Neo. scalabiensis*#**	**CAA1029**	**MW969748**	**MW934611**	**MW959100**
Neo. sichuanensis	**CFCC 54338**	**MW166231**	**MW218524**	**MW199750**
***Neo. siciliana*#**	**CBS 149117**	**ON117813**	**ON209162**	**ON107273**
Neo. smilacis	**CGMCC 3.23500**	**OR247885**	**OR381033**	**OR361433**
Neo. sonneratiae	**MFLUCC 17-1745**	**MK764279**	**MK764345**	**MK764323**
Neo. steyaertii	**IMI 192475**	**KF582796**	**KF582794**	**KF582792**
Neo. subepidermalis	**CFCC 55160**	**OK560699**	**OM117690**	**OM622425**
Neo. suphanburiensis	**MFLUCC 22-0126**	**OP497994**	**OP752135**	**OP753372**
Neo. surinamensis	**CBS 450.74**	**KM199351**	**KM199465**	**KM199518**
Neo. terricola#	CGMCC 3.23553	OP082294	OP235982	OP204796
Neo. thailandica	**MFLUCC 17-1730**	**MK764281**	**MK764347**	**MK764325**
***Neo. theobromicola*#**	**MFLUCC 24-0253**	**PQ198764**	**PQ671951**	**PQ671945**
***Neo. vaccinii*#**	**CAA1059**	**MW969747**	**MW934610**	**MW959099**
***Neo. vacciniicola*#**	**CAA1055**	**MW969751**	**MW934614**	**MW959103**
Neo. vheenae	**BRIP 72293a**	**MZ303792**	**MZ312685**	**MZ344177**
***Neo. vitis*#**	**MFLUCC 15-1265**	**KU140694**	**KU140685**	**KU140676**
Neo. xishuangbannaensis	**KUMCC 21-0424**	**ON426865**	**OR025934**	**OR025973**
Neo. zakeelii	**BRIP 72282a**	**MZ303789**	**MZ312682**	**MZ344174**
Neo. zimbabwana	**CBS 111495**	**JX556231**	**KM199456**	**KM199545**
Neo. zingiberis	**HGUP10001**	**MW930715**	**MZ683390**	**MZ683389**

Ex-type/ex-epitype/ex-neotype/ex-lectotype strains and voucher strains are in bold. Sequences that are not available are represented by N/A. Species confirmed with pathogenicity studies are marked with #.

135. *Neosetophoma* Gruyter, Aveskamp & Verkley, in Gruyter et al., Mycologia 102(5): 1075 (2010)

Type species: *Neosetophoma samararum* (Desm.) Gruyter, Aveskamp & Verkley

Classification: *Dothideomycetes*, *Pleosporales*, *Phaeosphaeriaceae*

Background: *Neosetophoma* was described as an asexual morph with *Ne. samararum* as the type species (Gruyter et al. 2010). Members have been reported as pathogens, endophytes, or saprobes in a wide range of habitats (Phookamsak et al. 2014, Hernandez-Restrepo et al. 2016, Karunarathna et al. 2017, Wanasinghe et al. 2018). *Neosetophoma* is characterized by globose to irregular conidiomata, with papillate ostioles, and yellowish conidia that are attenuated at one end (De Gruyter et al. 2010, Liu et al. 2015).

Distribution: worldwide (Farr & Rossman 2025)

Disease symptoms: *Neosetophoma* species are known to cause a variety of plant disease symptoms, although their pathogenic roles are not as extensively documented. *Neosetophoma* typically infects the leaves, stems, or bark of host plants, leading to symptoms such as leaf spots, necrotic lesions, blight, and canker formation (Gruyter et al. 2010, Marin-Felix et al. 2019a). The leaf spots are usually small to medium in size, brown to dark brown, often with a yellow halo, and may coalesce, causing extensive tissue death (Marin-Felix et al. 2019a, Ebrahimi & Fotouhifar 2021). *Neosetophoma* has also been associated with stem dieback or branch decline in woody plants as well as decline symptoms in fruit trees and elms, respectively (Hashemi & Mohammadi 2016, Ebrahimi & Fotouhifar 2021).

Hosts: *Neosetophoma* species have been isolated from various host families, viz. *Brassicaceae*, *Caprifoliaceae*, *Iridaceae*, *Malvaceae*, *Ranunculaceae* and *Salicaceae* (Phookamsak et al. 2014, Karunarathna et al. 2017). They have been found on both monocotyledons and dicotyledons, including trees, shrubs, grasses, and herbaceous crops (Alidadi et al. 2019, Farr & Rossman 2025). They have also been reported from economically and ecologically important species such as apple (*Malus domestica*), elm (*Ulmus* spp.), ash (*Fraxinus* spp.), and various plants in *Poaceae* (Ebrahimi & Fotouhifar 2021). *Neosetophoma* species have been reported from legumes, maples, other hardwood trees and soil, often as saprobes or endophytes (Gruyter et al. 2010, Karunarathna et al. 2017, Marin-Felix et al. 2019a). This broad host range underlines the genus's adaptability and potential impact on both natural ecosystems and agricultural systems.

Pathogen biology, disease cycle and epidemiology: The disease cycle of *Neosetophoma* species is not fully understood. *Neosetophoma* produce conidiomata on

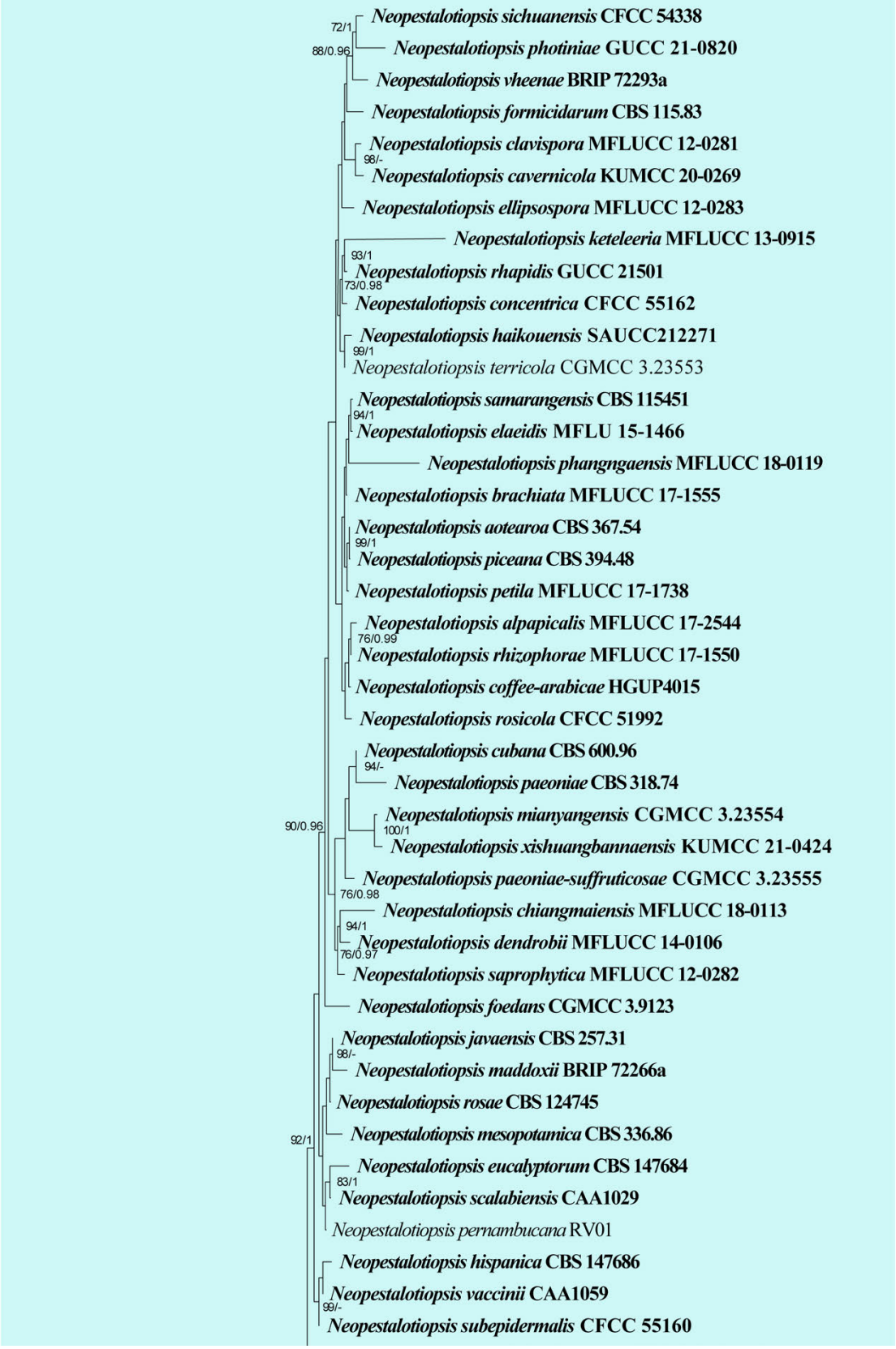

Fig. 20 Maximum likelihood tree of *Neopestalotiopsis* species based on the concatenated ITS, *tub2* and *tef* sequence data. The best scoring RAxML tree had a final likelihood value of -8335.116. The tree was rooted to *Pseudopestalotiopsis avicenniae* (MFLUCC 17-0434) and *P. myanmarina* (NBRC 112264). Estimated base frequencies were as follows: A = 0.223971, C = 0.279581, G = 0.195564, and T = 0.300884; substitution rates AC = 0.68043, AG = 2.40364, AT = 1.29389, CG = 0.68043, CT = 4.20028, and GT = 1.000000. ML bootstrap support values over 70% and Bayesian posterior probabilities (BPP) greater than 0.95 are indicated. Type strains are in bold. Scale bar indicates the number of substitutions per site. Hyphens (-) represent support values less than BS 70%/BPP 0.95.

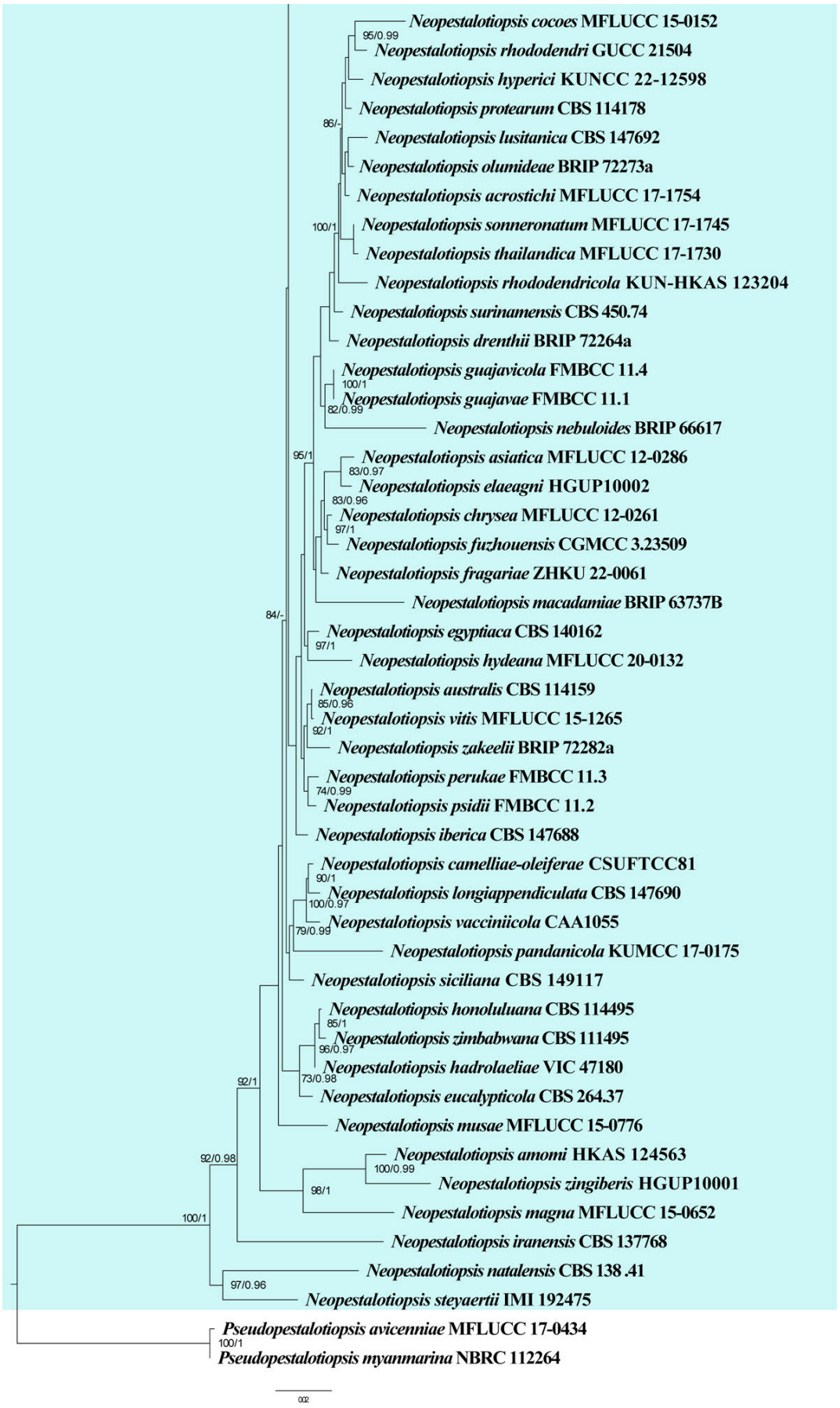

Fig. 20 (continued)

infected plant tissues, which release conidia that serve as primary inoculum (Alidadi et al. 2019, Ebrahimi & Fotouhifar 2021). The conidia are disseminated by wind or water splashes, particularly during wet conditions, allowing them to infect new host tissues through natural openings or wounds (Magyar et al. 2016). Once established, the fungus may remain asymptomatic or cause symptoms such as leaf spots, necrosis, and stem lesions (Ebrahimi & Fotouhifar 2021). In some species, pseudothecia develop later in the disease cycle, contributing to long-term survival. The fungus may overwinter in infected plant debris or woody tissues, serving as a reservoir for infection in subsequent growing seasons. *Neosetophoma* can act as a primary pathogen, secondary invader or latent colonizer (Magyar et al. 2016). More studies are needed to clarify the infection strategies and disease cycles of *Neosetophoma* species.

Morphological-based identification: The identification of *Neosetophoma* was primarily based on a combination of macroscopic and microscopic characteristics. The colonies (PDA or MEA) range from olivaceous to dark gray or brown, often with a darkly pigmented reverse (Gruyter et al. 2010, Marin-Felix et al. 2019a). The conidiomata are pycnidial, globose to pyriform, brown to black, and sometimes possess setae around the ostioles, a distinctive feature that contributes to the genus name (Fig. 21). Conidiogenous cells are usually phialidic or annellidic, ampulliform to cylindrical, and line the inner walls of the pycnidia. The conidia are hyaline to pale brown, ellipsoidal to cylindrical, mostly 1-septate, and smooth-walled. The sexual morph is characterized by globose to subglobose, unilocular and ostiolate ascomata (Phookamsak et al. 2014, Mehrabi & Asgari 2024). The hamathecium comprises numerous, filiform, hyaline, pseudoparaphyses. Asci are bitunicate, fissitunicate, cylindrical and 8-spored. Ascospores are fusiform, smooth-walled, hyaline to brown and 1–3-septate, without a gelatinous sheath. Although these morphological traits are useful for preliminary identification, they often overlap with other genera such as *Phoma* and *Didymella*, making molecular analysis essential for accurate species-level classification.

Molecular-based identification: Molecular-based identification of *Neosetophoma* has become increasingly important due to the morphological overlap with other genera. Gruyter et al. (2010) introduced *Neosetophoma* and *Setophoma* in *Phaeosphaeriaceae* to accommodate *Phoma* species based on LSU and SSU sequences. The placement of the genus in *Phaeosphaeriaceae* was confirmed by several studies (De Gruyter et al. 2012, Zhang et al. 2012b, Hyde et al. 2013, Quaedvlieg et al. 2013, Phookamsak et al. 2014). Several novel species were further introduced based on morphology and multi-gene phylogeny (Hernandez-Restrepo et al. 2016, Karunarathna et al. 2017, Wanasinghe et al. 2018, Marin-Felix et al. 2019a). This study provides an updated phylogeny of *Neosetophoma* based on combined ITS, LSU, SSU, *rpb2*, *tef* and *tub2* sequence data (Fig. 22, Table 11).

Recommended genetic markers (genus level): ITS and LSU

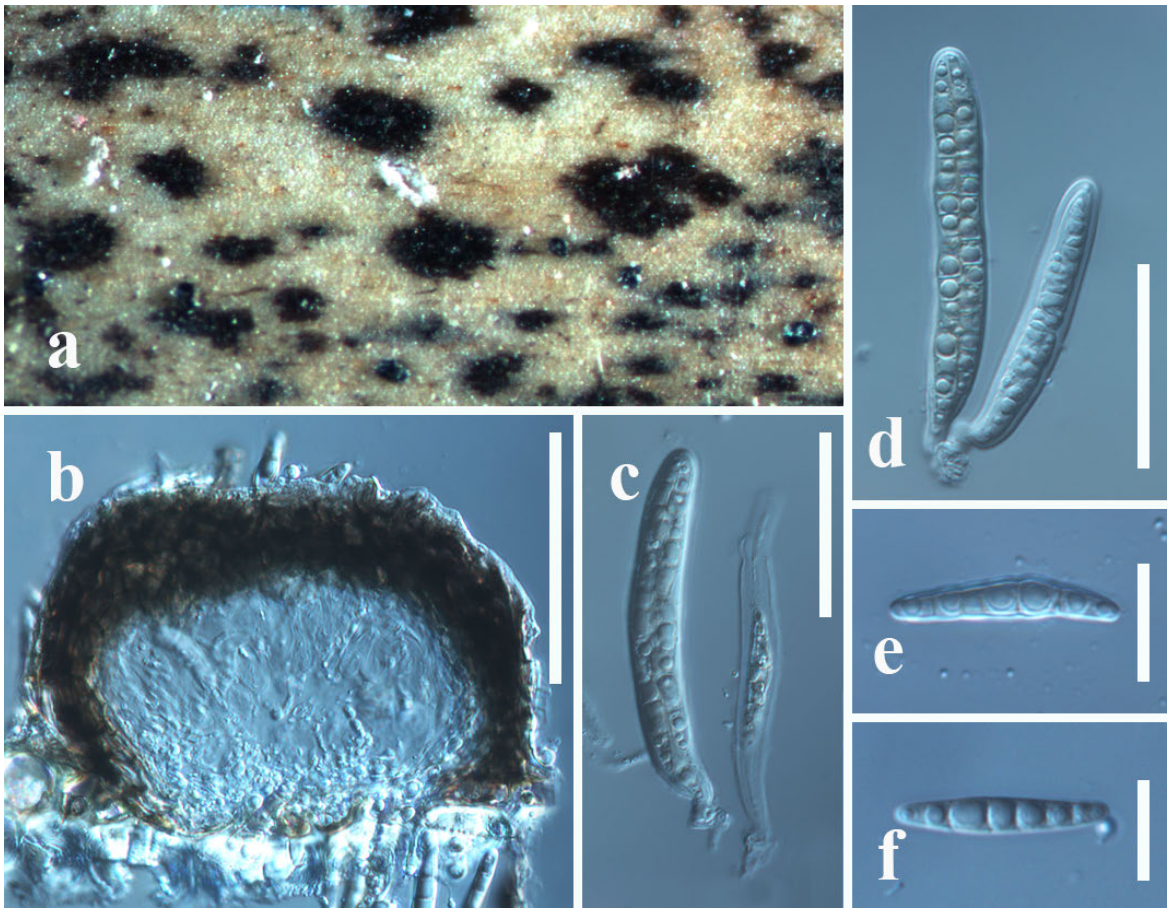

Figure 21 *Neosetophoma poaceicola.* a Ascomata on host. b Vertical section through ascoma. c-d Asci. e-f Ascospores. Scale bar: b = 50 µm, c-d = 30 µm, e-f = 15 µm. This picture is copyright of Danushka S Tennakoon (Tennakoon et al. 2020).

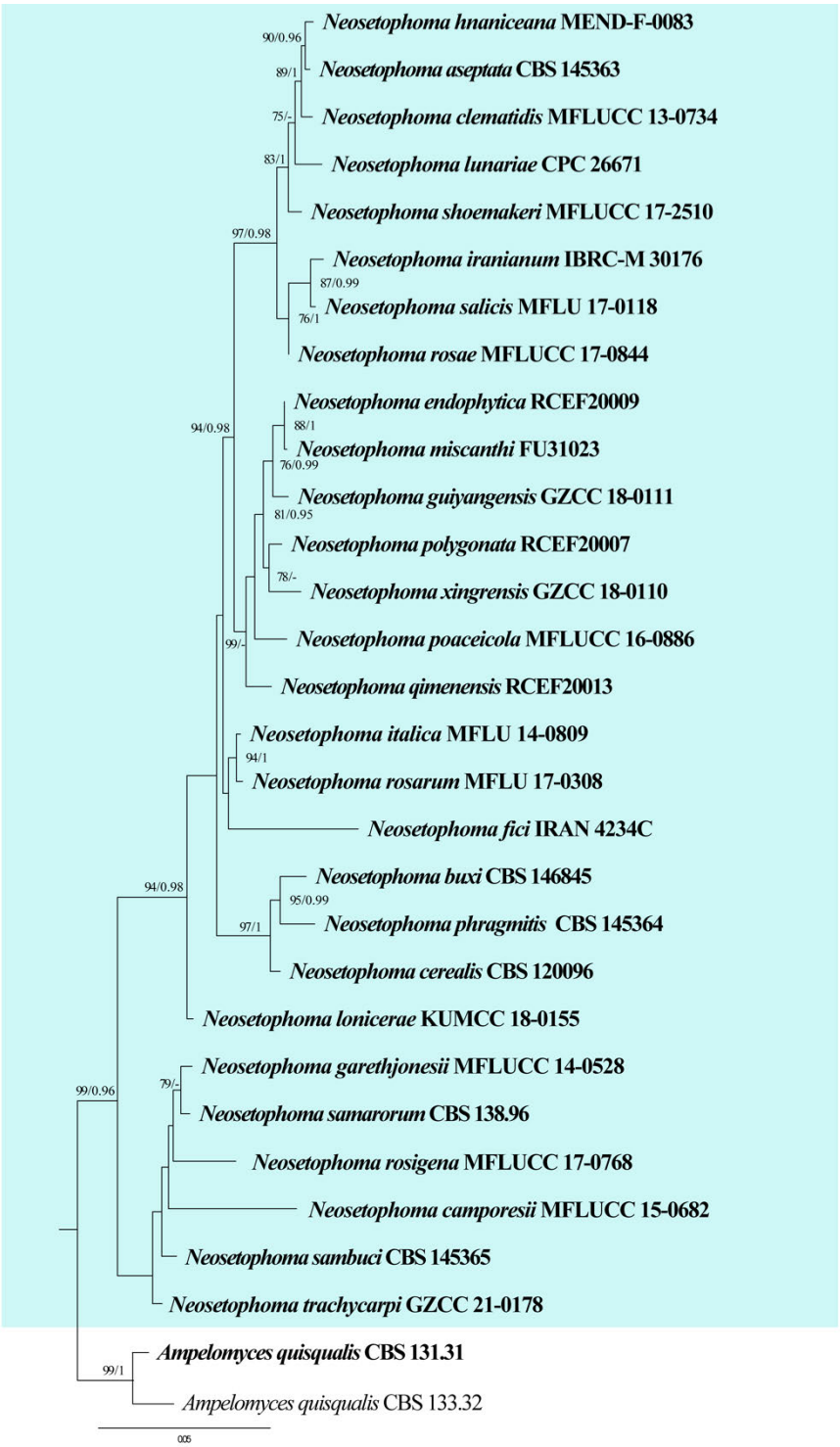

Fig. 22 Maximum likelihood tree of *Neosetophoma* species based on the concatenated ITS, LSU, SSU, *rpb2*, *tef* and *tub2* sequence data. The best scoring RAxML tree had a final likelihood value of -9494.891. The tree was rooted with *Ampelomyces quisqualis* (CBS 131.31 and CBS 133.32). Estimated base frequencies were as follows: A = 0.250, C = 0.250, G = 0.250, T = 0.250; substitution rates AC = 1.68999, AG = 5.54503, AT = 1.68999, CG = 1.00000, CT = 13.78932, GT = 1.000000. ML bootstrap support values over 70% and Bayesian posterior probabilities (BPP) greater than 0.95 are indicated. Type strains are in bold. Scale bar indicates the number of substitutions per site. Hyphens (-) represent support values less than BS 70%/BPP 0.95.

Table 11 DNA barcodes for accepted species of *Neosetophoma*.

Species	Strain	GenBank accession numbers					
		ITS	LSU	SSU	*rpb2*	*tef*	*tub2*
Neosetophoma aseptata	**CBS 145363**	**MK539953**	**MK540024**	**N/A**	**MK540084**	**N/A**	**N/A**
Ne. buxi	**CBS 146845**	**MW621494**	**MW620993**	**N/A**	**MW628872**	**MW628871**	**N/A**
Ne. camporesii	**MFLUCC 15-0682**	**N/A**	**N/A**	**NG_070320**	**N/A**	**N/A**	**N/A**
Ne. cerealis	**CBS 120096**	**MH863077**	**MH874630**	**N/A**	**N/A**	**N/A**	**N/A**
Ne. clematidis	**MFLUCC 13-0734**	**KP744450**	**KP684153**	**KP684154**	**N/A**	**N/A**	**N/A**
Ne. endophytica	**RCEF20009**	**OR985037**	**OR985064**	**OR985054**	**N/A**	**OR989985**	**N/A**
Ne. fici	**IRAN 4234C**	**OP806395**	**OP805934**	**N/A**	**OP838919**	**N/A**	**OP838921**
Ne. garethjonesii	**MFLUCC 14-0528**	**KY496758**	**KY496738**	**N/A**	**N/A**	**KY514402**	**N/A**
Ne. guiyangensis	**GZCC 18-0111**	**MH018134**	**MH018132**	**MH018136**	**N/A**	**MH051889**	**N/A**
Ne. hnaniceana	**MEND-F-0083**	**MT119769**	**MT119767**	**N/A**	**MT119768**	**N/A**	**N/A**
Ne. iranianum	**IBRC-M 30176**	**MF684861**	**MF684866**	**MF684868**	**N/A**	**N/A**	**N/A**
Ne. italica	**MFLU 14-0809**	**KP711356**	**KP711361**	**KP711366**	**N/A**	**N/A**	**N/A**
Ne. lonicerae	**KUMCC 18-0155**	**MK356375**	**MK356349**	**MK356363**	**N/A**	**MK359067**	**N/A**
Ne. lunariae	**CPC 26671**	**KX306763**	**KX306789**	**N/A**	**N/A**	**N/A**	**N/A**
Ne. miscanthi	**FU31023**	**MK503820**	**MK503826**	**MK503832**	**N/A**	**N/A**	**N/A**
Ne. phragmitis	**CBS 145364**	**MK539954**	**MK540025**	**N/A**	**MK540085**	**MK540148**	**N/A**
Ne. poaceicola	**MFLUCC 16-0886**	**KY568986**	**KY550382**	**KY550383**	**N/A**	**N/A**	**N/A**
Ne. polygonata	**RCEF20007**	**OR985035**	**OR985062**	**OR985052**	**N/A**	**N/A**	**N/A**
Ne. qimenensis	**RCEF20013**	**OR985041**	**OR985068**	**OR985058**	**N/A**	**N/A**	**N/A**
Ne. rosae	**MFLUCC 17-0844**	**MG828926**	**MG829035**	**MG829141**	**N/A**	**MG829219**	**N/A**
Ne. rosarum	**MFLU 17-0308**	**MG828927**	**MG829036**	**MG829142**	**N/A**	**N/A**	**N/A**
Ne. rosigena	**MFLUCC 17-0768**	**MG828928**	**MG829037**	**MG829143**	**N/A**	**N/A**	**N/A**
Ne. salicis	**MFLU 17-0118**	**MK608025**	**MK608026**	**N/A**	**N/A**	**N/A**	**N/A**
Ne. samarorum#	**CBS 138.96**	**MH862569**	**MH874195**	**GQ387517**	**KF252168**	**KF253119**	**KF252655**
Ne. sambuci	**CBS 145365**	**MK539955**	**MK540026**	**N/A**	**MK540086**	**MK540149**	**N/A**
Ne. shoemakeri	**MFLUCC 17-2510**	**MG602203**	**MG602199**	**MG602201**	**N/A**	**MG739515**	**N/A**
Ne. trachycarpi	**GZCC 21-0178**	**PP592444**	**PP621068**	**PP627324**	**PP780243**	**PP760996**	**N/A**
Ne. xingrensis	**GZCC 18-0110**	**MH018135**	**MH018133**	**N/A**	**N/A**	**N/A**	**N/A**

Ex-type/ex-epitype/ex-neotype/ex-lectotype strains and voucher strains are in bold. Sequences that are not available are represented by N/A. Species confirmed with pathogenicity studies are marked with #.

Recommended genetic markers (species level): ITS, LSU, SSU, *rpb2*, *tef* and *tub2*

Accepted number of species: 28

References: Gruyter et al. (2010), Karunarathna et al. (2017), Alidadi et al. (2019), Marin-Felix et al. (2019a), Ebrahimi & Fotouhifar (2021) (morphology and phylogeny)

136. *Nigrospora* Zimm., Centbl. Bakt. ParasitKde, Abt. I 8: 220 (1902)

Type species: *Nigrospora panici* Zimm.

Classification: *Sordariomycetes*, *Amphisphaeriales*, *Apiosporaceae*

Background: *Nigrospora* is an important genus in ascomycetes with a cosmopolitan distribution and wide host range (Wang et al. 2017b). *Nigrospora* species are endophytes and saprobes of various hosts and have also been commonly recorded as plant pathogens with diverse host ranges including important economic crops, fruits and ornamentals (Sun et al. 2011, Wang et al. 2017b, Rashmi et al. 2019, Manawasinghe et al. 2025). In addition, this fungus can cause onychomycosis, corneal ulcers, hay fever, respiratory and allergic diseases in humans (De Hoog et al. 2000, Fan et al. 2009, Ananya et al. 2014).

Distribution: worldwide (Farr & Rossman 2025)

Disease symptoms: *Nigrospora* species can cause leaf spot as well as leaf, twigs, shoot and stem blight (Fig. 23). *Nigrospora oryzae* can cause minute black pustules on rice leaves, necrotic spots on rice grains and blight on glumes and culms, while on rice stems it produces grey to black lesions (Hajano et al. 2011). This species was reported to be highly pathogenic on cotton forming grey mycelium on bolls that later become discolored bolls (Palmateer et al. 2003, Sharma et al. 2013). This fungus also causes ear rot disease in maize with characteristic symptoms including superficial, dark grey to black lesions with a slight bluish cast on the lower internodes (Sharma et al. 2013). *Nigrospora oryzae* also induces foliar symptoms in Kentucky bluegrass (*Poa pratensis*) in Ontario, Canada (Zheng et al. 2012). It was reported as seed-borne on barley, sorghum, and wheat and has been associated with postharvest diseases of citrus (Jagdish et al. 1985, Fakhrunnisa et al. 2006). Stem blight disease was observed on the lower portions of *Brassica juncea* stems during the cropping season, which was caused by *Ni. oryzae* in India (Sharma et al. 2013). *Nigrospora sphaerica* causes leaf blight symptoms on tea leaves in China and India (Dutta et al. 2015, Liu et al. 2016, 2020). Infected leaves have irregular-shaped yellow to brown leaf lesions, and later the entire leaf is infected and leaves turns dark brown and withered (Liu et al. 2020). *Nigrospora sphaerica* is an opportunistic pathogen causing onychomycosis in humans (De Hoog et al. 2000, Fan et al. 2009) and corneal ulcers (Ananya et al. 2014, Kindo et al. 2014, Motswaledi et al. 2018). *Nigrospora musae* is commonly known for causing squirter disease on banana plants (Jones and Stover 2000). The fungus resides on banana debris and sporulates after rainfall

or after tree watering, and the disease develops during transportation and ripening of the fruit (Meredith 1961). The initial disease symptoms are a dark core or dark-red line of rubbery material along the center core or near the end of the banana fruit (Meredith 1961). This disease occurs in Australia, Jamaica, and Nigeria (Meredith 1961, https://agrobaseapp.com/).

Hosts: *Nigrospora* does not display evidence of host or geographical limitation (Palmateer et al. 2003, Wu et al. 2014a, Eken et al. 2016, Wang et al. 2017b, Orina et al. 2025). More than 900 records are found in the Fungal database (Farr & Rossman 2025). Hao et al. (2020) isolated five *Nigrospora* species from Shandong, China and found 13 novel host associations. Nigronapthaphenyl, a new compound was extracted from *Ni. sphaerica* (an endophyte) on *Bruguiera gymnorrhyza* (Ukwatta et al. 2019). *Nigrospora sphaerica* causes leaf spots, twigs and shoot blight of blueberry (*Vaccinium corymbosum*) (Wright et al. 2008). Foliar and cane rot of *Arundo donax* are caused by *Ni. oryzae* in Europe (Widmer et al. 2006). The same species caused lint rot or leaf spots of cotton in Alabama, China (Palmateer et al. 2003, Zhang et al. 2012a), stem blight on *Brassica juncea* in India (Sharma et al. 2013) and leaf spots in *Aloe vera* in China (Zhai et al. 2013). *Nigrospora oryzae* also causes leaf spots on *Dendrobium candidum* in China (Wu et al. 2014a) and on Kentucky bluegrass (*Poa pratensis*) in Ontario (Zheng et al. 2012). *Nigrospora oryzae* and *Ni. sphaerica* causes leaf spots on date palm leaves (Abass et al. 2014). Leaf blight on *Stenotaphrum secundatum* was caused by *Nigrospora osmanthi* in China (Mei et al. 2019). *Nigrospora sphaerica* causes leaf blight on *Camellia sinensis* and *Cunninghamia lanceolata* in China (Liu et al. 2016, Xu et al. 2017) and leaf spots of *Kinnow mandarin* in Pakistan (Alam et al. 2017, 2020). Reddish brown spot disease of dragon fruit (*Hylocereus polyrhizus*) was caused by *Ni. lacticolonia* and *Ni. sphaerica* in Malaysia (Kee et al. 2019).

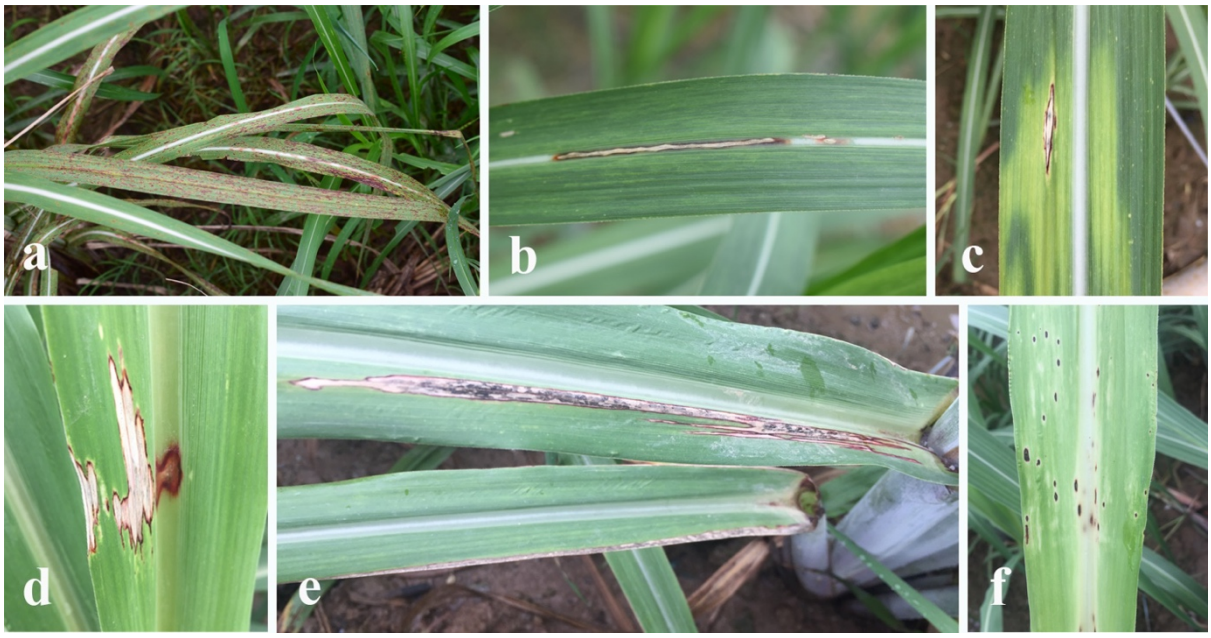

Fig. 23 a-f Symptoms caused by *Nigrospora* sp. on sugarcane (*Saccharum officinarum*). This picture is copyright of Mubashar Raza (Raza et al. 2019).

Pathogen biology, disease cycle and epidemiology: *Nigrospora* spp., particularly *Nigrospora oryzae*, are primarily saprobes but can become weak pathogens under favourable conditions (Wang et al. 2017b). They produce dark, single-celled conidia in abundance, which are easily dispersed by wind, rain splash, and mechanical means (Magyar et al. 2016). The disease cycle typically begins when conidia land on senescing or wounded plant tissue and germinate under warm and humid conditions, hence colonizing the host (Doohan and Zhou 2017). Infection is often facilitated by plant stress or injury (Doohan and Zhou 2017). Disease development is favoured by warm temperatures and high humidity, especially in tropical and subtropical regions (Palmateer et al. 2003, Eken et al. 2016, Wang et al. 2017b, Orina et al. 2025). The pathogen survives in plant debris and infected plant parts, serving as the primary inoculum source for subsequent infections (Wang et al. 2017b).

Morphological-based identification: Species delimitation in *Nigrospora* was previously based on morphological characters, especially conidial dimensions (Mason 1927, 1933). The generic concept of *Nigrospora* has branched micronematous or semi-macronematous conidiophores, monoblastic conidiogenous cells and black, shiny, globose or subglobose, aseptate conidia while the sexual morphs comprise perithecial ascomata, short-stalked asci with biseriate ascospores (Webster 1952, Wang et al. 2017b, Raza et al. 2019). It was found that some key morphological characters (conidial dimensions) overlap, but there are phylogenetically distinct species of *Nigrospora* (Wang et al. 2017b). Thus, Wang et al. (2017) suggested using a combination of morphological and molecular data to distinguish *Nigrospora* species. The type of the genus, *Ni. panici*, was reported from *Panicum amphibium* from Java (Zimmerman 1902), but the holotype was lost (Wang et al. 2017b). Also, several species (*Ni. aerophila, Ni. arundinacea, Ni. canescens, Ni. gallarum, Ni. gossypii, Ni. javanica, Ni. maydis, Ni. padwickii*) are not available for molecular study, which to some extent has impeded the full resolution of

species relationships (Wang et al. 2017b). Therefore, there is a need to find suitable specimens for epitypification of the type species and some other species.

Molecular-based identification: The phylogenetic investigations by Wang et al. (2017) significantly stabilized the taxonomy of the genus and affirmed the generic placement in *Apiosporaceae* (*Xylariales*) based on multi-locus molecular phylogeny of ITS, *tef* and *tub2* gene regions. This study provides an updated phylogeny of *Nigrospora* based on combined ITS, *tub2* and *tef* sequence data (Fig. 24, Table 12).

Recommended genetic markers (genus level): ITS and *tub2*

Recommended genetic markers (species level): ITS, *tef* and *tub2*

Accepted number of species: 46

References: Palmateer et al. (2003), Wu et al. (2014), Eken et al. (2016), Wang et al. (2017), Raza et al. (2019) (morphology and phylogeny)

Table 12 DNA barcodes for accepted species of *Nigrospora*.

Species	Strain	GenBank accession numbers		
		ITS	*tub2*	*tef*
Nigrospora aurantiaca	**CGMCC 3.18130**	**KX986064**	**KY019465**	**KY019295**
Ni. bambusae	**CGMCC 3.18327**	**KY385307**	**KY385319**	**KY385313**
Ni. brasiliensis	**CMM 1214**	**KY569629**	**MK720816**	**MK753271**
Ni. camelliae-sinensis	**CGMCC 3.18125**	**KX985986**	**KY019460**	**KY019293**
Ni. chinensis	**CGMCC 3.18127**	**KX986023**	**KY019462**	**KY019422**
Ni. cooperae	**BRIP 72408b**	**OP035047**	**OP039537**	**OP039538**
Ni. covidalis	**CGMCC 3.20538**	**OK335209**	**OK431479**	**OK431485**
Ni. dactylidis	**KUNCC 25-19191**	**PV608639**	**PV613325**	**PV626508**
Ni. dicranopteridis	**KUNCC 23-14199**	**PV138724**	**PV222011**	**PV177116**
Ni. endophytica	**URM8462**	**OM265233**	**OP572420**	**OP572416**
Ni. falsivesicularis	**CGMCC 3.19678**	**MN215778**	**MN329942**	**MN264017**
Ni. ficuum	**ZHKUCC 22-0143**	**OR164911**	**OR166318**	**N/A**
Ni. globosa	**CGMCC 3.19633**	**MK329121**	**MK336134**	**MK336056**
Ni. globospora	**CGMCC 3.20539**	**OK335211**	**OK431481**	**OK431487**
Ni. gorlenkoana	**CBS 480.73**	**KX986048**	**KY019456**	**KY019420**
Ni. guangdongensis	**CFCC 53917**	**MT017509**	**MT024495**	**MT024493**
Ni. guangxiensis	**KUNCC23-16747**	**PQ553688**	**PQ613610**	**PQ613605**
Ni. guilinensis	**CGMCC 3.18124**	**KX985983**	**KY019459**	**KY019292**
Ni. hainanensis	**CGMCC 3.18129**	**KX986091**	**KY019464**	**KY019415**
Ni. humicola	**CFCC 56884**	**ON555686**	**ON557392**	**ON557394**
Ni. lacticolonia	**GMCC 3.18123**	**KX985978**	**KY019458**	**KY019291**
Ni. macarangae	**MFLUCC 18-0553**	**MW063171**	**N/A**	**N/A**
Ni. magnoliae	**MFLUCC 19-0112**	**MW285092**	**MW438334**	**N/A**
Ni. manihoticola	**URM8461**	**OM265224**	**OM869479**	**OM914791**
Ni. marylouisemclawsiae	**BRIP 74865b**	**PP125567**	**PP209362**	**PP209361**
Ni. mercuriadeae	**BRIP 75764a**	**PP707904**	**PP712794**	**PP712793**
Ni. musae	**CBS 319.34**	**KX986076**	**KY019455**	**KY019419**
Ni. oryzae	LC 6761	KX986056	KY019574	KY019376
Ni. osmanthi	**CGMCC 3.18126**	**KX986010**	**KY019461**	**KY019421**
Ni. pernambucoensis	**URM8463**	**OM265234**	**OM869481**	**OM914793**
Ni. philosophiae-doctoris	**CGMCC 3.20540**	**OK335213**	**OK431483**	**OK431489**
Ni. platycladi	**CFCC 72632**	**PV759478**	**PV855114**	**PV820528**
Ni. pubelensis	**KUNCC23-16745**	**PQ553686**	**PQ613608**	**PQ613603**
Ni. pyriformis	**CGMCC 3.18122**	**KX985940**	**KY019457**	**KY019290**
Ni. rubi	**CGMCC 3.18326**	**KX985948**	**KY019475**	**KY019302**
Ni. saccharicola	**CGMCC 3.19362**	**MN215788**	**MN329951**	**MN264027**
Ni. sacchari-officinarum	**CGMCC 3.19335**	**MN215791**	**MN329954**	**MN264030**
Ni. shadeganensis	**IRAN 4332C**	**OR478184**	**OR482438**	**OR482439**
Ni. singularis	**CGMCC 3.19334**	**MN215793**	**MN329956**	**MN264032**
Ni. sphaerica	LC 7312	KX985935	KY019618	KY019414
Ni. stoneae	**BRIP 75019a**	**OR608743**	**OR604066**	**OR604064**
Ni. tomentosae	**ZHKUCC 22-0340**	**PP759659**	**PP763296**	**PP763294**
Ni. vesicularifera	**CGMCC 3.19333**	**MN215812**	**MN329975**	**MN264051**
Ni. vesicularis	**CGMCC 3.18128**	**KX986088**	**KY019463**	**KY019294**
Ni. yunnanensis	**GUCC24-0008**	**PP915796**	**PP947937**	**PP947933**
Ni. zimmermanii	**CBS 290.62**	**KY385309**	**KY385317**	**KY385311**

Ex-type/ex-epitype/ex-neotype/ex-lectotype strains and voucher strains are in bold. Sequences that are not available are represented by N/A.

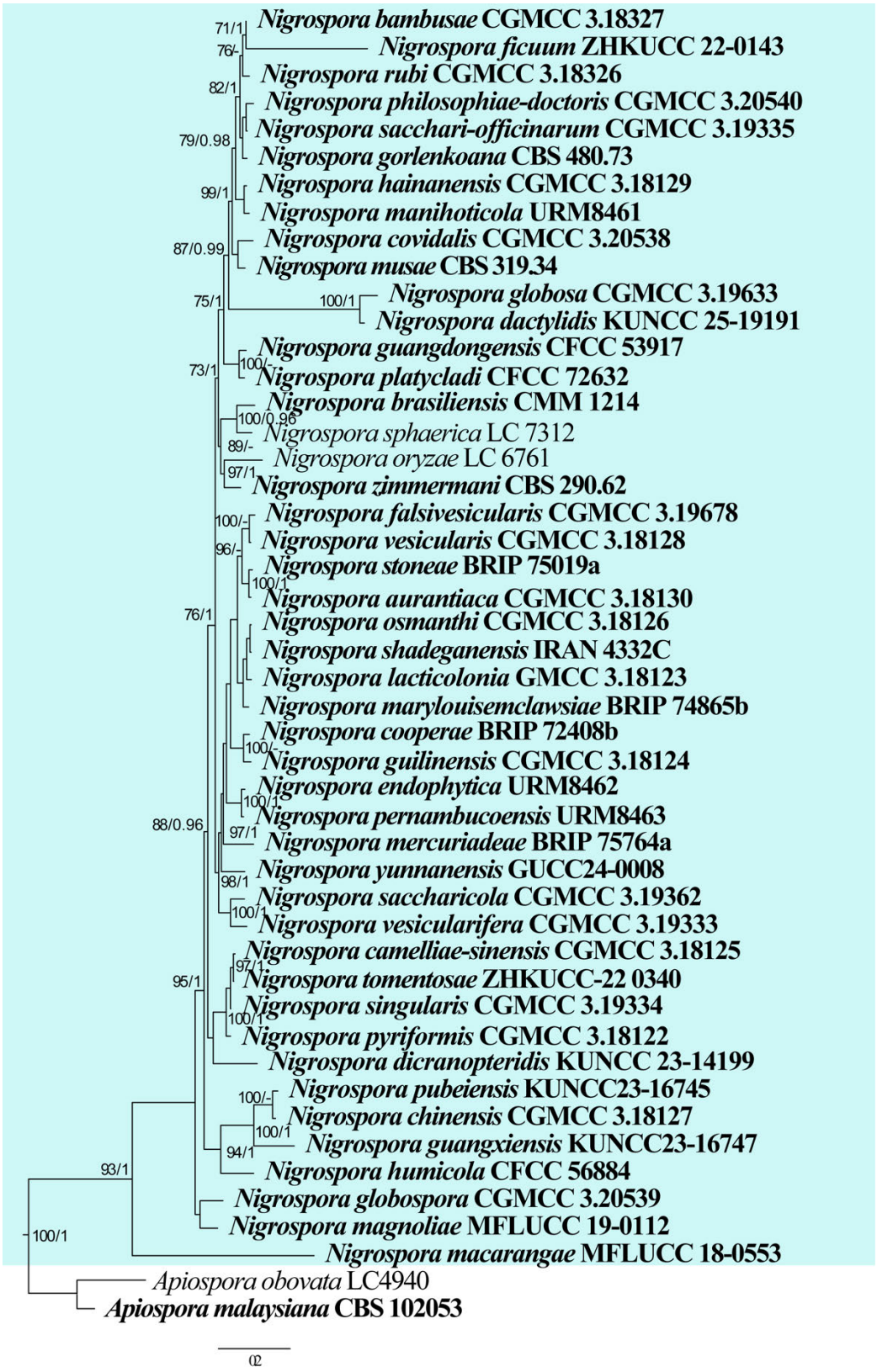

Fig. 24 Maximum likelihood tree of *Nigrospora* species based on the concatenated ITS, *tub2*, and *tef* sequence data. The best scoring RAxML tree had a final likelihood value of -12521.122218. The tree was rooted with *Apiospora* species. Estimated base frequencies were as follows: A = 0.215197, C = 0.302061, G = 0.242950, T = 0.239792; substitution rates AC = 1.163224, AG = 3.223818, AT = 0.979868, CG = 1.107217, CT = 4.753930, GT = 1.000000. ML bootstrap support values over 70% and Bayesian posterior probabilities (BPP) greater than 0.95 are indicated. Type strains are in bold. Scale bar indicates the number of substitutions per site. Hyphens (-) represent support values less than BS 70%/BPP 0.95.

137. *Oculimacula* Crous & W. Gams, Eur. J. Pl. Path. 109: 845. (2003)

Type species: *Oculimacula yallundae* (Wallwork & Spooner) Crous & W. Gams

Classification: *Leotiomycetes*, *Helotiales*, *Ploettnerulaceae*

Background: To resolve the phylogenetic position and affinity of the genus *Ramulispora* and the sexual state of the eyespot fungi in the genus *Tapesia*, Crous et al. (2003) established *Oculimacula* to accommodate *Tapesia* and *Helgardia*, the asexual morph of *Oculimacula*. Following the one fungus, one name system, Johnston et al. (2014) treated the name *Oculimacula* as the eyespot disease complex instead of using *Helgardia*. They also placed *H. aestiva* (Nirenberg) Crous & W. Gams and *H. anguioides* (Nirenberg) Crous & W. Gams in *Oculimacula* as *O. aestiva* (Nirenberg) Crous and *O. anguioides* (Nirenberg) Crous, respectively (Johnston et al. 2014). Marin-Felix et al. (2019b) provided details of *Oculimacula* and provided the genetic information to identify the genus. Crous et al. (2021a) redefined *Oculimacula* by analysis of genetic sequence comparisons of ITS, *tef*, *act*, *rpb1, rpb2* and LSU sequences. Subsequently, *Oculimacula* was reduced to two species, *O. acuformis* and *O. yallundae*, with *O. aestiva* placed in *Cyphellophora* and *O. anguioides* accommodated in a new genus, *Helgardiomyces* (Crous et al. 2021a, King et al. 2021). *Oculimacula yallundae* and *O. acuformis* induce the disease eyespot (Robertse et al. 1995, Crous et al. 2003, Ray et al. 2006, King et al. 2021). In temperate climates, eyespot is regarded as the most serious stem base disease of cereals (Crous et al. 2003, Ray et al. 2006). Field diagnosis of eyespot can be difficult since other diseases cause similar symptoms, complicating eyespot therapy techniques (King et al. 2021).

Distribution: Africa, Australasia, USA, UK, Western Europe, and other temperate areas of the world (Farr & Rossman 2025)

Disease symptoms: *Oculimacula* species are soil-borne, facultative fungi that cause eyespot disease of wheat (Fig. 25). It comprises a major component of the stem-base disease complex of wheat in temperate regions of the world with a cool and wet climate (Lucas et al. 2000, Crous et al. 2003, Wei et al. 2011). Eyespot disease of wheat generally occurs in autumn. The pathogen first infects the coleoptiles of wheat, then develops into the stem sheaths and stalks, producing typical eyespot lesions. In general, eyespot lesions form on leaf sheaths and culms that are close to the soil. The lesions cause yellowing of the straw, often with a black pupil-like spot in the center surrounded by a green-brown to dark brown ring. When the infection is severe, the wheat stems are weakened at the point of infection, making them prone to lodging, twisting, bending, and even breaking from the lesions (Lucas et al. 2000, Prescott et al. 2007, Wei et al. 2011, King et al. 2021). Eyespot lesions can cause moderate or severe damage to wheat, interfering with the movement of nutrients and water through the stem, resulting in a loss of wheat yield (Glynne & Salt 1958, Clarkson 1981, Lucas et al. 2000, Crous et al. 2003).

Hosts: *Oculimacula* has a wide range of hosts in cereals and wild grass species belonging to *Poaceae*, such as *Bromus diandrus*, *Hordeum leporinum*, *Holcus lanatus*, wheat, barley, rye, and oats with wheat being the most susceptible (Wallwork 1987, Murray et al. 1994, Lucas et al. 2000, Dyer & Bradshaw 2002, Chapman et al. 2008, Farr & Rossman 2025).

Pathogen biology, disease cycle and epidemiology: Eyespot is caused by the pathogens *Oculimacula acuformis* and *O. yallundae* (Marin-Felix et al. 2019b). Both *Oculimacula* species can enter the outer leaf sheath of the host directly through the epidermal cells or more commonly through the stomata. Normally, the fungi form a stroma on the host surface, from where infection occurs, and they then continue to grow, forming a pupil-like lesion and killing the tiller before the host head sprouts (Sprague & Fellows 1934). *Oculimacula* spp. develop in the host and produce many conidia in spring and autumn. The conidia are spread by rain splash. *Oculimacula* also reproduce sexually, producing ascospores that can lead to more infections. There is a second pathway of dispersal for spores in that a few spores can be transmitted and infect new hosts through the air, but Foëx and Rosella (1930) indicated that this conclusion needs to be confirmed by further research. *Oculimacula* spp. overwinter on diseased plants, and in spring produce spores that infect the newly seeded host (Sprague & Fellows 1934, Murray 1996, Douhan et al. 2002).

Morphological-based identification: *Oculimacula* produces sessile ascomata that are gregarious, circular to lobate and are formed on a subiculum of white to dark brown hyphae that are linked to the substrate by a superficial mat of light brown substratum. The apothecia are grey with a pale grey margin, emarginate and flattened to convex when they reach maturity. The receptacle is cup-shaped and pale brown to grey-brown. The medullary excipulum is composed of multiseptate, hyaline hyphae. The ectal excipulum of thin-walled, dark brown, angular cells, becomes more elongated towards the margin. Filiform paraphyses have obtuse ends and are as long as the asci. Asci are 8-spored, clavate to subcylindrical or fusoid, with a short stalk and an apical pore that can be stained blue by Melzer's reagent. Ascospores are mostly straight, bi- to multiseriate, hyaline, smooth, aseptate, fusoid to subcylindrical or clavate with rounded ends (Crous et al. 2003, Marin-Felix et al. 2019b).

Molecular-based identification: Crous et al. (2003) established this genus by using ITS and LSU sequences. The phylogenetic analysis indicates that there are four species in this genus (including the asexual morph of *Oculimacula*). Johnston et al. (2014) treated *Oculimacula* to include the asexual morph, *Helgardia*, based on the principle of “One fungus one name”. Marin-Felix et al. (2019b) provided identification of genes from species to genus and species levels. Crous et al. (2021a) redefined *Oculimacula* based on ITS, *tef*, *act*, *rpb1*, *rpb2*, and LSU sequences. When combined with morphological features, this genus is restricted to two species, both of which are important wheat pathogens (Crous et al. 2021a, King et al. 2021). This study provides an updated phylogeny of *Oculimacula* based on combined ITS, LSU, *act*, *rpb2* and *tef* sequence data (Fig. 26, Table 13).

Recommended genetic markers (genus level): LSU

Recommended genetic markers (species level): ITS, LSU, *act*, *rpb2* and *tef*

Accepted number of species: two

Reference: Crous et al. (2021a) (morphology and phylogeny)

138. *Phaeosphaeriopsis* M.P.S. Câmara, M.E. Palm & A.W. Ramaley, in Câmara et al., Mycol. Res. 10(5): 51 (2003)

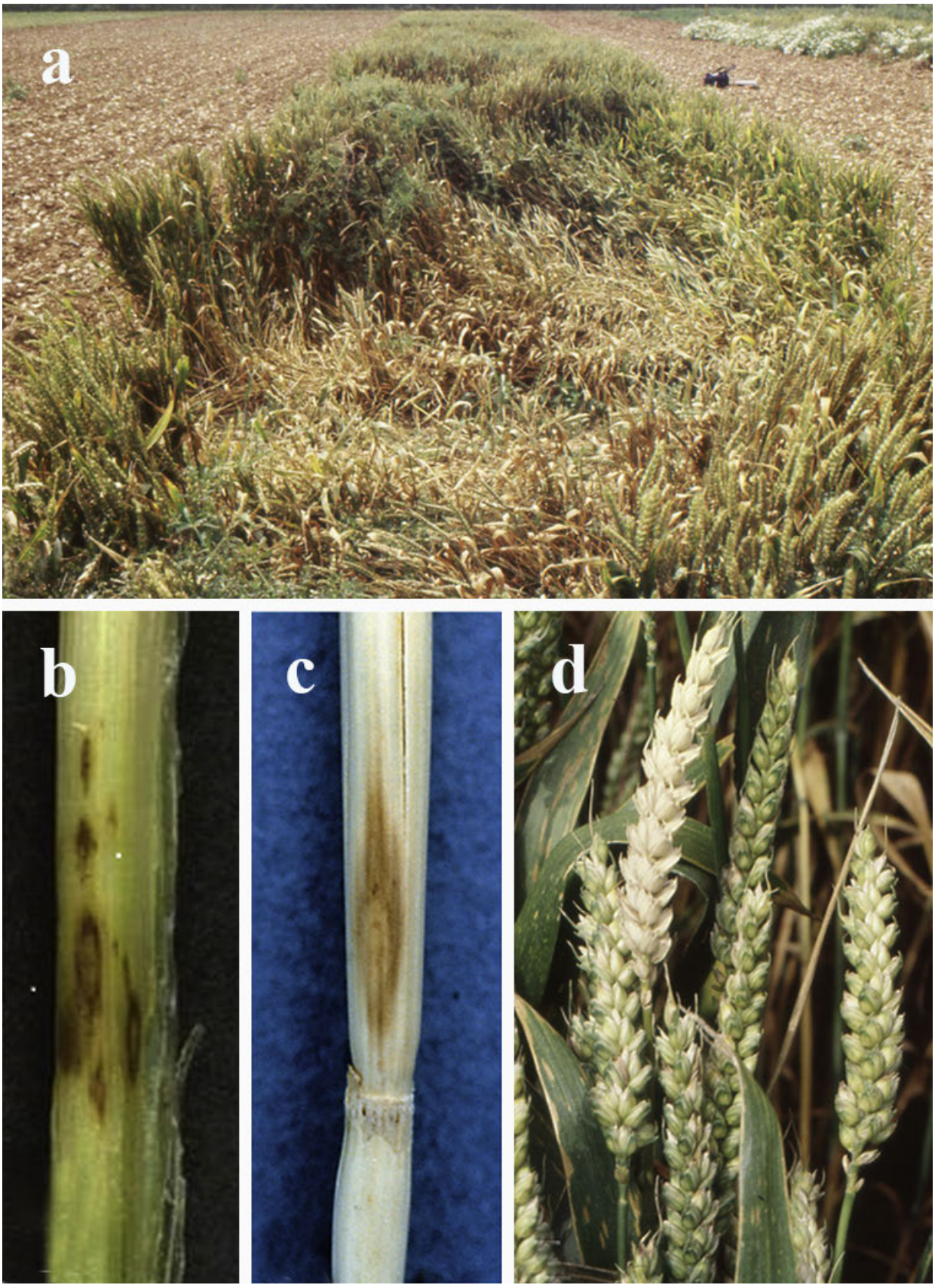

Fig. 25 Symptoms caused by *Oculimacula* sp. on wheat. a Eyespot lodging. b-c Eyespots. d Whiteheads of wheat. This picture is copyright of Pedro Crous (Marin-Felix et al. 2019b).

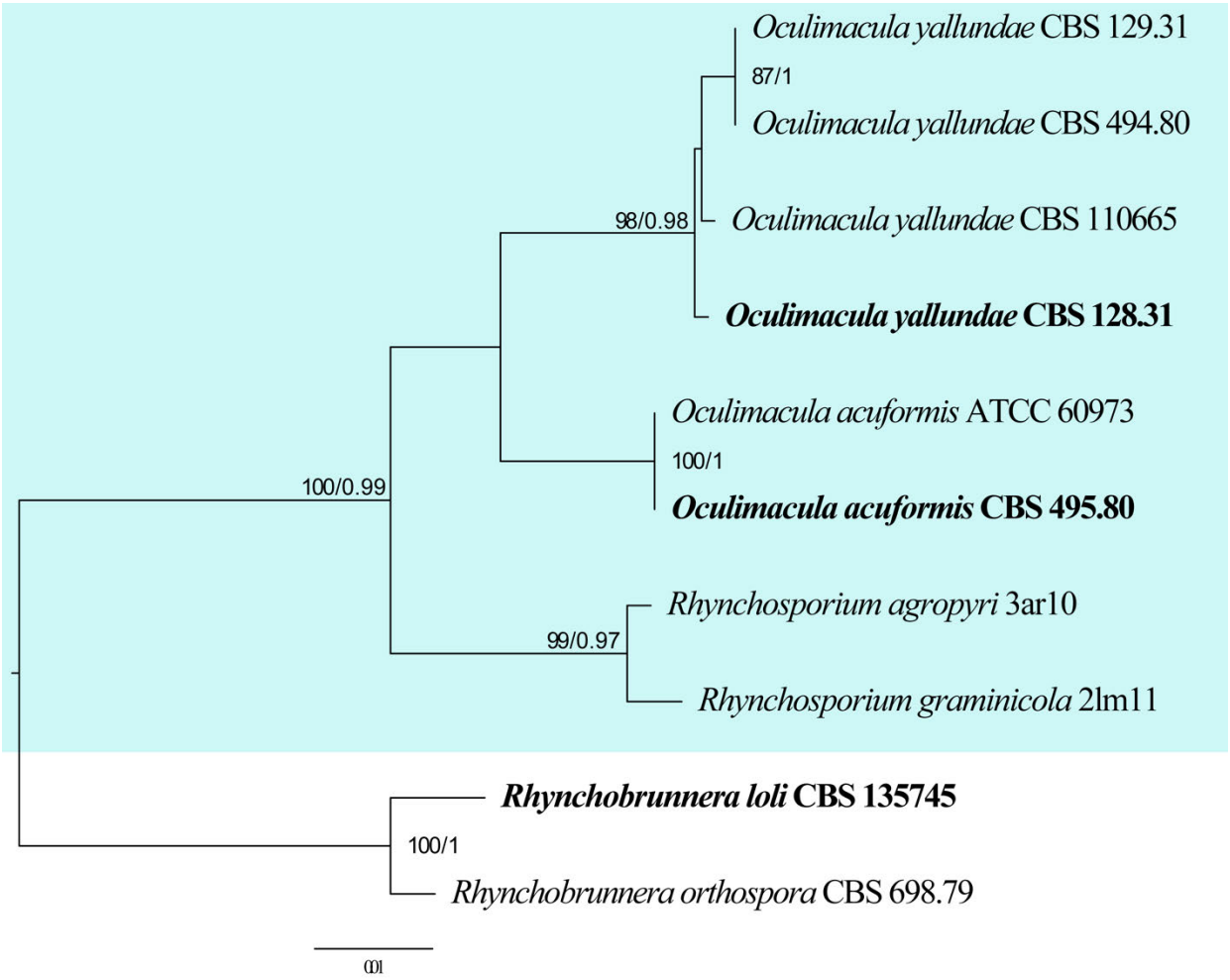

Fig. 26 Maximum likelihood tree of *Oculimacula* species based on the concatenated ITS, LSU, *act*, *rpb2* and *tef* sequence data. The best scoring RAxML tree had a final likelihood value of -6423.795453. The tree was rooted with *Rhynchobrunnera agropyri* (CBS 146762). Estimated base frequencies were as follows: A = 0.245708, C = 0.247574, G = 0.253386, T = 0.253333; substitution rates AC = 1.294731, AG = 2.248453, AT = 1.136711, CG = 0.484296, CT = 6.594746, GT = 1.000000. ML bootstrap support values over 70% and Bayesian posterior probabilities (BPP) greater than 0.95 are indicated. Scale bar indicates the number of substitutions per site. Hyphens (-) represent support values less than BS 70%/BPP 0.95.

Table 13 DNA barcodes for accepted species of *Oculimacula*.

Species	Strain	GenBank accession numbers				
		ITS	LSU	*act*	*rpb2*	*tef*
Oculimacula acuformis	**CBS 495.80**	**MH861289**	**MW298379**	**MW297203**	**MW297374**	**MG934497**
O. acuformis	ATCC 60973	AY266146	N/A	N/A	N/A	N/A
O. yallundae	**CBS 128.31**	**MG934457**	**MW298401**	**MW297224**	**MW297395**	**MG934499**
O. yallundae	CBS 129.31	MH855155	MH866603	MW297225	MW297396	N/A
O. yallundae	CBS 494.80	JF412009	MW298402	N/A	N/A	MG934500
O. yallundae	CBS 110665	MG934456	MW298399	MW297223	MW297394	MG934498

Ex-type/ex-epitype/ex-neotype/ex-lectotype strains and voucher strains are in bold. Sequences that are not available are represented by N/A.

Type species: *Phaeosphaeriopsis glaucopunctata* (Grev.) M.P.S. Câmara, M.E. Palm & A.W. Ramaley

Classification: *Dothideomycetes*, *Pleosporales*, *Phaeosphaeriaceae*

Background: *Phaeosphaeriopsis* was established by Câmara et a l. (2003) to include several species which could not be categorized as *Paraphaeosphaeria* based on morphological characters and SSU molecular data. Câmara et al. (2003) transferred *Paraphaeosphaeria agavensis*, *Pa. glauco-punctata*, *Pa. nolinae* and *Pa. obtusispora* to *Phaeosphaeriopsis* and described a new species *P. amblyspora*. *Phaeosphaeriopsis* represents species that produce uni- or

multi-loculate stromata, 4–5-septate, punctate or verrucose ascospores and have asexual morphs characterized by 0–3-septate, cylindrical, brown conidia or sometimes bacillar microconidia (Câmara et al. 2003, Phookamsak et al. 2014, Thambugala et al. 2014, Marin-Felix et al. 2019a).

Distribution: worldwide (Farr & Rossman 2025)

Disease symptoms: *Phaeosphaeriopsis* species can cause leaf spots and leaf on several hosts (Fig. 27). *Phaeosphaeriopsis glauco-punctata* has been reported as the causative agent (as "*Paraphaeosphaeria glauco-punctata*" in earlier studies) of leaf spot and necrosis on *Ruscus* (Camara et al. 2001). The symptoms are 2 mm wide, discoloured lesions that gradually develop into larger brown necrotic lesions. When infection is severe, these lesions coalesce and form large necrotic regions sometimes leading to leaf necrosis (Camara et al. 2001, Golzar & Wang 2012).

Hosts: *Phaeosphaeriopsis glauco-punctata* and *Pa. triseptata* have been reported on various *Ruscus* spp. from Europe. *Phaeosphaeriopsis amblyspora* was described from dead leaves of *Yucca baccata* (Câmara et al. 2003). *Phaeosphaeriopsis agapanthi* was isolated from *Agapanthus precox*. *Phaeosphaeriopsis agavacearum* and *Pa. pseudo-agavacearum* have been reported from *Agave* sp. (Crous et al. 2016a, b). *Phaeosphaeriopsis aloes* and *Pa. aloicola*, were both recorded from leaves of *Aloe* sp. in the USA (Marin-Felix et al. 2019a). *Phaeosphaeriopsis musae* was associated with leaf spots on *Musa* sp. (Arzanlou and Crous 2006). *Phaeosphaeriopsis dracaenicola* was reported from *Dracaena loureiroi* in Thailand (Phookamsak et al. 2014), while *Phaeosphaeriopsis grevilleae* was collected on leaves of *Grevillea* sp. from Queensland, Australia (Marin-Felix et al. 2019a). *Phaeosphaeriopsis beaucarneae* was isolated from dead leaves of *Beaucarnea recurvata* (Tennakoon et al. 2020). *Phaeosphaeriopsis omaniana, Pa. sansevieriae* and *Pa. triseptata* were isolated from the leaves of *Dracaena serrulata*, *Sansevieria hyacinthoides* and *Ruscus aculeatus*, respectively (Thambugala et al. 2014, Al-Jaradi et al. 2020, Crous et al. 2021b, Farr & Rossman 2025).

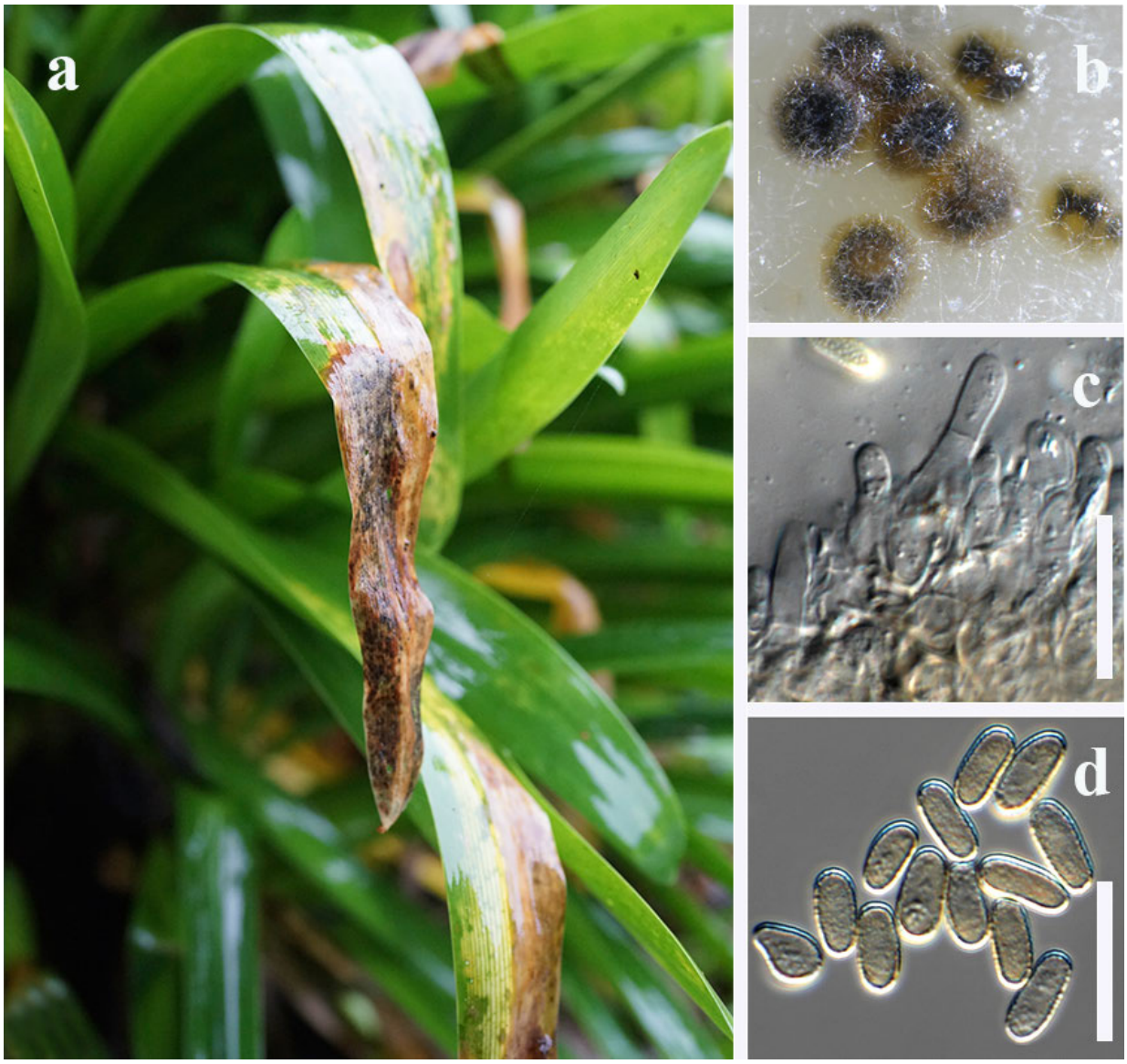

Fig. 27 a Symptoms caused by *Phaeosphaeriopsis* sp. on *Agapanthus precox*. b Conidiomata sporulating on pine needle agar. c Conidiogenous cells giving rise to conidia. d Conidia. Scale bars: c-d = 10 µm. This picture is copyright of Pedro Crous (Crous et al. (2016b) and Marin-Felix et al. (2019a)).

Phaeosphaeriopsis consists mostly of saprobic species. However, *Phaeosphaeriopsis glaucopunctata* has been reported to cause leaf spot and necrosis in *Ruscus aculeatus* (Câmara et al. 2003, Golzar & Wang 2012). *Phaeosphaeriopsis agapanthi* on *Agapanthus precox* and *P. dracaenicola* on *Dracaena lourieri* have been associated with causing necrotic leaf spots on these hosts (Phookamsak et al. 2014, Crous et al. 2016a). *Phaeosphaeriopsis musae* is assumed to be a weak pathogen or secondary invader (Arzanlou & Crous 2006) as it has often been found associated with leaf lesions of *Mycosphaerella fijiensis, Sphaerulina musae* and *Cordana musae*. The first report of *Pa. glaucopunctata* causing leaf spot and foliage necrosis on *Ruscus aculeatus* in Australia was reported by Golzar & Wang (2012).

Pathogen biology, disease cycle and epidemiology: Many *Phaeosphaeriopsis* species are associated with leaf spots, blights, or necrotic lesions (Camara et al. 2001, Golzar & Wang 2012). *Phaeosphaeriopsis* are generally considered necrotrophic pathogens and they often affect stressed or senescing plant material (Phookamsak et al. 2014, Thambugala et al. 2014, Marin-Felix et al. 2019a). *Phaeosphaeriopsis* species release spores under moist conditions, which are spread by rain splash, wind, or mechanical means (van Niekerk et al. 2010). The disease cycle begins when spores land on susceptible plant surfaces and germinate under high humidity or prolonged leaf wetness. Infection often starts at the leaf margins or tips, especially where mechanical damage or stress is present (Adaskaveg et al. 2008, Gonçalves et al. 2013). Lesions typically expand during periods of wet weather, favouring rapid disease development. The fungus survives between growing seasons as saprobes on crop residues or in infected plant tissue (Adaskaveg et al. 2008, van Niekerk et al. 2010).

Morphological-based identification: *Phaeosphaeriopsis* species produce uni- or multi-loculate stromata, scattered, semi-immersed to erumpent, globose to subglobose, ostiolate ascomata, cylindrical to broadly fusoid or clavate asci and 4–5-septate, yellowish to light brown, verrucose ascospores. The asexual morph is coniothyrium-like or phaeostagonospora-like (Câmara et al. 2003, Quaedvlieg et al. 2013, Thambugala et al. 2014, Marin-Felix et al. 2019a). Morphologically, the conidia are similar to *Paraphaeosphaeria* species but can be distinguished based on the different number of septa in ascospores (4–5-septate conidia vs. 2-septate ascospores) and asexual morphs (Câmara et al. 2003). Only a few species have both sexual and asexual morphs e.g. *Pa. beaucarneae* isolated from *Beaucarnea recurvata* (Tennakoon et al. 2020). For species such as *Pa. agapanthi*, *Pa. aloes*, *Pa. grevilleae*, *Pa. pseudoagavacearum*, *Pa. sansevieriae* and *Pa. triseptata*, only the asexual morph is known and for example in *Pa. aloicola* and *Pa. obtusispora* only the sexual morph is known. The asexual morphs of *Pa. amblyspora* and *Pa. agavensis* produce hyaline, bacillar conidia from simple phialides. The asexual morphs of *Pa. glauco-punctata*, *Pa. obtusispora*, and *Pa. nolinae* produce brown conidia from percurrently proliferating conidiogenous cells. In *Pa. nolinae*, the conidia are 3-septate and in *Pa. glauco-punctata* often 1-septate, while those in *Pa. obtusispora* are usually aseptate (Câmara et al. 2003, Thambugala et al. 2014). Thambugala et al. (2014) suggested that it was unlikely that *Pa. phacidiomorpha* belonged to *Phaeosphaeriopsis* due to its different asci characters, hyaline ascospores and microsphaeropsis-like asexual morphs. This requires further investigation. Thus, *Phaeosphaeriopsis* is a genus that requires more collections in order to establish its taxonomic boundaries, sexual-asexual connections and diversity.

Molecular-based identification: Thambugala et al. (2014) accepted seven species in *Phaeosphaeriopsis* based on multi-gene analysis of LSU, SSU, ITS and *rpb2* regions but excluded *P. musae*. However, in our phylogenetic analysis, the type strain of *P. musae* was included, and it grouped with other species of the genus. Marin-Felix et al. (2019a) accepted 15 species, including four new species in *Phaeosphaeriopsis* based on multi-gene analysis of ITS, LSU, *rpb2*, *tef* and *tub2* genes.

Phaeosphaeriopsis pseudoagavacearum is closely related to *Pa. agavacearum* (Marin-Felix et al. 2019a) and both were recorded from *Agave* sp. However, *Pa. aloes* and *Pa. aloicola*, which were isolated from *Aloe* sp. are phylogenetically distant, with *Pa. aloes* more closely related to *Pa. obtusispora* and *Pa. aloicola* to *Pa. agapanthi* (Marin-Felix et al. 2019a). A similar result was also observed in our phylogenetic analysis. This study provides an updated phylogeny of *Phaeosphaeriopsis* based on combined ITS, LSU, *rpb2* and *tef* sequence data (Fig. 28, Table 14).

Recommended genetic markers (genus level): LSU

Recommended genetic markers (species level): ITS, LSU, *rpb2* and *tef*

Accepted number of species: 20

References: Câmara et al. (2003), Thambugala et al. (2014), Marin-Felix et al. (2019a), Sun et al. (2025) (morphology and phylogeny); Golzar & Wang (2012) (pathogenicity)

Table 14 GenBank accession numbers for accepted species of *Phaeosphaeriopsis*.

Species	Strain	GenBank accession numbers			
		ITS	LSU	*rpb2*	*tef*
Phaeosphaeriopsis agapanthi	**CPC 26303**	**KX228260**	**KX228311**	**MK540094**	**MK540157**
P. agavacearum	**CPC 29122**	**KY173430**	**KY173520**	**KY173591**	**MK540158**
P. agavensis	**CBS 102206**	**KY090635**	**KY090669**	**KY090685**	**N/A**
P. aloes	**CBS 145367**	**MK539959**	**MK540030**	**MK540090**	**MK540153**
P. aloicola	**CBS 145368**	**MK539960**	**MK540031**	**MK540091**	**MK540154**
P. amblyospora	**CBS 110131**	**MH862851**	**MH874443**	**N/A**	**N/A**
P. beaucarneae	**MFLU 18-2586**	**MT321799**	**MT321813**	**N/A**	**MT328756**
P. dracaenicola	**MFLUCC 11-0157**	**KM434273**	**KM434283**	**KM434310**	**KM434301**
P. glaucopunctata#	**MFLUCC 13-0265**	**KJ522473**	**KJ522477**	**N/A**	**MG520918**

P. grevilleae	**CBS 145369**	**MK539961**	**MK540032**	**MK540092**	**MK540155**
P. musae	**CPC 11238**	**DQ885894**	**GU301862**	**GU357748**	**GU349037**
P. nolinae	CBS 102205	KY090637	KY090667	KY090686	N/A
P. oblongispora	**GUCC 24-0087**	**PQ325281**	**PQ578307**	**N/A**	**N/A**
P. obtusispora	CBS 246.64	KY090644	JX681119	KY090688	N/A
P. omanana	**SQUCC:14333**	**MT075840**	**MT075849**	**N/A**	**N/A**
P. phacidiomorpha	**CBS 198.35**	**FJ462742**	**AF275496**	**N/A**	**N/A**
P. pseudoagavacearum	**CBS 145370**	**MK539962**	**MK540033**	**MK540093**	**MK540156**
P. sansevieriae	**CBS 146984**	**MZ064438**	**MZ064495**	**MZ078204**	**N/A**
P. triseptata	**MFLUCC 13-0271**	**KJ522475**	**KJ522479**	**KJ522485**	**MG520919**
P. yuccae	**MFLUCC 16-0558**	**KY554482**	**KY554481**	**N/A**	**MG520920**

Ex-type/ex-epitype strains are in bold. Sequences that are not available are represented by N/A. Species confirmed with pathogenicity studies are marked with #.

139. *Phakopsora* Dietel, Ber. Dtsch. Bot. Ges.13: 333 (1895)

Type species: *Phakopsora punctiformis* (Barclay & Dietel) Dietel

Classification: *Pucciniomycetes, Pucciniales, Phakopsoraceae*

Background: *Phakopsora* was proposed by Dietel (1895) with *Phakopsora punctiformis* as the type species. *Phakopsora* is commonly known to cause rust disease on soybeans. With 116 named species (Wijayawardene et al. 2020, 2022), *Phakopsora* has been reported to occur all over the world on more than 150 genera and 30 families of monocots and dicots (Cummins & Hiratsuka 2003). Asian soybean rust, a disease of global importance caused by these fungi proved their significance to be studied all across the globe. Apart from soybeans and other members of *Fabaceae*, these fungi also cause serious leaf rust diseases on grapevine and other vitaceous plants (Chatasiri & Ono 2008, Okane & Ono 2018), cotton (Gjaerum 1985), *Eucalyptus* (Maier et al. 2016) and many more agricultural, horticultural and forest plant hosts. Species of *Phakopsora* has become well known and widely studied globally; becoming a fungus of plant quarantine importance. Recently, this fungus has been reported from the western hemisphere for the first time. Although reported continuously from Asia for decades, its virulence on important soybean crops and first-time entry in this region poses a serious threat to these crops (Frederick 2002). These fungi, however, are distributed mostly in warmer regions of the world.

Distribution: Africa, Australia, Bangladesh, Bolivia, Brazil, Cameroon, China, Chile, Costa Rica, Ecuador, Eritrea, Ghana, India, Ivory Coast, Indonesia, Japan, Kenya, Madagascar, Myanmar, Namibia, Pakistan, Philippines, South Africa, Sudan, Tanzania, Tibet, Uganda, USA and Venezuela (Farr & Rossman 2025)

Host: on species of *Alseis*, *Campomanesia*, *Desmodium*, *Dicotyledonae*, *Erythrina*, *Eucalyptus*, *Ficus*, *Glochidion*, *Grewia*, *Kirganelia*, *Kraunhia*, *Litsea*, *Loudetia*, *Mallotus*, *Melhania*, *Merremia*, *Myrtaceae*, *Odina*, *Pachyrhizus, Phyllanthus*, *Psoralea*, *Randia*, *Schrebera*, *Senna*, *Setaria*, *Sickingia*, *Sterculia*, *Stereospermum*, *Terminalia*, *Tiarella*, *Vernonia*, *Vitis* (Farr & Rossman 2025).

Disease symptoms: *Phakopsora* is most commonly known to occur on soybeans and other members of *Fabaceae* (Fig. 29). The disease symptoms start as small tan or red-brown lesions mostly on the lower leaf surface in which pustules (Uredinia) are formed. Each small lesion often has several pustules (uredinia) which ultimately contain urediniospores. At the time of sporulation, the raised pustules (uredinia) can be seen. These small pustules turn into brown to brownish pustules (telia) with the progression of the disease. Most of the disease symptoms appear on leaves, but can also be seen on petioles, stems and even on cotyledons. However, the characteristics (symptoms and signs) of rust lesions/pustules (uredia and telia) of these fungi may differ slightly on different hosts.

Pathogen biology, disease cycle and epidemiology: *Phakopsora pachyrhizi* on Soybean, and *Ph. gossypii* on cotton, are economically important rust fungi. Soybean rust disease starts with the infection due to arrival of airborne inoculum (urediniospores). *Phakopsora* penetrates the leaf tissue directly through stomata, forming haustoria that extract nutrients and suppress host defences. The disease cycle is polycyclic, with multiple generations of urediniospores produced throughout the growing season, contributing to epidemics under conducive environmental conditions (Hartman et al. 2005). Many alternative hosts may act as sources of inoculum of this rust genus. *Desmodium* sp. (clover), *Cassia occidentalis* (coffee senna) and *Macroptilium lathyroides* are some alternative hosts of soybean rusts reported by Torres et al. (2012). The spores of these rust fungi are sensitive to ultraviolet radiations, the areas that experience chilling temperatures and frost may protect them from these radiations. In addition, storms may favour the long-distance movement of these rust spores (Rupe & Sconyers 2008).

Morphological-based identification: Morphological and microscopic studies of *Phakopsora* spp. shows that these fungi have subcuticular, Group IV (type 7) spermogonia. This genus produces subepidermal, erumpent aecia which are of *Calidion*-type or *Milesia*-type. The aeciospores are similar to urediniospores and borne singly. Uredinia are sub-epidermal, erumpent, with or without paraphyses. In cases, with peripheral, surmounting peridial tissue, uredinia are of *Malupa*- and *Calidion*-type, while *Uredo*-type are without paraphyses. Urediniospores are brownish or nearly colourless with scattered and equatorial pores, echinulate and borne singly. Telia are sub-epidermal, form coverings of 2 or more cells deep, laterally supportive to teliospores. Teliospores are 1-celled with brown or brownish walls, without stalk (sessile), borne in chain (catenulate) or arranged irregularly. Teliospores contain single apical germ pores and

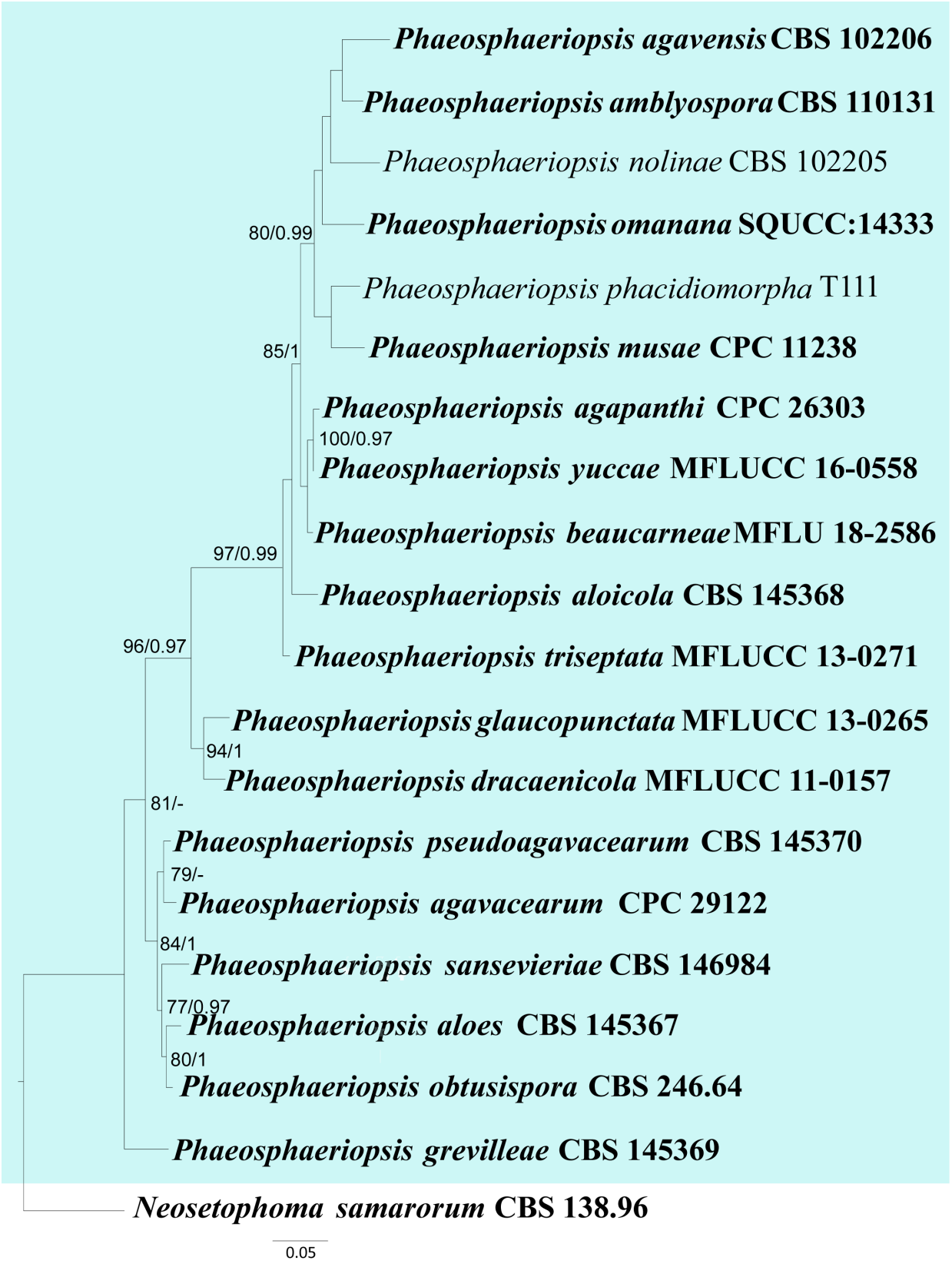

Fig. 28 Maximum likelihood tree of *Phaeosphaeriopsis* species based on the concatenated ITS, LSU, *rpb2* and *tef* sequence data. The best scoring RAxML tree had a final likelihood value of -125.662246. The tree was rooted to *Neosetophoma samarorum* (CBS 138.96). Estimated base frequencies were as follows: A = 0.245606, C = 0.2343, G = 0.26123, T = 0.254233; substitution rates AC = 1.356002, AG = 3.20, AT = 1.2506, CG = 0.3613, CT = .31121, GT = 1.000000. ML bootstrap support values over 70% and Bayesian posterior probabilities (BPP) greater than 0.95 are indicated. Type strains are in bold. Scale bar indicates the number of substitutions per site. Hyphens (-) represent support values less than BS 70%/BPP 0.95.

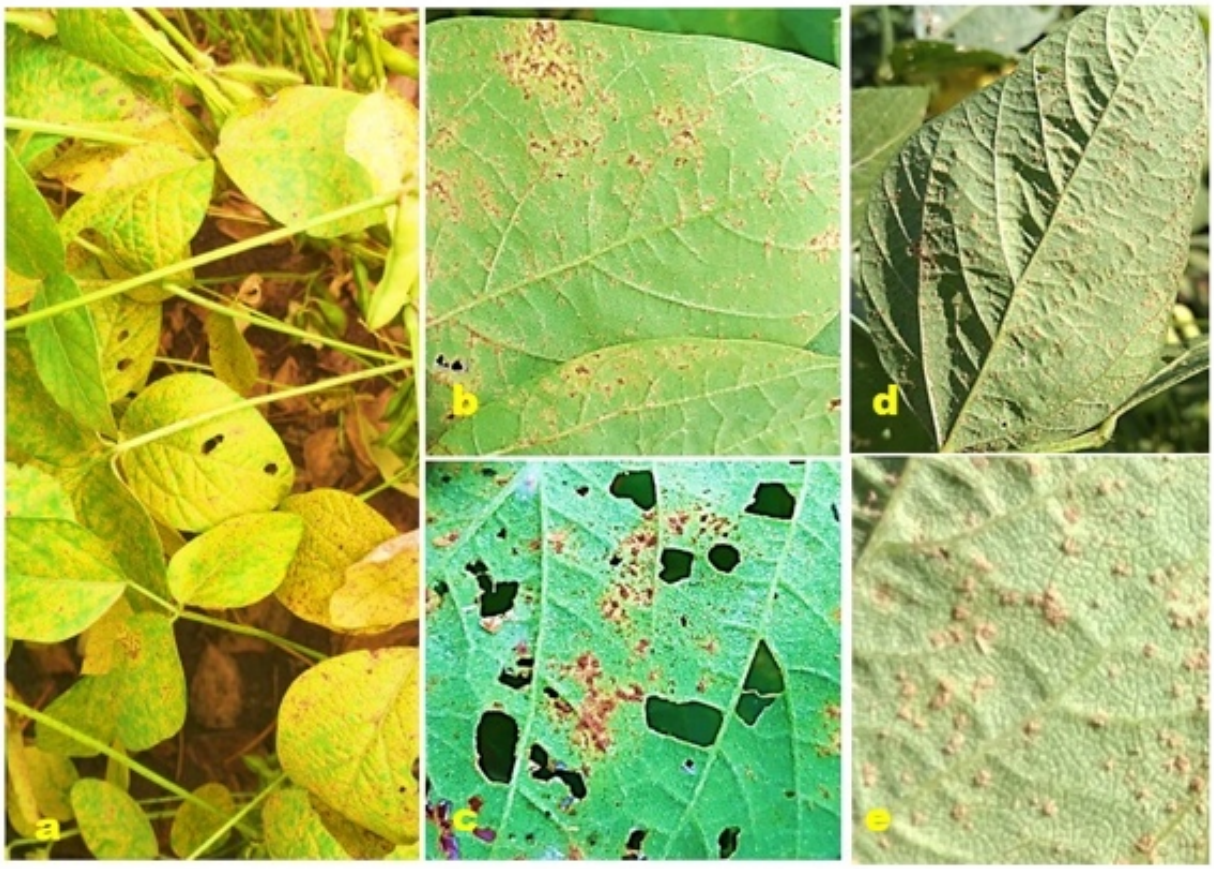

Fig. 29 *Phakopsora* sp. on *Glycine max* (Soybean). a Infected leaves of Soybean with *Phakopsora* sp., b-e Infected host plant with rust sori at various stages of infection. This picture is copyright of Ajay Kumar Gautam, Shubhi Avasthi and Rajnish Kumar Verma.

germinate generally after the dormancy period. These fungi comprise external basidia (Cummins and Hiratsuka 2003).

Molecular-based identification: The molecular studies of *Phakopsora* using different gene loci have been carried out. Two closely related species of *Phakopsora* viz. *Ph. pachyrhizi* and *Ph. meibomiae* reported to cause soybean rust, were identified using nucleotide sequence of the internally transcribed spacer (ITS) region (Frederick et al. 2002). The molecular analyses of 45 collections (44 with ITS2 and 33 with D1/D2 sequences, 32 common in both ITS and D1/D2 sequences analyses) of heteroecious *Ph. euvitis*, *Ph. vitis*, and *Ph. ampelopsidis*, autoecious *Ph. meliosmae* grouped them into seven clades *(*Chatasiri & Ono 2008). The analysis of the mitochondrial (*mt*) genomes of *Ph. pachyrhizi* and *Ph. meibomiae* was carried out by Stone et al. (2010). The circular *mt* genome of both species consists of 31,825 base pair with a mean GC content of 34.6% in *Ph. pachyrhizi* compared to 32,520 base pair with a mean GC content of 34.9% in *Ph. meibomiae.* Phylogenetic analysis of 14 protein-coding genes in *mt* genomes of both species of *Phakopsora* confirmed their taxonomic identity (Stone et al. 2010). Analysis of the 28S ribosomal DNA, specifically D1/D2 domains of a group of 40 rust fungi collected from diverse plants in the Colombian Andean region supported the validity of rust families like *Pucciniaceae, Phragmidiaceae, Pileolariaceae, Mikronegeriaceae, Coleosporiaceae, Cronartiaceae* including *Phakopsoraceae* (Zuluaga et al. 2011). A rust disease on Asian Soybean was analyzed for the identification of the pathogen based on sequence data, and BLAST searches of the ITS region. The results of molecular analyses along with morphological characters identified the pathogen as *Phakopsora pachyrhizi* (de Jensen et al. 2013). Rust fungi on the plant *genus Annona* (*Annonaceae*) with special reference to genus *Phakopsora* were investigated morphologically and using DNA sequences. The phylogenetic analyses based on the ITS1–5.8S–ITS2 region, partial LSU and SSU of the nuclear rDNA, and the mitochondrial cytochrome oxidase subunit 3 revealed that the genus *Batistopsora* is a synonym of *Phakopsora* and was described as new species of *Phakopsora* i.e. *Ph. annonae-sylvaticae* (Beenken 2014). A rust pathogen of eucalyptus plantations and nurseries in Kenya was identified using morphological and molecular data based on ITS and LSU rDNA. After systematic evaluation, the rust pathogen was identified as *Phakopsora myrtacearum* (Maier et al. 2016). A large number of intraspecific and intragenomic variations in the ITS region of *Phakopsora pachyrhizi* was detected by Rush et al. (2019). They detected polymorphic copies of ITS within single leaf samples and even within single rust sori. This study raises caution about the use of multicopy genes (e.g., ITS) in single-gene detection assays. A recent study carried out by Aime et al. (2019) on the molecular phylogenetic analysis of *Phakopsora* revealed that *Ph. pachyrhizi* and the closely related *Ph. meibomiae* cluster in a monophyletic clade with other economically important species of *Phakopsora*, such as *Ph. myrtacearum*, *Ph. ampelopsidis* and *Ph. euvitis.* They also proposed to conserve *Phakopsora* with the new type, *Ph. pachyrhizi*, the causal organism of the globally important disease Asian

soybean rust. Recently, fresh or herbarium material of *Phakopsora* spp. (*Ph. crucis-filii, Ph. fici* and *Ph. pachyrhizi*) was examined for morpho-taxonomic analysis. Three gene loci (LSU, SSU, and *cox*) extracted from sample material were sequenced and analyzed phylogenetically which provided a better understanding in resolving an updated higher-rank classification for *Pucciniales* (Aime & McTaggart 2020). The genus has 116 accepted species based on morpho-taxonomy (Wijayawardene et al. 2020, 2022). However, sequence data is available only for 14 species of *Phakopsora* with ITS and LSU gene loci more commonly used in phylogenetic analyses. Similarly, Gautam et al. (2021) included seven species of *Phakopsora* in the phylogenetic analyses of Indian *Pucciniales* based on ITS and LSU gene regions of rDNA. This study provides an updated phylogeny of *Phakopsora* based on combined LSU and ITS sequence data (Fig. 30, Table 15).

Recommended genetic marker (genus level): ITS

Recommended genetic marker (species level): ITS, LSU

Accepted number of species: 116

References: Frederick et al. (2002), Chatasiri & Ono (2008), Stone et al. (2010), Zuluaga et al. (2011), de Jensen et al. (2013), Beenken (2014), Liu et al. (2015), Maier et al. (2016), Rush et al. (2019), Aime & McTaggart (2020), Crous et al. (2024), Sun et al. (2024) (morphology and phylogeny)

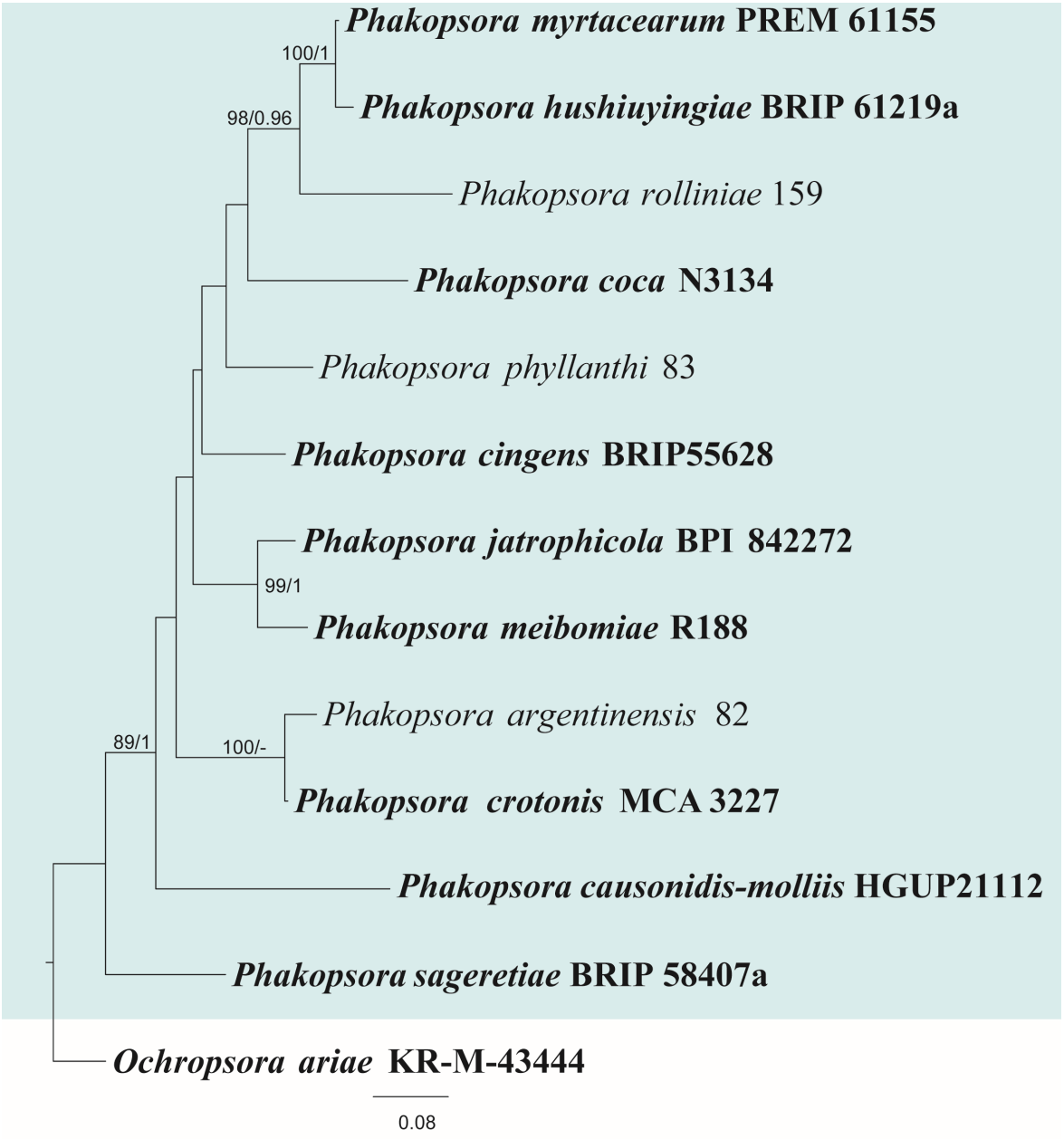

Fig. 30 Maximum likelihood tree of *Phakopsora* species based on the concatenated LSU and ITS sequence data. The best scoring RAxML tree had a final likelihood value of -8012.311729. The tree was rooted to *Ochropsora ariae* (KR-M-43444). Estimated base frequencies were as follows: A = 0.309790, C = 0.158926, G = 0.226227, and T = 0.305058; substitution rates AC = 1.138546, AG = 3.284213, AT = 2.829326, CG = 0.442988, CT = 5.536758, and GT = 1.000000. ML bootstrap support values over 70% and Bayesian posterior probabilities (BPP) greater than 0.95 are indicated. Type strains are in bold. Scale bar indicates the number of substitutions per site. Hyphens (-) represent support values less than BS 70%/BPP 0.95.

Table 15 DNA barcodes for accepted species of *Phakopsora*.

Species	Strain	GenBank accession numbers	
		ITS	LSU
Phakopsora argentinensis	82	KF528009	KF528009
Ph. causonidis-molliis	**HGUP21112**	**OR462111**	**OR462116**
Ph. cingens	**BRIP55628**	**N/A**	**KP729474**
Ph. coca	**N3134**	**HQ317532**	**HQ317532**
Ph. crotonis	**MCA 3227**	**MH790110**	**MH790110**
Ph. ericksoniae	**BRIP 60953a**	**N/A**	**PP800293**
Ph. hushiuyingiae	**BRIP 61219a**	**N/A**	**PP800294**
Ph. jatrophicola	**BPI 842272**	**N/A**	**KY764076**
Ph. meibomiae	**R188**	**N/A**	**EU851164**
Ph. myrtacearum	**PREM61155**	**NR_132913**	**NG_060142**
Ph. parthenocissi-tricuspidatae	**HGUP21115**	**OR462114**	**N/A**
Ph. phyllanthi	83	KF528025	KF528025
Ph. rolliniae	159	KF528036	KF528036
Ph. sageretiae	**BRIP 58407a**	**N/A**	**PP973746**
Ph. sophorae	**HMAS350010**	**MK488221**	**MK518529**

Ex-type/ex-epitype/ex-neotype/ex-lectotype strains and voucher strains are in bold. Sequences that are not available are represented by N/A.

140. *Pleiocarpon* L. Lombard & D. Aiello, in Aiello et al., IMA Fungus 8(1): 73 (2017)

Type species: *Pleiocarpon strelitziae* L. Lombard & D. Aiello

Classification: *Sordariomycetes*, *Hypocreales*, *Nectriaceae*

Background: *Pleiocarpon* was introduced by Aiello et al. (2017). *Pleiocarpon* was established to accommodate *Pl. strelitziae*, which causes a severe basal rot disease in *Strelitzia reginae*. The genus is known for its distinctive ascomata and spore structures. *Pleiocarpon* species have been isolated from decaying plant material or soil, suggesting a possible role in decomposition or plant interactions (Aigoun-Mouhous et al. 2019). Further studies are needed to understand the host range and distribution of *Pleiocarpon*.

Distribution: Algeria, French Guiana, Italy and Sri Lanka (Farr & Rossman 2025)

Disease symptoms: *Pleiocarpon* are primarily associated with root and basal stem infections, often leading to rot, wilting, and plant death in both ornamental and agricultural hosts (Aiello et al. 2017, Aigoun-Mouhous et al. 2019, Fig. 31). Infected plants typically exhibit wilting, yellowing, and progressive necrosis at the base of the stem and roots, ultimately collapsing and dying within a few weeks. In peony (*Paeonia suffruticosa*), *Pleiocarpon algeriense* was associated with root discoloration, decay, and growth decline, while in palms (*Livistona rotundifolia*) and avocado (*Persea americana*), infections were linked to crown rot, often accompanied by internal tissue browning and reduced vigor (Aiello et al. 2020, Ni et al. 2023). These symptoms are similar to those caused by other soilborne pathogens such as *Ilyonectria* or *Cylindrocladiella* (Aiello et al. 2020), highlighting the importance of accurate identification.

Hosts: *Pleiocarpon* has been reported from a number of ornamental and economically important plants (Farr & Rossman 2025). The species are capable of infecting a diverse group of monocot and dicot hosts, indicating its potential as a broad-spectrum plant pathogen (Aiello et al. 2017, 2020, Aigoun-Mouhous et al. 2019, Lechat & Fournier 2019).

Pathogen biology, disease cycle and epidemiology: The disease cycle of *Pleiocarpon* is not well understood due to its relatively recent classification and limited number of described species (Aigoun-Mouhous et al. 2019). *Pleiocarpon* species behave as typical soilborne pathogens, infecting plants through the roots or basal stem tissues, particularly under moist and warm environmental conditions (Capote et al. 2022). The fungi produce macroconidia and microconidia, which serve as primary inoculum and are likely dispersed through contaminated soil, water, or infected planting material (Aiello et al. 2017). Once inside the host, the pathogen colonizes vascular and cortical tissues, leading to rot, vascular discoloration, and eventual plant death. *Pleiocarpon* may survive in the soil or plant debris as chlamydospores or persistent mycelium, acting as overwintering structures similar to other members of *Nectriaceae* (Lombard et al. 2015).

Morphological-based identification: *Pleiocarpon* has cylindrocarpon-like asexual morph which is typical of *Neonectria sensu lato* (Aiello et al. 2017, 2020). Colonies typically grow slowly on standard media and produce both macroconidia and microconidia, a distinguishing feature. The macroconidia are hyaline, straight or slightly curved, multiseptate and cylindrical with rounded ends (Aigoun-Mouhous et al. 2019). Microconidia are abundant, aseptate, and typically ellipsoidal to ovoid. The high production of microconidia distinguishes *Pleiocarpon* from the closely related genus *Thelonectria*, which rarely produce microconidia and often have larger macroconidia with more septa (Salgado-Salazar et al. 2016). The sexual morph has red to orange ascomata that turn purple in potassium hydroxide. Due to overlapping features with other genera in *Nectriaceae*, phylogenetic analyses coupled with morphology is recommended for accurate species identification (Lombard et al. 2015).

Molecular-based identification: The genus was established by Aiello et al. (2017) through phylogenetic analysis using ITS, LSU, *tef*, *tub2*, *his3*, and *rpb2* sequences. Aiello et al. (2020) introduced *Pleiocarpon algeriense* from avocado trees in Italy. Aigoun-Mouhous et al. (2019) reported *Pl. algeriense* in Algerian grapevine nurseries, supporting its wider distribution and host range. Lechat & Fournier (2019)

described *Pl. gardiennetii* from dead pyrenolichen, *Astrothelium* sp. in French Guiana. Further studies are needed using broader taxon sampling, especially from underexplored habitats to better understand the diversity, ecological role, and evolutionary significance of *Pleiocarpon*. This study provides an updated phylogeny of *Pleiocarpon* based on combined ITS, LSU, *his3*, *rpb2*, *tef* and *tub2* sequence data (Fig. 32, Table 16). *Pleiocarpon gardiennetii* is excluded from our analysis as only the ITS region is available which cannot be used for accurate species identification.

Recommended genetic marker (genus level): LSU

Recommended genetic markers (species level): ITS, LSU, *his3*, *rpb2*, *tef* and *tub2*

Accepted number of species: three

References: Aiello et al. (2017, 2020), Aigoun-Mouhous et al. (2019), Lechat and Fournier (2019), Ni et al. (2023) (morphology and phylogeny)

Fig. 31 a-b Symptoms caused by *Pleiocarpon* sp. on *Strelitzia reginae*. c-e Basal rot and wilting. This picture is copyright of Pedro Crous (Aiello et al. (2017) and Marin-Felix et al. (2019a)).

Table 16 DNA barcodes of accepted *Peliocarpon*.

Species	Strain	GenBank accession numbers					
		ITS	LSU	*his3*	*rpb2*	*tef*	*tub2*
Pleiocarpon algeriense#	**CBS 144964**	**MH587320**	**MH587321**	**MH587296**	**MH587322**	**MH587323**	**MH587324**
Pl. livistonae	**CBS 145030**	**MK539963**	**N/A**	**MK540234**	**MK540095**	**MK540165**	**MK540179**
Pl. strelitziae#	**CBS 142251**	**KY304644**	**KY304672**	**KY304616**	**KY304697**	**KY304722**	**KY304750**

Ex-type/ex-epitype/ex-neotype/ex-lectotype strains and voucher strains are in bold. Sequences that are not available are represented by N/A. Species confirmed with pathogenicity studies are marked with #.

141. *Pseudopestalotiopsis* Maharachch., K.D. Hyde & Crous 2014

Type species: *Pseudopestalotiopsis theae* (Sawada) Maharachch., K.D. Hyde & Crous

Classification: *Sordariomycetes*, *Amphisphaeriales*, *Sporocadaceae*

Background: *Pseudopestalotiopsis* was introduced by Maharachchikumbura et al. (2014b) with *Pseudopestalotiopsis theae* as the type species. *Pseudopestalotiopsis* is characterized by having brown to dark brown or olivaceous median cells, with or without knobbed apical appendages (Maharachchikumbura et al. 2014b, 2016). *Pseudopestalotiopsis* species have mainly been recorded as plant pathogens on various hosts (Liu et al. 2017, Nozawa et al. 2017, Chen et al. 2018, Heng et al. 2025). *Pseudopestalotiopsis theae* is an economically significant pathogen that reduces the yield of tea worldwide (Maharachchikumbura et al. 2011, 2013a, b, 2016). Various secondary metabolites have

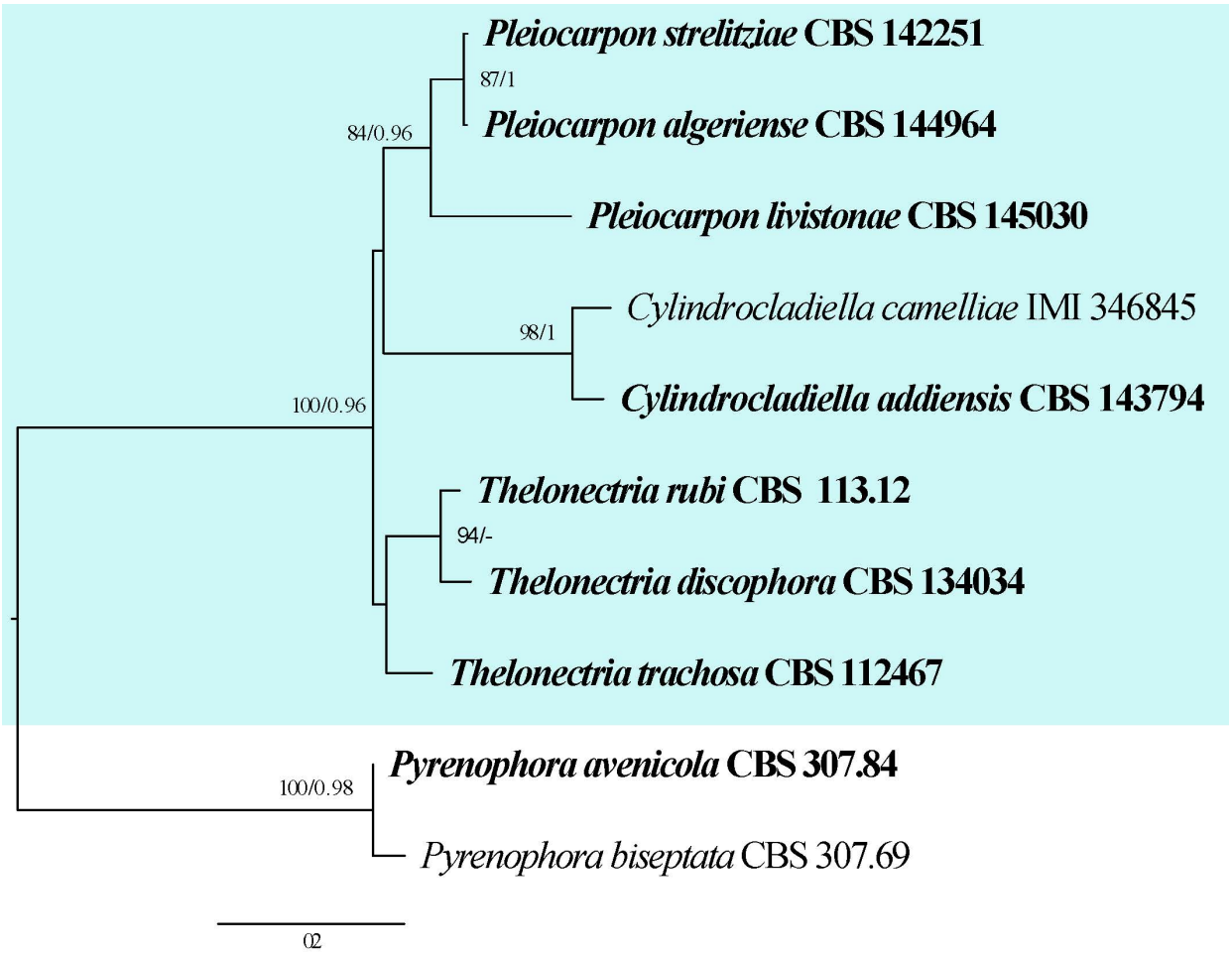

Fig. 32 Maximum likelihood tree of *Pleiocarpon* and selected genera in *Nectriaceae* based on the concatenated ITS, LSU, *his3*, *rpb2*, *tef* and *tub2* sequence data. The best scoring RAxML tree had a final likelihood value of -12394.429. The tree was rooted with *Pyrenophora avenicola* (CBS 307.84) and *Pyrenophora biseptata* (CBS 307.69). Estimated base frequencies were as follows: A = 0.250, C = 0.250, G = 0.250, T = 0.250; substitution rates AC = 1.34435, AG = 2.17858, AT = 1.34435, CG = 1.00000, CT = 5.46713, GT = 1.000000. ML bootstrap support values over 70% and Bayesian posterior probabilities (BPP) greater than 0.95 are indicated. Type strains are in bold. Scale bar indicates the number of substitutions per site. Hyphens (-) represent support values less than BS 70%/BPP 0.95.

been reported from *Pseudopestalotiopsis* including anti-tumour, antifungal, antimicrobial and other activities (Ding et al. 2008, Maharachchikumbura et al. 2011, 2016).

Distribution: Brazil, China, India, Indonesia, Italy, Malaysia, Myanmar, Thailand and Vietnam (Maharachchikumbura et al. 2016, Jayawardena et al. 2018, Farr & Rossman 2025)

Disease symptoms: *Pseudopestalotiopsis* species are known to cause a range of disease symptoms primarily on leaves, fruits, and stems of various host plants (Maharachchikumbura et al. 2016, Tsai et al. 2018, Shahriar et al. 2022, Heng et al. 2025, Fig. 33). Infected plants typically exhibit leaf spots that start as small, water-soaked lesions which gradually enlarge and turn necrotic with irregular brown or black margins. These spots may coalesce, leading to extensive blighting and premature leaf drop, which can significantly reduce photosynthetic capacity (Norphanphoun et al. 2019, Heng et al. 2025). On fruits, infection often results in soft rot or sunken lesions, sometimes covered with fungal fruiting bodies or spores, leading to decay and post-harvest losses. *Pseudopestalotiopsis theae* causes grey blight in tea (Maharachchikumbura et al. 2016, Shahriar et al. 2022). The pathogen initially causes circular to irregular leaf spots that turn grey with brown margins when mature, covering up to half of the leaf with acervuli (Maharachchikumbura et al. 2016). *Pseudopestalotiopsis ixorae* and *P. taiwanensis* cause leaf spot which are initially small, circular, ash-coloured spots which later turn into brown spots (Tsai et al. 2018).

Hosts: *Acacia* sp., *Averrhoa carambola*, *Avicennia marina*, *Camellia* sp., *Celtis sinensis*, *Cinnamomum* sp., *Cocos nucifera*, *Cycas revoluta*, *Diospyros crassiflora*, *Elaeis guineensis*, *Fragaria* sp., *Hibiscus rosa-sinensis*, *Holarrhena antidysenterica*, *Indocalamus tessellatus*, *Ixora* sp., *Kandelia obovata*, *Litsea verticillata*, *Macaranga* sp., *Mangifera indica*, *Pandanus odoratissimus*, *Pharus latifolius*, *Phoenix dactylifera*, *Podocarpus macrophyllus*, *Prunus* sp., *Rhizophora* sp., *Terminalia arjuna*, *Thea sinensis* and *Vitis* sp. (Farr & Rossman 2025)

Pathogen biology, disease cycle and epidemiology: *Pseudopestalotiopsis* species are characterized by their production of multicellular conidia with distinctive appendages, which aid in dispersal (Maharachchikumbura et al. 2016, Tsai et al. 2018). They survive in plant debris, soil, and infected plant tissues, serving as inoculum sources for new infections. The disease cycle typically begins when

conidia are dispersed by wind or water splashes to susceptible plant parts, where they germinate under favourable conditions (Shu et al. 2020). The pathogen penetrates host tissues either directly or through natural openings and wounds, leading to symptom development. *Pseudopestalotiopsis* species thrives in tropical and subtropical climates where warm, moist conditions prevail, facilitating rapid disease spread (Heng et al. 2025).

Morphological-based identification: *Neopestalotiopsis*, *Pestalotiopsis* and *Pseudopestalotiopsis* have similar conidia comprising five cells, including three pigmented median cells, an apical hyaline cell with one or many appendages, and a basal cell with one appendage (Maharachchikumbura et al. 2014b, 2016). These three genera can be distinguished based on variations in the color of the three pigmented cells in the conidia (Steyaert 1949, Nag Raj 1993, Maharachchikumbura et al. 2011, 2012, 2014b). *Pseudopestalotiopsis* can be distinguished from *Neopestalotiopsis* and *Pestalotiopsis* by its dark concolourous median cells with indistinct conidiophores (Maharachchikumbura et al. 2014b, 2016). While morphological traits provide valuable preliminary identification, they can often overlap among taxa, making accurate identification based solely on morphology challenging.

Molecular-based identification: Molecular data is vital to identify different pestalotioid species (Maharachchikumbura et al. 2014b, 2016). The ITS sequence alone lacks resolution at the species level within *Pseudopestalotiopsis*. Therefore, it is recommended to use a multi-locus dataset of ITS, *tub2* and *tef* for better resolution as compared to single gene phylogeny (Maharachchikumbura et al. 2012). Phylogenetic analyses based on multi-locus data sets have revealed cryptic *Pseudopestalotiopsis* species in several studies (Liu et al. 2017, Norphanphoun et al. 2019, Monkai et al. 2025). This study provides an updated phylogeny of *Pseudopestalotiopsis* based on combined ITS, *tub2* and *tef* sequence data (Fig. 34, Table 17).

Recommended genetic markers (genus level): LSU

Recommended genetic markers (species level): ITS, *tub2* and *tef*

Accepted number of species: 32

References: Maharachchikumbura et al. (2013a, b), (2014b), (2016b), Tsai et al. (2018), Shahriar et al. (2022), Weerasekara et al. (2024), Heng et al. (2025) (morphology and phylogeny)

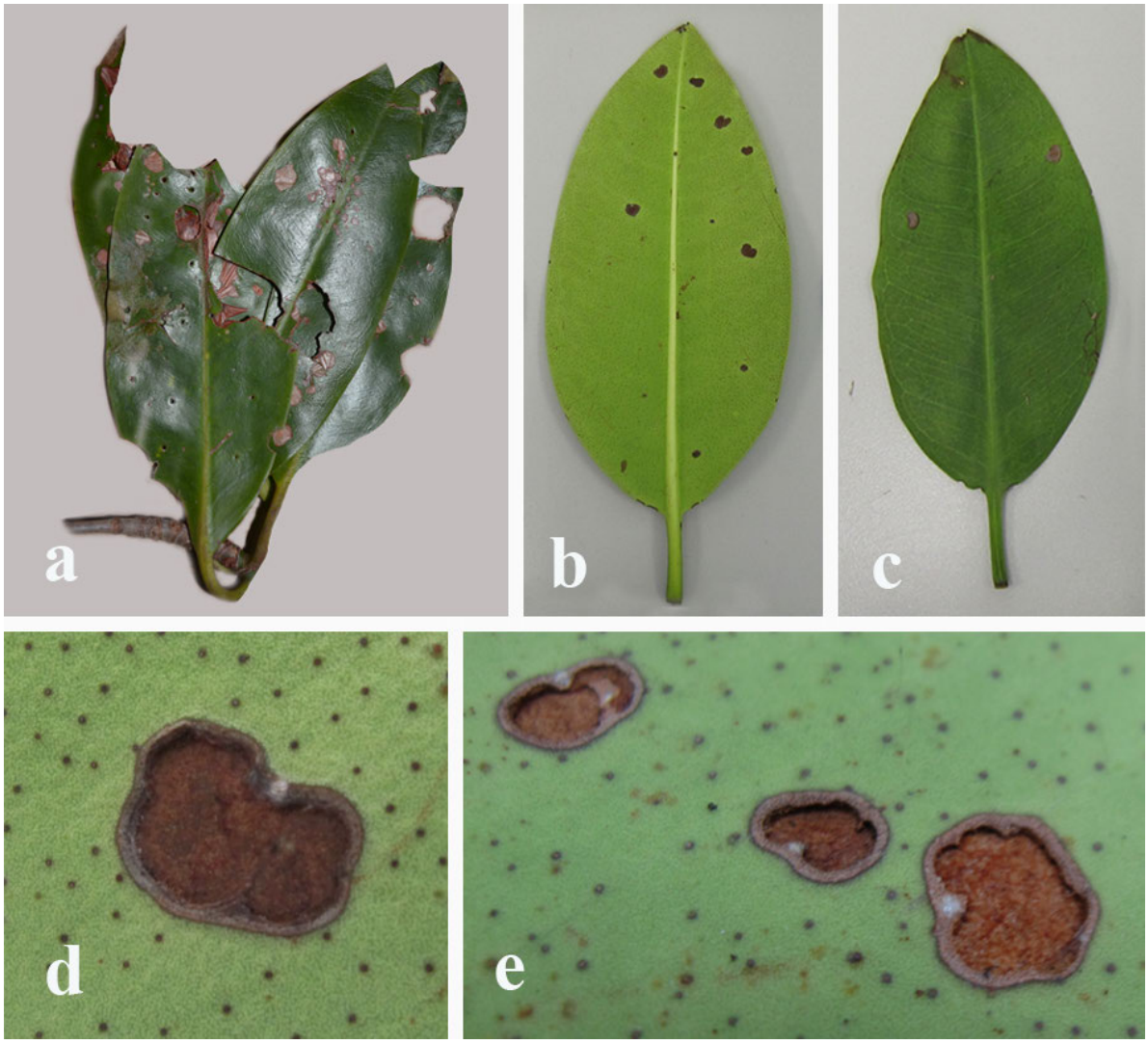

Fig. 33 Symptoms caused by *Pseudopestalotiopsis* sp. a Leaf spots on *Rhizophora apiculata.* b-e Leaf spots on *Rhizophora mucronata.* This picture is copyright of Chada Norphanphoun (Norphanphoun et al. 2019).

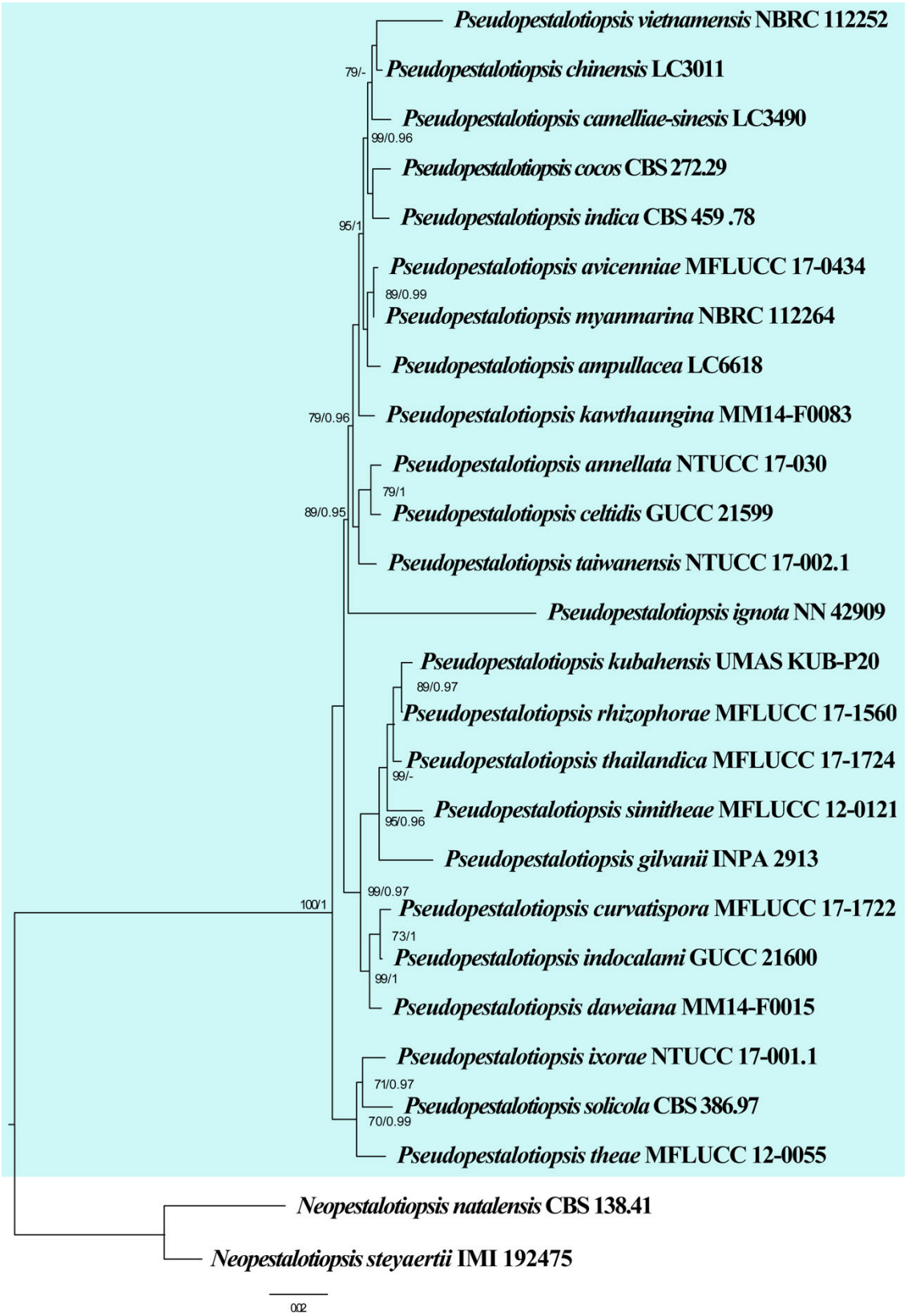

Fig. 34 Maximum likelihood tree of *Pseudopestalotiopsis* species based on the concatenated ITS, *tub2* and *tef* sequence data. The best scoring RAxML tree had a final likelihood value of -4938.689. The tree was rooted to *Neopestalotiopsis natalensis* (CBS 138.41) and *N. steyaertii* (IMI 192475). Estimated base frequencies were as follows: A = 0.230000, C = 0.279283, G = 0.206189, and T = 0.284528; substitution rates AC = 1.035460, AG = 2.28890, AT = 2.139899, CG =0.975180, CT = 4.74831, and GT = 1.000000. ML bootstrap support values over 70% and Bayesian posterior probabilities (BPP) greater than 0.95 are indicated. Type strains are in bold. Scale bar indicates the number of substitutions per site. Hyphens (-) represent support values less than BS 70%/BPP 0.95.

Table 17 DNA barcodes of accepted *Pseudopestalotiopsis*.

Species	Strain	GenBank accession numbers		
		ITS	*tub2*	*tef*
Pseudopestalotiopsis ampullacea	**LC6618**	**KX895025**	**KX895358**	**KX895244**
Ps. annellata	**NTUCC 17-030**	**MT322087**	**MT321889**	**MT321988**
Ps. avicenniae	**MFLUCC 17-0434**	**MK764287**	**MK764353**	**MK764331**
Ps. camelliae-sinensis	**LC3490**	**KX894985**	**KX895316**	**KX895202**
Ps. celtidis	**GUCC 21599**	**OL423535**	**OL439010**	**OL439012**
Ps. chinensis	**LC3011**	**KX894937**	**KX895269**	**KX895154**
Ps. cocos	**CBS 272.29**	**KM199378**	**KM199467**	**KM199553**
Ps. curvatispora	**MFLUCC 17-1722**	**MK764288**	**MK764354**	**MK764332**
Ps. daweiana	**MM14-F0015**	**LC324750**	**LC324751**	**LC324752**
Ps. elaeidis	**CBS 413.62**	**MH554044**	**MH554720**	**MH554479**
***Ps. gilvanii*#**	**INPA 2913**	**MN385951**	**MN385954**	**MN385957**
Ps. hydei	**NTUCC 17-003.1**	**MG816313**	**MG816323**	**MG816333**
Ps. ignota	**NN 42909**	**KU500020**	**N/A**	**KU500016**
Ps. indica	**CBS 459.78**	**KM199381**	**KM199470**	**KM199560**
Ps. indocalami	**GUCC 21600**	**OL423536**	**OL439011**	**OL439013**
Ps. iteae	**KUNCC 24-18921**	**PQ521230**	**PQ560703**	**PQ529181**
***Ps. ixorae*#**	**NTUCC 17-001.1**	**MG816316**	**MG816326**	**MG816336**
Ps. kawthaungina	**MM14-F0083**	**LC324753**	**LC324754**	**LC324755**
Ps. kubahensis	**UMAS KUB-P20**	**KT006749**	**N/A**	**N/A**
Ps. myanmarina	**NBRC 112264**	**LC114025**	**LC114045**	**LC114065**
***Ps. petchii*#**	**USJCC-0159**	**PP077199**	**PP196144**	**PP263678**
***Ps. ratnapurensis*#**	**USJCC-0157**	**PP077191**	**PP196136**	**PP263671**
Ps. rhizophorae	**MFLUCC 17-1560**	**MK764291**	**MK764357**	**MK764335**
***Ps. rossmaniae*#**	**USJCC-0158**	**PP077196**	**PP196141**	**PP263676**
Ps. simitheae	**MFLUCC 12-0121**	**KJ503812**	**KJ503815**	**KJ503818**
Ps. solicola	**CBS 386.97**	**MH554039**	**MH554715**	**MH554474**
***Ps. srilankensis*#**	**USJCC-0160**	**PP077203**	**PP196148**	**PP263682**
***Ps. taiwanensis*#**	**NTUCC 17-002.1**	**MG816319**	**MG816329**	**MG816339**
Ps. thailandica	**MFLUCC 17-1724**	**MK764292**	**MK764358**	**MK764336**
Ps. theae	**MFLUCC 12-0055**	**JQ683727**	**JQ683711**	**JQ683743**
Ps. vietnamensis	**NBRC 112252**	**LC114034**	**LC114054**	**LC114074**
Ps. zhangzhouensis	**CGMCC 3.28547**	**PQ681341**	**PQ687600**	**PQ687594**

Ex-type/ex-epitype/ex-neotype/ex-lectotype strains and voucher strains are in bold. Sequences that are not available are represented by N/A. Species confirmed with pathogenicity studies are marked with #.

142. *Pseudogymnoascus* Raillo, Centbl. Bakt. ParasitKde, Abt. II 78: 520 (1929)

Type species: *Pseudogymnoascus vinaceus* Raillo

Classification: *Leotiomycetes*, *Thelebolales*, *Pseudeurotiaceae*

Background: *Pseudogymnoascus* is a psychrophilic genus, known for its adaptation to cold environments (Lorch et al. 2013, Carvalho et al. 2019, Hoyt et al. 2021). The sexual morph of *Pseudogymnoascus* is characterized by the production of gymnothecial ascocarps containing sub-spherical to spherical asci (Raillo 1929, Rice & Currah 2006, Minnis & Lindner 2013). The genus was originally classified in *Myxotrichaceae* based on morphology, but phylogenetic analyses have since shown that *Pseudogymnoascus* is not

related to the family (Currah 1985, Wang et al. 2006, Lorch et al. 2013). *Pseudogymnoascus* drew significant scientific interest, when the newly emerging disease, white-nose syndrome (WNS) began devastating bat populations in North America (Minnis & Lindner 2013, Hoyt et al. 2021, Villanueva et al. 2021). The causal agent of WNS was initially identified as *Geomyces destructans*, but was later reclassified as *Pseudogymnoascus destructans* based on molecular evidence as it is distinct from *Geomyces* (Gargas et al. 2009, Lorch et al 2011, Minnis & Lindner 2013).

Distribution: *Pseudogymnoascus* species have a global distribution, with a strong affinity for cold and temperate regions, particularly those with subterranean or low-temperature habitats (Rice & Currah 2006, Villanueva et al. 2021, Childress et al. 2025, Farr & Rossman 2025). They are commonly found in caves, soils, permafrost, and other cryoenvironments, where their psychrophilic nature allows them to thrive. Members have been isolated from various continents, including North America, Europe, Asia, and Antarctica, indicating their wide ecological amplitude and adaptability to harsh conditions (Rice & Currah 2006, Villanueva et al. 2021, Childress et al. 2025). Their presence in both natural ecosystems and anthropogenically influenced environments (e.g., mines and artificial caves) suggests that *Pseudogymnoascus* species are well-adapted generalists within cold ecosystems, capable of both saprobic and pathogenic lifestyles (Rice & Currah 2006, Veselská et al. 2020, Childress et al. 2025).

Disease symptoms: The most well-known disease symptoms associated with *Pseudogymnoascus*, specifically *Pseudogymnoascus destructans*, are observed in bats affected by WNS. Infected bats typically exhibit a white, powdery growth on the muzzle, ears, and wings (Meteyer et al. 2009, Forsythe et al. 2021, Childress et al. 2025). Affected bats often show abnormal behaviours during hibernation, such as premature emergence from hibernacula, and daytime activity in freezing temperatures, all of which contribute to fat reserve depletion and eventual death (Zukal et al. 2017, Fritze et al. 2021). *Pseudogymnoascus destructans* does not cause immediate death through systemic infection, however, its impact is physiological, weakening the host over time (Zukal et al. 2017, Fritze et al. 2021).

Hosts: *Pseudogymnoascus* are ecologically diverse, having been isolated from a wide range of substrates, including soil, rocks, caves, bat hibernacula, and even decomposing meat (Lorch et al. 2013, Minnis & Lindner 2013, Carvalho et al. 2019, Crous et al. 2019, 2020, Urbina et al. 2021). The species have also been isolated from a wide range of hosts including *Picea abies*, *Triticum aestivum* and *Vitis* sp. (Kwasna & Bateman 2008, Mułenko et al. 2008, Childress et al. 2025).

Pathogen biology, disease cycle and epidemiology: *Pseudogymnoascus*, particularly *Pse. destructans*, exhibits a unique pathogen biology closely tied to its psychrophilic nature and the hibernation biology of bats (Lorch et al. 2013, Carvalho et al. 2019, Hoyt et al. 2021). *Pseudogymnoascus destructans* grows optimally at 4–15 °C and it infects bats during hibernation, when their body temperatures drop and immune responses are suppressed (Donaldson et al. 2018, Campbell et al. 2020). *Pseudogymnoascus* invades the skin tissues of the wings, leading to ulceration, necrosis, and disruption of physiological functions such as water balance and thermoregulation (Veselská et al. 2020, Hoyt et al. 2021). The disease cycle begins when bats enter hibernation sites already contaminated with fungal spores or come into contact with infected individuals (Veselská et al. 2020, Hoyt et al. 2021). Spores adhere to the skin, germinate, and slowly invade tissues over weeks. Upon death or emergence from hibernation, the fungus persists in the environment, surviving as conidia or hyphal fragments on cave surfaces or in organic debris. Human-mediated movement of spores is also a potential vector (Ballmann et al. 2017).

Morphological-based identification: The colonies of *Pseudogymnoascus* typically exhibit slow growth and appear white to greyish, with a powdery to velvety texture, often developing a yellowish or tan pigmentation over time (Forsythe et al. 2021, Villanueva et al. 2021). Species produce hyaline to lightly pigmented, septate hyphae, and conidia that are typically unicellular, hyaline, and ellipsoidal to cylindrical in shape, often formed singly or in short chains (Rice & Currah 2006, Villanueva et al. 2021, Fig. 35). The genus is also known for producing gymnothecial ascocarps with loosely woven fruiting bodies that contain sub-spherical to spherical asci, each bearing eight ascospores. These sexual characters were part of the basis for the classification by Raillo (1929). However, morphological features alone are insufficient for distinguishing *Pseudogymnoascus* from related genera like *Geomyces*, due to overlapping characteristics (Samson 1972, Rice & Currah 2006, Minnis & Lindner 2013). Therefore, molecular data is are used for accurate species-level identification.

Molecular-based identification: Several *Pseudogymnoascus* species have been introduced based primarily on morphological characters (Villanueva et al. 2021). A number of different markers have been used in the molecular analyses of *Pseudogymnoascus* species (Gargas et al. 2009, Minnis & Lindner 2013, Luo et al. 2016). Rice & Currah (2006) performed the first polyphasic study using ITS region and described the new species *Pse. appendiculatus* and *Pse. verrucosus*. Gargas et al. (2009) described *Pse. destructans* using ITS and SSU sequences. Minnis & Lindner (2013) employed multi-locus phylogenetic analysis using ITS, LSU, *mcm7*, *rpb2* and *tef* sequences and transfered several species into *Pseudogymnoascus*. Crous et al. (2019) described *Pse. lindneri* and *Pse. turneri* while Crous et al. (2020) identified *Pse. palmeri* using ITS, *rpb2* and *tef* sequences. Several new species were also introduced using ITS, LSU, *rpb2*, *mcm7*, and *tef* sequences (Zhang et al. 2020, Villanueva et al. 2021). This study provides an updated phylogeny of *Pseudogymnoascus* based on combined ITS, LSU, *mcm7*, *rpb2* and *tef* sequence data (Fig. 36, Table 18). *Pseudogymnoascus guiyangensis* was not included in the phylogeny as it only has the ITS region (Luo et al. 2016), which can be used for generic placement only.

Recommended genetic markers (genus level): ITS

Recommended genetic markers (species level): ITS, LSU, *mcm7*, *rpb2* and *tef*

Accepted number of species: 28

References: Rice and Currah (2006), Gargas et al. (2009), Lorch et al (2011), Minnis and Lindner (2013), Crous et al. (2020), Villanueva et al. (2021), Childress et al. (2025) (morphology and phylogeny)

143. *Pyrenophora* Fr., Summa veg. Scand., Sectio Post. (Stockholm): 397 (1849)

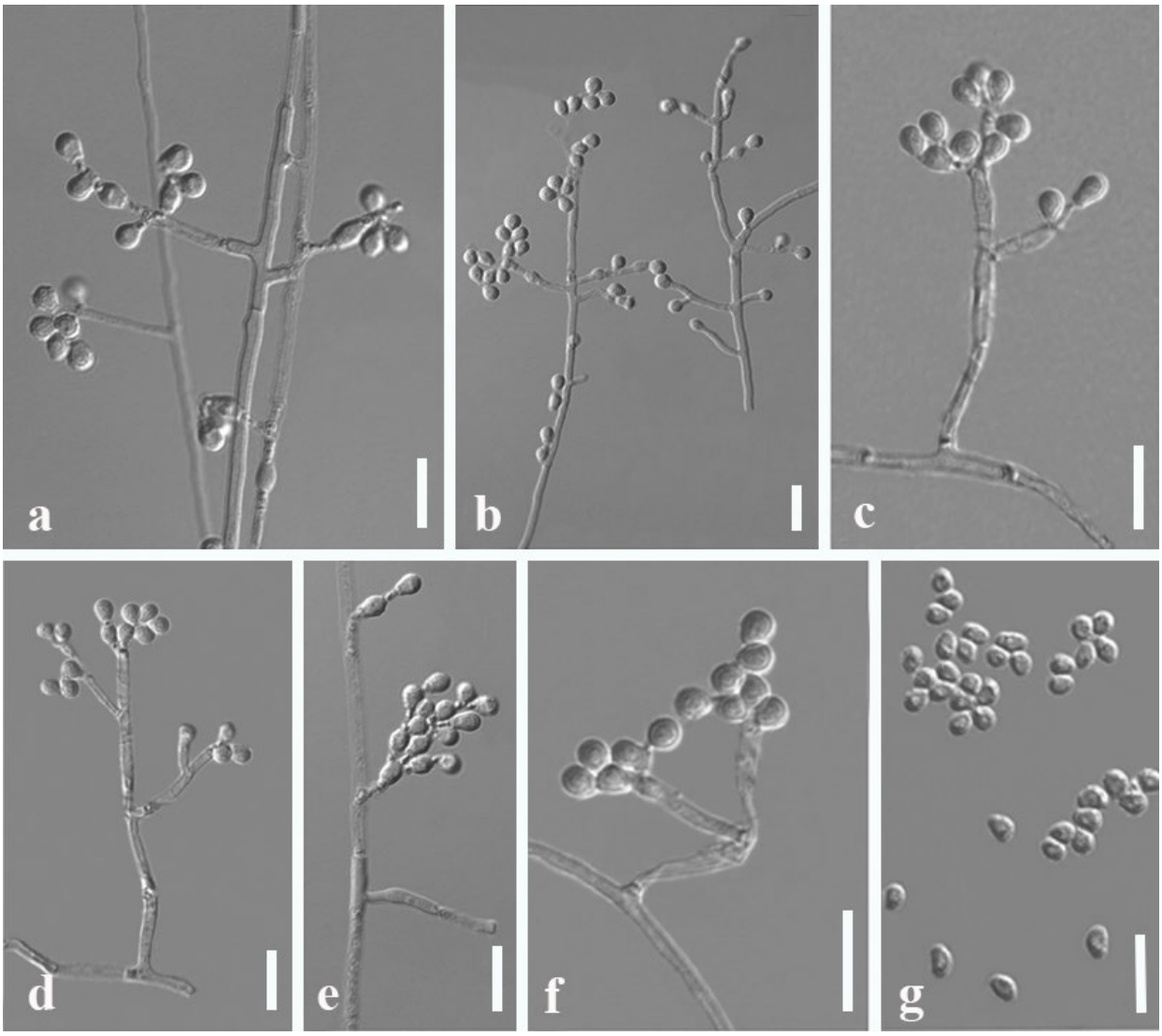

Fig. 35 *Pseudogymnoascus* sp. a-f Conidiophores and conidia. g Conidia. Scale bars: a-g = 10 μm. This picture is copyright of Yan-Feng Han (Zhang et al. 2021b).

Type species: *Pyrenophora phaeocomes* (Rebent.) Fr.

Classification: *Dothideomycetes*, *Pleosporales*, *Pleosporaceae*

Background: *Pyrenophora phaeocomes*, the type species of *Pyrenophora*, was introduced as *Sphaeria phaeocomes* by Rebentisch (1804) and was placed in *Xylariaceae*. Fries (1849) reclassified the genus as *Pyrenophora* within *Pleosporales*. Wehmeyer (1961) dealt with the genera *Pleospora*, *Platyspora*, *Clathrospora*, and *Pyrenophora,* and placed *Pyrenophora* in *Pleosporaceae,* a placement confirmed by further studies (Berbee 1996, Hyde et al. 2013). *Pyrenophora* includes pathogens, saprobes, and endophytes in terrestrial habitats with a worldwide distribution (Balance et al. 1996, Zhang & Berbee 2001, Leisova 2005, Liu et al. 2011, Abdullah et al. 2017). *Pyrenophora teres, Py. graminea* and *Py. tritici-repenti* are serious plant pathogens of grasses, especially barley, wheat, and oats. Infected leaves turn yellow or the whole plant may die, resulting in reduced yield and economic losses (Shabeer & Bockus 1988, Bankina & Priekule 2011, Liu et al. 2011, Ariyawansa et al. 2014, Abdullah et al. 2017). *Pyrenophora* species have potential in biological control, for example, pyrenophoric acid was isolated from *Py. semeniperda*, and can be a mycoherbicide for biocontrol of cheatgrass and other annual bromes (Ariyawansa et al. 2014).

Pyrenophora was linked to the asexual morphs in *Drechslera,* which was confirmed by Zhang and Berbee (2001). Based on muti-gene phylogenetic analyses, Ariyawansa et al. (2014) synonymised *Drechslera* under *Pyrenophora.* The asexual morph of *Pyrenophora* is similar to *Bipolaris, Curvularia* and *Setosphaeria,* the sexual morph resembles *Clathrospora* and *Platyspora* (Zhang & Berbee 2001, Ariyawansa et al. 2014, Marin-Felix et al. 2019a). To better distinguish these genera, multi-gene data are essential for analysis, with LSU, ITS, *gapdh* sequences (Ariyawansa et al. 2014). Marin-Felix et al. (2019a) reanalyzed the genus using ITS, *gapdh* and *rpb2* genes.

Distribution: worldwide (Farr & Rossman 2025)

Disease symptoms: *Pyrenophora* species cause various symptoms including leaf blight, yellow leaf blotch, leaf spot, leaf stripe, tan spot, seedling blight (Fig. 37). For example, *Py. teres* causes net blotch on barley (Friis et al. 1991, Liu et al. 2011). *Pyrenophora graminea* causes barley stripe (Mathre 1997, Mokrani et al. 2012) and *Py. tritici-repentis* is a necrotrophic pathogen causing tan spot (Aboukhaddour et al.

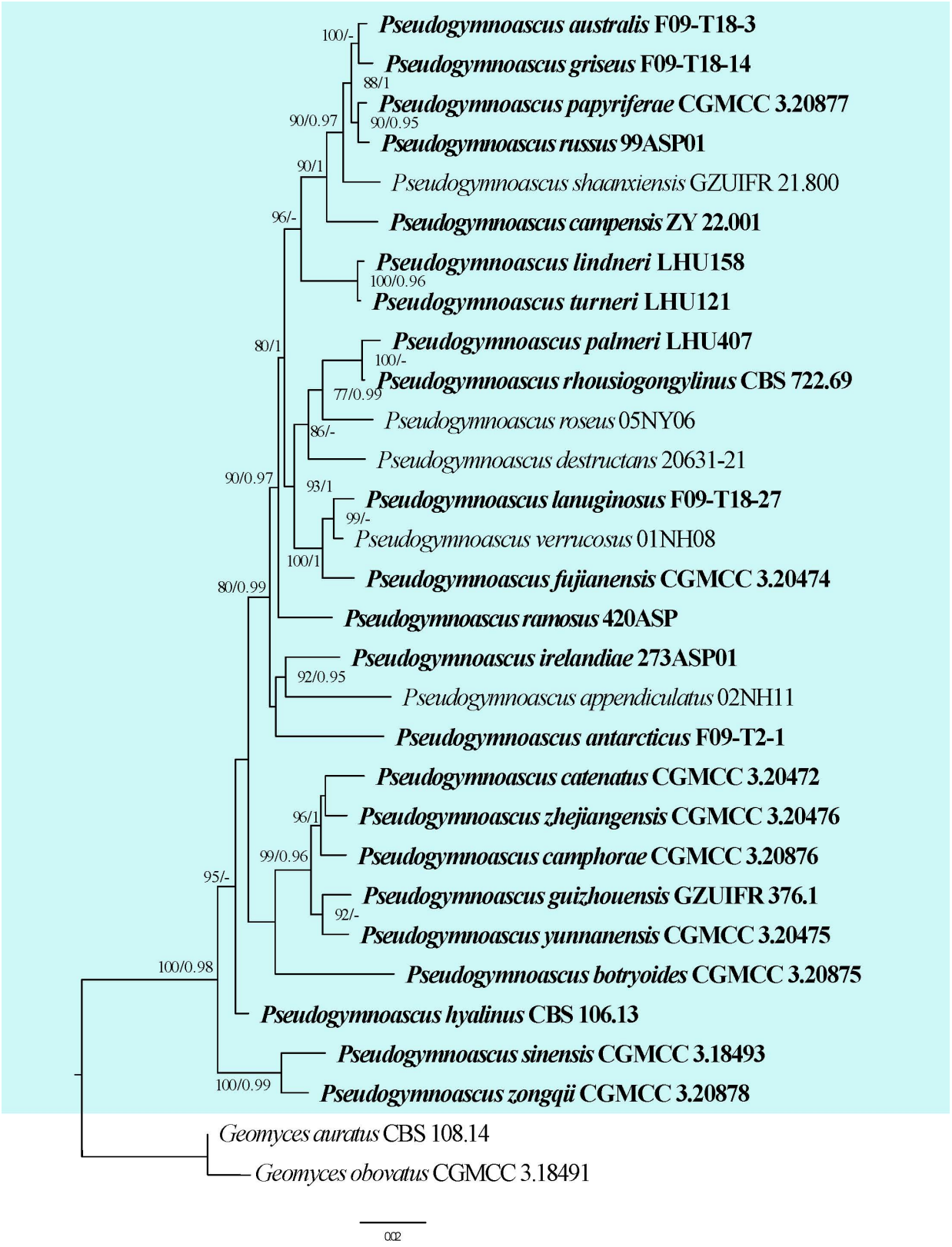

Fig. 36 Posterior probabilities of *Pseudogymnoascus* species based on the concatenated ITS, LSU, *mcm7*, *rpb2* and *tef* sequence data. The best scoring RAxML tree had a final likelihood value of -14600.702. The tree was rooted with *Geomyces auratus* (CBS 108.14) and *Geomyces obovatus* (CGMCC 3.18491). Estimated base frequencies were as follows: A = 0.250, C = 0.250, G = 0.250, T = 0.250; substitution rates AC = 1.00000, AG = 4.01339, AT = 1.00000, CG = 1.00000, CT = 6.14273, GT = 1.000000. ML bootstrap support values over 70% and Bayesian posterior probabilities (BPP) greater than 0.95 are indicated. Type strains are in bold. Scale bar indicates the number of substitutions per site. Hyphens (-) represent support values less than BS 70%/BPP 0.95.

2013, Abdullah et al. 2017). *Pyrenophora seminiperda* is a minor pathogen that causes leaf spots on many graminicolous hosts, while *Py. avenae* causes seedling blight of oats (Ariyawansa et al. 2014). Initial leaf lesions are yellow to brown spots that expand to larger irregular shapes, including stripes, spots, and blotch, which eventually dry out and cause leaf shedding or leaf death. Under favourable conditions, conidia are produced which may infect the head/spikes causing grey or brownish glumes (Liu et al. 2011, Aboukhaddour et al. 2013, Ariyawansa et al. 2014).

Hosts: *Poaceae* (especially barley, oats, and wheat) and *Proteaceae* (Farr & Rossman 2025)

Pathogen biology, disease cycle and epidemiology: The conidia and ascospores of the pathogen require specific temperature, relative humidity, and leaf wetness for dispersal and germination. They produce lesions on leaf surfaces following infection from appressorium and an infection peg. Spores can also infect plants in neighbouring fields serving as primary inoculum spread by wind and rain, creating a polycyclic disease cycle (Liu et al. 2011).

Morphological-based identification: *Drechslera* is the asexual morph of *Pyrenophora* and they clustered together in phylogenetic analyses (Zhang & Berbee 2001, Ariyawansa et al. 2014). In accordance with the ''One Fungus, one name'' concept, the sexual name *Pyrenophora* was protected over *Drechslera*. The sexual morph is characterized by immersed to semi-immersed ascomata and neck covered with brown to reddish-brown setae, lack of pseudoparaphyses, 8-spored, bitunicate, fissitunicate, clavate to saccate asci, with or without a large apical ring, and muriform terete ascospores (Ariyawansa et al. 2014, Marin-Felix et al. 2019a). The asexual morph has macronematous, mononematous, subhyaline to brown conidiophores, polytretic, integrated or terminal conidiogenous cells and solitary, acropleurogenous, simple, straight or curved, pale to dark brown or olivaceous brown conidia of various shapes (Marin-Felix et al. 2019a). Species have overlapping characters making identification based on morphology difficult. Therefore, the use of DNA sequence data is important in identifying these species.

Molecular-based identification: The first multi-gene (ITS and *gapdh*) phylogenetic analysis for *Pyrenophora* and *Drechslera* by Zhang and Berbee (2001) showed these genera to be congeneric and monophyletic. Zhang et al. (2012) refined *Pleosporales* based on analyses of LSU, SSU, *rpb2* and *tef* and placed *Pyrenophora* in *Pleosporaceae.* Ariyawansa et al. (2014) confirmed this result based on LSU, SSU and *rpb2* analyses. Marin-Felix et al. (2019a) introduced six new *Pyrenophora* species and synonymized five *Drechslera* species under *Pyrenophora* based on analyses of ITS, LSU, *gapdh* and *rpb2* sequences. Here we reconstruct the phylogenetic tree of *Pyrenophora* based on ITS, LSU and *gapdh* sequence data, which provided similar result to previous studies (Ariyawansa et al. 2014, Marin-Felix et al. 2019a). This study provides an updated phylogeny of *Pyrenophora* based on combined ITS, LSU and *gapdh* sequence data (Fig. 38, Table 19).

Recommended genetic markers (genus level): LSU and ITS

Recommended genetic markers (species level): ITS, LSU and *gapdh*

Accepted number of species: 31

References: Liu et al. (2011), Mokrani et al. (2012) (morphology); Zhang & Berbee (2001), Ariyawansa et al. (2014), Abdullah et al. (2017), Marin-Felix et al. (2019a), Jayawardena et al. (2022) (phylogeny)

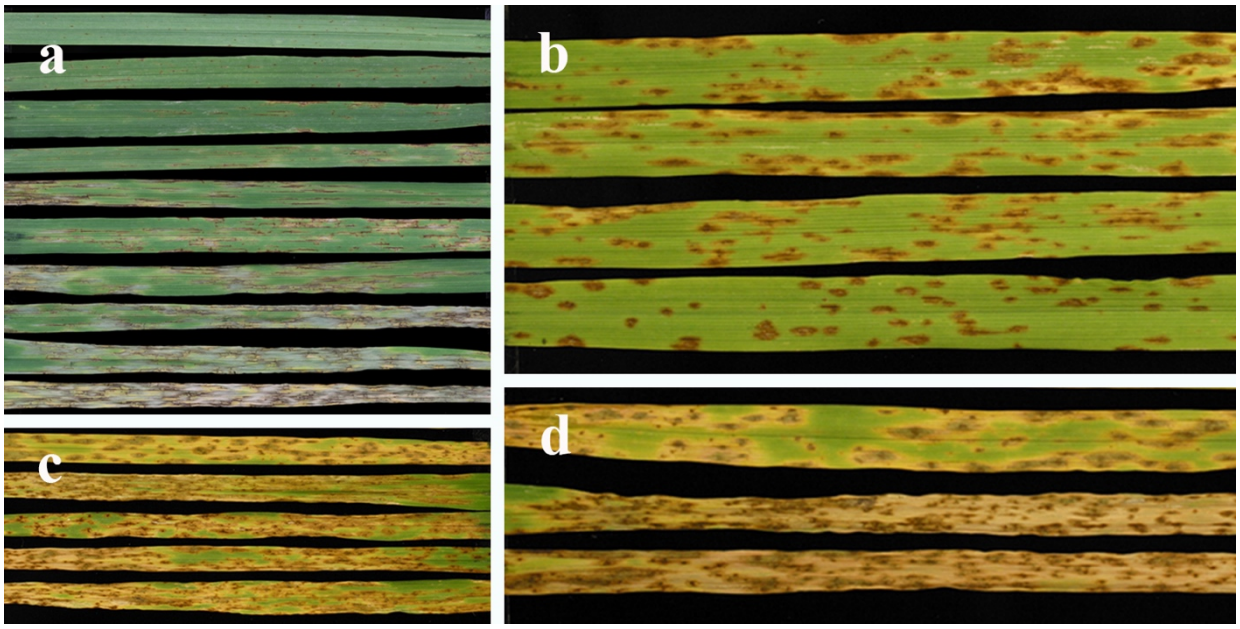

Fig. 37 a-d Spot form net blotch and net form net blotch caused by *Pyrenophora* sp. on barley. This picture is copyright of Timothy L Friesen.

144. *Ramichloridium* Stahel ex de Hoog, Studies in Mycology. 15: 59 (1977)

Type species: *Ramichloridium apiculatum* (J.H. Mill., Giddens & A.A. Foster) de Hoog

Classification: *Dothideomycetes*, *Mycosphaerellales*, *Dissoconiaceae*

Background: Most *Ramichloridium* species were placed in *Rhinocladiella* by Schol-Schwarz (1968). *Ramichloridium* was originally established by Stahel (1937) and typified by *R. musae* Stahel. However, the genus was invalid due to lacking

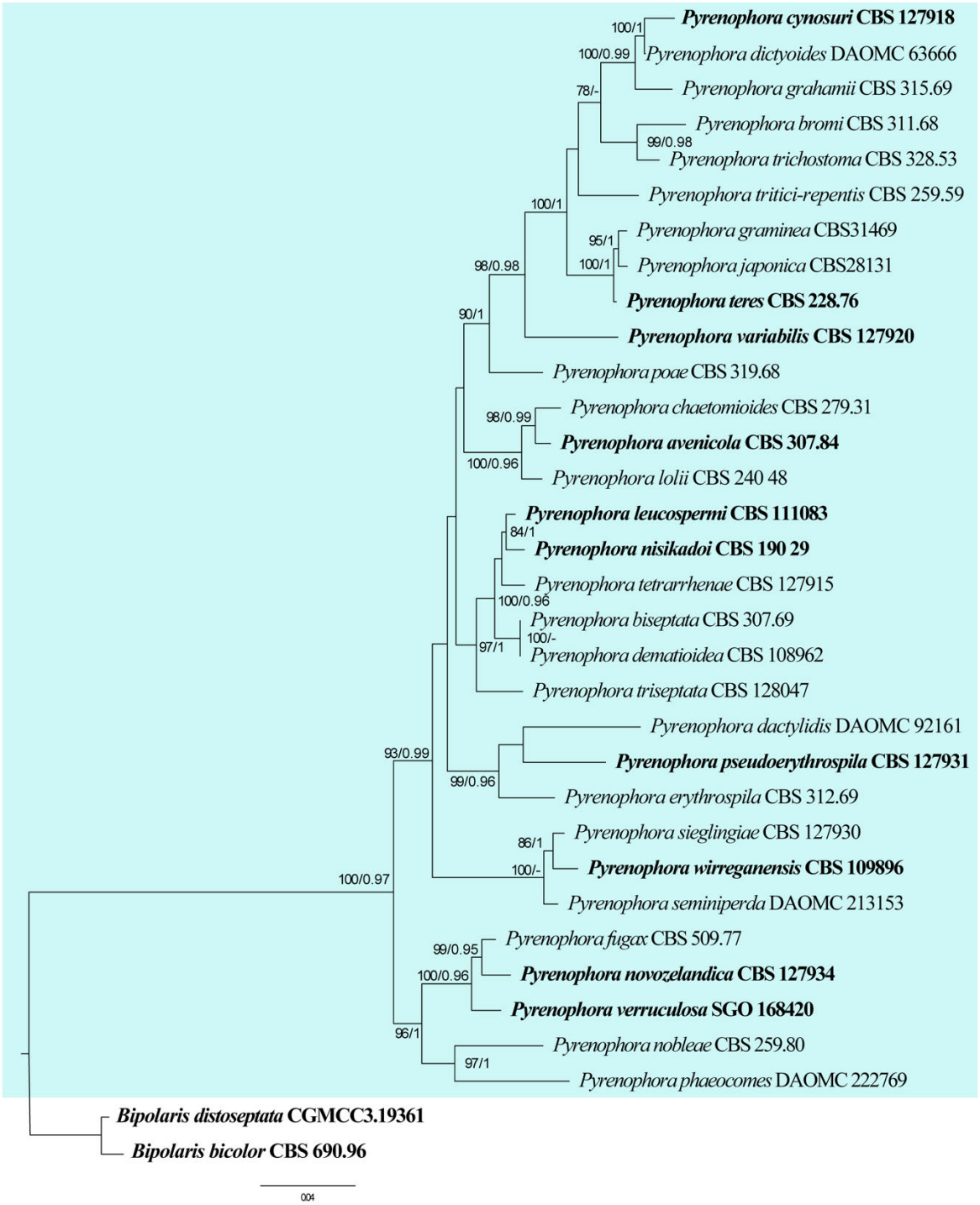

Fig. 38 Maximum likelihood tree of *Pyrenophora* species based on the concatenated ITS, LSU and *gapdh* sequence data. The best scoring RAxML tree had a final likelihood value of -9923.179825. The tree was rooted with *Bipolaris bicolor* (CBS 690.96) and *B. distoseptata* (CGMCC3.19361). Estimated base frequencies were as follows: A = 0.244864, C = 0.251782, G = 0.268257, T = 0.235097; substitution rates AC = 1.218177, AG = 2.450247, AT = 1.097347, CG = 0.861679, CT = 4.648617, GT = 1.000000. ML bootstrap support values over 70% and Bayesian posterior probabilities (BPP) greater than 0.95 are indicated. Type strains are in bold. Scale bar indicates the number of substitutions per site. Hyphens (-) represent support values less than BS 70%/BPP 0.95.

Table 19 DNA barcodes of accepted *Pyrenophora*.

Species	Isolate	GenBank accession numbers		
		ITS	LSU	*gapdh*
Pyrenophora avenicola	**CBS 307.84**	**MK539972**	**MK540042**	**MK540180**

Py. biseptata	CBS 307.69	MK539973	MK540043	MK540181
Py. bromi	CBS 311.68	MK539976	MH870851	MK540184
Py. chaetomioides	CBS 279.31	MK539977	MK540045	MK540185
Py. cynosuri	**CBS 127918**	**MK539980**	**MK540047**	**MK540188**
Py. dactylidis	DAOMC 92161	JN943667	JN940087	AY004812
Py. dematioidea	CBS 108962	JN712465	JN712531	N/A
Py. dictyoides	DAOMC 63666	JN943653	JN940080	AY004836
Py. erythrospila	CBS 312.69	MK539983	MK540051	MK540192
Py. fugax	CBS 509.77	MK539985	MK540053	MK540194
Py. grahamii	CBS 315.69	MK539986	MK540054	MK540195
Py. graminea	CBS31469	MH859313	MH871047	N/A
Py. japonica	CBS28131	MH855214	MH866663	N/A
P. leucospermi	**CBS 111083**	**JN712467**	**JN712533**	**MK540198**
Py. lolii	CBS 240 48	MK539991	MK540055	MK540201
Py. nisikadoi	**CBS 190 29**	**KM257054**	**KM243296**	**KM257057**
Py. nobleae	CBS 259.80	MK539994	MK540058	MK540206
Py. novozelandica	**CBS 127934**	**MK539997**	**MK540061**	**MK540209**
Py. phaeocomes	DAOMC 222769	JN943649	JN940093	N/A
Py. poae	CBS 319.68	MK539998	MK540062	MK540210
Py. pseudoerythrospila	**CBS 127931**	**MK540000**	**MK540063**	**MK540212**
Py. seminiperda	DAOMC 213153	JN943665	JN940088	AY004826
Py. sieglingiae	CBS 127930	MK540002	MK540065	MK540214
Py. teres	**CBS 228.76**	**MK540003**	**MK540066**	**MK540215**
Py. tetrarrhenae	CBS 127915	MK540010	MH877964	MK540222
Py. trichostoma	CBS 328.53	MK540012	MK540072	MK540224
Py. triseptata	CBS 128047	MK540015	MH877983	MK540227
Py. tritici-repentis	CBS 259.59	MK540017	MK540075	AM884276
Py. variabilis	**CBS 127920**	**MK540020**	**MK540078**	**MK540231**
Py. verruculosa	**SGO 168420**	**ON722346**	**N/A**	**ON736764**
Py. wirreganensis	**CBS 109896**	**MK540021**	**MK540079**	**MK540232**

Ex-type/ex-epitype/ex-neotype/ex-lectotype strains and voucher strains are in bold. Sequences that are not available are represented by N/A.

a Latin diagnosis. De Hoog (1977) reintroduced *Ramichloridium* and treated *R. apiculatum* as the type species. *Ramichloridium* includes human or plant pathogens, saprobes, endophytes, airborne fungi and lichenicolous fungi from aquatic and terrestrial habitats (De Hoog 1977, Arzanlou et al. 2007, Braun et al. 2009, Li et al. 2012, Crous et al. 2014, Diederich et al. 2017, Zheng et al. 2020).

Distribution: Belgium, Canada, China, Chile, Czechoslovakia, Denmark, Ecuador, France, India, Jamaica, Japan, Malaysia, Netherlands, Peru, Rhodesia, Seychelles, South Africa, U.K, U.S.A, U.S.S.R (Farr & Rossman 2025)

Disease symptoms: Some *Ramichloridium* species are related to sooty blotch and flyspeck on fruits, for example, *R. punctatum* and *R. cucurbitae* cause disease on the surface of winter squash while *R. luteum* causes symptoms on the surface of apples (Li et al. 2012). Arzanlou et al. (2007) reported *R. musae* and *R. biverticillatum* were involved in banana speckle disease, however, Videira et al. (2017) regarded *R. musae* and *R. biverticillatum* to be conspecific, and applied the name *Zasmidium biverticillatum* to both species.

Hosts: Air, *Amomum krervanh* (*Zingiberaceae*), *Alnus glutinosa* (*Betulaceae*), *Alocasia odora* (*Araceae*), *Bambusa* sp. (*Poaceae*), *Brassica* sp. (*Brassicaceae*), *Carica papaya* (*Caricaceae*), *Carissa carandas* (*Apocynaceae*), *Cladonia portentosa* (*Cladoniaceae*), *Cladonia stygia* (*Cladoniaceae*), *Crataegus flava* (*Rosaceae*), *Cucurbita maxima* (*Cucurbitaceae*), *Erythrina tomentosa* (*Fabaceae*), *Euclea undulata* (*Ebenaceae*), *Fagus sylvatica* (*Fagaceae*), *Malus domestica,* (*Rosaceae*), *Malus pumila* (*Rosaceae*), *Musa* sp. (*Musaceae*), *Palmae*, *Picea engelmannii* (*Pinaceae*), *Potamogeton pectinatus* (*Potamogetonaceae*), *Solanum torvum* (*Solanaceae*), soil, *Tilia cordata* (*Malvaceae*), *Wissadula* sp. (*Malvaceae*) (Farr & Rossman 2025)

Pathogen biology, disease cycle and epidemiology: *Ramichloridium* survives on plant debris, senescing tissue, or as epiphytes, and can persist in the environment due to their melanized (pigmented) cell walls, which confer resistance to UV and desiccation (Wang et al. 2017a). The disease cycle begins with the dissemination of conidia via wind, rain splash, or insect vectors, which land on host surfaces (Ploetz et al. 2003, Wang et al. 2017a). Infection typically occurs in warm, humid conditions, where conidia germinate and colonize the cuticle or epidermal layers (Wang et al. 2017a). Unlike more aggressive pathogens, *Ramichloridium* species rarely penetrate deeply into host tissues, often remaining superficial, which contributes to their classification as blemish or surface pathogens (Brandt & Warnock 2003, Wang et al. 2017a). Epidemiologically, outbreaks are linked to prolonged leaf wetness, high humidity, and dense canopy structure that limits airflow (Brandt & Warnock 2003, Wang et al. 2017a).

Morphological-based identification: *Ramichloridium* is characterized by macronematous, mononematous, solitary, erect, dark, branched or unbranched, straight to curved or sinuous, septate conidiophores, polyblastic, integrated, terminal, solitary, pale to brown conidiogenous cells and solitary, pale to brown, obovate to subglobose, oblong, or clavate conidia (De Hoog 1977, Arzanlou et al. 2007, Zheng et

al. 2020, Fig. 39). The sexual morph is unknown.

It is difficult to identify *Ramichloridium* based solely on morphology since the characters are similar to those of other *Ramichloridium*-like fungi, such as *Cladosporium*, *Rhinocladiella* and *Veronaea. Rhinocladiella* differs from *Ramichloridium* in having exophiala-type budding cells (De Hoog 1977, De Hoog et al. 1983, Arzanlou et al. 2007). *Cladosporium* differs from *Ramichloridium* in having conspicuous, protuberant, darkened and thickened, coronate conidial scars, and catenate conidia (Arzanlou et al. 2007). Molecular analyses are necessary to separate *Ramichloridium* from *Veronaea*.

Molecular-based identification: The first multi-gene (LSU and ITS) phylogenetic analysis which included *Ramichloridium* and allied genera was performed by Arzanlou et al. (2007). They reclassified *Ramichloridium* and placed it in *Mycosphaerellaceae* (*Capnodiales*). Crous et al. (2009) reconstructed the phylogenetic analyses for *Capnodiales* and established a new family, *Dissoconiaceae* to accommodate *Dissoconium* and *Ramichloridium* based on ITS, LSU, and SSU sequence data. Five genera, *Dissoconium, Globoramichloridium, Pseudoveronaea, Ramichloridium* and *Uwebraunia* were accepted in *Dissoconiaceae* based on molecular analyses (Marin-Felix et al. 2019a, Hongsanan et al. 2020b, Zheng et al. 2020). This study provides an updated phylogeny of *Ramichloridium* based on combined ITS, LSU and *tef* sequence data (Fig. 40, Table 20) and the result is similar to previous study (Zheng et al. 2020).

Recommended genetic markers (genus level): LSU

Recommended genetic markers (species level): ITS, LSU, *tef*

Accepted number of species: seven

References: De Hoog (1977) (morphology); Arzanlou et al. (2007); Crous et al. (2014), Zheng et al. (2020) (phylogeny)

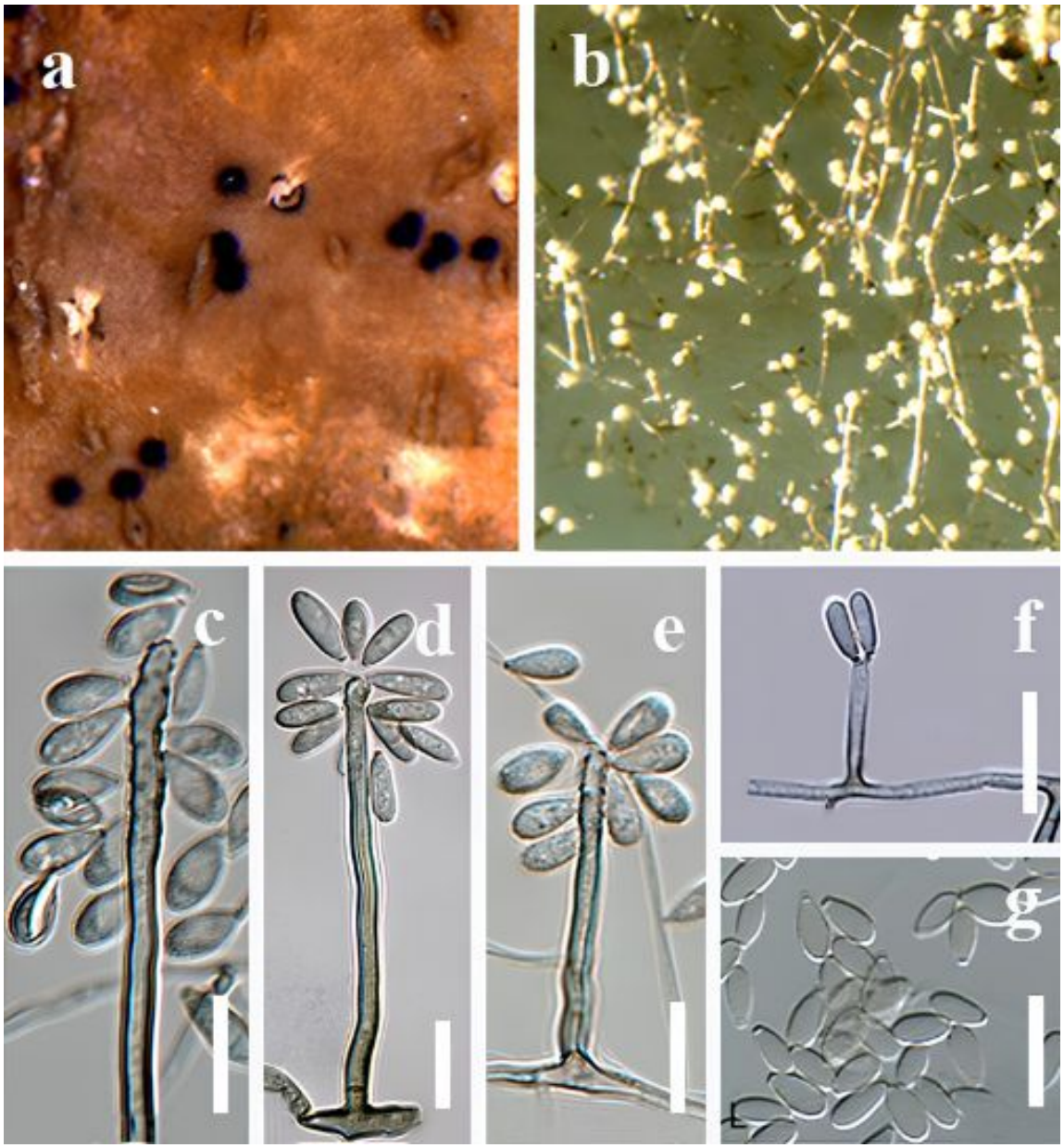

Fig. 39 *Ramichloridium* sp. a *Ramichloridium* sp. on apple. b Sporulating colony. c-e Conidiophores with conidiogenous cells giving rise to a conidium-bearing rachis. f Conidiophores reduced to conidiogenous cells. g Conidia. Scale bars: c-g = 10 µm. This picture is copyright of Pedro Crous (Arzanlou et al. (2007) and Marin-Felix et al. (2019a)).

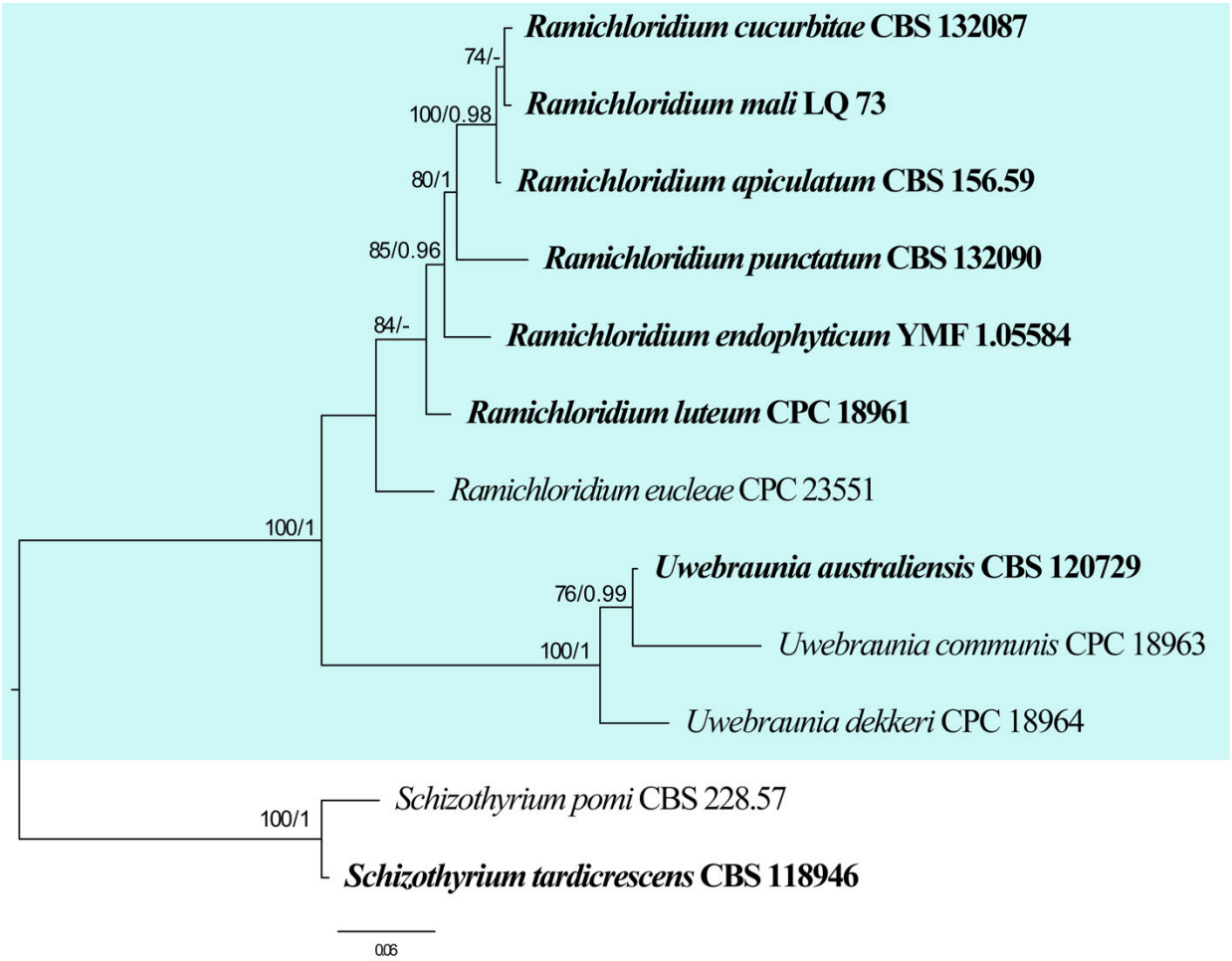

Fig. 40 Maximum likelihood tree of *Ramichloridium* and related species based on the concatenated ITS, LSU and *tef* sequence data. The best scoring RAxML tree had a final likelihood value of -6278.128. The tree was rooted with *Schizothyrium pomi* (CBS 228.57) and *S. tardicrescens* (CBS 118946). Estimated base frequencies were as follows: A = 0.234313, C = 0.260471, G = 0.293042, T = 0.212174; substitution rates AC = 1.783781, AG = 2.739194, AT = 1.812124, CG = 1.712212, CT = 7.492617, GT = 1.000000. ML bootstrap support values over 70% and Bayesian posterior probabilities (BPP) greater than 0.95 are indicated. Type strains are in bold. Scale bar indicates the number of substitutions per site. Hyphens (-) represent support values less than BS 70%/BPP 0.95.

Table 20 DNA barcodes of accepted *Ramichloridium*.

Species	Strain	GenBank accession numbers		
		ITS	LSU	*tef*
Ramichloridium apiculatum	**CBS 156.59**	**NR_145091**	**NG_069690**	**N/A**
R. cucurbitae	**CBS 132087**	**JQ622087**	**NG_042613**	**JQ622112**
R. endophyticum	**YMF 1.05584**	**NR_172411**	**MK836098**	**MN307070**
R. eucleae	CPC 23551	KJ869155	NG_058086	N/A
R. luteum	**CPC 18961**	**EU329730**	**NG_042615**	**JQ622116**
R. mali	**LQ 73**	**EF627452**	**N/A**	**N/A**
R. punctatum	**CBS 132090**	**JQ622086**	**NG_042612**	**JQ622111**

Ex-type/ex-epitype/ex-neotype/ex-lectotype strains and voucher strains are in bold. Sequences that are not available are represented by N/A.

145. *Ravenelia* Berk. Gard. Chron., London 13: 132 (1853)

Type species: *Ravenelia glanduliformis* Berk. & M.A. Curtis

Classification: *Pucciniomycetes, Pucciniales, Raveneliaceae*

Background: *Ravenelia* is the third largest genus with more than 250 described species within the rust fungi (*Pucciniales*) (Hernández & Hennen 2002, Cummins & Hiratsuka 2003, Wijayawardene et al. 2020). This genus was introduced by Berkeley (1853) with *Ravenelia glanduliformis* as the type species on leaves of *Tephrosia* sp. in South

Carolina and Georgia. Initially, *Ravenelia* was comprised of *Ra. glandulosa* and *Ra. indica*. *Ravenelia glandulosa* was transferred from *Sphaeria epiphylla* (found on *Tephrosia virginiana*) while *Ra. indica* (on *Acacia* sp.) was described as a new species. Based on morphological diversity and variability in the life cycle, Sydow (1921) proposed a broad taxonomic classification for *Ravenelia* and distinguished eight species. With the addition of many new species and records throughout the world, *Ravenelia* became the third most species-rich rust fungal genus after *Puccinia* and *Uromyces*. Interestingly, an edible rust fungus *Ra. esculenta* was described from India (Narasimhan and Thirumalachar 1961). The genus is widely distributed in subtropical and tropical regions, but so far there are no reports of *Ravenelia* from Europe and Australia, and exclusively on *Fabaceae* (Cummins and Hiratsuka 2003). After the discovery of the type species, Dietel correctly recombined the type species *Ra. glandulosa* and *Ra. glanduliformis* as synonym of *Ra. epiphylla* (Schwein.) Dietel (Dietel 1894).

Distribution: Africa, Brazil, China, Chile, Mexico, India, Argentina, Spain, Bahamas, Colombia, Cuba, Formosa, Japan, Zambia, France, Pakistan, Panama, Philippines, Sri Lanka, Uganda, USA and Venezuela (Farr & Rossman 2025).

Hosts: Species of *Abrus, Acacia, Albizia, Aloe, Anadenanthera, Andira, Brogniartia, Bulnesia, Caesalpinia, Calliandra, Cassia, Cassiaria, Cenostigma, Chamaecrista, Cracca, Cratylia, Dichrostachys, Elephantorrhiza, Entada, Enterolobium, Erythrina, Gleditsia, Indigofera, Leucaena, Leucania, Lonchocarpus, Lysiloma, Megonemium, Millettia, Mimosa, Parkia, Phyllanthus, Piptadenia, Piscidia, Pithecellobium, Plathymenia, Poinciana, Pongamia, Prosopis, Pseudopiptadenia, Senegalia, Senna, Sesbania, Siderocarpos, Swartzia, Tephrosia* and *Vachellia* (Farr & Rossman 2025).

Disease symptoms: *Ravenelia* species are characterized by the appearance of ochraceous to light brown and chestnut to dark brown pustules on the abaxial as well as adaxial leaf surface (Fig. 41). The aecial stage of several macrocyclic *Ravenelia* spp. may induce galls and witches' brooms in infected host tissues. Production of uredinoid aecia in many *Ravenelia* spp. is another feature of these rust fungi (Cummins1959, Cummins & Hiratsuka 2003).

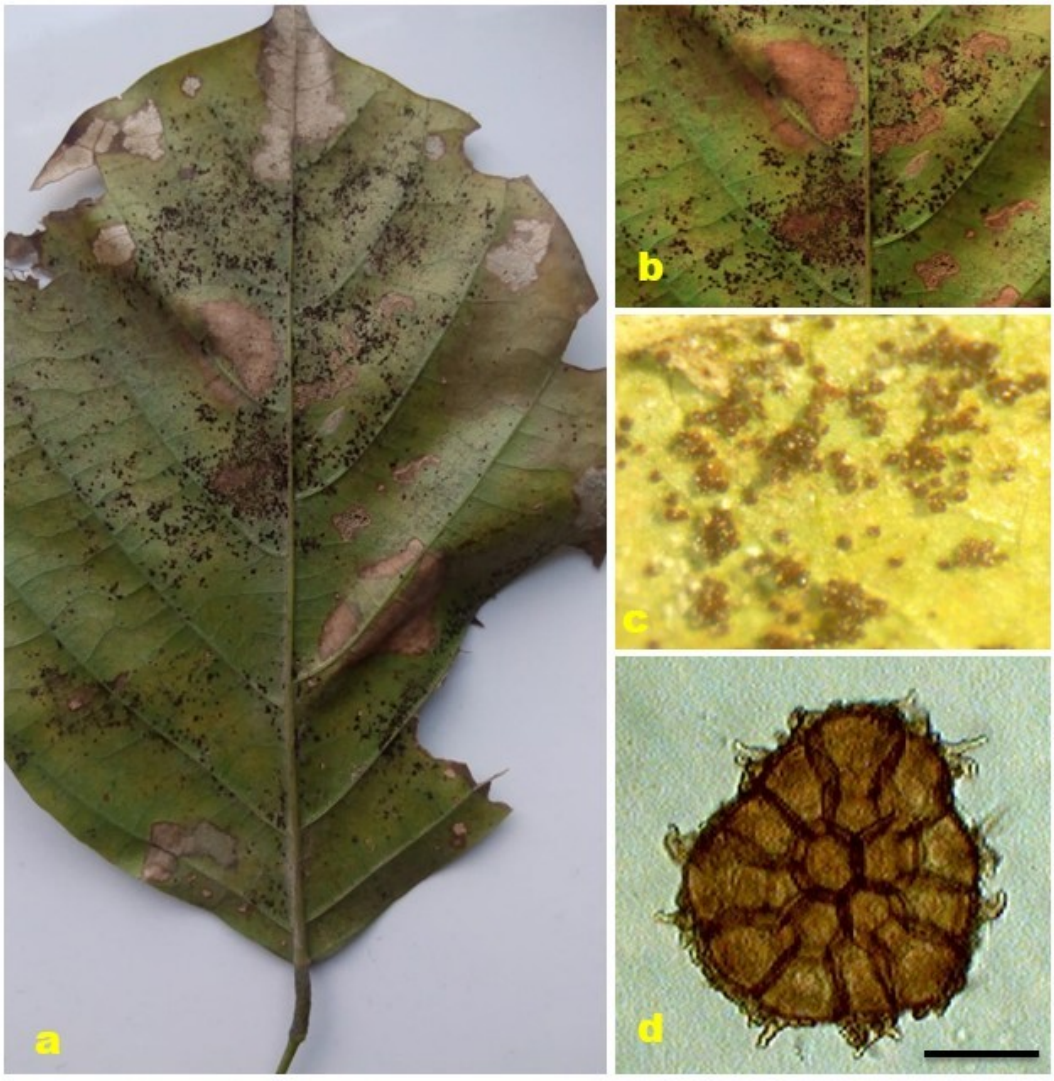

Fig. 41 *Ravenelia* sp. on *Pongamia* sp. a Infected leaf with rust fungus. b-c Sori at various stages of infection. d Teliospore of *Ravenelia* sp. Scale bar: 10 µm. This picture is copyright of Ajay Kumar Gautam, Shubhi Avasthi and Rajnish Kumar Verma.

Pathogen biology, disease cycle and epidemiology: *Ravenelia* spp. are autoecious with life cycles ranging from macro- and demi- to hemi-, and more rarely to microcyclic (Cummins & Hiratsuka 2003). Members of this genus parasitize a diverse range of host plants mostly belonging to the legume family i.e. *Fabaceae* (Hennen et al. 2005). Infection starts when wind-dispersed urediniospores germinate on leaves, penetrating through stomata to form haustoria that extract nutrients from host cells. Urediniospores are repeatedly produced in successive cycles during the growing season, enabling rapid, polycyclic epidemics under favourable conditions. Teliospores develop later, often aggregated in sori or galls, providing overwintering survival and serving as inoculum for the next season (Avasthi et al. 2024).

Morphological-based identification: The most prominent morphological characters shared by all species of *Ravenelia* are the multicellular teliospores, borne on compound pedicels composed of two to several hyphae. These spores have an ellipsoidal, reniform, or almost hemispherical shape in side view and bear a variable number of pendent hygroscopic cysts. Spermogonia are mostly subcuticular, group VI (type 5), however, subepidermal in a few cases with type 7 spermogonia (Cummins & Hiratsuka 2003). Aecia are subepidermal (subcuticular also) and erumpent, containing pedicellate spores (*Uredo* type) or catenulate spores in some cases with or without peridium (*Aecidium*- or *Caeoma*- type). Uredinia are of *Uredo*-type, subepidermal mostly (subcuticular and erumpent) containing echinulate urediniospores borne singly on pedicels. Telia are mostly abaxial, subepidermal (sometimes subcuticular), dark brown to nearly black. The multicellular, ellipsoidal, reniform, or almost hemispherical shaped teliospores consisting of 1 cell (2 cells thick in some species) thick discoid heads are borne on compound pedicels composed of two to several hyphae. There is a single germ pore present in each cell of teliospores. This genus contains external basidia (Cummins & Hiratsuka 2003, Ebinghaus et al. 2020).

Molecular-based identification: DNA sequence data from LSU, SSU, and *cox* genes have been used for phylogenetic analyses. *Ravenelia* have been recorded on various plant hosts. Most of the identifications are based on morpho-taxonomic characteristics; however, there are a few records also available where only molecular data has been used. In a study on rust fungi (*Pucciniales*) by Aime (2006), the 18S and 28S regions of nuclear rDNA were studied to provide a better systematic outline. Herbarium specimens or dried materials and field collections of rust fungi, including *Ravenelia havanensis* collected on *Enterolobium contortisiliquum* from Argentina, were used for DNA extraction and for further molecular analyses. In addition, previously accessioned DNA sequences from GenBank were also utilized to provide a complete framework. Gandhe and Kuvalekar (2007) evaluated the phylogenetic position of *Ravenelia esculenta* among other rust fungi based on the 18S rDNA region and put forth the phylogenetic correlation between molecular and morphological data. This was the first report of DNA sequencing and phylogenetic positioning in the genus *Ravenelia* from India. The rust disease on the plant *Vachellia* caused by *Ravenelia* spp. in South Africa was reported by Ebinghaus et al. (2018). These rust fungi were identified and characterized as *Ra. macowaniana* and *Ra. evansii* based on DNA sequence data of LSU and ITS rDNA regions analyses along with morphological examinations. Similarly, based on molecular phylogenetic analyses of 28S rDNA sequence data, *Ra. piepenbringiae* and *Ra. hernandezii* were identified as representatives of *Senegalia* rusts from Panama and Costa Rica (Ebinghaus & Begerow 2018). Ebinghaus et al. (2020) conducted phylogenetic analyses of *Ravenelia* with a special focus on South African species using 28S rDNA and Cytochrome-c-oxidase subunit 3 sequences. As a result, six novel *Ravenelia* species were reported from South Africa. Aime & McTaggart (2020) presented an updated taxonomy for *Pucciniales*, which is the result of the examination of phylogenetic data of sequences from type species or type species proxies. Molecular data from three loci (LSU, SSU and *cox*) of about 113 rust genera were used to propose a stable higher-rank classification. Gautam et al. (2021) provided a taxonomic outline of Indian *Pucciniales* using ITS and LSU sequences of five species of *Ravenelia*, along with 25 other genera of rust fungi. This study provides an updated phylogeny of *Ravenelia* based on combined ITS and LSU sequence data (Fig. 42, Table 21).

Recommended genetic marker (genus level): ITS

Recommended genetic marker (species level): ITS, LSU

Accepted number of species: 250

References: Aime (2006), Scholler & Aime (2006), Gandhe & Kuvalekar (2007), McTaggart et al. (2015), Aime et al. (2018), Ebinghaus & Begerow (2018), Ebinghaus et al. (2018), Ebinghaus et al. (2020), Aime & McTaggart (2020) (morphology and phylogeny)

146. *Seiridium* Nees, Syst. Pilze (Würzburg): 22 (1817)

Type species: *Seiridium marginatum* Nees, Syst. Pilze (Würzburg)

Classification: *Sordariomycetes*, *Amphisphaeriales, Sporocadaceae*

Background: *Seiridium* was established by Nees (1817) based on *Seiridium marginatum*, and epitypified by Jaklitsch et al. (2016). Members are predominantly known as plant pathogens, often causing serious diseases in woody plants and trees (Graniti 1998, Barnes et al. 2001, Bonthond et al. 2018, Li et al. 2022). The most notable species is *Seiridium cardinale* which is the causal agent of cypress canker, a devastating disease affecting cypress and related conifer species worldwide (Graniti 1986). The genus has historically been taxonomically challenging due to morphological similarities with related genera, however, the use of multi-locus phylogeny has helped clarify species boundaries and evolutionary relationships within this group.

Distribution: worldwide (Farr & Rossman 2025)

Disease symptoms: *Seiridium* species, particularly those pathogenic to conifers, cause a range of disease symptoms (Graniti 1998, Bonthond et al. 2018). Infection usually occurs through wounds by environmental factors such as wind, frost, insect activity, or natural openings (La Porta et al. 2008, Bonthond et al. 2018). After penetration, necrotic bark lesions spread rapidly through the cortical parenchyma and more slowly within the phloem while in severe cases, the cambium and all surrounding tissues turn brown and die (Graniti 1998). Infected trees typically develop sunken, necrotic lesions on branches and stems, which may exude resin or sap. These cankers often start as small, discoloured areas that expand over time, girdling branches or main stems and leading to

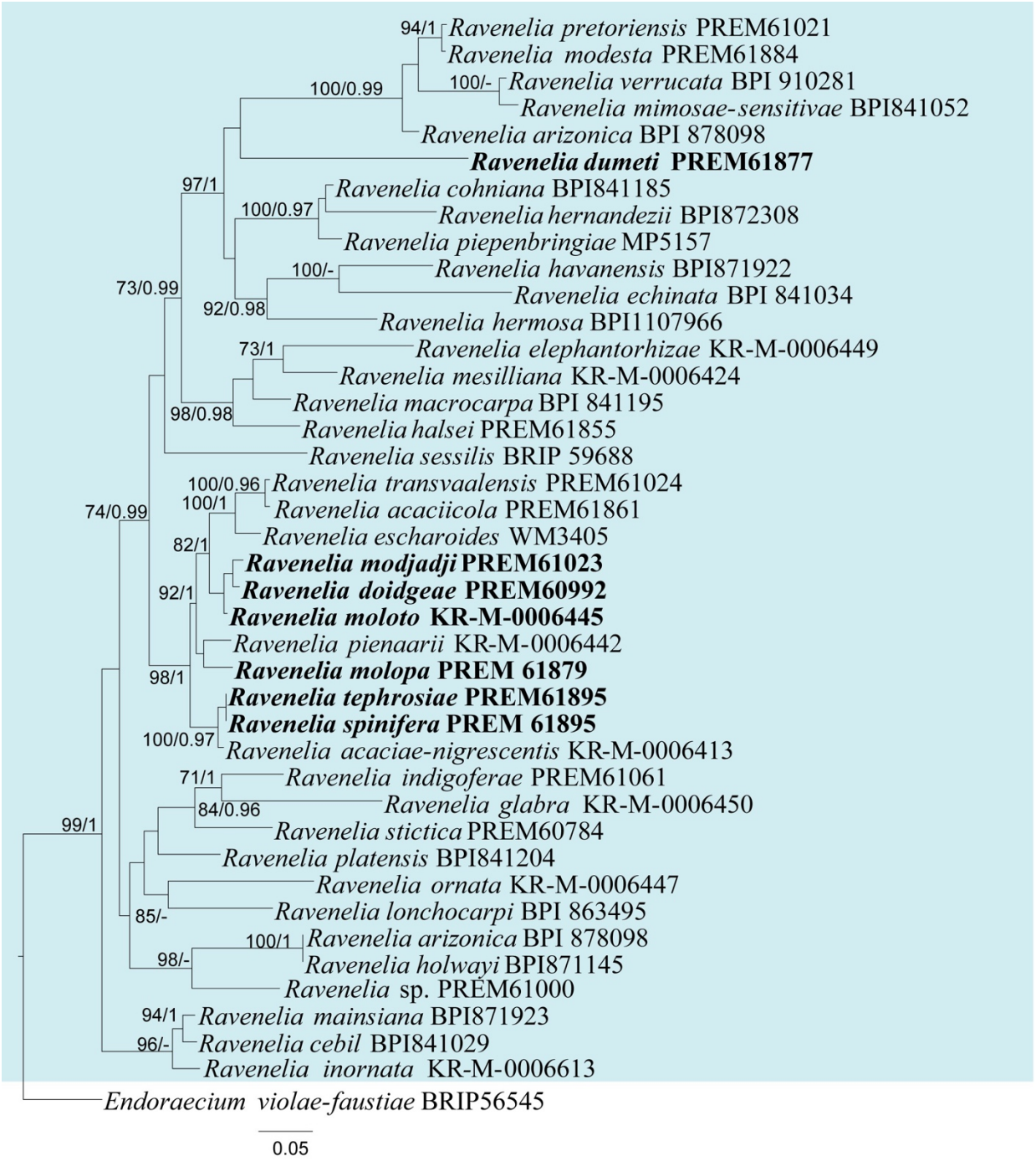

Fig. 42 Maximum likelihood tree of *Ravenelia* species based on the concatenated ITS and LSU sequence data. The best scoring RAxML tree had a final likelihood value of -10939.992725. The tree was rooted to *Endoraecium violae-faustiae* (BRIP56545). Estimated base frequencies were as follows: A = 0.297698, C = 0.159517, G = 0.260564, and T = 0.282220; substitution rates AC = 1.260199, AG = 3.686171, AT = 1.534708, CG = 0.647813, CT = 5.324166, and GT = 1.000000. ML bootstrap support values over 70% and Bayesian posterior probabilities (BPP) greater than 0.95 are indicated. Type strains are in bold. Scale bar indicates the number of substitutions per site. Hyphens (-) represent support values less than BS 70%/BPP 0.95.

Table 21 DNA barcodes for accepted species of *Ravenelia*.

Species	Strain	GenBank accession numbers	
		ITS	LSU
Ravenelia acaciae-nigrescentis	KR-M-0006413	N/A	MN072686
Ra. acaciicola	PREM61861	N/A	MN072683

Ra. arizonica	BPI 878098	N/A	MW147032
Ra. cebil	BPI841029	N/A	MN072649
Ra. cohniana	BPI841185	N/A	MG954487
Ra. doidgeae	**PREM60992**	**N/A**	**MN072672**
Ra. dumeti	**PREM61877**	**N/A**	**MN072681**
Ra. echinata	BPI841034	N/A	DQ323925
Ra. elephantorhizae	KR-M-0006449	MN072702	MN072702
Ra. escharoides	WM3405	N/A	MG954480
Ra. glabra	KR-M-0006450	N/A	MN072691
Ra. halsei	PREM61855	N/A	MG954484
Ra. havanensis	BPI871922	N/A	MN275524
Ra. hermosa	BPI1107966	N/A	MN072657
Ra. hernandezii	BPI872308	N/A	MG954488
Ra. holwayi	BPI871145	N/A	MN072656
Ra. indigoferae	PREM61061	N/A	MN072664
Ra. inornata	KR-M-0006613	N/A	MN072666
Ra. lonchocarpi	BPI 863495	N/A	MW147034
Ra. macrocarpa	BPI841195	N/A	DQ323926
Ra. mainsiana	BPI871923	N/A	MN275525
Ra. mesilliana	KR-M-0006424	N/A	MN072693
Ra. mimosae-sensitivae	BPI841052	N/A	MN072650
Ra. modesta	PREM61884	N/A	MN072688
Ra. modjadji	**PREM61023**	**N/A**	**MN072667**
Ra. molopa	**PREM61879**	**N/A**	**NG_068900**
Ra. moloto	**KR-M-0006445**	**N/A**	**MN072697**
Ra. ornata	KR-M-0006447	N/A	MN072687
Ra. pienaarii	KR-M-0006442	N/A	MN072699
Ra. piepenbringiae	MP5157	N/A	MG954489
Ra. platensis	BPI841204	N/A	MN072652
Ra. pretoriensis	PREM61021	N/A	MN072665
Ra. sessilis	BRIP 59688	N/A	MW147035
Ra. spinifera	**PREM 61895**	**N/A**	**NG_068903**
Ra. stictica	PREM60784	N/A	MN072663
Ra. tephrosiae	**PREM61895**	**N/A**	**MN072698**
Ra. transvaalensis	PREM61024	N/A	MN072669
Ra. verrucata	BPI 910281	KY764176	KY764176

Ex-type/ex-epitype/ex-neotype/ex-lectotype strains and voucher strains are in bold. Sequences that are not available are represented by N/A.

dieback of the affected tissues (Graniti 1998, Danti et al. 2014, Bonthond et al. 2018). In severe cases, the infection can cause extensive bark cracking, resin bleeding, and eventual death of large portions of the tree crown (Bonthond et al. 2018). Needle discoloration, wilting, and premature needle drop are common secondary symptoms as the vascular tissues become impaired. The progression of the disease can lead to structural weakening of the tree and increased susceptibility to other pathogens or environmental stressors (Bonthond et al. 2018).

Hosts: *Seiridium* has a wide range of hosts, including several economical plant genera, such as *Camellia*, *Eucalyptus*, *Juniperus* and *Rosa* (Graniti 1998, Barnes et al. 2001, Tsopelas et al. 2007, Bonthond et al. 2018, Marin-Felix et al. 2019a, Li et al. 2022, Farr & Rossman 2025). The genus is also well-known to be associated with *Cupressaceae* including cypress, juniper, arborvitae, and related conifers (Danti et al., 2014, Aylward et al. 2025, Farr & Rossman 2025).

Pathogen biology, disease cycle and epidemiology: *Seiridium* species form acervuli on infected bark that produce conidia, that serve as infectious propagules (Bonthond et al. 2018). The disease cycle begins when the conidia infect trees through wounds or natural openings (La Porta et al. 2008). These wounds are often caused by pruning, insect damage, mechanical injury, or environmental stress. Once the conidia land on these entry points, especially during warm, moist weather, they establish beneath the bark to form resinous and necrotic cankers, which disrupt vascular flow and eventually lead to branch dieback and tree mortality (Graniti 1998; Danti et al. 2014). The spores can also be dispersed by rain splash, wind, insects, or contaminated pruning tools, enabling the pathogen to spread and cause new infections on nearby trees (Ghelardini et al. 2017). *Seiridium* species have been responsible for significant global outbreaks of cypress canker. *Seiridium cardinale* spread to several continents, resulting in a global outbreak of cypress canker, with particularly severe impacts in Mediterranean climates (Graniti 1998, Aylward et al. 2025).

Morphological-based identification: *Seiridium* produces acervular to pycnidial conidiomata that are semi-immersed or erumpent and brown or black (Bonthond et al. 2018, Jiang et al. 2019, Fig. 43). Conidia are fusiform, multi-septate, bearing two appendages, with pale-hyaline end cells and brown-pigmented median cells that are smooth or striated. Distinguishing *Seiridium* from morphologically similar genera such as *Pestalotiopsis*, *Neopestalotiopsis*, and *Monochaetia* can be challenging due to overlapping conidial characteristics (Graniti 1998, Bonthond et al. 2018). *Seiridium* typically differ from these morphologically similar genera as they have conidia with lighter pigmentation and smoother walls. The

presence, position, and morphology of conidial appendages have been used as key diagnostic features for distinguishing *Seiridium* species (Bonthond et al. 2018). However, these morphological traits can be variable and overlap among species, making identification challenging.

Molecular-based identification: Molecular-based analyses are important for accurate delimitation of *Seiridium* species due to the morphological overlap. Barnes et al. (2001) highlighted the limitations of morphological identification and demonstrated that the ITS region lacked resolution for distinguishing *Seiridium* species. Many isolates previously identified as *S. unicorne* based on morphology were found to be genetically distinct (Cunnington et al. 2007). Jaklitsch et al. (2016) and Bonthond et al. (2018) applied a polyphasic approach to resolve cryptic species within *Sporocadaceae* using ITS, *tef*, *tub2*, and *rpb2* sequences. Bonthond et al. (2018) also contributed to the designation of epitypes. Razaghi et al. (2024) used LSU, ITS, *tef*, *tub2*, and *rpb2* sequences of *Sporocadaceae* from numerous plant hosts mainly from China to significantly broadened the diversity within the family. This study provides an updated phylogeny of *Seiridium* based on combined ITS, *rpb2*, *tef*, and *tub2* sequence data (Fig. 44, Table 22).

Recommended genetic markers (genus level): ITS

Recommended genetic markers (species level): ITS, *rpb2*, *tef*, and *tub2*

Accepted number of species: 29

References: Barnes et al. (2001), Cunnington et al. (2007), Jaklitsch et al. (2016), Bonthond et al. (2018), Razaghi et al. (2024) (morphology and phylogeny)

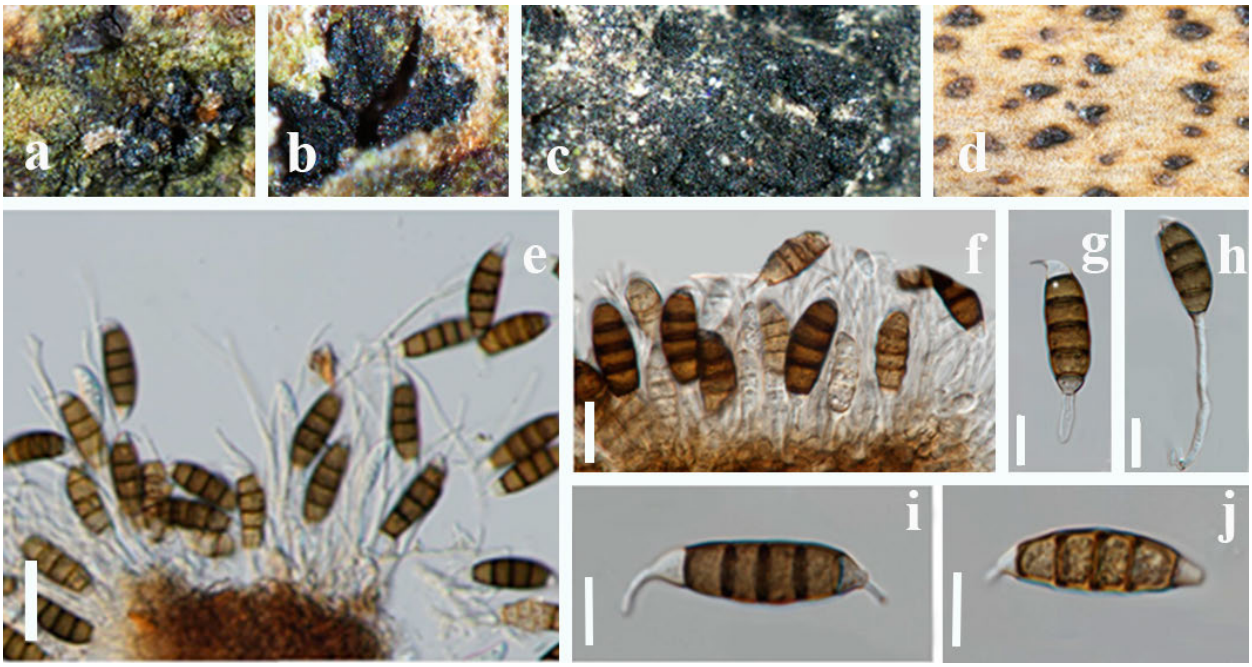

Fig. 43 *Seiridium* sp. on branches of: a, b *Vernicia fordii*. c *Olea europaea*. d *Paeonia suffruticosa.* e-f Conidiogenous cells and conidia. g-h Conidiophore and conidia. i-j Conidia. Scale bars: e = 20 µm, f-j = 10 µm. This picture is copyright of Jian-Kui (Jack) Liu (Li et al. 2022).

147. *Stenocarpella* Syd. & P. Syd., Annls mycol. 15(3/4): 258 (1917)

Type species: *Stenocarpella macrospora* (Earle) B. Sutton

Classification: *Sordariomycetes*, *Diaporthales*, *Diaporthaceae*

Background: *Stenocarpella* was introduced and illustrated by Sydow & Sydow (1917), who treated *St. zeae* as the type species. Sutton (1977) provided evidence that *St. zeae* is a synonym of *Diplodia macrospora* and named *St. macrospora* as the type species. Initially, *Stenocarpella* was placed in *Botryosphaeriaceae* (*Botryosphaeriales*) due to morphological similarity with *Diplodia* (Lamprecht et al. 2011). Crous et al. (2006a, b) and Senanayake et al. (2018) found that *Stenocarpella* belongs to *Diaporthaceae* (*Diaporthales*) based on LSU sequences. Subsequently, Lamprecht et al. (2011) confirmed its placement using ITS and *tef* sequence.

Distribution: worldwide (Farr & Rossman 2025)

Disease symptoms: *Stemocarpella macrospora* and *St. maydis* cause seed rot, seedling blight, stem and ear rot, and leaf spots of maize (Fig. 45). When ears are affected, these fungi are usually the predominant grain rot causative agent (Latterell & Rossi 1983, Casa et al. 2006, Lamprecht et al. 2011, Da Silva et al. 2014, Senanayake et al. 2018, Hyde et al. 2020). *Stenocarpella maydis* causes a dry rot of maize ears, and occurs in practically every maize cultivation worldwide (Sutton & Waterston 1966, Dorrance et al. 1998, Wicklow et al. 2011, Matiello et al. 2015). When switching from conventional to conservation tillage, the severity of *St. maydis* rot increases (Kerr 1965, Kruger 1970, Byrnes & Carroll 1986, Flett & Wehner 1990). *Stenocarpella maydis* can be found in the residue of maize stalks, ears, and fallen grains between seasons. *Stenocarpella maydis* may cause a reduction in seed germination and vigor of emerged seedlings and is associated with neuro mycotoxicosis in cattle grazing harvested maize fields in southern Africa and Argentina (da Silva Siqueira et al. 2014). Initially, the symptoms caused by *St. maydis* are yellowing and drying of infected leaves on the green maize plant (Rossouw 2001). The second symptom is discolored kernel embryos that can only be seen if the ear is broken; this symptom is called "hidden diplodia" in South

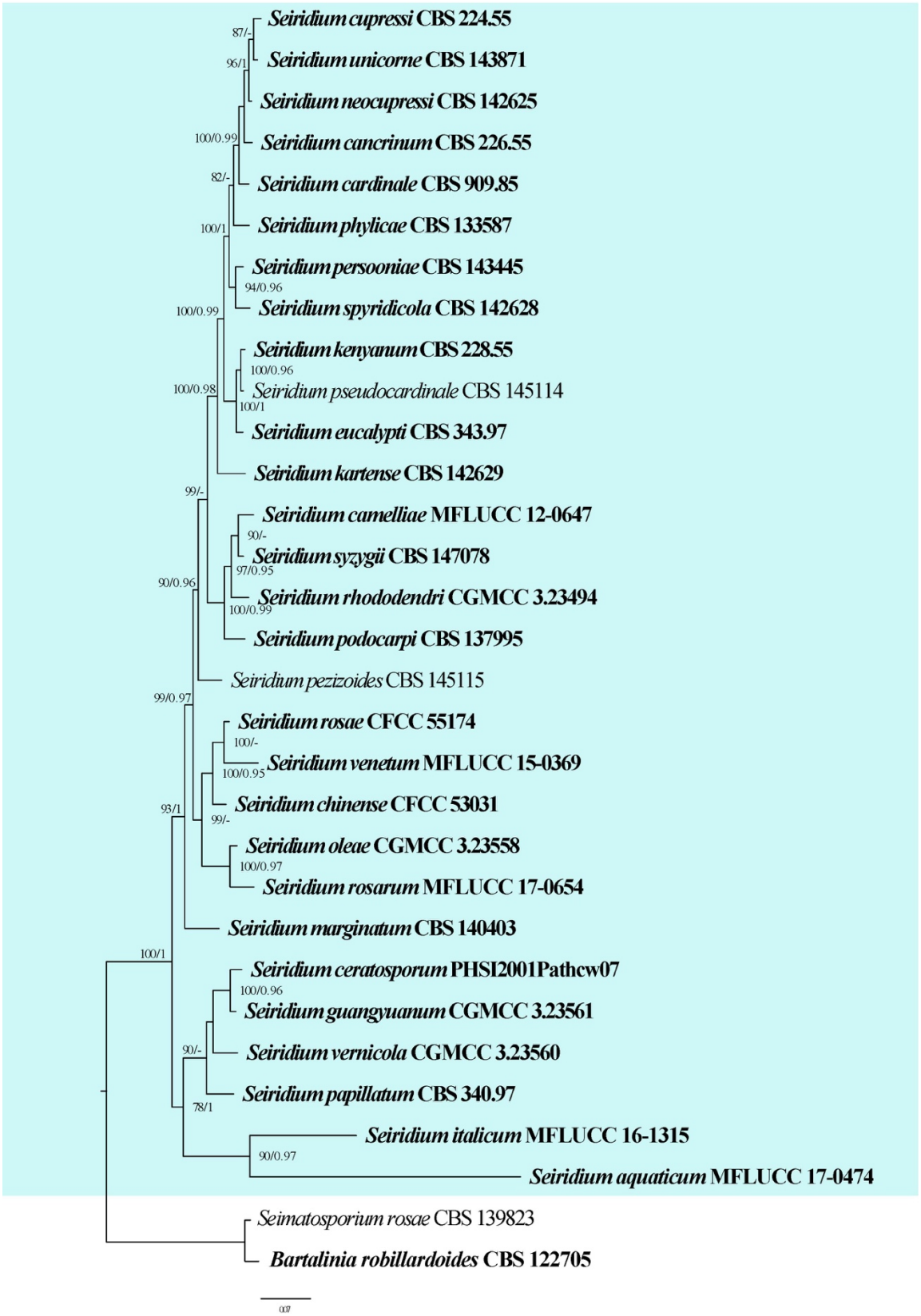

Fig. 44 Maximum likelihood tree of *Seiridium* species based on the concatenated ITS, *rpb2*, *tef*, and *tub2* sequence data. The best scoring RAxML tree had a final likelihood value of -18579.142. The tree was rooted with *Bartalinia robillardoides* (CBS 122705) and *Seimatosporium rosae* (CBS 139823). Estimated base frequencies were as follows: A = 0.250, C = 0.250, G = 0.250, T = 0.250; substitution rates AC = 1.00000, AG = 3.45694, AT = 1.00000, CG = 1.00000, CT = 4.30822, GT = 1.000000. ML bootstrap support values over 70% and Bayesian posterior probabilities (BPP) greater than 0.95 are indicated. Type strains are in bold. Scale bar indicates the number of substitutions per site. Hyphens (-) represent support values less than BS 70%/BPP 0.95.

Table 22 DNA barcodes for accepted species of *Seiridium*.

Species	Strain	GenBank accession numbers			
		ITS	*rpb2*	*tef*	*tub2*
Seiridium aquaticum	**MFLUCC 17-0474**	**MK828605**	**MN156531**	**MN194101**	**N/A**
S. camelliae	**MFLUCC 12-0647**	**JQ683725**	**N/A**	**JQ683741**	**JQ683709**
S. cancrinum	**CBS 226.55**	**LT853089**	**LT853137**	**LT853186**	**LT853236**
***S. cardinale*#**	**CBS 909.85**	**LT853064**	**LT853113**	**LT853161**	**LT853211**
S. ceratosporum	**PHSI2001Pathcw07**	**AY687314**	**N/A**	**N/A**	**DQ137857**
S. chinense	**CFCC 53031**	**MK353158**	**MK351796**	**MK351799**	**MK351802**
***S. cupressi*#**	**CBS 224.55**	**LT853083**	**LT853131**	**LT853180**	**LT853230**
S. eucalypti	**CBS 343.97**	**LT853099**	**LT853146**	**LT853196**	**LT853246**
S. guangyuanum#	**CGMCC 3.23561**	**OP082305**	**OP204826**	**OP204809**	**OP235995**
S. italicum	**MFLUCC 16-1315**	**MW240643**	**MW658630**	**MW759527**	**MW775600**
S. kartense	**CBS 142629**	**LT853100**	**LT853147**	**LT853197**	**LT853247**
S. kenyanum	**CBS 228.55**	**LT853098**	**LT853145**	**LT853195**	**LT853245**
S. marginatum	**CBS 140403**	**KT949914**	**LT853149**	**LT853199**	**LT853249**
S. neocupressi	**CBS 142625**	**LT853079**	**LT853127**	**LT853176**	**LT853226**
S. oleae#	**CGMCC 3.23558**	**OP082313**	**OP204833**	**OP204817**	**OP236003**
S. papillatum	**CBS 340.97**	**LT853102**	**LT853150**	**LT853200**	**LT853250**
S. persooniae	**CBS 143445**	**MG386033**	**N/A**	**N/A**	**MG386163**
S. pezizoides	CBS 145115	MK079342	MK058475	MK058480	MK058485
***S. phylicae*#**	**CBS 133587**	**LT853091**	**LT853139**	**LT853188**	**LT853238**
S. podocarpi	**CBS 137995**	**LT853101**	**LT853148**	**LT853198**	**LT853248**
S. pseudocardinale	CBS 145114	MK079341	MK058479	MK058484	MK058489
S. rhododendri	**CGMCC 3.23494**	**OR247929**	**OR792179**	**OR361507**	**OR381088**
S. rosae	**CFCC 55174**	**OK560681**	**OL742151**	**OL814533**	**OM313314**
S. rosarum	**MFLUCC 17-0654**	**MG828961**	**N/A**	**N/A**	**N/A**
S. spyridicola	**CBS 142628**	**LT853095**	**LT853142**	**LT853192**	**LT853242**
S. syzygii	**CBS 147078**	**MZ064444**	**N/A**	**N/A**	**N/A**
S. unicorne#	**CBS 143871**	**MK079339**	**MK058477**	**MK058482**	**MK058487**
S. venetum	**MFLUCC 15-0369**	**KT438836**	**N/A**	**N/A**	**KT438837**
S. vernicola	**CGMCC 3.23560**	**OP082319**	**OP204838**	**OP204823**	**OP236008**

Ex-type/ex-epitype/ex-neotype/ex-lectotype strains and voucher strains are in bold. Sequences that are not available are represented by N/A. Species confirmed with pathogenicity studies are marked with #.

Africa (Flett 1999, Rossouw 2001). Normally it is invisible when the ear is closed, only seen at harvest when the prominent symptom is discolored kernel embryos, therefore resulting in yield loss (Rossouw 2001). Infections that cause maize ear rot are particularly important because they cause considerable decreases in maize output. The symptoms caused by *St. macrospora* first form an infection point, and then continue spreading till necrotic. The infection develops into a light brown spot, surrounded by a yellowish halo, decreasing the photosynthetic area of the leaf. In the area of symptoms, dark patches emerge, which are pycnidia. These produce spores that are conveyed and infect the base of the ear and can move to the apex, in the form of white or yellowish, cottony mycelium, and from the cob to the grains, resulting in lowering grain quality (grains burning) (Duarte et al. 2009). *Stenocarpella* species are frequently isolated from infected maize crops throughout the world, especially during humid seasons. This so-called "maize ear rot" can cause both weight reduction and quality losses in the grain (Odriozola et al. 2005). Maize ear rot diseases are one of the world's most significant food and feed safety threats to maize production (Mesterházy et al. 2012, Matiello et al. 2015).

Hosts: *Stenocarpella* species have a wide distribution, especially on maize crops, causing stalk and ear rot, seed rot, seedling blight, and leaf spot. They are considered the most important pathogen in maize (Bressan & Figueiredo 2003, Casa et al. 2006, Lamprecht et al. 2011, Rossouw 2001, Da Silva et al. 2014, Senanayake et al. 2018). While maize is the primary host, *Stenocarpella* can survive on crop residues and infect grass-related species under favorable conditions (Jia et al. 2023).

Pathogen biology, disease cycle and epidemiology: *Stenocarpella* species can damage the embryo of maize seeds, decrease germination and seedling vigor, and cause rot in the stem and ears, even impairing its functioning, resulting in stem base breaking, lodging, and, untimely plant death (Vincelli 1997, Fedrigo et al. 2016). When infected by *Stenocarpella* species, the host will exhibit symptoms such as ear rot, seed rot, seedling blight, and leaf spot, which will gradually develop and eventually lead to widespread infection and finally kill the host. When the fruiting bodies mature, the pycnidia open and the spores extrude, and they are spread by raindrops, wind, insects, and infected seeds (Vincelli 1997, Matiello et al. 2015, Bermúdez-Cardona et al.

2016, Fedrigo et al. 2016). The mycelium of *Stenocarpella* species can survive and overwinter in residue stalks, ears, and fallen grains of maize, resulting in a new round of infection under favourable conditions (Bermúdez-Cardona et al. 2016, Fedrigo et al. 2016).

Morphological-based identification: *Stenocarpella* species have been extensively published as species of *Diplodia* due to having similar morphology (Lamprecht et al. 2011). *Stenocarpella macrospora* and *St. maydis* have unique characteristics of conidiogenous cells and are distinct from *Diplodia*. The sexual morph of *Stenocarpella* is unknown. *Stenocarpella* is characterised by unilocular, pycnidial, solitary, or occasionally confluent, subepidermal, globose or elongated, dark brown, ostiolate conidiomata with thick-walled dark brown cells of *textura angularis*. The conidiomata are papillate with a single, circular ostiole. The conidiophores are usually reduced to phialidic conidiogenous cells that are cylindrical, determinate, discrete, with a collarette and a minute channel. The periclinal wall is thickened and the conidiogenous cells proliferate percurrently, producing cylindrical, fusiform, straight or curved conidia with an obtuse apex and a tapered, truncate base. The conidia are brown, septate, smooth, thin-walled, subcylindrical to narrowly obclavate (Crous et al. 2006, Senanayake et al. 2018, Jia et al. 2023).

Molecular-based identification: In the past, *Stenocarpella* species were placed in *Botryosphaeriaceae.* Crous et al. (2006a) recollected species of *Stenocarpella* and revealed *Stenocarpella* belong to *Diaporthales* with the evidence of molecular phylogenetic studies (LSU sequence). Lamprecht et al. (2011) confirmed its placement in *Diaporthaceae* using LSU sequence in the phylogenetic analysis for the generic placement, and ITS and *tef* to determine species-level relationships. Wijayawardene et al. (2016b) also provided evidence that *Stenocarpella* belongs to the *Diaporthaceae* based on LSU and ITS sequences. Thambugala & Hyde (2018) presented a phylogenetic tree with *Stenocarpella* in *Diaporthaceae* based on ITS, LSU, and *tef* sequences. This study provides an updated phylogeny of *Stenocarpella* based on combined ITS, LSU and *tef* sequence data (Fig. 46, Table 23).

Recommended genetic markers (genus level): LSU

Recommended genetic markers (species level): ITS, LSU and *tef*

Accepted number of species: three

References: Matiello et al. (2015), Bermúdez-Cardona et al. (2016), Jia et al. (2023) (morphology and phylogeny)

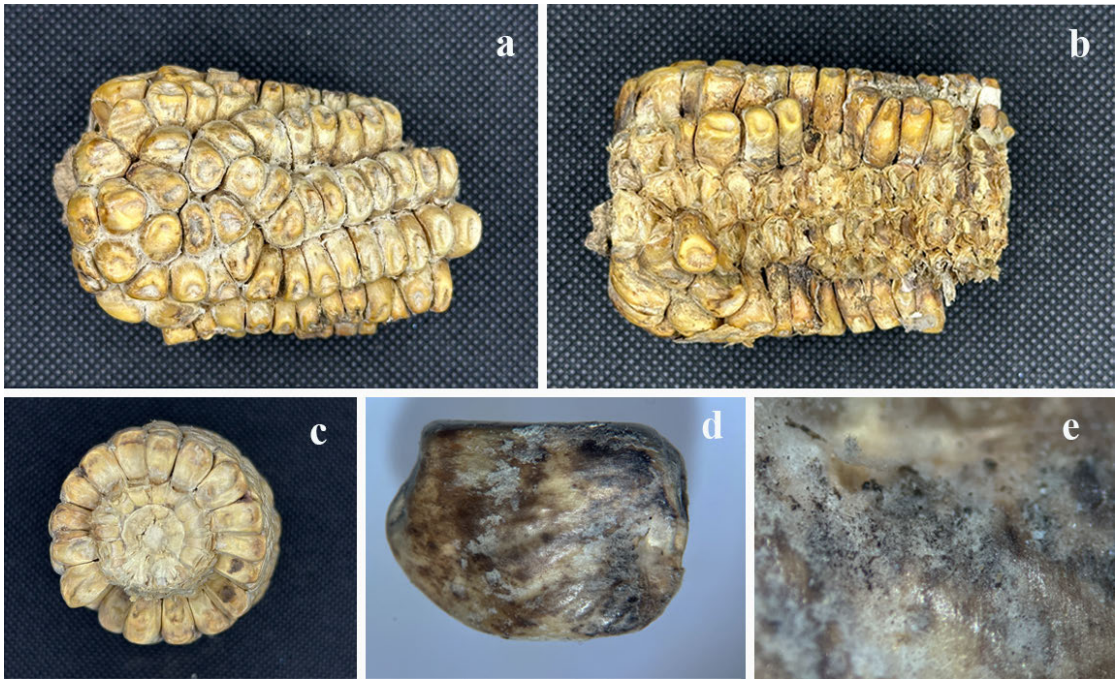

Fig. 45 Symptoms caused by *Stenocarpella* sp. a-e Maize ears and kernels infected with *Stenocarpella maydis.* This picture is copyright of Guillermo Márquez-Licona (García-Reyes et al. 2022).

Table 23 DNA barcodes for accepted species of *Stenocarpella* species used in the analysis.

Species	Strain	GenBank accession numbers		
		ITS	LSU	*tef*
Stenocarpella chrysopogonis#	**GDMCC 3.684**	**OL780795**	**OL780802**	**OL944433**
St. macrospora#	**CBS 117560**	**FR748048**	**DQ377934**	**N/A**
St. macrospora	CPC 11863	FR748049	N/A	N/A
St. maydis#	**CBS 117558**	**FR748051**	**DQ377936**	**FR748080**
St. maydis	CPC 16785	FR748060	FR748113	FR748089

Ex-type/ex-epitype/ex-neotype/ex-lectotype strains and voucher strains are in bold. Sequences that are not available are represented by N/A. Species confirmed with pathogenicity studies are marked with #.

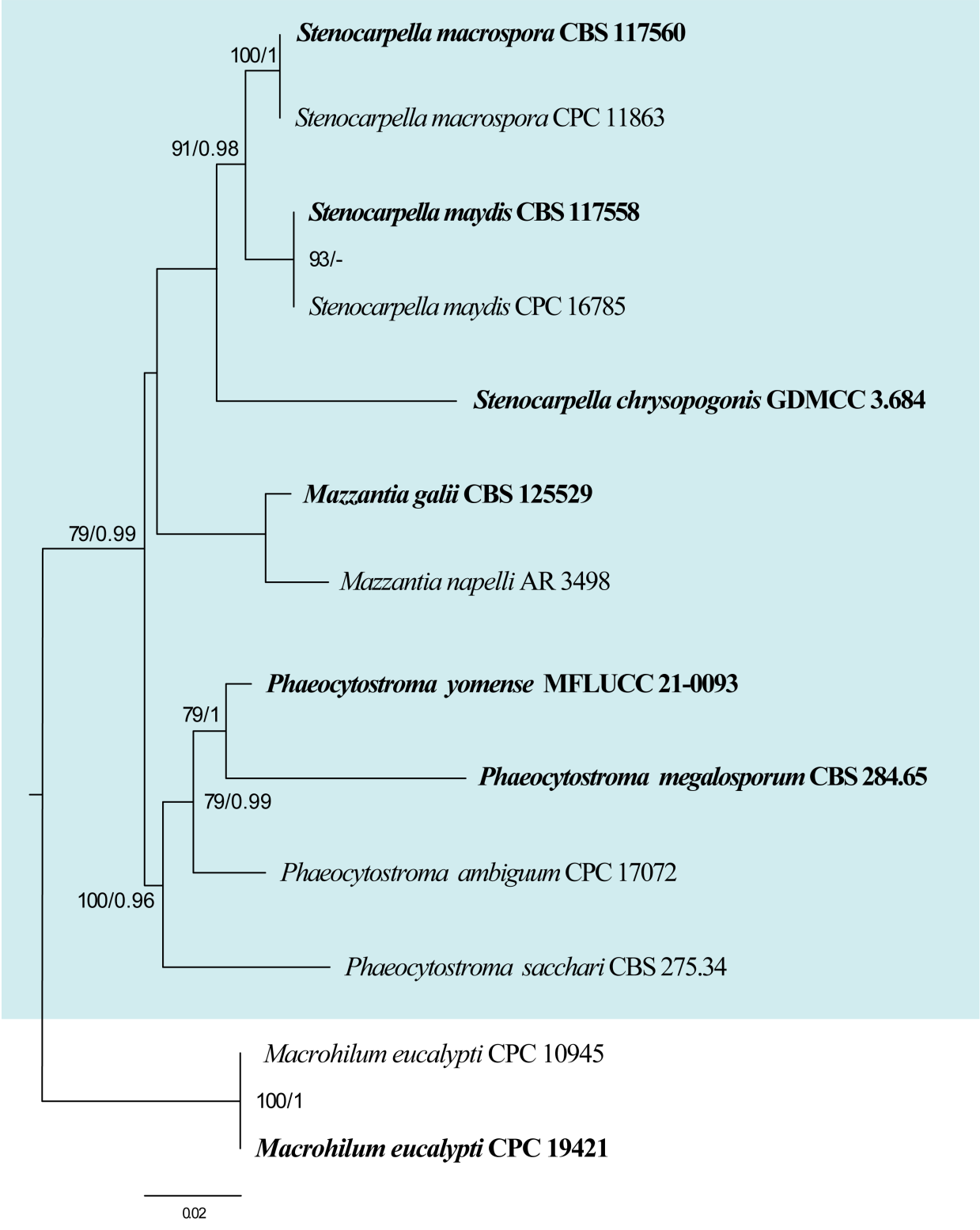

Fig. 46 Maximum likelihood tree of *Stenocarpella* and related species based on the concatenated ITS, LSU and *tef* sequence data. The best scoring RAxML tree had a final likelihood value of -10313.925489. The tree was rooted with *Macrohilum eucalypti* (CPC 10945 and CPC 19421). Estimated base frequencies were as follows: A = 0.241440, C = 0.270829, G = 0.279735, T = 0.207997; substitution rates AC = 1.586014, AG = 2.680785, AT = 1.670079, CG = 1.612357, CT = 6.629624, GT = 1.000000. ML bootstrap support values over 70% and Bayesian posterior probabilities (BPP) greater than 0.95 are indicated. Type strains are in bold. Scale bar indicates the number of substitutions per site. Hyphens (-) represent support values less than BS 70%/BPP 0.95.

148. *Tubakia* B. Sutton, Trans. Brit. Mycol. Soc. 60: 164. (1973)

Type species: *Tubakia japonica* (Sacc.) B. Sutton

Classification: *Sordariomycetes*, *Diaporthales*, *Tubakiaceae*

Background: *Tubakia* was introduced by Sutton (1973) and the genus is known for causing leaf spot diseases on a variety of hardwood trees, particularly oaks (*Quercus* spp.) (Harrington et al. 2012). *Tubakia* species are endophytes in leaves and twigs of many tree species (Cohen 1999). *Tubakia* species are common in temperate and subtropical regions, where they infect host plants through leaf surfaces, especially during warm and wet weather. The most notable species, *Tubakia dryina*, produces characteristic brown or reddish circular lesions on leaves, which may coalesce and lead to premature defoliation (Braun et al. 2018). While generally considered a secondary pathogen or stress-related invader, severe infections can reduce tree vigor over time.

Distribution: worldwide (Farr & Rossman 2025)

Disease symptoms: Tubakia leaf spot primarily affects the foliage of hardwood trees, especially oaks, with symptoms typically appearing in mid to late summer (Harrington et al. 2012, Fig. 47). The disease is characterized by small, circular to irregularly shaped leaf spots that are brown, reddish-brown, or tan in color, often with darker margins (Braun et al. 2018, Yun & Kim 2018). These lesions can vary in size and may coalesce to form larger dead areas on the leaf surface (Kowalski 2006). In severe cases, infected leaves may curl, become scorched, and fall prematurely, leading to significant defoliation (Kowalski 2006). The symptoms often begin on older or lower leaves and progress upward through the canopy (Fallon et al. 2020). While the disease is generally cosmetic and not fatal to healthy trees, repeated defoliation over consecutive seasons can weaken trees, making them more vulnerable to other stresses such as drought or insect infestations (Kowalski 2006).

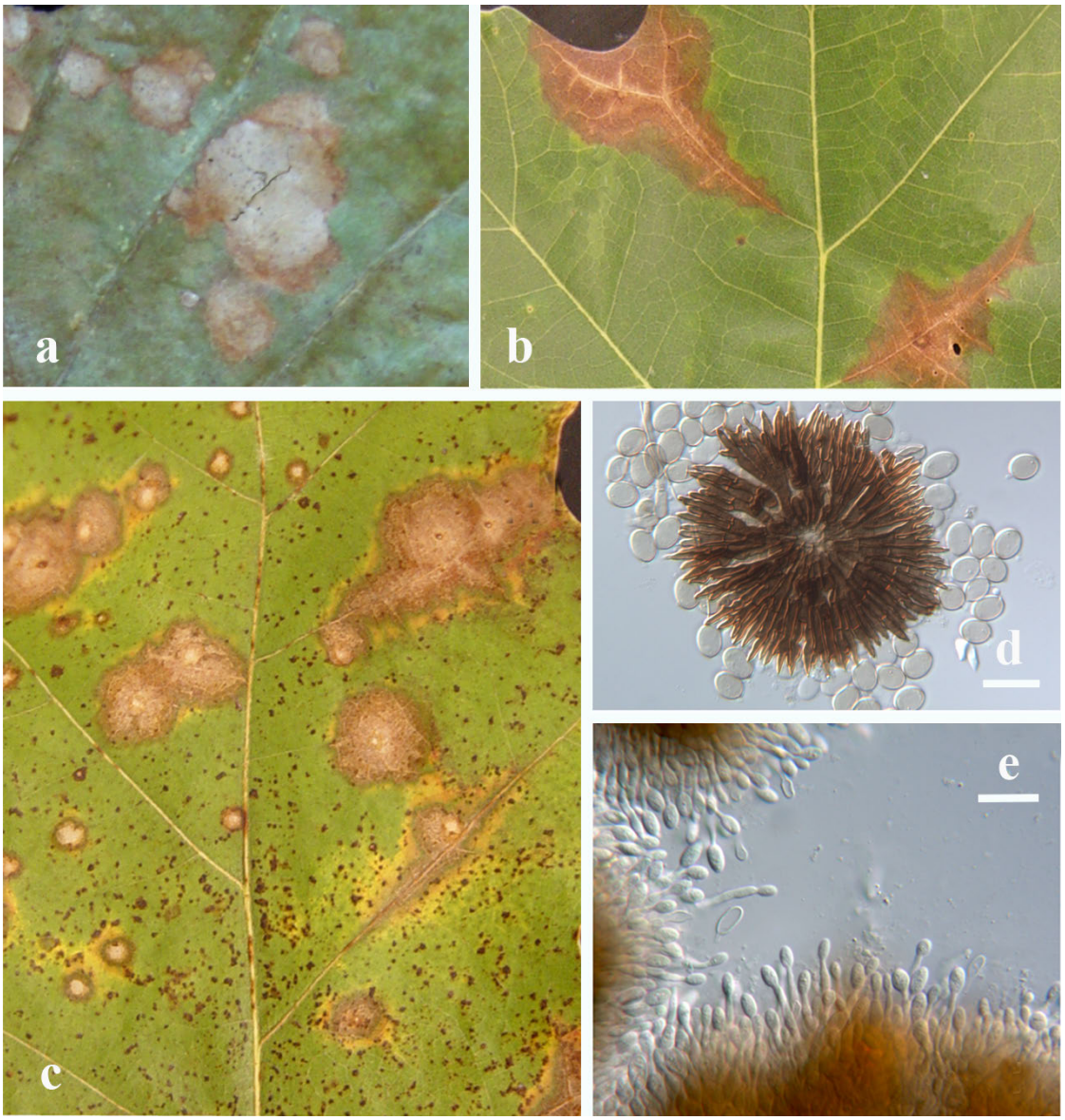

Fig. 47 Symptoms caused by *Tubakia* sp. on leaves of *Quercus stellata*. a Leaf spots. b Veinal necrosis. c Necrotic flecks and leaf spots. d Pycnothyrium with conidia. e Conidiophores and conidia. Scale bars: 20 μm. This picture is copyright of Thomas C. Harrington (Harrington & McNew 2018).

Hosts: *Tubakia* species primarily infect hardwood trees, with oaks being the most common and susceptible hosts (Harrington et al. 2012). Both red and white oak groups are affected, although red oaks tend to show more severe symptoms (Harrington & McNew 2018). *Tubakia* has also been reported on other deciduous trees and shrubs, including maple (*Acer* spp.), chestnut (*Castanea* spp.), elm (*Ulmus* spp.), ash (*Fraxinus* spp.), and tupelo (*Nyssa* spp.) (Farr & Rossman 2025). However, infections on these hosts are less frequent and typically less severe.

Pathogen biology, disease cycle and epidemiology: *Tubakia* species are fungal pathogens that survive the winter in infected fallen leaves and twigs, primarily as conidia or mycelium (Harrington et al. 2012). Under warm and humid conditions, the fungus produces conidia that are spread by wind and rain splash to newly emerging leaves. Infection typically begins on older or lower leaves, with symptoms appearing later in the season. The disease cycle continues throughout the growing season as multiple generations of spores are produced, leading to secondary infections (Zlatković et al. 2024). Extended leaf wetness from rain, dew, or irrigation greatly enhances the pathogen ability to infect. Although it does not usually infect healthy leaf tissue aggressively, trees under stress such as those suffering from drought, nutrient deficiencies, or other diseases, are more vulnerable (Kowalski 2006).

Morphological-based identification: *Tubakia* produces pycnothyrial or stromatic conidiomata on infected leaves and twigs, typically embedded within necrotic lesions (Holdenrieder & Kowalski 1989). These conidiomata are superficial, dark brown to black, and may appear scattered or aggregated. Conidia are usually single-celled, ellipsoidal to oblong, thick-walled, and pigmented, ranging from light to dark brown as they mature (Braun et al. 2018). The conidial size, septation, and wall texture were previously used to differentiate species. However, the morphological characteristics of *Tubakia* species can be highly variable depending on environmental conditions, substrate, and host species, which makes species delimitation based solely on morphology problematic (Harrington & McNew 2018). Therefore, traditional identification methods often failed to differentiate cryptic species and a polyphasic approach is recommended

Molecular-based identification: Molecular-based identification has revolutionized the taxonomy of *Tubakia* as traditional classification proved insufficient for distinguishing closely related or cryptic species (Harrington & McNew 2018). *Tubakia* was previously assigned to *Diaporthales* (Yokoyama & Tubaki 1971, Yun & Rossman 2011) and *Melanconiellaceae* (Senanayake et al. 2017). Braun et al. (2018) introduced *Tubakiaceae* to accommodate *Tubakia* s based on sequences retrieved from material of the type species. Several studies have employed multi-gene approaches to resolve species boundaries in *Tubakia* (Harrington et al. 2012, Braun et al. 2018, Marin-Felix et al. 2019a). Harrington et al. (2012) described the new species *Tubakia iowensis* which was initially misidentified as *Tubakia dryina*. Braun et al. (2018) revealed that the diversity of *Tubakia* had been significantly underestimated. Several new species were also reported based on molecular and phylogenetic studies (Yun & Kim 2018, Zhang et al. 2021a, Cho et al. 2024). This study provides an updated phylogeny of *Tubakia* based on combined ITS, *rpb2*, *tef* and *tub2* sequence data (Fig. 48, Table 24).

Recommended genetic markers (genus level): ITS

Recommended genetic markers (species level): ITS, *rpb2*, *tef* and *tub2*

Accepted number of species: 23

References: Harrington et al. (2012), Harrington and McNew (2018), Marin-Felix et al. (2019a) (morphology and phylogeny); Braun et al. (2018), Zhu et al. (2022) (morphology, pathogenicity, and phylogeny)

Table 24 DNA barcodes for accepted species of *Tubakia*.

Species	Isolate	GenBank accession numbers			
		ITS	*rpb2*	*tef*	*tub2*
Tubakia americana	CBS 129014	MG591873	MG976449	MG592058	MG592152
T. byeongjinii	CDH040	OR727896	N/A	OR732731	N/A
T. californica	CBS 143670	MG591835	MG976451	MG592023	MG592117
T. cyclobalanopsidis#	CFCC 55979	OP114639	N/A	OP254247	OP329290
T. dryina#	CBS 112097	MG591851	MG976455	MG592039	MG592133
T. dryinoides	NBRC 9267	MG591878	MG976461	MG592063	MG592157
T. glaucae	CGMCC 3.28256	PQ340136	PQ367358	PQ358339	PQ358363
T. hallii	CBS 129013	MG591880	MG976462	MG592065	MG592159
T. iowensis#	CBS 129012	MG591879	N/A	MG592064	MG592158
T. japonica	MUCC2296	MG591886	MG976465	MG592071	MG592165
T. koreana	KCTC 46072	KP886837	N/A	N/A	N/A
T. liquidambaris	CBS 139744	MG605068	N/A	MG603578	N/A
T. lushanensis	SAUCC 1923	MW784678	MW842267	MW842261	MW842264
T. macnabbii	CBS 137349	MG605069	N/A	MG603579	N/A
T. meinikiana	CPC 32255	MG591893	MG976472	MG592080	MG592174
T. oblongispora	NBRC 9885	MG591897	MG976474	MG592084	MG592178
T. paradryinoides	NBRC 9884	MG591898	MG976475	MG592085	MG592179
T. quercicola#	CFCC 55106	OP114635	N/A	OP254243	OP254289
T. seoraksanensis	CBS 127492	MG591908	MG976485	MG592096	MG592188

T. sierrafriensis	**CPC 33020**	**MG591910**	**MG976486**	**MG592099**	**MG592191**
T. suttoniana	**CBS 639.93**	**MG591921**	**MG976493**	**MG592110**	**MG592202**
T. tiffanyae	**CBS 137345**	**MG605081**	**N/A**	**N/A**	**N/A**
T. variabilis	**CGMCC 3.28249**	**PQ340126**	**PQ367348**	**PQ358329**	**PQ358353**

Ex-type/ex-epitype/ex-neotype/ex-lectotype strains and voucher strains are in bold. Sequences that are not available are represented by N/A. Species confirmed with pathogenicity studies are marked with #.

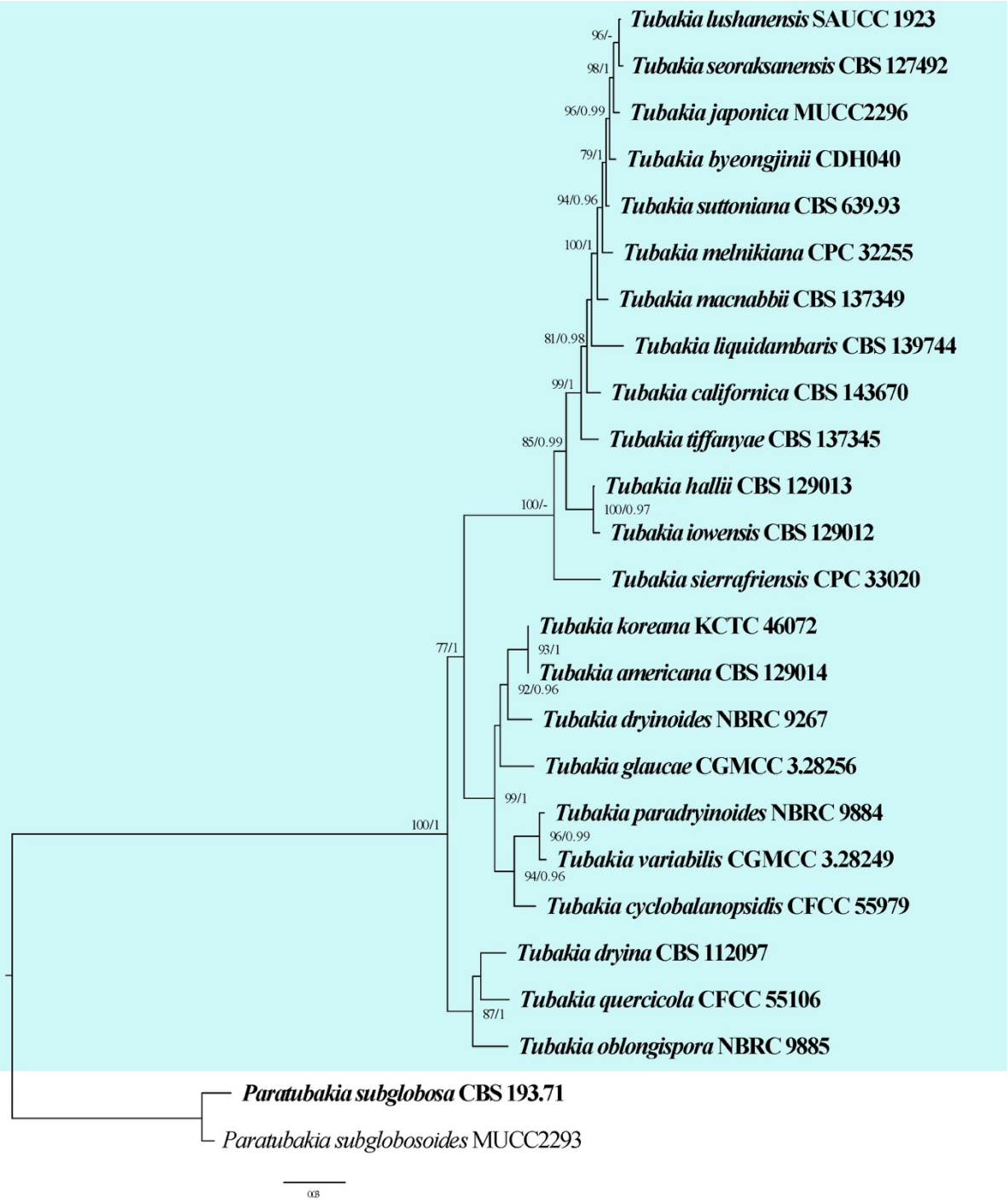

Fig. 48 Maximum likelihood tree of *Tubakia* species based on the concatenated ITS, *rpb2*, *tef*, and *tub2* sequence data. The best scoring RAxML tree had a final likelihood value of -10338.339. The tree was rooted with *Paratubakia subglobosa* (CBS 193.71) and *Paratubakia subglobosoides* (MUCC2293). Estimated base frequencies were as follows: A = 0.223, C = 0.298, G = 0.248, T = 0.231; substitution rates AC = 1.48724, AG = 4.21500, AT = 1.48724, CG = 1.00000, CT = 7.42148, GT = 1.000000. ML bootstrap support values over 70% and Bayesian posterior probabilities (BPP) greater than 0.95 are indicated. Type strains are in bold. Scale bar indicates the number of substitutions per site. Hyphens (-) represent support values less than BS 70%/BPP 0.95.

149. *Zasmidium* Fr., Summa veg. Scand., Sectio Post. (Stockholm): 407 (1849)

Type species: *Zasmidium cellare* (Pers.) Fr.

Classification: *Dothideomycetes*, *Mycosphaerellales*, *Mycosphaerellaceae*

Background: *Zasmidium* was introduced by Fries (1849) with *Z. cellare* as the type species. The taxonomy of *Zasmidium* has been debatable due to its similarities with stenella-like hyphomycetes (Braun et al. 2013). Arzanlou et al. (2007) showed that *Zasmidium* is the oldest name for stenella-like hyphomycetes within *Mycosphaerellaceae*, which have conidiogenous loci and conidia with truncate hila (Bensch et al. 2012, Braun et al. 2013). Subsequently, numerous *Stenella* species were transferred to *Zasmidium* (Braun et al. 2010, 2013).

Distribution: worldwide (Farr & Rossman 2025)

Disease symptoms: *Zasmidium* mostly causes leaf spots in a wide range of host species (Fig. 49). The infection spots can be amphigenous, brown or blackish brown, circular to sub-circular or irregular, at first yellow or yellowish brown, later with pale centre and brown margin, coalescing and spreading to cover most of the leaf surface (e.g. *Z. cassines*, *Z. dioscorinum*, *Z. fabaceicola*, *Z. micromeli*, *Z. pavettae*, *Z. robustum*) (Phengsintham et al. 2013, Singh et al. 2014, Kharwar et al. 2015, Videira et al. 2017). Some *Zasmidium* infections do not cause leaf spots and infected areas only have chlorosis corresponding to the areas delimited by veins (e.g. *Z. australiense*) (Braun et al. 2013). Citrus greasy spot caused by *Zasmidium citri-griseum* is one of the most important fungal diseases in the USA. Infection typically shows yellow mottle on the upper surface of leaves and yellow-brown spots, slightly raised pustules on the lower surface, resulting in premature defoliation and yield reduction (Aguilera-Cogley & Vicent 2020). Some *Zasmidium* species infect fresh fruits causing sooty blotch and flyspeck disease. which are characterized by blemishes in the epicuticular wax layer, decreasing the aesthetic appearance and sale value of fresh-market fruits. For example, Li et al. (2012) described *Zasmidium angulare* from the surface of apple fruit, where it causes discrete specks consisting of shiny, black, irregular or rounded to angular sclerotium-like bodies. Subsequently, sooty blotch and flyspeck disease caused by *Z. litseae* were recorded from the petiole of *Litsea glutinosa* in China (Zhao et al. 2016).

Hosts: *Zasmidium* species have been recorded from a wide range of hosts worldwide. They have been recorded from *Achyranthes aspera* (Laos), *Alocasia odora* (China), *Brabejum stellatifolium* (South Africa), *Daviesia mimosoides* (Australia), *Dioscorea oppositifolia* (India), *Elaeocarpus kirtonii* (Australia), *Eucalyptus* sp. (Brazil, Colombia, Indonesia, Thailand), *Geniostoma rupestre* (New Zealand), *Grevillea* sp. (Australia), *Hakea undulata* (Australia), *Ischyrolepis subverticillata* (South Africa), *Itea parviflora* (China), *Lonicera japonica* (Korea), *Lythrum salicaria* (Poland), *Mangifera indica* (Thailand), *Maianthemum bifolium* (Poland), *Malus domestica* (USA), *Musa sapientum* (Australia, Europe), *Pittosporum tenuifolium* (New Zealand), *Ravenala madagascariensi* (China), *Sasa* sp. (Japan), *Citrus limon* (China, USA), *Scaevola taccada* (Australia), *Schinus terebinthifolia* (Brazil), *Smilax china* (China), *Smilax glyciphylla* (Australia), *Smilax prolifera* (India), *Strelitzia nicolai* (South Africa), *Syzygium cordatum* (South Africa), and *Tsuga heterophylla* (USA) (Hao et al. 2013, Phengsintham et al. 2013, Singh et al. 2014, Videira et al. 2017, Świderska-burek 2020, Tan et al. 2022, Armand et al. 2025, Farr & Rossman 2025).

Pathogen biology, disease cycle and epidemiology: The main source of inoculum is the ascospores for *Zasmidium citri-griseum* which is the cause of citrus greasy spot disease. Ascospores are deposited on the underside of the leaves, germinate and form epiphytic mycelia on the surface (Fig. 50). Appressoria form over stomata, and the fungus penetrates the leaf mesophyll. Even in highly susceptible species under favourable conditions, leaf colonization is very slow, with symptoms appearing after 45 to 60 days (Mondal & Timmer 2006, Aguilera-Cogley et al. 2017).

Morphological-based identification: *Zasmidium* has hyphomycetes asexual morphs and mycosphaerella-like sexual morphs (Videira et al. 2017). The members are saprobic or mostly biotrophic, usually foliicolous, symptomless or causing various lesions, ranging from yellowish discolourations to distinct leaf spots. Mycelium are mostly immersed or superficial; hyphae branched, septate, hyaline or pale olivaceous to brown, thin walled to somewhat thickened, immersed hyphae smooth or faintly rough, external hyphae distinctly verruculose to verrucose. Stromata are lacking to well-developed, pigmented. Conidiophores are solitary, arising from superficial hyphae, lateral, occasionally terminal. Conidia are solitary or catenate, in simple or branched acropetal chains, shape and size variable, ranging from amero- to scolecosporous, subhyaline to pigmented, pale olivaceous to brown, hila somewhat thickened and darkened-refractive, planate, conidial secession schizolytic. Species delimitation based on morphological characteristics, such as shape and size of conidia and conidiophores is difficult as these characteristics are often shared between species (Videira et al. 2017).

Molecular-based identification: *Zasmidium* are similar to *Stenella* based on morphology. A molecular revision (based on LSU) of *Zasmidium* and *Stenella* confirmed that they should be separated despite morphological similarities (Arzanlou et al. 2007). Some *Zasmidium* species cluster in *Teratosphaeriaceae*, whereas others are in *Mycosphaerellaceae* (Arzanlou et al. 2007). Consequently, Braun et al. (2010) reallocated some stenella-like species that clustered in *Mycosphaerellaceae* to *Zasmidium*. Most recently, *Zasmidium* taxonomy studies were based on multi-genes (LSU, ITS and *rpb2*) (Videira et al. 2017, An et al. 2021, Hongsanan et al. 2025). This study provides an updated phylogeny of *Zasmidium* based on combined LSU, ITS and *rpb2* sequence data (Fig. 51, Table 25).

Recommended genetic markers (genus level): LSU, ITS

Recommended genetic markers (species level): LSU, ITS and *rpb2*

Accepted number of species: 56

References: Braun et al. (2010), (2013), Świderska-burek (2020) (morphology); Arzanlou et al. (2007), Hongsanan et al. (2020b), (2025), An et al. (2021) (phylogeny)

150. *Zymoseptoria* Quaedvl. & Crous, in Quaedvlieg, Kema, Groenewald, Verkley, Seifbarghi, Razavi, Mirzadi Gohari, Mehrabi & Crous, Persoonia 26: 64 (2011)

Type species: *Zymoseptoria tritici* (Roberge ex Desm.) Quaedvl. & Crous

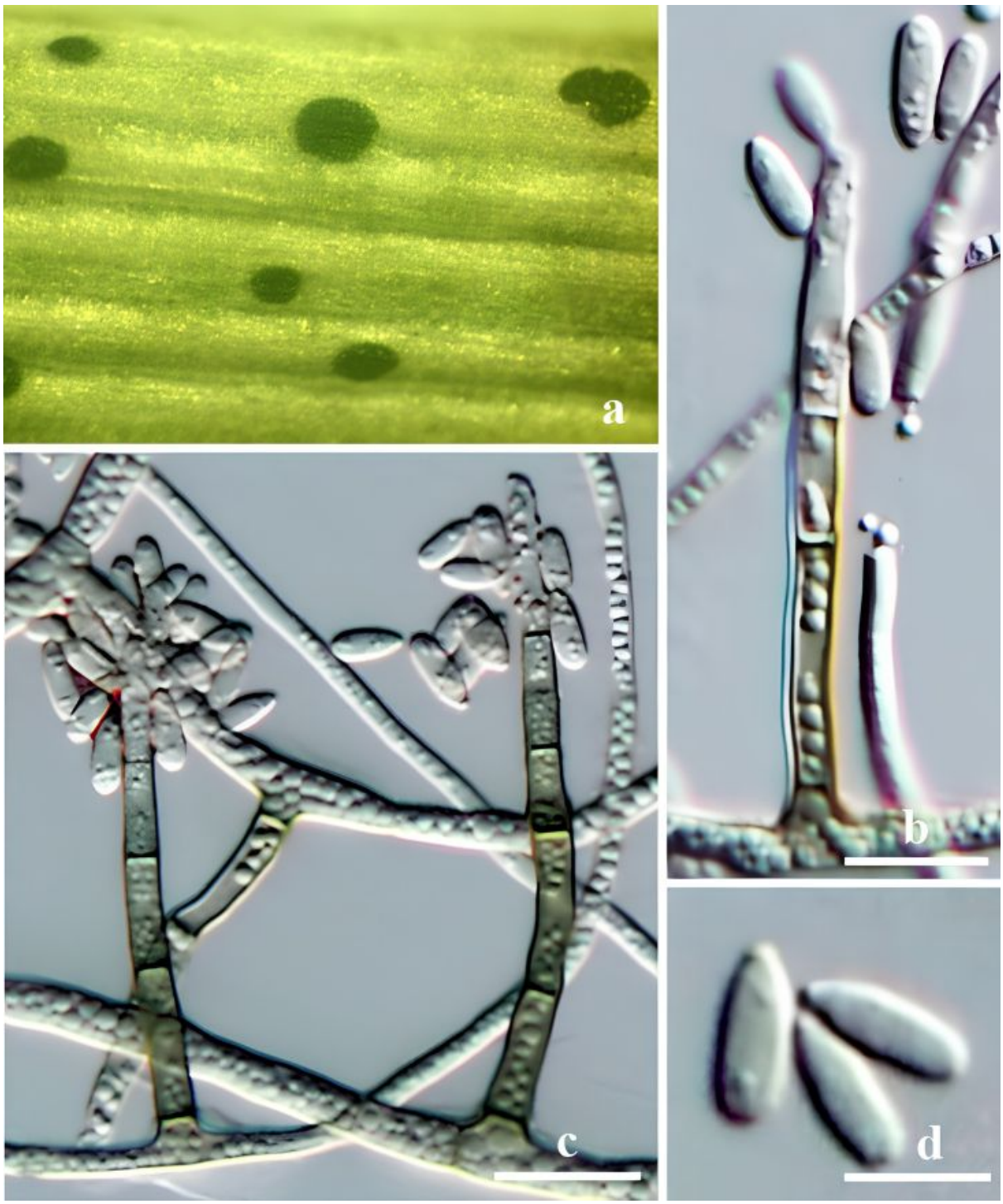

Fig. 49 *Zasmidium strelitziae* on stem of *Ravenala madagascariensi.* a Flyspeck disease symptom. b-c Conidiophores. d Conidia. Scale bars: 10 μm. This picture is copyright of Guangyu Sun (Hao et al. 2013).

Table 25 DNA barcodes for accepted species of *Zasmidium*.

Species	Strain	GenBank accession numbers		
		LSU	ITS	*rpb2*
Zasmidium angulare	**CBS 132094**	**JQ622096**	**JQ622088**	**MF951690**
Z. anthurilicola	**CBS 118742**	**FJ839662**	**FJ839626**	**MF951691**
Z. arcuatum	**CBS 113477**	**EU041836**	**EU041779**	**MF951692**
Z. aucklandicum	CPC 13569	MF951280	MF951409	MF951733
Z. biverticillatum	CBS 335.36	EU041853	EU041796	N/A

Z. cellare	**CBS 146.36**	**EU041878**	**EU041821**	**MF951693**
Z. cerophillum	**CBS 103.59**	**GU214485**	**EU041798**	**MF951694**
Z. citri-griseum#	CBS 122455	KF902151	KF901792	MF951695
Z. commune	**CBS 142530**	**KY979820**	**NR_156003**	**N/A**
Z. corymbiae	**CBS 145047**	**NG_066279**	**NR_161118**	**MK047534**
Z. daviesiae	CBS 116002	FJ839669	FJ839633	MF951698
Z. ducassei	**BRIP 53367**	**N/A**	**NR_164517**	**N/A**
Z. elaeocarpi	**CBS 142187**	**MF951263**	**MF951398**	**MF951699**
Z. eucalypticola	**CBS 142186**	**MF951265**	**MF951400**	**MF951701**
Z. eucalyptorum	**CBS 118500**	**MF951266**	**KF901652**	**MF951702**
Z. faygaleae	**BRIP 72890b**	**OR673899**	**OR673894**	**OR680058**
Z. fructicola	**CBS 139625**	**KP895922**	**KP896052**	**MF951703**
Z. fructigenum	**CBS 139626**	**KP895926**	**KP896056**	**MF951704**
Z. grevilleae	**CBS 124107**	**FJ839670**	**FJ839634**	**MF951705**
Z. gupoyu	CBS 122099	MF951267	MF951401	MF951706
Z. guttulatum	**CGMCC 3.28955**	**PX214436**	**PX214418**	**PX640850**
Z. hakeae	**CBS 142185**	**MF951268**	**MF951402**	**MF951707**
Z. hakeicola	**CBS 144590**	**NG_066335**	**NR_163384**	**MK442687**
Z. hydei	**MBSZU 25-013**	**PQ898039**	**PQ898043**	**PV016591**
Z. indonesianum	**CBS 139627**	**KF902086**	**KF901739**	**MF951710**
Z. iteae	**CBS 113094**	**MF951271**	**MF951405**	**MF951711**
Z. johnsoniae	**BRIP 72385e**	**N/A**	**OP256852**	**OP289001**
Z. liboense	**GUCC 1720.2**	**MT712180**	**MT683373**	**MT700486**
Z. longisporum	**CGMCC 3.28954**	**PX214438**	**PX214420**	**PX640852**
Z. lonicericola	**CBS 125008**	**KF251787**	**KF251283**	**MF951712**
Z. mangiferae#	**MFLUCC 24-0391**	**PQ638521**	**PQ639273**	**N/A**
Z. mangrovei	**CBS142048**	**MW046214**	**KY290860**	**N/A**
Z. morrisoniae	**BRIP 70485a**	**PP707924**	**PP707907**	**PP712796**
Z. musae#	CBS 121384	MF951272	EU514292	MF951713
Z. musae-banksii	**CBS 121710**	**EU041852**	**EU041795**	**MF951716**
Z. musicola	**CBS 122479**	**MF951275**	**EU514294**	**MF951717**
Z. musigenum	CBS 190.63	EU041857	EU041800	MF951718
Z. nancybirdwaltoniae	**BRIP 72888b**	**N/A**	**OR290131**	**N/A**
Z. nocoxi	**CBS 125009**	**KF251788**	**KF251284**	**MF951719**
Z. pearceae	**BRIP 72388b**	**N/A**	**OP023117**	**OP021641**
Z. pitospori	CBS 122274	MF951276	MF951406	MF951720
Z. podocarpi	CBS 142529	KY979821	NR_156004	N/A
Z. proteacearum	CBS 116003	FJ839671	FJ839635	MF951721
Z. pseudoparkii	**CBS 110999**	**JF700965**	**DQ303023**	**MF951723**
Z. pseudotsugae	rapssd	EF114704	EF114687	N/A
Z. pseudovespa	**CBS 121159**	**KF901836**	**MF951407**	**MF951724**
Z. queenslandicum	**CBS 122475**	**MF951277**	**EU514295**	**MF951725**
Z. scaevolicola	**CBS 127009**	**KF251789**	**KF251285**	**MF951726**
Z. schini	**CBS 142188**	**MF951278**	**MF951408**	**MF951727**
Z. strelitziae	**CBS 121711**	**EU041860**	**EU041803**	**MF951729**
Z. suregadae	P36	KC677939	KC677914	N/A
Z. syzygii	**CBS 133580**	**KC005798**	**KC005777**	**MF951730**
Z. thailandicum	**CBS 145027**	**NG_066342**	**NR_164463**	**N/A**
Z. tsugae	ratstk	EF114705	EF114688	N/A
Z. velutinum	**CBS 101948**	**EU041838**	**EU041781**	**MF951731**
Z. xenoparkii	**CBS 111185**	**JF700966**	**DQ303028**	**MF951732**

Ex-type/ex-epitype/ex-neotype/ex-lectotype strains and voucher strains are in bold. Sequences that are not available are represented by N/A. Species confirmed with pathogenicity studies are marked with #.

Classification: *Dothideomycetes*, *Capnodiales*, *Mycosphaerellaceae*

Background: Quaedvlieg et al. (2011) introduced *Zymoseptoria* to accommodate *Septoria*-like species occurring on graminicolous hosts based on the LSU sequences. *Zymoseptoria* species produce yeast-like growth in culture and produce three different types of conidia. *Zymoseptoria tritici* and *Zy. passerinii* are well-known pathogens (Quaedvlieg et al. 2011). It was suggested that *Zymoseptoria* species became pathogens during wheat domestication as they are mostly found in natural and domesticated grasses (Stukenbrock et al. 2007).

Distribution: worldwide (Farr & Rossman 2025)

Disease symptoms: *Zymoseptoria tritici* is the most damaging pathogen of wheat (*Triticum aestivum*) in Europe and an important pathogen in all major wheat growing

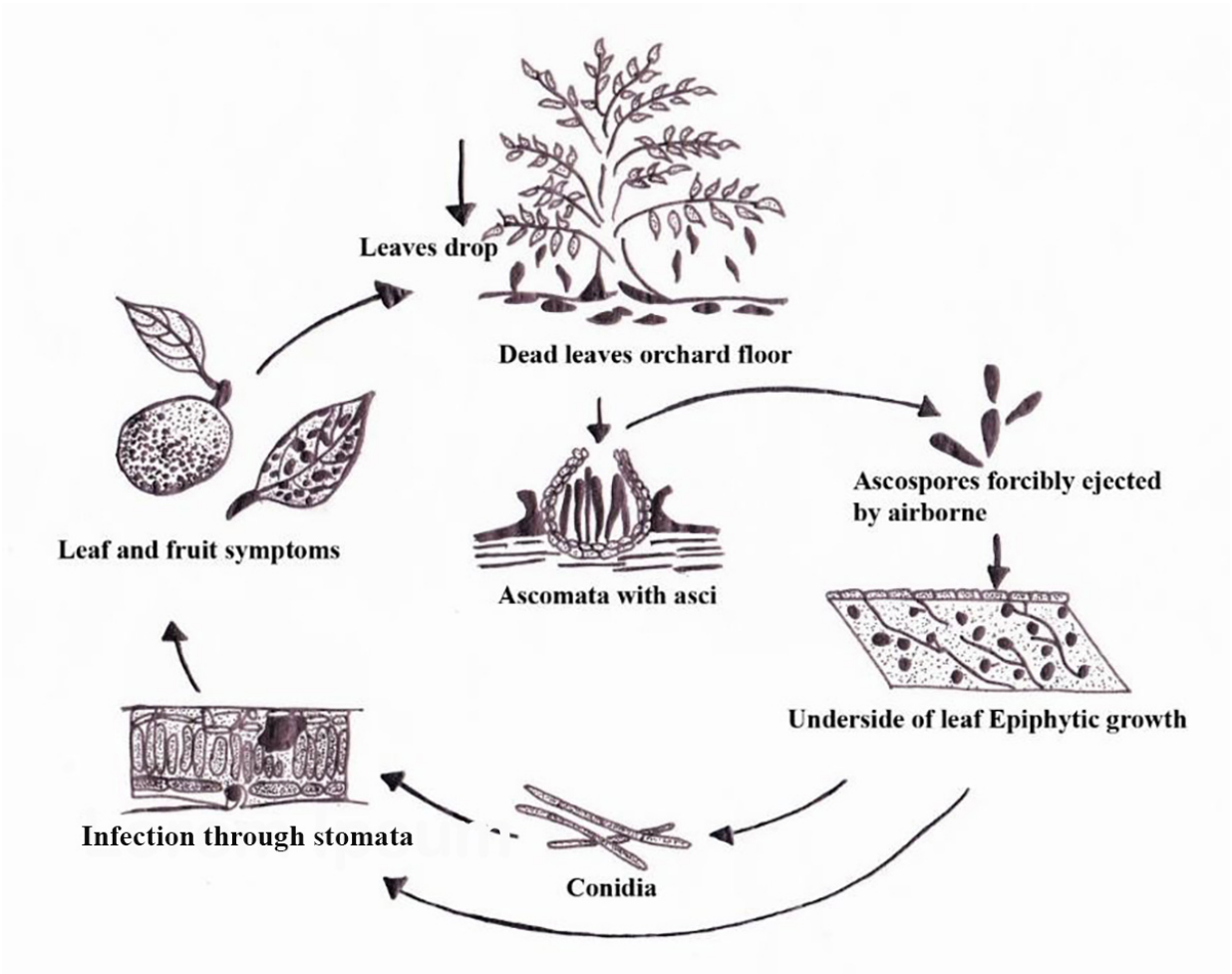

Fig. 50 Disease cycle of a *Zasmidium* species. Redrawn from Futch (2001).

countries worldwide (Fones and Gurr 2015). Septoria tritici blotch caused by *Zymoseptoria tritici* is characterized by necrotic lesions on leaves or stems. The lesions then enlarge with a light tan and develop darker-colored fruiting bodies (Ponomarenko et al. 2011). *Zymoseptoria passerinii* causes septoria speckled leaf blotch on barley (*Hordeum vulgare*) (Mathre 1997, Cunfer & Ueng 1999, Goodwin & Zismann 2001, Ware et al. 2007, Fig. 52).

Hosts: *Zymoseptoria ardabiliae* was isolated from *Lolium* sp. in Iran (Stukenbrock et al. 2012) while *Zy. brevis* was isolated from *Phalaris* sp. in Iran (Quaedvlieg et al. 2011). *Zymoseptoria halophila* and *Zy. passerinii* were isolated from *Hordeum* sp. from Iran and Italy (Quaedvlieg et al. 2011). *Zymoseptoria pseudotritici* was found in *Dactylis* sp. in Iran (Stukenbrock et al. 2012). *Zymoseptoria tritici* was found in *Triticum* sp. in France (Quaedvlieg et al. 2011). *Zymoseptoria verkleyi* was found in *Poa annua* in the Netherlands (Crous et al. 2012) and *Zy. crescenta* from *Aegilops triuncialis* in Iran (Crous et al. 2018).

Pathogen biology, disease cycle and epidemiology: *Zymoseptoria tritici* is the causal agent of septoria tritici blotch. Initially, the spores of *Zy. tritici* are splash dispersed during rainstorms as they need humid conditions for successful infection. After landing on the leaves of host plants, the spores produce a germ tube that enters the host leaf via the stomata. Initial growth appears to be biotrophic but it switches to necrotrophic growth beginning up to two weeks after penetration and epidemics can develop rapidly (Shaw & Royle 1993, Kema et al. 1996, Ponomarenko et al. 2011, Fig. 53). The next growing season will be continuous if debris from heavily infected leaves and stems remains in fields after harvest (Ponomarenko et al. 2011).

Morphological-based identification: *Zymoseptoria* is characterized by forming different types of conidia in vitro (pycnidial, phragmosporous and yeast-like) (Quaedvlieg et al. 2011). Conidia can be hyaline, narrowly cylindrical to subulate, tapering towards an acutely rounded apex with a bluntly rounded to truncate base, and transversely euseptate. Phragmosporous conidia are microcyclic conidiation with yeast-like growth and microcyclic conidia have also been reported (Quaedvlieg et al. 2011).

Molecular-based identification: *Zymoseptoria* is a segregation of grass-inhabiting species which cluster apart from *Septoria sensu stricto* (Quaedvlieg et al. 2011). Both single gene (LSU) and multi-locus datasets (*act*, *cal*, *rpb2*, *tub2* and ITS) will resolve the identity of *Septoria*-like species occurring on graminicolous hosts (Quaedvlieg et al. 2011). This study provides an updated phylogeny of *Zymoseptoria* based on combined *act*, *cal*, ITS, *tub2*, *rpb2*, LSU and *tef* sequence data (Fig. 54, Table 26).

Recommended genetic markers (genus level): ITS and *rpb2*

Recommended genetic markers (species level): *act*, *cal*, ITS, *tub2*, *rpb2*, LSU and *tef*

Fig. 51 Maximum likelihood tree of *Zasmidium* species based on the concatenated LSU, ITS and *rpb2* sequence data. The best scoring RAxML tree had a final likelihood value of -18887.668. The tree was rooted with *Nothopericoniella perseamacranthae* (CBS 122097 and CBS 122282). Estimated base frequencies were as follows: A = 0.240, C = 0.258, G = 0.289, T = 0.213; substitution rates AC = 1.26001, AG = 3.69613, AT = 1.26001, CG = 1.00000, CT = 7.66522, GT = 1.000000. ML bootstrap support values over 70% and Bayesian posterior probabilities (BPP) greater than 0.95 are indicated. Type strains are in bold. Scale bar indicates the number of substitutions per site. Hyphens (-) represent support values less than BS 70%/BPP 0.95.

Table 26 DNA barcodes for accepted species of *Zymoseptoria*.

Species	Strain	GenBank accession numbers						
		act	*cal*	ITS	*tub2*	*rpb2*	LSU	*tef*
Zymoseptoria ardabiliae	**CBS 130977**	**JN982477**	**JN982479**	**JQ739806**	**JN982485**	**JN982483**	**JQ739846**	**JQ739790**
Zy. brevis	**CBS 128853**	**JF701036**	**JF701104**	**JF700867**	**JF700968**	**JF700798**	**JQ739833**	**JQ739777**
Zy. crescenta	**CPC 24053**	**N/A**	**N/A**	**MH259304**	**N/A**	**MH271695**	**MH267287**	**MH271694**
Zy. halophila	**CBS 128854**	**JF701045**	**JF701113**	**JF700876**	**JF700977**	**JF700808**	**JQ739842**	**JQ739786**

Zy. passerinii	CBS 120384	JF701047	JF701115	JF700878	JF700979	JF700810	JQ739844	JQ739788
Zy. pseudotritici	**CBS 130976**	**JN982476**	**JN982478**	**JN982480**	**JN982484**	**JN982482**	**JQ739828**	**JQ739772**
Zy. sheehyskeffingtoniae	**BRIP 71809a**	**OR964971**	**N/A**	**OR947073**	**N/A**	**OR964972**	**OR947080**	**OR964973**
Zy. tritici	CBS 392.59	JF701055	JF701123	AY152603	JF700987	JF700818	JQ739850	JQ739794
Zy. verkleyi	**CBS 133618**	**N/A**	**N/A**	**KC005781**	**N/A**	**N/A**	**KC005802**	**N/A**

Ex-type/ex-epitype/ex-neotype/ex-lectotype strains and voucher strains are in bold. Sequences that are not available are represented by N/A.

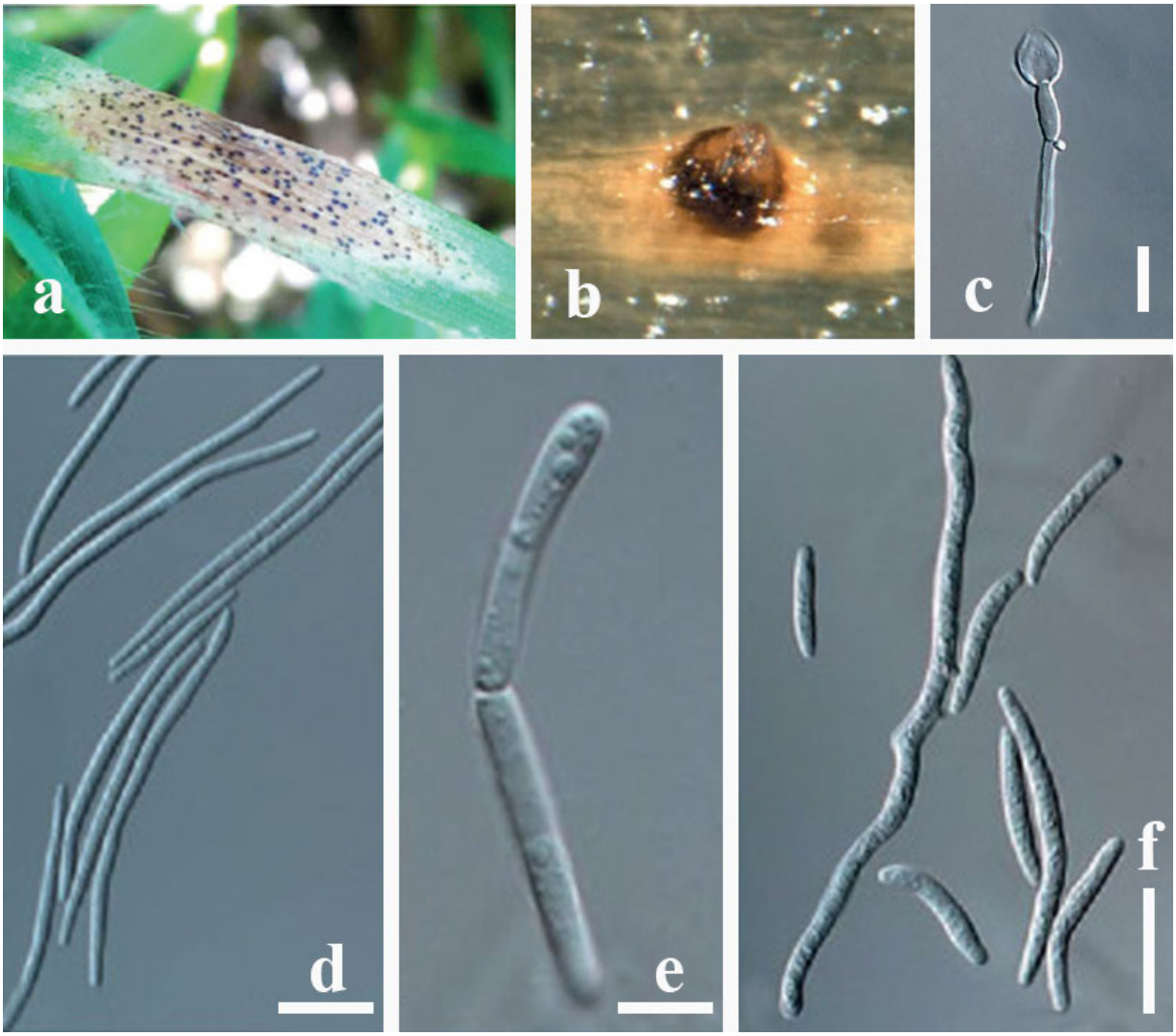

Fig. 52 *Zymoseptoria* sp. a Disease symptom of *Z. crescent* on leaves of *Aegilops triuncialis*. b Pycnidium of *Z. brevis* on the leaves of *Hordeum vulgare.* c Conidiogenous cell of *Z. passerinii*. d-f Conidia (d: Type I, e: Type II and f: Type III). Scale bars = 10 μm. This picture is copyright of Pedro Crous (Quaedvlieg et al. (2011) and Chen et al. (2022)).

Accepted number of species: nine

References: Stukenbrock et al. (2007), Ponomarenko et al. (2011), Quaedvlieg et al. (2011) (morphology and phylogeny)

Discussion

Fungal pathogens pose significant threats to agriculture, forestry, and human health, causing devastating diseases. The impact of fungal pathogens on global food security is increasingly pronounced under intensifying agricultural practices, climate change, and expanding international trade. Despite substantial advances in fungal systematics and molecular phylogenetics, knowledge of pathogenic genera remains taxonomically fragmented and inconsistently synthesized, limiting comparative evolutionary analyses and constraining disease diagnostics and management strategies. The “One Stop Shop series” not only provides updated backbone trees and comprehensive information on plant pathogens, but also consolidates scattered data into a single accessible resource at http://www.onestopshopfungi.org. This work enhances taxonomic clarity and facilitates cross-genus comparisons critical for understanding host specificity, pathogenic evolution, and lineage diversification. The introduction of the novel species *Dichotomophthora conlute*

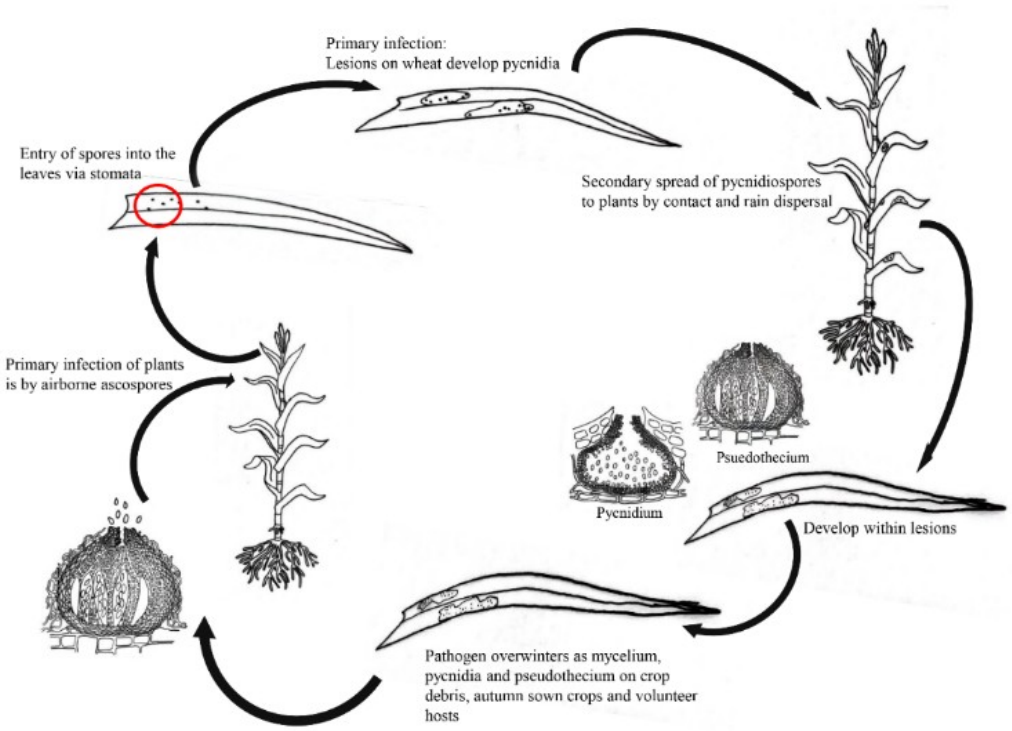

Fig. 53 Disease cycle of *Zymoseptoria tritici* the causal agent of septoria tritici blotch. Redrawn from Ponomarenko et al. (2011).

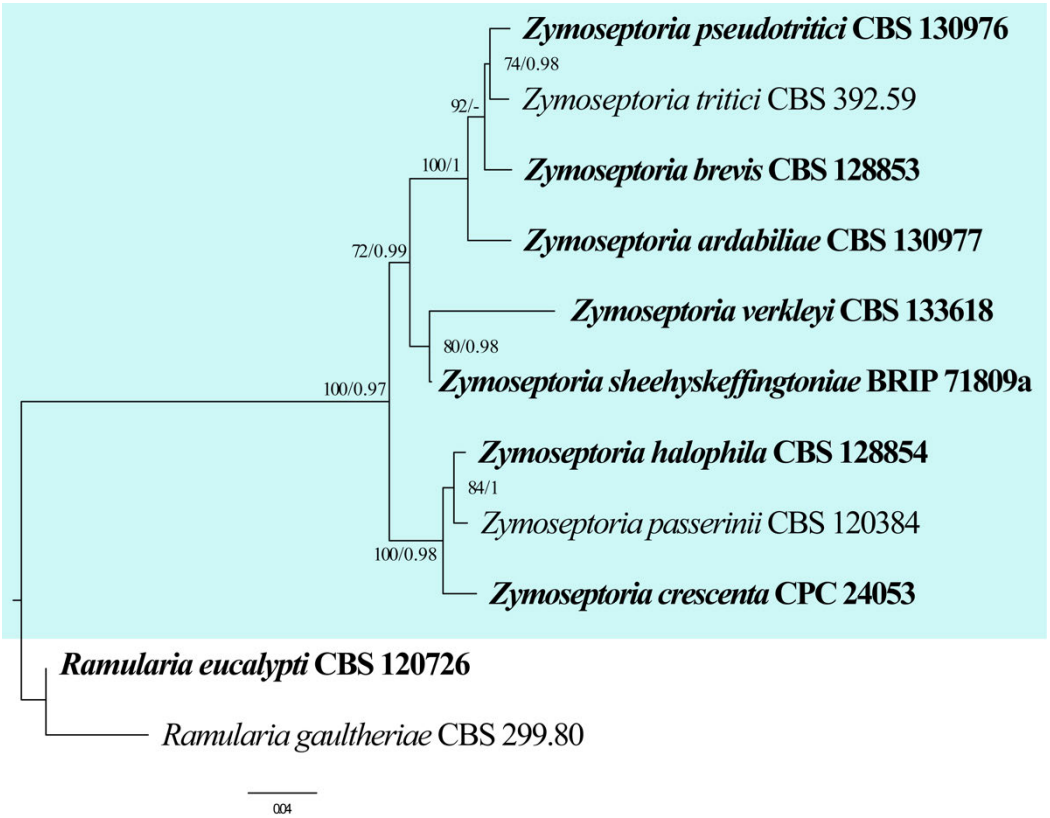

Fig. 54 Maximum likelihood tree of *Zymoseptoria* species based on the concatenated *act*, *cal*, ITS, *tub2*, *rpb2*, LSU and *tef* sequences. The best scoring RAxML tree had a final likelihood value of -7943.951. The tree was rooted with *Ramularia eucalypti* (CBS 120726) and *R. gaultheriae* (CBS 299.80). Estimated base frequencies were as follows: A = 0.235, C = 0.283, G = 0.268, T = 0.214; substitution rates AC = 2.18805, AG = 3.38306, AT = 2.18805, CG = 1.00000, CT = 7.61291, GT = 1.000000. ML bootstrap support values over 70% and Bayesian posterior probabilities (BPP) greater than 0.95 are indicated. Type strains are in bold. Scale bar indicates the number of substitutions per site. Hyphens (-) represent support values less than BS 70%/BPP 0.95.

together with the new combinations *Digitiseta chiangmaiensis* and *Myxospora thailandica*, further refines the current systematic frameworks and underscores the dynamic nature of fungal taxonomy. These taxonomic updates not only contribute to nomenclatural stability but also have practical implications for accurate pathogen identification, surveillance, and quarantine efforts.

The study of fungal pathogens relies on interdisciplinary collaboration including microbiology, genetics, ecology, and agronomy. Collectively, this study strengthens the foundation for integrative plant pathology research by linking updated phylogenetic frameworks with applied disease knowledge. Nevertheless, continued incorporation of genome-scale datasets, expanded geographic sampling, and integration of functional and epidemiological data will be essential to maintain relevance and improve predictive capacity in the face of emerging pathogens.

Acknowledgments

This work was supported by the following projects: the Natural Science Special Research Fund of Guizhou University, Special Post Gui Da Ling Jun He Zi [2024] 07), National Natural Science Foundation of China (Grant no. 31972222), Program of Introducing Talents of Discipline to Universities of China (111 Program, D20023), and Guizhou Key Laboratory of Agricultural Biosecurity [Qian Ke He ZSYS (2025)024]. Chitrabhanu S. Bhunjun would like to thank the National Research Council of Thailand (NRCT) grant "Diversity and application of micro-fungi in Northern Thailand for agricultural waste degradation" (Grant no. N42A690265). The authors extend their appreciation to Taif University for supporting this work through the Highly Cited Researchers Supporting Project (TURSP-HC2026/13), Taif University, Saudi Arabia. Samantha C. Karunarathna and Saowaluck Tibpromma thank the National Natural Science Foundation of China (No. 32260004), the High-Level Talent Recruitment Plan of Yunnan Province, and the Key Laboratory of Yunnan Provincial Department of Education of the Deep-Time Evolution on Biodiversity from the Origin of the Pearl River. Chitrabhanu S Bhunjun sincerely thanks Dr. Chada Norphanphoun, Dr. Danushka Tennakoon, Dr. Prof. Guangyu Sun, Dr. Guillermo Márquez Licona, Prof. Jian-Kui (Jack) Liu, Dr. Mubashar Raza, Prof. Pedro Crous, Dr. Qian Chen, Prof. Thomas C. Harrington, Dr. Timothy L Friesen and Dr. Yan-Feng Han for granting permission to utilise the images in this publication. The authors also thank Dr. Shaun Pennycook from Manaaki Whenua, Landcare Research, New Zealand.

Author contributions

The author contributions are already provided at the start of the paper under "Table of Contents and contributors"

ORCID

Chitrabhanu S Bhunjun: https://orcid.org/0000-0001-8098-3390
Yong Wang: https://orcid.org/0000-0003-3831-2117
Feng-Quan Liu: https://orcid.org/0000-0001-8999-9241

Conflict of interest statement

The author list includes members of the Editorial Board of Fungal Diversity. They were not involved in the journal's review of, or decisions related to, this manuscript. The authors declare no competing interests.

Data availability

All sequences generated in this study were submitted to GenBank.

Supplementary Information

The online version contains supplemental information available at https://doi.org/10.65390/fdiv.2026.136009. The maximum likelihood tree of *Myrothecium* and related genera in Stachybotryaceae is provided in Supplementary File S1.

References

Abass MH, Mohammed NH (2014) Morphological, molecular and pathological study on *Nigrospora oryzae* and *Nigrospora sphaerica*, the leaf spot fungi of date palm. Basra Journal for Date Palm Researches 13: 26–38.

Abdulla ZK (2021) *Dichotomophthora portulacae*, a new record from Iraq. Mycotaxon 136: 215–218. https://doi.org/10.5248/136.215

Abdullah S, Sehgal SK, Ali S, Liatukas Z, Ittu M, Kaur N (2017) Characterization of *Pyrenophora tritici-repentis* (tan spot of wheat) races in Baltic States and Romania. The Plant Pathology Journal 33: 133–139. https://doi.org/10.5423/ppj.oa.10.2016.0214

Abler SW, Couch HB, Baudoin CAB (2003) Ecology and taxonomy of *Leptosphaerulina* spp. associated with Turfgrasses in the United States. Ph.D. thesis. Virginia Tech, USA.

Aboukhaddour R, Turkington TK, Strelkov SE (2013) Race structure of *Pyrenophora triciti-repentis* (tan spot of wheat) in Alberta, Canada. Canadian Journal of Plant Pathology 35: 256–268. https://doi.org/10.1080/07060661.2013.782470

Adaskaveg JE, Schnabel G, Förster H (2008) Diseases of peach caused by fungi and fungal-like organisms: biology, epidemiology and management. In The peach: botany, production and uses. CABI Wallingford, UK. https://doi.org/10.1079/9781845933869.0352

Agarwal DK (2010) *Macrophomina*: Taxonomy, ecology, diseases and their management. Taxonomy and Ecology of Indian Fungi; IK International Publishing House: New Delhi, India.

Aguilera-Cogley V, Vicent A (2020) Sensitivity of *Zasmidium citrigriseum* to Fenbuconazole and control of citrus greasy spot in Panama. Agronomy 10: 1577. https://doi.org/10.3390/agronomy10101577

Aguilera-Cogley VA, Berbegal M, Català S, Brentu FC, Armengol J, Vicent A (2017) Characterization of *Mycosphaerellaceae* species associated with citrus greasy spot in Panama and Spain. PloS One 12: e0189585. https://doi.org/10.1371/journal.pone.0189585

Ahrazem O, Gómez-Miranda B, Prieto A, Bernabé M, Leal JA (2000) Heterogeneity of the genus *Myrothecium* as revealed by cell wall polysaccharides. Archives of Microbiology 173: 296–302. https://doi.org/10.1007/s002030000149

Aiello D, Gusella G, Vitale A, Guarnaccia V, Polizzi G (2020) *Cylindrocladiella peruviana* and *Pleiocarpon algeriense*

causing stem and crown rot on avocado (*Persea americana*). European Journal of Plant Pathology 158: 419–430. https://doi.org/10.1007/s10658-020-02082-x

Aiello D, Polizzi G, Crous PW, Lombard L (2017) *Pleiocarpon* gen. nov. and a new species of *Ilyonectria* causing basal rot of *Strelitzia reginae* in Italy. IMA Fungus 8: 65–76. https://doi.org/10.5598/imafungus.2017.08.01.05

Aigoun-Mouhous W, Elena G, Cabral A, León M, Sabaou N, Armengol J, Chaouia C, Mahamedi AE, Berraf-Tebbal A (2019) Characterization and pathogenicity of Cylindrocarpon-like asexual morphs associated with black foot disease in Algerian grapevine nurseries, with the description of *Pleiocarpon algeriense* sp. nov. European Journal of Plant Pathology 154: 887–901. https://doi.org/10.1007/s10658-019-01708-z

Aime MC (2006) Toward resolving family-level relationships in rust fungi (*Uredinales*). Mycoscience 47: 112–122. https://doi.org/10.1007/s10267-006-0281-0

Aime MC, Bell C, Wilson A (2018) Deconstructing the evolutionary complexity between rust fungi (*Pucciniales*) and their plant hosts. Studies in Mycology 89: 143–152. https://doi.org/10.1016/j.simyco.2018.02.002

Aime MC, Matheny PB, Henk DA, Frieders EM, Nilsson RH, Piepenbring M, McLaughlin DJ, Szabo LJ, Begerow D, Sampaio JP, Bauer R, Weiß M, Oberwinkler F, Hibbett D (2006) An overview of the higher-level classification of *Pucciniomycotina* based on combined analyses of nuclear large and small subunit rDNA sequences. Mycologia 98: 896–905. https://doi.org/10.1080/15572536.2006.11832619

Aime MC, McTaggart AR (2020) A higher-rank classification for rust fungi, with notes on genera. Fungal Systematics and Evolution 7: 21–47. https://doi.org/10.3114/fuse.2021.07.02

Aime MC, Rossman AY, Ono Y, Castlebury LA (2019) (2688) Proposal to conserve the name *Phakopsora* (*Basidiomycota*, *Pucciniales*) with a conserved type. Taxon 68: 592. https://doi.org/10.1002/tax.12076

Akinsanmi OA, Nisa S, Jeffego OS, Drenth A (2016) Multiple *Pestalotiopsis* and *Neopestalotiopsis* species cause flower bight of macadamia in Australia. Phytopathology 106: 122.

Alam MW, Rehman A, Ahmad S, Sarwar M, Nawaz A, Khan SM, Ali S, Aslam S, Mannan A (2020) First report of *Nigrospora sphaerica* causing leaf spot of date palm in Pakistan. Journal of Plant Pathology 102: 223. https://doi.org/10.1007/s42161-019-00360-0

Alam MW, Rehman A, Gleason ML, Riaz K, Saira M, Aslam S, Rosli H, Muhammad S (2017) First report of *Nigrospora sphaerica* causing leaf spot of Kinnow mandarin in Pakistan. Journal of Plant Pathology 99: 295.

Alfieri Jr SA, Langdon KR, Wehlburg C, Kimbrough JW (1984) Index of plant diseases in Florida (Revised). Florida Department of Agriculture and Consumer Services, Division of Plant Industries, Bulletin 11: 1–389.

Ali B, Sohail Y, Toome-Heller M, Mumtaz AS (2016) *Melampsora pakistanica* sp. nov., a new rust fungus on *Euphorbia helioscopia* (Sun spurge) from Pakistan. Mycological Progress 15: 1285–1292. https://doi.org/10.1007/s11557-016-1244-2

Alidadi A, Kowsari M, Javan-Nikkhah M, Jouzani GR, Rastaghi ME (2019) New pathogenic and endophytic fungal species associated with Persian oak in Iran. European Journal of Plant Pathology 155: 1017–1032. https://doi.org/10.1007/s10658-019-01830-y

Al-Jaradi AJ, Maharachchikumbura SS, Al-Sadi AM (2020) *Phaeosphaeriopsis omaniana* (*Phaeosphaeriaceae*, *Pleosporales*), a novel fungus from Oman. Phytotaxa 436: 1–12. https://doi.org/10.11646/phytotaxa.436.2.8

Alves DR, da Silva WMB, dos Santos DL, de Oliveira Freire FD, Vasconcelos FR, de Morais SM (2020) Atividades antioxidante, anticolinesterasica e citotóxica de metabolitos de fungos endofiticos. Brazilian Journal of Development 6: 73684–73691. https://doi.org/10.34117/bjdv6n9-721

Alves JL, Barreto RW, Pereira OL (2010) Additions to the mycobiota of the invasive weed *Miconia calvescens* (*Melastomataceae*). Mycologia 102: 69–82. https://doi.org/10.3852/09-070

An YY, Zeng XY, Geng K, Hyde KD, Wang Y (2021) One new species and one new record of *Zasmidium* in China. Biodiversity Data Journal 9: e59001. https://doi.org/10.3897/bdj.9.e59001

Anahosur KH, Fazalnoor K (1972) Studies on foliicolar fungi of soybean crop. Indian Phytopathology 25: 504–508.

Ananya TS, Kindo AJ, Subramanian A, Suresh K (2014) *Nigrospora sphaerica* causing corneal ulcer in an immunocompetent woman: A Case Report. International Journal of Case Reports and Images (IJCRI) 5: 675–679. https://doi.org/10.5348/ijcri-2014119-cr-10430

Ariyawansa HA, Kang JC, Alias SA, Chukeatirote E, Hyde KD (2014) *Pyrenophora*. Mycosphere 5: 351–362. https://doi.org/10.5943/mycosphere/5/2/9

Armand A, Fallahi M, Absalan S, Rathnayaka AR, Braun U, Taylor PW, Khongphinitbunjong K, McKenzie EH, Hyde KD, Al-Otibi F, Jayawardena RS (2025) Mango microcosm: Unveiling the species diversity and pathogenic potential of fungi isolated from mango (*Mangifera indica*) in northern Thailand. Fungal Biology 129: 101552. https://doi.org/10.1016/j.funbio.2025.101552

Armstrong-Cho C, Banniza S (2020) Pathogens of caraway and coriander blossoms in western Canada. Canadian Journal of Plant Pathology 42: 367–376. https://doi.org/10.1080/07060661.2019.1681515

Arthur JC (1934) Manual of the Rusts in United States and Canada. Purdue Research Foundation, Lafayette, New York, Hafner Publishing.

Arzanlou M, Crous PW (2006) Fungal Planet 9-*Phaeosphaeriopsis musae*. In Fungal Planet–A Global Initiative to promote the Study of Fungal Biodiversity 2006. CBS-KNAW Fungal Biodiversity Centre.

Arzanlou M, Groenewald JZ, Gams W, Braun U, Shin HD, Crous PW (2007) Phylogenetic and morphotaxonomic revision of *Ramichloridium* and allied genera. Studies in Mycology 58: 57–93. https://doi.org/10.3114/sim.2007.58.03

Ashby SF (1927) *Macrophomina phaseoli* (Maubl.) comb. nov. the pycnidial stage of *Rhizoctonia bataticola* (Taub.) Butl. Transactions of the British Mycological Society 12: 141–147.

Avasthi S, Gautam AK, Verma RK, Rajeshkumar KC, Niranjan M, Sharma A, Karunarathna SC, Suwannarach N (2024) The genus Ravenelia: Insights on taxonomy, diversity and distribution. Pathogens 13: 775. https://doi.org/10.3390/pathogens13090775

Aveskamp MM, de Gruyter J, Woudenberg JHC, Verkley GJM, Crous PW (2010) Highlights of the *Didymellaceae*: a polyphasic approach to characterise *Phoma* and related

pleosporalean genera. Studies in Mycology 65: 1–60. https://doi.org/10.1016/s0166-0616(14)60107-x

Aylward J, Atkins S, Roets F, Wingfield BD, Wingfield MJ (2025) Several *Seiridium* species (*Sporocadaceae*: *Xylariales*) cause cypress canker in South Africa. Fungal Biology 129: 101528. https://doi.org/10.1016/j.funbio.2024.101528

Ayoubi N, Soleimani MJ (2016) Strawberry fruit rot caused by *Neopestalotiopsis iranensis* sp. nov., and *N. mesopotamica*. Current Microbiology 72: 329–336. https://doi.org/10.1007/s00284-015-0955-y

Babadoost M, Zitter TA (2009) Fruit rots of pumpkin: A serious threat to the pumpkin industry. Plant Disease 93: 772–782. https://doi.org/10.1094/pdis-93-8-0772

Babu BK, Saikia R, Arora DK (2010) Molecular characterization and diagnosis of *Macrophomina phaseolina*: a charcoal rot fungus. In: Y. Gherbawy and K. Voigt (eds.), Molecular Identification of Fungi, Springer-Verlag Berlin Heidelberg. https://doi.org/10.1007/978-3-642-05042-8_9

Balance GM, Lamari L, Kowatsch R, Bernier CC (1996) Cloning, expression and occurrence of the gene encoding the Ptr necrosis toxin from *Pyrenophora tritici-repentis.* Molecular Plant Pathology 1209.

Ballmann AE, Torkelson MR, Bohuski EA, Russell RE, Blehert DS (2017) Dispersal hazards of *Pseudogymnoascus destructans* by bats and human activity at hibernacula in summer. Journal of Wildlife Diseases 53: 725–735. https://doi.org/10.7589/2016-09-206

Bankina B, Priekule I (2011) A review of tan spot research in Baltic countries: occurrence, biology and possibilities of control. Žemdirbystė (Agriculture) 98: 3–10.

Barbetti MJ (2000) Fungal diseases of canola in Western Australia. Bulletin, Western Australia. Agriculture Western Australia.

Barnes I, Roux J, Wingfield MJ, Coetzee MP, Wingfield BD (2001) Characterization of *Seiridium* spp. associated with cypress canker based on *ß-tubulin* and *Histone* sequences. Plant Disease 85: 317–321. https://doi.org/10.1094/pdis.2001.85.3.317

Barr ME (1982) On the *Pleomassariaceae* (*Pleosporales*) in North America [Fungi, new taxa]. Mycotaxon 15: 349–383.

Baudoin ABAM (1986) First Report of *Dichotomophthora indica* on common purslane in Virginia. Plant Disease 70: 352. https://doi.org/10.1094/pd-70-352a

Beenken L (2014) *Pucciniales* on Annona (*Annonaceae*) with special focus on the genus *Phakopsora*. Mycological Progress 13: 791–809. https://doi.org/10.1007/s11557-014-0963-5

Beenken L, Lutz M, Scholler M (2017) DNA barcoding and phylogenetic analyses of the genus *Coleosporium* (*Pucciniales*) reveal that the North American goldenrod rust *C. solidaginis* is a neomycete on introduced and native *Solidago* species in Europe. Mycological Progress 16: 1073–1085. https://doi.org/10.1007/s11557-017-1357-2

Belisário R, Aucique-Pérez CE, Abreu LM, Salcedo SS, Oliveira WD, Furtado GQ (2020) Infection by *Neopestalotiopsis* spp. occurs on unwounded eucalyptus leaves and is favoured by long periods of leaf wetness. Plant Pathology 69: 194–204. https://doi.org/10.1111/ppa.13132

Ben HY, Gao W, Qu HY, Chai AL, Shi YX, Xie XW, Li BJ (2016) New host record of *Myrothecium roridum* causing leaf spot on *Abutilon megapotamicum* from China. Journal of Phytopathology 164: 563–566. https://doi.org/10.1111/jph.12439

Bensch K, Braun U, Groenewald JZ, Crous PW (2012) The genus *Cladosporium*. Studies in Mycology 72: 1–401. https://doi.org/10.1016/s0166-0616(14)60070-1

Berbee ML (1996) *Loculoascomycete* origins and evolution of filamentous ascomycete morphology based on 18s rRNA gene sequence data. Molecular Biology and Evolution 13: 462–470. https://doi.org/10.1093/oxfordjournals.molbev.a025607

Berkeley (1853) *Ravenelia* gen. nov. Gard Chron, London.

Bhunjun CS, Chen YJ, Phukhamsakda C, Boekhout T, Groenewald JZ, McKenzie EH, Francisco EC, Frisvad JC, Groenewald M, Hurdeal VG, Luangsa-Ard J, Perrone G, Visagie CM, Bai FY, Błaszkowski J et al. (2024) What are the 100 most cited fungal genera? Studies in Mycology 108: 1–411. https://doi.org/10.3114/sim.2024.108.01

Bhunjun CS, Niskanen T, Suwannarach N, Wannathes N, Chen YJ, McKenzie EHC, Maharachchikumbura SSN, Buyck B, Zhao CL, Fan YG, Zhang JY, Dissanayake AJ, Marasinghe DS, Jayawardena RS, Kumla J et al. (2022) The numbers of fungi: are the most speciose genera truly diverse? Fungal Diversity 114: 387–462. https://doi.org/10.1007/s13225-022-00501-4

Blancard D (2012) Diagnosis of parasitic and nonparasitic diseases. Tomato Diseases 2: 35–411. https://doi.org/10.1016/b978-0-12-387737-6.50002-9

Blehert DS, Hicks AC, Behr M, Meteyer CU, Berlowski-Zier BM, Buckles EL, Coleman JT, Darling SR, Gargas A, Niver R, Okoniewski JC (2009) Bat white-nose syndrome: an emerging fungal pathogen? Science 323: 227. https://doi.org/10.1126/science.1163874

Boerema G, Verhoeven A (1977) Check-list for scientific names of common parasitic fungi. Series 2b: Fungi on field crops: cereals and grasses. Netherlands Journal of Plant Pathology 83: 165–204. https://doi.org/10.1007/bf01976647

Bonthond G, Sandoval-Denis M, Groenewald JZ, Crous PW (2018) *Seiridium* (*Sporocadaceae*): an important genus of plant pathogenic fungi. Persoonia 40: 96–118. https://doi.org/10.3767/persoonia.2018.40.04

Borrero C, Castaño R, Avilés M (2017) First report of *Pestalotiopsis clavispora* (*Neopestalotiopsis clavispora*) causing canker and twig dieback on blueberry bushes in Spain. Plant Disease 102: 1178. https://doi.org/10.1094/pdis-10-17-1529-pdn

Brandt ME, Warnock DW (2003) Epidemiology, clinical manifestations, and therapy of infections caused by dematiaceous fungi. Journal of Chemotherapy 15: 36–47. https://doi.org/10.1179/joc.2003.15.supplement-2.36

Braun U (1995) A monograph of *Cercosporella*, *Ramularia*, and allied genera (phytopathogenic hyphomycetes). Ihw-Verlag Eching.

Braun U, Crous PW, Schubert K, Shin HD (2010) Some reallocations of *Stenella* species to *Zasmidium*. Schlechtendalia 20: 99–104.

Braun U, Heuchert B, Diederich P (2009) Two new and another interesting lichenicolous hyphomycete. Herzogia 22: 165–171.

Braun U, Nakashima C, Crous PW (2013) Cercosporoid fungi (*Mycosphaerellaceae*) 1. Species on other fungi, *Pteridophyta* and *Gymnospermae*. IMA Fungus 4: 265–345. https://doi.org/10.5598/imafungus.2013.04.02.12

Braun U, Nakashima C, Crous PW, Groenewald JZ, Moreno-Rico O, Rooney-Latham S, Blomquist CL, Haas J, Marmolejo J (2018) Phylogeny and taxonomy of the genus *Tubakia s. lat*.

Fungal Systematics and Evolution 1: 41–99. https://doi.org/10.3114/fuse.2018.01.04

Brian PW, Hemming HG, Jefferys EG (1948) Production of antibiotics by species of *Myrothecium*. Mycologia 40: 363–368. https://doi.org/10.1080/00275514.1944.12017714

Brito ACQ, Mello JF, Michereff SJ, de Souza-Motta CM, Machado AR (2019) First report of *Macrophomina pseudophaseolina* causing stem dry rot in cassava in Brazil. Journal of Plant Pathology 101: 1245. https://doi.org/10.1007/s42161-019-00309-3

Busby PE, Aime MC, Newcombe G (2012) Foliar pathogens of *Populus angustifolia* are consistent with a hypothesis of Beringian migration into North America. Fungal Biology 116: 792–801. https://doi.org/10.1016/j.funbio.2012.04.012

Câmara MPS, Ramaley AW, Castlebury LA, Palm ME (2003) *Neophaeosphaeria* and *Phaeosphaeriopsis*, segregates of *Paraphaeosphaeria*. Mycological Research 10: 516–522. https://doi.org/10.1017/s0953756203007731

Campbell LJ, Walsh DP, Blehert DS, Lorch JM (2020) Long-term survival of *Pseudogymnoascus destructans* at elevated temperatures. The Journal of Wildlife Diseases 56: 278–287. https://doi.org/10.7589/2019-04-106

Capote N, Del Río MÁ, Herencia JF, Arroyo FT (2022) Molecular and pathogenic characterization of Cylindrocarpon-like anamorphs causing root and basal rot of almonds. Plants 11: 984. https://doi.org/10.3390/plants11070984

Carmody SM (2017) Light leaf spot and white leaf spot of *Brassicaceae* in Washington State. Doctoral dissertation, Washington State University, USA.

Carvalho CRD, Santiago IF, Costa Coelho LD, Câmara PEAS, Silva MC, Stech M, Rosa CA, Rosa LH (2019) Fungi associated with plants and lichens of Antarctica. In Fungi of Antarctica. Cham: Springer International Publishing. https://doi.org/10.1007/978-3-030-18367-7_8

Casa RT, Reis EM, Zambolim L (2006) Doenças do milho causadas por fungos do gênero *Stenocarpella*. Fitopatologia Brasileira 31: 427–439. https://doi.org/10.1590/s0100-41582006000500001

Casadevall A (2019) Global catastrophic threats from the fungal kingdom: fungal catastrophic threats. Global Catastrophic Biological Risks 424: 21–32. https://doi.org/10.1007/82_2019_161

Chamorro M, Aguado A, De los Santos B (2016) First report of root and crown rot caused by *Pestalotiopsis clavispora* (*Neopestalotiopsis clavispora*) on strawberry in Spain. Plant Disease 100: 1495. https://doi.org/10.1094/pdis-11-15-1308-pdn

Chapell TM, Rausher MD (2016) Evolution of host range in *Coleosporium ipomoeae*, a plant pathogen with multiple hosts. Proceedings of the National Academy of Sciences 113: 5346–5351. https://doi.org/10.1073/pnas.1522997113

Chapman N, Burt C, Dong H, Nicholson P (2008) The development of PCR-based markers for the selection of eyespot resistance genes *Pch1* and *Pch2*. Theoretical and Applied Genetics 117: 425–433. https://doi.org/10.1007/s00122-008-0786-3

Chatasiri S, Ono Y (2008) Phylogeny and taxonomy of the Asian grapevine leaf rust fungus, *Phakopsora euvitis*, and its allies (*Uredinales*). Mycoscience 49: 66–74. https://doi.org/10.1007/s10267-007-0390-4

Chen Q, Bakhshi M, Balci Y, Broders KD, Cheewangkoon R, Chen SF, Fan XL, Gramaje D, Halleen F, Jung MH, Jiang N, Jung T, Májek T, Marincowitz S, Milenković I et al. (2022) Genera of phytopathogenic fungi: GOPHY 4. Studies in Mycology 101: 417–564. https://doi.org/10.3114/sim.2022.101.06

Chen Q, Hou LW, Duan WJ, Crous PW, Cai L (2017) *Didymellaceae* revisited. Studies in Mycology 87: 77–103. https://doi.org/10.1016/j.simyco.2017.06.002

Chen Q, Jiang JR, Zhang GZ, Cai L, Crous PW (2015) Resolving the *Phoma* enigma. Studies in Mycology 82: 137–217. https://doi.org/10.1016/j.simyco.2015.10.003

Chen Y, Ran SF, Dai DQ, Wang Y, Hyde KD, Wu YM, Jiang YL (2016) Mycosphere essays 2. *Myrothecium*. Mycosphere 7: 64–80. https://doi.org/10.5943/mycosphere/7/1/7

Chen Y, Zeng L, Shu N, Jiang M, Wang H, Huang Y, Tong H (2018) Pestalotiopsis-like species causing gray blight disease on *Camellia sinensis* in China. Plant Disease 102: 98–106. https://doi.org/10.1094/pdis-05-17-0642-re

Childress MK, Dragone NB, Young BD, Adams BJ, Fierer N, Quandt CA (2025) Three new *Pseudogymnoascus* species (*Pseudeurotiaceae*, *Thelebolales*) described from Antarctic soils. IMA Fungus 16: e142219. https://doi.org/10.3897/imafungus.16.142219

Cho SE, Shin K, Kim YH, Lee DH (2024) *Tubakia byeongjinii*, a new species of *Tubakiaceae*, isolated from *Quercus variabilis* in South Korea. Phytotaxa 638: 294–300. https://doi.org/10.11646/phytotaxa.638.3.9

Clarkson JDS (1981) Relationship between eyespot severity and yield loss in winter wheat. Plant Pathology 30: 125–131. https://doi.org/10.1111/j.1365-3059.1981.tb01243.x

Cohen R, Elkabetz M, Paris HS, Gur A, Dai N, Rabinovitz O,Freeman S (2022a) Occurrence of Macrophomina phaseolina in Israel: Challenges for disease management and crop germplasm enhancement. Plant Disease 106: 15–25. https://doi.org/10.1094/pdis-07-21-1390-fe

Cohen R, Elkabetz M. Paris HS, Freeman S, Gur A (2022b) Charcoal rot (Macrophomina phaseolina) across melon diversity: evaluating the interaction between the pathogen, plant age and environmental conditions as a step towards breeding for resistance. European Journal of Plant Pathology 163: 601–613. https://doi.org/10.1007/s10658-022-02500-2

Cohen SD (1999) Technique for large scale isolation of *Discula umbrinella* and other foliar endophytic fungi from *Quercus* species. Mycologia 91: 917–922. https://doi.org/10.1080/00275514.1999.12061099

Corlett M (1981) A taxonomic survey of some species of *Didymella* and *Didymella*-like species. Canadian Journal of Botany 59: 2016–2042. https://doi.org/10.1139/b81-264

Couch HB (1962) Diseases of turfgrasses. Rheinhold Publishing Corp, Chapman and Hall, New York, USA.

Crossan D (1954) Cercosporella leafspot of crucifers. Technical Bulletin. North Carolina Agricultural Experiment Station.

Crous PW, Braun U, McDonald BA, Lennox CL, Edwards J, Mann RC, Zaveri A, Linde CC, Dyer PS, Groenewald JZ (2021a) Redefining genera of cereal pathogens: *Oculimacula*, *Rhynchosporium* and *Spermospora*. Fungal Systematics and Evolution 7: 67–98. https://doi.org/10.3114/fuse.2021.07.04

Crous PW, Cowan DA, Maggs-Kölling G, Yilmaz N, Larsson E, Angelini C, Brandrud TE, Dearnaley JDW, Dima B, Dovana F, Fechner N, García D, Gené J, Halling RE, Houbraken J et al. (2020) Fungal Planet description sheets: 1112–1181. Persoonia 45: 251–409. https://doi.org/10.3767/persoonia.2020.45.10

Crous PW, Cowan DA, Maggs-Kölling G, Yilmaz N, Thangavel R, Wingfield MJ, Noordeloos ME, Dima B, Brandrud TE, Jansen GM, Morozova OV, Vila J, Shivas RG, Tan YP, Bishop-Hurley S et al. (2021b) Fungal Planet description sheets: 1182–1283. Persoonia 46: 313–352. https://doi.org/10.3767/persoonia.2021.46.11

Crous PW, Shivas RG, Quaedvlieg WV, Van der Bank M, Zhang Y, Summerell BA, Guarro J, Wingfield MJ, Wood AR, Alfenas AC, Braun U, Cano-Lira JF, García D, Marin-Felix Y, Alvarado P et al. (2014) Fungal Planet description sheets: 214–280. Persoonia 32: 184–306. https://doi.org/10.3767/003158514X682395

Crous PW, Shivas RG, Wingfield MJ, Summerell BA, Rossman AY, Alves JL, Adams GC, Barreto RW, Bell A, Coutinho ML, Flory SL, Gates G, Grice KR, Hardy GE, Kleczewski NM et al. (2012) Fungal Planet description sheets: 128–153. Persoonia 29: 146–201. https://doi.org/10.3767/003158512X661589

Crous PW, Slippers B, Wingfield MJ, Rheeder J, Marasas WF, Philips AJ, Alves A, Burgess T, Barber P, Groenewald JZ (2006a) Phylogenetic lineages in the *Botryosphaeriaceae*. Studies in Mycology 55: 235–253. https://doi.org/10.3114/sim.55.1.235

Crous PW, Wingfield MJ, Burgess TI, Hardy GE, Crane C, Barrett S, Cano-Lira JF, Le Roux JJ, Thangavel R, Guarro J, Stchigel AM, Martín MP, Alfredo DS, Barber PA, Barreto RW et al. (2016a) Fungal Planet description sheets: 469–557. Persoonia 3: 21–403. https://doi.org/10.3767/003158516X694499

Crous PW, Wingfield MJ, Burgess TI, Hardy GS, Gené J, Guarro J, Baseia IG, García D, Gusmão LFP, Souza-Motta CM, Thangavel R, Adamčík S, Barili A, Barnes CW, Bezerra JDP et al. (2018) Fungal Planet description sheets: 716–784. Persoonia 40: 240–393. https://doi.org/10.3767/persoonia.2018.40.10

Crous PW, Wingfield MJ, Jurjević Ž, Balashov S, Osieck ER, Marin-Felix Y, Luangsa-Ard JJ, Mejía LC, Cappelli A, Parra LA, Lucchini G, Chen J, Moreno G, Faraoni M, Zhao RL et al. (2024) Fungal Planet description sheets: 1697–1780. Fungal Systematics and Evolution 14: 325–577. https://doi.org/10.3114/fuse.2024.14.19

Crous PW, Wingfield MJ, Lombard L, Roets F, Swart WJ, Alvarado P, Carnegie AJ, Moreno G, Luangsaard J, Thangavel R, Alexandrova AV, Baseia IG, Bellanger JM, Bessette AE, Bessette AR et al. (2019) Fungal Planet description sheets: 951–1041. Persoonia 43: 223–425. https://doi.org/10.3767/persoonia.2019.43.06

Crous PW, Wingfield MJ, Mansilla JP, Alfenas AC, Groenewald JZ (2006b) Phylogenetic reassessment of *Mycosphaerella* spp. and their anamorphs occurring on eucalyptus. Studies in Mycology 55: 99–131. https://doi.org/10.3114/sim.55.1.99

Crous PW, Wingfield MJ, Richardson DM, Le Roux JJ, Strasberg D, Edwards J, Roets F, Hubka V, Taylor PW, Heykoop M, Martín MP, Moreno G, Sutton DA, Wiederhold NP, Barnes CW et al. (2016b) Fungal Planet description sheets: 400–468. Persoonia 36: 316–345. https://doi.org/10.3767/003158516X692185

Cummins GB (1959) Illustrated genera of rust fungi. Minneapolis. Burgess Publishing Company. https://doi.org/10.2307/3756263

Cummins GB, Hiratsuka Y (2003) Illustrated genera of rust fungi, 3rd ed. American Phytopathological Society, St. Paul, Minnesota. https://doi.org/10.1046/j.1439-0434.2003.00804.x

Cunfer BM, Ueng PP (1999) Taxonomy and identification of *Septoria* and *Stagonospora* species on small grain cereals. Annual Review of Phytopathology 37: 267–284. https://doi.org/10.1094/pdis.1997.81.5.427

Cunnington JH (2007) *Seiridium cupressi* is the common cause of cypress canker in south-eastern Australia. Australas Plant Disease Notes 2: 53–55. https://doi.org/10.1071/dn07014

Currah RS (1985) Taxonomy of the *Onygenales*: *Arthrodermataceae*, *Gymnoascaceae*, *Myxotrichaceae* and *Onygenaceae*. Mycotaxon 24: 1–216. https://doi.org/10.5962/p.417019

Dai DQ, Phookamsak R, Wijayawardene NN, Li WJ, Bhat DJ, Xu JC, Taylor JE, Hyde KD, Chukeatirote E (2017) Bambusicolous fungi. Fungal Diversity 82: 1–105. https://doi.org/10.1007/s13225-016-0367-8

Damadi SM, Pei MH, Smith JA, Abbasi M (2011) A new species of *Melampsora* rust on *Salix elbursensis* from Iran. Forest Pathology 41: 392–397. https://doi.org/10.1111/j.1439-0329.2010.00699.x

Danti R, Barberini S, Pecchioli A, Di Lonardo V, Della Rocca G (2014) The epidemic spread of *Seiridium cardinale* on Leyland cypress severely limits its use in the Mediterranean. Plant Disease 98: 1081–1087. https://doi.org/10.1094/pdis-12-13-1237-re

Deb D, Khan A, Dey N (2020) Phoma diseases: Epidemiology and control. Plant Pathology 69: 1203–1217. https://doi.org/10.1111/ppa.13221

De Gruyter J, Aveskamp MM, Woudenberg JHC, Verkley GJ, Groenewald JZ, Crous PW (2009) Molecular phylogeny of *Phoma* and allied anamorph genera: towards a reclassification of the *Phoma* complex. Mycological Research 113: 508–519. https://doi.org/10.1016/j.mycres.2009.01.002

De Gruyter J, Woudenberg JHC, Aveskamp AA, Verkley GJM, Groenewald JZ, Crous PW (2012) Redisposition of phoma-like anamorphs in *Pleosporales*. Studies in Mycology 75: 1–36. https://doi.org/10.3114/sim0004

De Hoog GS (1977) *Rhinocladiella* and allied genera. Studies in Mycology 15: 1–140.

De Hoog G, van Oorschot A (1983) Taxonomy of the *Dactylaria* complex. I. Notes on the genus *Dichotomophthora*. Proceeding of the Koninklijk Nederlandse Akademische Wetenschappen.

De Hoog GS, Guarro J, Gené J, Figueras MJ (2000) Atlas of clinical fungi:708–711. Centraalbureau voor Schimmelcultures, Utrecht, The Netherlands and Universitat Rovira i Virgili. Reus, Spain.

De Jensen CE, Harmon CL, Vitoreli A (2013) First report of Asian Soybean rust caused by *Phakopsora pachyrhizi* in Puerto Rico. Plant Disease 97: 1378. https://doi.org/10.1094/pdis-01-13-0108-pdn

Deighton F (1973) Studies on *Cercospora* and allied genera. IV. *Cercosporella* Sacc., *Pseudocercosporella* gen. nov. and

Pseudocercosporidium gen. nov. Mycological Papers 133: 62. https://doi.org/10.1016/s0007-1536(75)80210-5

Diederich P, Lücking R, Aptroot A, Sipman HJM, Braun U, Ahti T, Ertz D (2017) New species and new records of lichens and lichenicolous fungi from the Seychelles. Herzogia 30: 182–236. https://doi.org/10.13158/heia.30.1.2017.182

Dietel P (1894) Die Gattung *Ravenelia*. Hedwigia 33: 22–69.

Dhingra OD, Sinclair JB (1978) Biology and pathology of *Macrophomina phaseolina*. Imprensa Universitária, Universidade Federal de Viçosa, Viçosa, Brazil.

Diogo E, Gonçalves CI, Silva AC, Valente C, Bragança H, Phillips AJ (2021) Five new species of *Neopestalotiopsis* associated with diseased *Eucalyptus* spp. in Portugal. Mycological Progress 20: 1441–1456. https://doi.org/10.1007/s11557-021-01741-5

Donaldson ME, Davy CM, Vanderwolf KJ, Willis CK, Saville BJ, Kyle CJ (2018) Growth medium and incubation temperature alter the *Pseudogymnoascus destructans* transcriptome: implications in identifying virulence factors. Mycologia 110: 300–315. https://doi.org/10.1080/00275514.2018.1438223

Doohan F, Zhou B (2017) Fungal pathogens of plants. Fungi: Biology and Applications. John Wiley & Sons, Inc. https://doi.org/10.1002/9781119374312.ch14

Douhan GW, Murray TD, Dyer PS (2002) Species and mating-type distribution of *Tapesia yallundae* and *T. acuformis* and occurrence of apothecia in the U.S. Pacific Northwest. Phytopathology 92: 703–709. https://doi.org/10.1094/phyto.2002.92.7.703

Duarte RT, Juliatti FC, Freitas PT (2009) Eficácia de diferentes fungicidas na cultura do milho. Bioscience Journal 25: 101–111.

Durrieu G (1980) Phylogeny of *Uredinales* on *Pinaceae*. Reports of the Tottori Mycological Institute 18: 283–290.

Dutta J, Gupta S, Thakur D, Handique PJ (2015) First report of Nigrospora leaf blight on tea caused by *Nigrospora sphaerica* in India. Plant Disease 99: 417. https://doi.org/10.1094/pdis-05-14-0545-pdn

Dyer PS, Bradshaw RE (2002) First report of apothecia of *Tapesia yallundae* occurring on the wild grass *Holcus lanatus* (Yorkshire Fog) in New Zealand. Plant Pathology 51: 806. https://doi.org/10.1046/j.1365-3059.2002.00774.x

Ebinghaus M, Begerow D (2018) *Ravenelia piepenbringiae* and *Ravenelia hernandezii*, two new rust species on *Senegalia* (*Fabaceae*, *Mimosoideae*) from Panama and Costa Rica. MycoKeys 41: 51–63. https://doi.org/10.3897/mycokeys.41.27694

Ebinghaus M, Maier W, Wingfield MJ, Begerow D (2018) New host associations and a novel species for the gall-inducing acacia rust genus *Ravenelia* in South Africa. MycoKeys 43: 1–21. https://doi.org/10.3897/mycokeys.42.25090

Ebinghaus M, Wingfield MJ, Begerow D, Maier W (2020) The genus *Ravenelia* (*Pucciniales*) in South Africa. Mycological Progress 19: 259–290. https://doi.org/10.1007/s11557-020-01556-w

Ebrahimi L, Fotouhifar KB (2021) First report of *Neosetophoma poaceicola* on apple leaf from Iran. Journal of Crop Protection 10: 350–357. https://doi.org/10.48311/jcp.2021.1544

Eken C (2003) *Dichotomophthora portulacae* on *Portulaca oleracea* in Turkey. Mycotaxon 87: 153–156. https://doi.org/10.5962/p.418403

Eken C, Spanbayev A, Tulegenova Z, Yechshzhanov T (2016) First report of *Nigrospora oryzae* on wheat in Kazakhstan. Plant Disease 100: 861. https://doi.org/10.1094/pdis-08-15-0915-pdn

Ellis MB (1971) Dematiaceous hyphomycetes. Commonwealth Mycological Institute, Kew, Surrey, England. https://doi.org/10.1079/9780851986180.0006

Eriksson OE (1993) Outline of the ascomycetes. Systema ascomycetum 12: 51–257.

Eriksson OE (2006) Outline of Ascomycota. Myconet 12: 1–82.

Espinoza JG, Briceño EX, Keith LM, Latorre BA (2008) Canker and twig dieback of blueberry caused by *Pestalotiopsis* spp. and a *Truncatella* sp. in Chile. Plant Disease 92: 1407–1414. https://doi.org/10.1094/pdis-92-10-1407

Fakhrunnisa MH, Ghaffar A (2006) Seed-borne mycoflora of wheat, sorghum and barley. Pakistan Journal of Botany 38: 185–192.

Fallon B, Yang A, Lapadat C, Armour I, Juzwik J, Montgomery RA, Cavender-Bares J (2020) Spectral differentiation of oak wilt from foliar fungal disease and drought is correlated with physiological changes. Tree Physiology 40: 377–390. https://doi.org/10.1093/treephys/tpaa005

Fan YM, Huang WM, Li W, Zhang GX (2009) Onychomycosis caused by *Nigrospora sphaerica* in an immunocompetent man. Archives of Dermatology 145: 611–612. https://doi.org/10.1001/archdermatol.2009.80

Farr DF, Rossman AY (2025) Fungal databases, US national fungus collections, ARS, USDA. Accessed on 30 September 2025. https://nt.ars-grin.gov/fungaldatabases/.

Feau N, Vialle A, Allaire M, Tanguay P, Joly DL, Frey P, Callan BE, Hamelin RC (2009) Fungal pathogen (mis-) identifications: a case study with DNA barcodes on *Melampsora* rusts of aspen and white poplar. Mycological Research 113: 713–724. https://doi.org/10.1016/j.mycres.2009.02.007

Fedrigo K, Giacomin RM, Faria CM, Da-Silva PR (2016) ISSR primers for analysis of genetic variability of *Stenocarpella maydis*. Tropical Plant Pathology 41: 270–275. https://doi.org/10.1007/s40858-016-0089-1

Fisher MC, Denning DW (2023) The WHO fungal priority pathogens list as a game-changer. Nature Reviews Microbiology 21: 211–212. https://doi.org/10.1038/s41579-023-00861-x

Fisher MC, Gurr SJ, Cuomo CA, Blehert DS, Jin H, Stukenbrock EH, Stajich JE, Kahmann R, Boone C, Denning DW, Gow NA (2020) Threats posed by the fungal kingdom to humans, wildlife, and agriculture. MBio 11: 10–128. https://doi.org/10.1128/mbio.00449-20

Fisher MC, Henk DA, Briggs CJ, Brownstein JS, Madoff LC, McCraw SL, Gurr SJ (2012) Emerging fungal threats to animal, plant and ecosystem health. Nature 12: 186–194. https://doi.org/10.1038/nature10947

Fitt B, Huang Y, Van Den Bosch F, West J (2006) Coexistence of related pathogen species on arable crops in space and time. Annual Review of Phytopathology 44: 163–182. https://doi.org/10.1146/annurev.phyto.44.070505.143417

Foëx E, Rosella E (1930) Recherches sur le piétin. Ann Épiphyties 16: 51–82.

Föller I, Paul V (2002) Investigations on diseases of false flax (*Camelina sativa* (l.) crtz.) with special regard to downy mildew (*Peronospora parasitica* (Pers.) Fr.). Soest Germany 25: 43–52.

Fones H, Gurr S (2015) The impact of *Septoria tritici* Blotch disease on wheat: An EU perspective. Fungal Genetics and Biology 79: 3–7. https://doi.org/10.1016/j.fgb.2015.04.004

Fones HN, Bebber DP, Chaloner TM, Kay WT, Steinberg G, Gurr SJ (2020) Threats to global food security from emerging fungal and oomycete crop pathogens. Nature Food 1: 332–342. https://doi.org/10.1038/s43016-020-0075-0

Forsythe A, Vanderwolf KJ, Xu J (2021) Landscape genetic connectivity and evidence for recombination in the North American population of the white-nose syndrome pathogen, *Pseudogymnoascus destructans*. Journal of Fungi 7: 182. https://doi.org/10.3390/jof7030182

Frederick RD, Snyder CL, Peterson GL, Bonde MR (2002) Polymerase chain reaction assays for the detection and discrimination of the Soybean rust pathogens *Phakopsora pachyrhizi* and *P. meibomiae*. Phytopathology 92: 217–227. https://doi.org/10.1094/phyto.2002.92.2.217

Fries EM (1849) Summa vegetabilium Scandinaviae, Typographia Academica, Uppsala.

Friis P, Olsen CE, Møller BL (1991) Toxin production in *Pyrenophora teres*, the ascomycete causing the net-spot blotch disease of barley (*Hordeum vulgare* L.). Journal of Biological Chemistry 266: 13329–13335. https://doi.org/10.1016/s0021-9258(18)98843-5

Fritze M, Puechmaille SJ, Costantini D, Fickel J, Voigt CC, Czirják GÁ (2021) Determinants of defence strategies of a hibernating European bat species towards the fungal pathogen *Pseudogymnoascus destructans*. Developmental & Comparative Immunology 119: 104017. https://doi.org/10.1016/j.dci.2021.104017

Fujinawa MF, Pontes NDC, Do Vale HMM, Santos NF, Halfeld-Vieira BA (2016) First report of *Myrothecium roridum* causing Myrothecium leaf spot on Begonia in Brazil. Plant Disease 100: 655. https://doi.org/10.1094/pdis-09-15-1097-pdn

Furtado JS, Olive LS (1971) Ascospore discharge and ultrastructure of the ascus in *Leptosphaerulina australis*. Nova Hedwigia 19: 799–823.

Futch SH (2001) A guide to citrus diseases. University of Florida Cooperative Extension Service, Institute of Food and Agriculture Sciences, EDIS.

Gandhe KR, Kuvalekar A (2007) Phylogenetic studies in *Ravenelia esculenta* and related rust fungi. Indian Journal of Microbiology 47: 212–218. https://doi.org/10.1007/s12088-007-0042-6

García-Reyes V, Solano-Báez AR, Leyva-Mir SG, De Leon-Garcia De Alba C, Rodríguez-Mendoza J, Quezada-Salinas A, Márquez-Licona G (2022) Molecular confirmation of *Stenocarpella maydis* causing ear rot of maize in Mexico. Journal of Plant Pathology 104: 775–779. https://doi.org/10.1007/s42161-022-01053-x

Gargas A, Trest MT, Christensen M, Volk TJ, Blehert DS (2009) *Geomyces destructans* sp. nov., associated with bat white-nose syndrome. Mycotaxon 108: 147–154. https://doi.org/10.5248/108.147

Gautam AK, Avasthi S, Verma RK, Devadatha B, Jayawardena RS, Sushma RK (2021) Indian *Pucciniales*: taxonomic outline with important descriptive notes. Mycosphere 12: 89–162. https://doi.org/10.5943/mycosphere/12/1/2

Ghelardini L, Luchi N, Pecori F, Pepori AL, Danti R, Della Rocca G, Capretti P, Tsopelas P, Santini A (2017) Ecology of invasive forest pathogens. Biological Invasions 19: 3183–3200. https://doi.org/10.1007/s10530-017-1487-0

Glynne MD, Salt GA (1958) Eyespot of wheat and barley. Report of Rothamsted Experimental Station 1958: 231–241.

Golzar H, Wang C (2012) First report of *Phaeosphaeriopsis glaucopunctata* as the cause of leaf spot and necrosis on *Ruscus aculeatus* in Australia. Australas Plant Disease Notes 7: 13–15. https://doi.org/10.1007/s13314-011-0035-5

Gonçalves RM, Figueiredo JE, Pedro ED, Meirelles WF, Leite RP, Sauer AV, Paccola-Meirelles LD (2013) Etiology of Phaeosphaeria leaf spot disease of maize. Journal of Plant Pathology 1: 559–569.

González P, Alaniz S, Montelongo MJ, Rauduviniche L, Rebellato J, Silvera-Pérez E, Mondino P (2012) First report of *Pestalotiopsis clavispora* causing dieback on blueberry in Uruguay. Plant Disease 96: 914. https://doi.org/10.1094/pdis-12-11-1070-pdn

Goodwin SB, Zismann VL (2001) Phylogenetic analyses of the ITS region of ribosomal DNA reveal that *Septoria passerinii* from barley is closely related to the wheat pathogen *Mycosphaerella graminicola*. Mycologia 93: 934–946. https://doi.org/10.1080/00275514.2001.12063227

Gorny AM, Kikkert JR, Shivas RG, Pethybridge SJ (2016) First report of *Didymella americana* on baby lima bean (*Phaseolus lunatus*). Canadian Journal of Plant Pathology 38: 389–394. https://doi.org/10.1080/07060661.2016.1195877

Graham JH (1961) Species of *Leptosphaerulina* on forage plants. Phytopathology 51: 680–693.

Graniti A (1986) *Seiridium cardinale* and other cypress cankers. EPPO Bulletin 16: 479–486. https://doi.org/10.1111/j.1365-2338.1986.tb00309.x

Graniti A (1998) Cypress canker: a pandemic in progress. Annual Review of Phytopathology 36: 91–114. https://doi.org/10.1146/annurev.phyto.36.1.91

Gruyter J, Woudenberg JH, Aveskamp MM, Verkley GJ, Groenewald JZ, Crous PW (2010) Systematic reappraisal of species in *Phoma* section *Paraphoma*, *Pyrenochaeta* and *Pleurophoma*. Mycologia 102: 1066–1081. https://doi.org/10.3852/09-240

Gudelj I, Fitt BD, Van Den Bosch F (2004) Evolution of sibling fungal plant pathogens in relation to host specialization. Phytopathology 94: 789–795. https://doi.org/10.1094/phyto.2004.94.7.789

Gunasinghe N, Barbetti M, You M, Burrell D, Neate S (2020) White leaf spot caused by *Neopseudocercosporella capsellae*: A re-emerging disease of *Brassicaceae*. Frontiers in Cellular and Infection Microbiology 10: 588090. https://doi.org/10.3389/fcimb.2020.588090

Gunasinghe N, Barbetti M, You M, Dehigaspitiya P, Neate S (2021) Dimorphism in *Neopseudocercosporella capsellae,* an emerging pathogen causing white leaf spot disease of *Brassicas*. Frontiers in Cellular and Infection Microbiology 11: 678231. https://doi.org/10.3389/fcimb.2021.678231

Gunasinghe N, You M, Barbetti M (2016) Phenotypic and phylogenetic studies associated with the crucifer white leaf spot pathogen, *Pseudocercosporella Capsellae*, in Western Australia. Plant Pathology 65: 205–217. https://doi.org/10.1111/ppa.12402

Guo Z, Xie H, Wang H, Huang Y, Chen Q, Xiang L, Yu Z, Yang X (2020) Leaf spot caused by *Didymella segeticola* on tobacco in China. Plant Disease 104: 1559. https://doi.org/10.1094/pdis-11-19-2398-pdn

Gupta GK, Sharma SK, Ramteke R (2012) Biology, epidemiology and management of the pathogenic fungus *Macrophomina phaseolina* (Tassi) goid with special reference to charcoal rot

of soybean (*Glycine max* (L.) Merrill). Journal of Phytopathology 160: 167–180. https://doi.org/10.1111/j.1439-0434.2012.01884.x

Hajano G, Pathan QA, Mubeen AL (2011) Rice blast-mycoflora, symptomatology and pathogenicity. Sindh Agriculture University Tandojam 5: 53–63. https://doi.org/10.5455/ijavms.20110226124750

Hall TA (1999) BioEdit: a user-friendly biological sequence alignment editor and analysis program for Windows 95/98/NT. In: Nucleic Acids Symposium Series; Information Retrieval Ltd, London, UK.

Han KS, Choi SK, Kim HH, Lee SC, Park JH, Cho MR, Park MJ (2014) First report of *Myrothecium roridum* causing leaf and stem rot disease on *Peperomia quadrangularis* in Korea. Mycobiology 42: 203–205. https://doi.org/10.5941/myco.2014.42.2.203

Hao B, Li W, Chen C, Gao L, Zhang R, Wang B, Sun G, Gleason ML (2013) *Ramichloridium strelitziae* associated with sooty blotch and flyspeck on *Ravenala madagascariensis* in China. Mycotaxon 124: 39–44. https://doi.org/10.5248/124.39

Hao Y, Aluthmuhandiram JV, Chethana KT, Manawasinghe IS, Li X, Liu M, Hyde KD, Phillips AJ, Zhang W (2020) *Nigrospora* species associated with various hosts from Shandong Peninsula, China. Mycobiology 48: 169–183. https://doi.org/10.1080/12298093.2020.1761747

Harrington TC, McNew D, Yun HY (2012) Bur oak blight, a new disease on *Quercus macrocarpa* caused by *Tubakia iowensis* sp. nov. Mycologia 104: 79–92. https://doi.org/10.3852/11-112

Harrington TC, McNew DL (2018) A re-evaluation of *Tubakia*, including three new species on *Quercus* and six new combinations. Antonie van Leeuwenhoek 111: 1003–1022. https://doi.org/10.1007/s10482-017-1001-9

Harrington TC, Wingfield MJ (2000) 19 Diseases and the ecology of indigenous and exotic pines. Ecology and Biogeography of *Pinus* 31: 381.

Hartman GL, Miles MR, Frederick RD (2005) Breeding for resistance to soybean rust. Plant Disease 89: 664–666. https://doi.org/10.1094/PD-89-0664

Hashemi H, Mohammadi H (2016) Identification and characterization of fungi associated with internal wood lesions and decline disease of willow and poplar trees in Iran. Forest Pathology 46: 341–352. https://doi.org/10.1111/efp.12269

Havenga M, Gatsi GM, Halleen F, Spies CF, van der Merwe R, Mostert L (2019) Canker and wood rot pathogens present in young apple trees and propagation material in the Western Cape of South Africa. Plant Disease 103: 3129–3141. https://doi.org/10.1094/pdis-04-19-0867-re

Hawksworth DL (1991) The fungal dimension of biodiversity: magnitude, significance, and conservation. Mycological Research 95: 641–655. https://doi.org/10.1016/s0953-7562(09)80810-1

Hedgcock G (1928) A key to the known aecial forms of *Coleosporium* occurring in the United States and a list of the host species. Mycologia 20: 97–100. https://doi.org/10.1080/00275514.1928.12016905

Heidari K, Farokhinejad R, Mehrabi-Koushki M (2018) Occurence of purslane leaf spot caused by *Dichotomophthora lutea* in Iran. Australas Plant Disease Notes 13: 33. https://doi.org/10.1007/s13314-018-0317-2

Heng ZA, Mu TC, Keyhani NO, Yang LX, Zheng MH, Lv HJ, Zhao ZY, Mao YC, Shang JY, Yang J, Pu HL (2025) Three new species of *Neopestalotiopsis* and *Pseudopestalotiopsis* (*Sporocadaceae*, *Amphisphaeriales*) associated with shrub leaf diseases from Fujian, China. MycoKeys 119: 1–28. https://doi.org/10.3897/mycokeys.119.148647

Hennen JF, Figueiredo MB, de Carvalho AA Jr, Hennnen PG (2005) Catalogue of the species of plant rust fungi (*Uredinales*) of Brazil. Instituto de Pesquisas, Jardim Botanico do Rio de Janeiro: Rio de Janeiro, Brazil.

Hernández JR, Hennen JF (2002) The genus *Ravenelia* in Argentina. Mycological Research 106: 954–974. https://doi.org/10.1017/s0953756202006226

Hernandez-Restrepo M, Schumacher RK, Wingfield MJ, Ahmad I, Cai L, Duong TA, Edwards J, Gene J, Groenewald JZ, Jabeen S, Khalid AN, Lombard L, Madrid H, Marin-Felix Y, Marincowitz S, Miller AN et al. (2016) Fungal systematics and evolution: FUSE 2. Sydowia 68: 193–230.

Hiratsuka N, Kaneko S (1975) Surface structure of *Coleosporium* spores. Rep. Reports of the Tottori Mycological Institute 12: 1–13.

Holcomb GE, Aime MC (2010) First Report of *Plumeria* spp. rust caused by *Coleosporium plumeriae* in Louisiana and Malaysia and *Catheranthus roseus*, a new host of this rust. Plant Disease 94: 272. https://doi.org/10.1094/pdis-94-2-0272c

Holdenrieder O, Kowalski T (1989) Pycnidial formation and pathogenicity in *Tubakia dryina*. Mycological Research 92: 166–169. https://doi.org/10.1016/s0953-7562(89)80007-3

Holliday P, Punithalingam E (1970) *Macrophomina phaseolina*. C.M.I. Descriptions of Pathogenic Fungi and Bacteria 275: 2.

Holm L (1975) Nomenclatural notes on *Pyrenomycetes*. Taxon 475–488. https://doi.org/10.2307/1219501

Hongsanan S, Hyde KD, Phookamsak R, Wanasinghe DN, McKenzie EHC, Sarma VV, Boonmee S, Lücking R, Pem D, Bhat JD, et al. (2020a) Refined families of *Dothideomycetes*: *Dothideomycetidae* and *Pleosporomycetidae*. Mycosphere 11: 1553–2107. https://doi.org/10.5943/mycosphere/11/1/13

Hongsanan S, Hyde KD, Phookamsak R, Wanasinghe DN, McKenzie EHC, Sarma VV, Lücking R, Boonmee S, Bhat JD, Liu NG, et al. (2020b) Refined families of *Dothideomycetes*: orders and families incertae sedis in *Dothideomycetes*. Fungal Diversity 105: 17–318. https://doi.org/10.1007/s13225-020-00462-6

Hongsanan S, Khuna S, Manawasinghe IS, Tibpromma S, Chethana KW, Xie N, Bagacay JF, Calabon MS, Chen C, Doilom M, Du HY, Gafforov Y, Huang SK, Li JX, Luangharn T et al. (2025) Mycosphere Notes 521–571: A special edition of fungal biodiversity to celebrate Kevin D. Hyde's 70th birthday and his exceptional contributions to Mycology. Mycosphere 16: 1–178. https://doi.org/10.5943/mycosphere/16/2/1

Hopkins EF (1923) The *Sphaerulina* leaf spot of clover. Phytopathology 13: 117–126.

Hou LW, Groenewald JZ, Pfenning LH, Yarden O, Crous PW, Cai L(2020) The phoma-like dilemma. Studies in Mycology 96: 309–396. https://doi.org/10.1016/j.simyco.2020.05.001

Hoyt JR, Kilpatrick AM, Langwig KE (2021) Ecology and impacts of white-nose syndrome on bats. Nature Reviews

Microbiology 19: 196–210.
https://doi.org/10.1038/s41579-020-00493-5

Huda-Shakirah AR, Kee YJ, Hafifi ABM, Mohamad Azni NN, Zakaria L, Mohd MH (2019) Identification and characterization of *Macrophomina phaseolina* causing leaf blight on white spider Lilies (*Crinum asiaticum* and *Hymenocallis littoralis*) in Malaysia. Mycobiology 47: 408–414.
https://doi.org/10.1080/12298093.2019.1682448

Hyde KD, Al-Hatmi AM, Andersen B, Boekhout T, , Buzina W, Dawson Jr TL, Eastwood DC, Jones EG, de Hoog S, Kang Y, Longcore JE (2018) The world's ten most feared fungi. Fungal Diversity 93: 161–194.
https://doi.org/10.1007/s13225-018-0413-9

Hyde KD, Jeewon R, Chen YJ, Bhunjun CS, Calabon MS, Jiang HB, Lin CG, Norphanphoun C, Sysouphanthong P, Pem D, Tibpromma S, Zhang Q, Doilom M, Jayawardena RS, Liu JK et al. (2020) The numbers of fungi: is the descriptive curve flattening? Fungal Diversity 103: 219–271.
https://doi.org/10.1007/s13225-020-00458-2

Hyde KD, Jones EBG, Liu JK, Ariyawansa H, Boehm E, Boonmee S, Braun U, Chomnunti P, Crous PW, Dai DQ, Diederich P, Dissanayake A, Doilom M, Doveri F, Hongsanan S et al. (2013) Families of *Dothideomycetes*. Fungal Diversity 63: 1–313.
https://doi.org/10.1007/s13225-013-0263-4

Hyde KD, Nilsson RH, Alias SA, Ariyawansa HA, Blair JE, Cai L, de Cock AWAM, Dissanayake AJ, Glockling SL, Goonasekara ID, Gorczak M, Hahn M, Jayawardena RS, van Kan JA, Laurence MH et al. (2014) One stop shop: backbones trees for important phytopathogenic genera: I. Fungal Diversity 67: 21–125.
https://doi.org/10.1007/s13225-014-0298-1

Hyde KD, Noorabadi MT, Thiyagaraja V, He MQ, Johnston PR, Wijesinghe SN, Armand A, Biketova AY, Chethana KWT, Erdoğdu M, Ge ZW, Groenewald JZ, Hongsanan S, Kušan I, Leontyev DV et al. (2024a) The 2024 Outline of Fungi and fungus-like taxa. Mycosphere 15: 5146–6239.
https://doi.org/10.5943/mycosphere/15/1/25

Hyde KD, Saleh A, Aumentado HDR, Boekhout T, Bera I, Khyaju S, Bhunjun CS, Chethana KWT, Phukhamsakda C, Doilom M, Thiyagaraja V, Mortimer PE, Maharachchikumbura SSN, Hongsanan S, Jayawardena RS et al. (2024b) Fungal numbers: global needs for a realistic assessment. Fungal Diversity 128: 191–225.
https://doi.org/10.1007/s13225-024-00545-8

Hyde KD, Tennakoon DS, Jeewon R, Bhat DJ, Maharachchikumbura SSN, Rossi W, Leonardi M, Lee HB, Mun HY, Houbraken J, Nguyen TTT, Jeon SJ, Frisvad JC, Wanasinghe DN, Lücking R et al. (2019) Fungal diversity notes 1036–1150: taxonomic and phylogenetic contributions on genera and species of fungal taxa. Fungal Diversity 96: 1–242.
https://doi.org/10.1007/s13225-019-00429-2

Indermaur EJ, Day CTC, Smart CD (2022) First Report of *Didymella rhei* causing leaf spot on rhubarb in New York. Plant Disease 107: 222.
https://doi.org/10.1094/pdis-03-22-0573-pdn

Index Fungorum (2025) Index Fungorum. Accessed 30 May 2025.
http://www.indexfungorum.org/names/names.asp.

Ingold CT (1971) Fungal spores. Their libération and dispersal. Oxford, Clarendon Press.
https://doi.org/10.2307/3757818

Inman AJ, Sivanesan A, Fitt BDL, Evans RL (1991) The biology of *Mycosphaerella capsellae* sp. nov., the teleomorph of *Pseudocercosporella capsellae*, cause of white leaf. Mycological Research 95: 1334–1342.
https://doi.org/10.1016/s0953-7562(09)80586-8

Jagdish BK, Laxminarayana P, Reddy SM (1985) New records of post harvest diseases of oranges (*Citrus reticulata*). Indian Phytopathology 38: 575.

Jaklitsch WM, Gardiennet A, Voglmayr H (2016) Resolution of morphology-based taxonomic delusions: *Acrocordiella*, *Basiseptospora*, *Blogiascospora*, *Clypeosphaeria*, *Hymenopleella*, *Lepteutypa*, *Pseudapiospora*, *Requienella*, *Seiridium* and *Strickeria*. Persoonia 37: 82–105.
https://doi.org/10.3767/003158516x690475

Jayasiri SC, Hyde KD, Jones EBG, Jeewon R, Ariyawansa HA, Bhat JD, Camporesi E, Kang JC (2017) Taxonomy and multigene phylogenetic evaluation of novel species in *Boeremia* and *Epicoccum* with new records of *Ascochyta* and *Didymella* (*Didymellaceae*). Mycosphere 8: 1080–1101.
https://doi.org/10.5943/mycosphere/8/8/9

Jayawardena RS, Hyde KD, Aumentado HD, Abeywickarama PD, Avasthi S, Dissanayake AJ, Gautam AK, Gajanayake AJ, Armand A, Balendres MAO, Calabon MS, Chen YJ, Chethana KWT, Ferdinandez HS, Gomdola Det al. (2025) One stop shop V: taxonomic update with molecular phylogeny for important phytopathogenic genera: 101–125 (2024). Fungal Diversity 18: 1–67.
https://doi.org/10.1007/s13225-024-00542-x

Jayawardena RS, Hyde KD, Chen YJ, Papp V, Bhunjun CS, Hurdeal VG, Senwanna C, Manawasinghe IS, Harischandra DL, Gautam AK, Avasthi S, Chuankid B, Goonasekara ID, Hongsanan S, Zeng XY et al. (2020) One stop shop IV: taxonomic update with molecular phylogeny for important phytopathogenic genera: 76–100. Fungal Diversity 103: 87–218.
https://doi.org/10.1007/s13225-020-00460-8

Jayawardena RS, Hyde KD, Jeewon R, Ghobad-Nejhad M, Wanasinghe DN, Liu N, Phillips AJL, Oliveira-Filho JRC, da Silva GA, Gibertoni TB, Abeywikrama P, Carris LM, Chethana KWT, Dissanayake AJ, Hongsanan S et al. (2019a) One stop shop II: taxonomic update with molecular phylogeny for important phytopathogenic genera: 26–50. Fungal Diversity 94: 41–129.
https://doi.org/10.1007/s13225-019-00418-5

Jayawardena RS, Hyde KD, McKenzie EHC, Jeewon R, Phillips AJL, Perera RH, de Silva NI, Maharachchikumburua SSN, Samarakoon MC, Ekanayake AH, Tennakoon DS, Dissanayake AJ, Norphanphoun C, Lin C, Manawasinghe IS et al. (2019b) One stop shop III: taxonomic update with molecular phylogeny for important phytopathogenic genera: 51–75. Fungal Diversity 98: 77–160.
https://doi.org/10.1007/s13225-019-00433-6

Jayawardena RS, Liu M, Maharachchikumbura SS, Zhang W, Xing Q, Hyde KD, Nilthong S, Li X, Yan J (2016) *Neopestalotiopsis vitis* sp. nov. causing grapevine leaf spot in China. Phytotaxa 258: 63–74.
https://doi.org/10.11646/phytotaxa.258.1.4

Jayawardena RS, Purahong W, Zhang W, Wubet T, Li X, Liu M, Zhao W, Hyde KD, Liu J, Yan J (2018) Biodiversity of fungi on *Vitis vinifera* L. revealed by traditional and high-resolution culture-independent approaches. Fungal Diversity 90: 1–84.
https://doi.org/10.1007/s13225-018-0398-4

Jayawardena RS, Zhang W, Liu M, Maharachchikumbura SS, Zhou Y, Huang JB, Nilthong S, Wang ZY, Li XH, Yan JY, Hyde KD (2015) Identification and characterization of pestalotiopsis-like fungi related to grapevine diseases in China. Fungal

Biology 119: 348–361.
https://doi.org/10.1016/j.funbio.2014.11.001

Ji JX, Wang Q, Li Z, Li Y, Makoto K (2016) Notes on rust fungi in China 2. Two species of *Coleosporium* on *Compositae*. Mycotaxon 131: 811–820.
https://doi.org/10.5248/131.811

Jia X, Zheng X, Damm U, Lu X, Niu X, Feng Y, Zhang W (2023) *Stenocarpella chrysopogonis*, a new species causing leaf streak disease of *Chrysopogon zizanioides* in southern China. Plant Disease 107: 3674–3686.
https://doi.org/10.1094/pdis-02-23-0383-sr

Jiang N, Fan X, Tian C (2021) Identification and characterization of leaf-inhabiting fungi from *Castanea* plantations in China. Journal of Fungi 7: 64.
https://doi.org/10.3390/jof7010064

Jiang N, Liang YM, Tian CM (2019) Morphological and phylogenic evidences reveal a new *Seiridium* species in China Phytotaxa 418: 287–293.
https://doi.org/10.11646/phytotaxa.418.3.4

Jiang YL, Wang HF, Pan HQ, Zhang TY (2014) *Myrothecium* (Hyphomycetes): Three new species, one variety and a key to species and varieties of the genus known from soil in China. Mycosystema 33: 7–14.

Jiang YL, Wu YM, Yang B, Xu JJ, Zhang ZG, Zhang YL, Zhang TY (2017) New species of *Cephalotrichum*, *Leptographium*, and *Myrothecium* from soil in China. Mycotaxon 132: 603–609.
https://doi.org/10.5248/132.603

Jing J, Diao LG, Lu BS, Li BD (2008) The finding of *Dichotomophthora portulacae* in China. Mycosystema 27: 601–603.

Jones DR, Baker RHA (2007) Introductions of non-native plant pathogens into Great Britain, 1970–2004. Plant Pathology 56: 891–910.
https://doi.org/10.1111/j.1365-3059.2007.01619.x

Jones DR, Stover RH (2000) Fungal diseases of banana fruit, preharvest diseases. Wallingford, UK CABI Publishing.
https://doi.org/10.1079/9781780647197.0255

Kaneko S (1981) The species of *Coleosporium*, the causes of pine needle rusts, in the Japanese Archipelago. Report of Tottori Mycological Institute 19: 159.

Karunarathna A, Papizadeh M, Senanayake IC, Jeewon R, Phookamsak R, Goonasekara ID, Wanasinghe DN, Wijayawardene NN, Amoozegar MA, Shahzadeh Fazeli SA, Camporesi E (2017) Novel fungal species of *Phaeosphaeriaceae* with an asexual/sexual morphconnection. Mycosphere 8: 1818–1834.
https://doi.org/10.5943/mycosphere/8/10/8

Katoh K, Rozewicki J, Yamada KD (2019) MAFFT online service: multiple sequence alignment, interactive sequence choice and visualization. Briefings in Bioinformatics 20: 1160–1166.
https://doi.org/10.1093/bib/bbx108

Kee YJ, Hafifi AB, Huda-Shakirah AR, Wong KL, Jin XL, Nordahliawate MS, Zakaria L, Mohd MH (2019) First report of reddish brown spot disease of red-fleshed dragon fruit (*Hylocereus polyrhizus*) caused by *Nigrospora lacticolonia* and *Nigrospora sphaerica* in Malaysia. Crop Protection 122: 165–170.
https://doi.org/10.1016/j.cropro.2019.05.006

Kehinde IA (2013) Characteristic symptoms of melon diseases caused by fungi in south western Nigeria. African Journal of Agricultural Research 8: 5791–5801.

Keinath AP (2008) Survival of *Didymella bryoniae* in infested muskmelon crowns in South Carolina. Plant Disease 92: 1223–1228.
https://doi.org/10.1094/pdis-92-8-1223

Kema G, Yu D, Rijkenberg F, Shaw MW, Baayen RP (1996) Histology of the pathogenesis of *Mycosphaerella graminicola* in wheat. Phytopathology 86: 777–786.
https://doi.org/10.1094/phyto-86-777

Khan SN (2007) *Macrophomina phaseolina* as causal agent for charcoal rot of sunflower. Mycopath 5: 111–118.

Khan TN, Timmerman-Vaughan GM, Rubiales D, Warkentin TD, Siddique KH, Erskine W, Barbetti MJ (2013) *Didymella pinodes* and its management in field pea: Challenges and opportunities. Field Crops Research 148: 61–77.
https://doi.org/10.1016/j.fcr.2013.04.003

Kharwar RN, Singh A, Singh R, Kumar S (2015) Two new species of *Zasmidium* from Nepal. Mycotaxon 130: 241–246.
https://doi.org/10.5248/130.241

King KM, Eyres GJ, West JS, Siraf C, Matusinsky P, Palicová J, Canning GG, Bateman GL, Fraaije BA, Dyer PS (2021) Novel multiplex and loop-mediated isothermal amplification assays for rapid species and mating-type identification of *Oculimacula acuformis* and *O. yallundae* (causal agents of cereal eyespot), and application for detection of ascospore dispersal and in planta use. Phytopathology 111: 582–592.
https://doi.org/10.1094/phyto-04-20-0116-r

Kirk PM, Cannon PF, David JC, Staplers JA (2001) Bisby's Dictionary of the Fungi. Ainsworth and Bisby's dictionary of the fungi: 9th edition. CABI, Wallingford, UK.

Kirk PM, Cannon PF, Minter DW, Stalpers JA (2008) Ainsworth & Bisby's Dictionary of the Fungi. 10th edn. Wallingford: CABI, Wallingford, UK.
https://doi.org/10.1108/09504120910969104

Klisiewicz JM (1985) Growth and reproduction of *Dichotomophthora portulacae* and its biological activity on Purslane. Plant Disease 69: 761–762.
https://doi.org/10.1094/pd-69-761

Klisiewicz JM, Clement SL, Norris RF (1983) Black stem: a fungal disease of common Purslane in California. Plant Disease 67: 1162.
https://doi.org/10.1094/pd-67-1162

Köhler JR, Hube B, Puccia R, Casadevall A, Perfect JR (2017) Fungi that infect humans. Microbiology Spectrum 30: 10–128.
https://doi.org/10.1128/9781555819583.ch39

Kolmer JA, Ordonez ME, Groth JV (2009) The rust fungi. In: Encyclopedia of Life Sciences (ELS). John Wiley & Sons, Ltd, Chicheste, UK.
https://doi.org/10.1002/9780470015902.a0021264

Kouadri MEA, Bekkar AA, Zaim S (2023) Morphological, molecular and pathogenic characterization of *Macrophomina pseudophaseolina* the causal agent of charcoal rot disease on lentil (*Lens culinaris*) in Algeria. Physiological and Molecular Plant Pathology 128: 102143.
https://doi.org/10.1016/j.pmpp.2023.102143

Kowalski T (2006) *Tubakia dryina*, symptoms and pathogenicity to *Quercus robur*. Acta Mycologica 41: 299–304.
https://doi.org/10.5586/am.2006.030

Krout-Greenberg, ND, Puschner B, Davidson MG, Depeters EJ (2013) Preliminary study to assess mycotoxin concentrations in whole corn in the California feed supply. Journal of Dairy Science 96: 2705–2712.
https://doi.org/10.3168/jds.2012-5957

Kwasna H, Bateman GL (2008) A new species of *Galactomyces* and first reports of four fungi on wheat roots in the United Kingdom. Sydowia 60: 69–92.

Lamprecht SC, Crous PW, Groenewald JZ, Tewoldemedhin YT, Marasas WF (2011) *Diaporthaceae* associated with root and crown rot of maize. IMA Fungus 2: 13–24. https://doi.org/10.5598/imafungus.2011.02.01.03

Lancaster R (2006) Diseases of vegetable brassicas. Farmnote 39/90. Perth, Australia. La Porta NI, Capretti PI, Thomsen IM, Kasanen R, Hietala AM, Von Weissenberg K (2008) Forest pathogens with higher damage potential due to climate change in Europe. Canadian Journal of Plant Pathology 30: 177–195. https://doi.org/10.1080/07060661.2008.10540534

La Porta NI, Capretti PI, Thomsen IM, Kasanen R, Hietala AM, Von Weissenberg K (2008) Forest pathogens with higher damage potential due to climate change in Europe. Canadian Journal of Plant Pathology 30: 177–195. https://doi.org/10.1080/07060661.2008.10540534

Larsson A (2014) AliView: a fast and lightweight alignment viewer and editor for large datasets. Bioinformatics 30: 3276–3278. https://doi.org/10.1093/bioinformatics/btu531

Latterell FM, Rossi AE (1983) *Stenocarpella macrospora* (= *Diplodia*) and *S. maydis* (= *D. maydis*) compared as pathogens of corn. Plant Disease 67: 725–729. https://doi.org/10.1094/pd-67-725

Lechat C, Fournier J (2019) *Pleiocarpon gardiennetii* (*Nectriaceae*), a new holomorphic species from French Guiana. Ascomycete.org 11: 33–36.

Lee HB, Kim JC, Hong KS, Kim CJ (2008) Evaluation of a fungal strain, *Myrothecium roridum* F0252, as a bioherbicide agent. Plant Pathology 24: 453–460. https://doi.org/10.5423/ppj.2008.24.4.453

Lee JE, Kim KB, Park JE, Kim DW, Shin YK, Yun SH, Chung YR (2019) First report of a bracken blight disease caused by *Didymella* sp. Research in Plant Disease 25: 143–148. https://doi.org/10.5423/rpd.2019.25.3.143

Leisova L, Kucera L, Minarikova V, Ovesna J (2005) AFLP-based PCR markers that differentiate spot and net forms of *Pyrenophora teres*. Plant Pathology 54: 66–73. https://doi.org/10.1111/j.1365-3059.2005.01117.x

Li H, Sun G, Zhai XR, Batzer JC, Mayfield DA, Crous PW, Groenewald JZ, Gleason ML (2012) *Dissoconiaceae* associated with sooty blotch and flyspeck on fruits in China and the United States. Persoonia 28: 113–125. https://doi.org/10.3767/003158512x651157

Li WL, Dissanayake AJ, Zhang T, Maharachchikumbura SS, Liu JK (2022) Identification and pathogenicity of pestalotiod fungi associated with woody oil plants in Sichuan Province, China. Journal of Fungi 8: 1175. https://doi.org/10.3390/jof8111175

Liang J, Li G, Hou L, Zhao M, Cai L (2021) *Leptosphaerulina* species isolated from golf turfgrass in China, with description of *L. macrospora*, sp. nov. Mycologia 113: 956–967. https://doi.org/10.1080/00275514.2021.1923298

Liang J, Li G, Zhou S, Zhao M, Cai L (2019) Myrothecium-like new species from turfgrasses and associated rhizosphere. MycoKeys 51: 29–53. https://doi.org/10.3897/mycokeys.51.31957

Link HF (1809) Observationes in ordines plantarum naturales. Dissertatio I. 3: 3–42.

Liu F, Hou L, Raza M, Cai L (2017) *Pestalotiopsis* and allied genera from *Camellia*, with description of 11 new species from China. Scientific Reports 7: 866. https://doi.org/10.1038/s41598-017-00972-5

Liu JK, Hyde KD, Jones EBG, Ariyawansa HA, Bhat DJ, Boonmee S, Maharachchikumbura SS, McKenzie EH, Phookamsak R, Phukhamsakda C, Shenoy BD, Abdel-Wahab MA, Buyck B, Chen J, Chethana KWT et al. (2015) Fungal diversity notes 1–110: taxonomic and phylogenetic contributions to fungal species. Fungal Diversity 72: 1–197. https://doi.org/10.1007/s13225-015-0324-y

Liu XP, Jing XM, Yan HX, Li GL, Luo YH (2019) First report of *Leptosphaerulina* leaf spot caused by *Leptosphaerulina trifolii* on Alfalfa in Heilongjiang Province, China. Plant Disease 103: 2673. https://doi.org/10.1094/pdis-04-19-0693-pdn

Liu YJ, Hu F, Chen LS, Xu SW (2020) First report of *Nigrospora sphaerica* causing leaf blight on oil tea (*Camellia oleifera*) in China. Plant Disease 104: 3252. https://doi.org/10.1094/pdis-03-20-0563-pdn

Liu YJ, Tang Q, Fang L (2016) First report of *Nigrospora sphaerica* causing leaf blight on *Camellia sinensis* in China. Plant Disease 100: 221. https://doi.org/10.1094/pdis-04-15-0493-pdn

Liu ZH, Ellwood SR, Oliver RP, Friesen TL (2011) *Pyrenophora teres*: profile of an increasingly damaging barley pathogen. Molecular Plant Pathology 12: 1–19. https://doi.org/10.1111/j.1364-3703.2010.00649.x

Lombard L, Houbraken J, Decock C, Samson RA, Meijer M, Réblová M, Groenewald JZ, Crous PW (2016) Generic hyper-diversity in *Stachybotriaceae*. Persoonia 36: 156–246. https://doi.org/10.3767/003158516x691582

Lombard L, Van der Merwe NA, Groenewald JZ, Crous PW (2015) Generic concepts in *Nectriaceae*. Studies in Mycology 80: 189–245. https://doi.org/10.1016/j.simyco.2014.12.002

Lorch JM, Lindner DL, Gargas A, Muller LK, , Minnis AM, Blehert DS (2013) A culture-based survey of fungi in soil from bat hibernacula in the eastern United States and its implications for detection of *Geomyces destructans*, the causal agent of bat white-nose syndrome. Mycologia 105: 237–252. https://doi.org/10.3852/12-207

Lorch JM, Meteyer CU, Behr MJ, Boyles JG, Cryan PM, Hicks AC, Ballmann AE, Coleman JT, Redell DN, Reeder DM, Blehert DS (2011) Experimental infection of bats with *Geomyces destructans* causes white-nose syndrome. Nature 480: 376–378. https://doi.org/10.1038/nature10590

Luo Y, Chen WH, Wang Y, Han YF, Liang ZQ (2016) A new *Geomyces* species producing melanin in the medium. Mycosystema 35: 123–130.

Luttrell ES (1955) The Ascostromatic Ascomycetes. Mycologia 47: 511–532. https://doi.org/10.1080/00275514.1955.12024473

Ma W, Yang J, Gao X, Han T, Liu J, Ding J, Zhao W, Peng YL, Bhadauria V (2022) First report of *Didymella glomerata* causing Didymella leaf blight on maize in China. Plant Disease 106: 2522. https://doi.org/10.1094/pdis-02-22-0282-pdn

Machado AR, Pinho DB, Soares DJ, Gomes AAM, Pereira OL (2019) Bayesian analyses of five gene regions reveal a new phylogenetic species of *Macrophomina* associated with charcoal rot on oilseed crops in Brazil. European Journal of Plant Pathology 153: 89–100. https://doi.org/10.1007/s10658-018-1545-1

Magyar D, Vass M, Li DW (2016) Dispersal strategies of microfungi. In Biology of Microfungi Cham: Springer International

Publishing.
https://doi.org/10.1007/978-3-319-29137-6_14

Mahapatra S, Banerjee J, Kumar K, Pramanik S, Pramanik K, Islam S, Das S (2018) Leaf spot and fruit rot of strawberry caused by *Neopestalotiopsis clavispora* in indo-gangetic plains of India. Indian Phytopathology 71: 1–5.
https://doi.org/10.1007/s42360-018-0043-x

Maharachchikumbura SS, Chen Y, Ariyawansa HA, Hyde KD, Haelewaters D, Perera RH, Samarakoon MC, Wanasinghe DN, Bustamante DE, Liu JK, Lawrence DP, Cheewangkoon R, Stadler M (2021) Integrative approaches for species delimitation in Ascomycota. Fungal Diversity 109: 155–179.
https://doi.org/10.1007/s13225-021-00486-6

Maharachchikumbura SS, Guo LD, Chukeatirote E, Bahkali AH, Hyde KD (2011) *Pestalotiopsis*-morphology, phylogeny, biochemistry and diversity. Fungal Diversity 50: 167–187.
https://doi.org/10.1007/s13225-011-0125-x

Maharachchikumbura SS, Guo LD, Chukeatirote E, Hyde KD (2014) Improving the backbone tree for the genus *Pestalotiopsis*; addition of *P. steyaertii* and *P. magna* sp. nov. Mycological Progress 13: 617–624.
https://doi.org/10.1007/s11557-013-0944-0

Maharachchikumbura SS, Guo LD, Liu ZY, Hyde KD (2016) *Pseudopestalotiopsis ignota* and *Ps. camelliae* spp. nov. associated with grey blight disease of tea in China. Mycological Progress 15: 22.
https://doi.org/10.1007/s11557-016-1162-3

Maharachchikumbura SSN, Chukeatirote E, Guo LD, Crous PW, Mckenzie EH, Hyde KD (2013a) *Pestalotiopsis* species associated with *Camellia sinensis* (tea). Mycotaxon 123: 47–61.
https://doi.org/10.5248/123.47

Maharachchikumbura SSN, Guo LD, Cai L, Chukeatirote E, Wu WP, Sun X, Crous PW, Bhat DJ, McKenzie EH, Bahkali AH, Hyde KD (2012) A multi-locus backbone tree for *Pestalotiopsis*, with a polyphasic characterization of 14 new species. Fungal Diversity 56: 95–129.
https://doi.org/10.1007/s13225-012-0198-1

Maharachchikumbura SSN, Guo LD, Chukeatirote E, McKenzie EHC, Hyde KD (2013b) A destructive new disease of *Syzygium samarangense* in Thailand caused by the new species *Pestalotiopsis samarangensis*. Tropical Plant Pathology 38: 227–235.
https://doi.org/10.1590/s1982-56762013005000002

Maier W, Begerow D, Weiss M, Oberwinkler F (2003) Phylogeny of the rust fungi: an approach using nuclear large subunit ribosomal DNA sequences. Canadian Journal of Botany 81: 12–23.
https://doi.org/10.1139/b02-113

Maier W, McTaggart AR, Roux J, Wingfield MJ (2016) *Phakopsora myrtacearum* sp. nov., a newly described rust (*Pucciniales*) on eucalypts in eastern and southern Africa. Plant Pathology 65: 189–195.
https://doi.org/10.1111/ppa.12406

Maji MD (2013) Assessment of crop loss in sericulture due to Myrothecium leaf spot (*Myrothecium roridum*). Bulletin of Indian Academy of Sericulture 17: 59–64.

Manawasinghe IS, Hyde KD, Wanasinghe DN, Karunarathna SC, Maharachchikumbura SS, Samarakoon MC, Voglmayr H, Pang KL, Chiang MW, Jones EG, Saxena RK, Kumar A, Rajeshkumar KC, Selbmann L, Coleine C et al. (2025) Fungal diversity notes 1818–1918: taxonomic and phylogenetic contributions on genera and species of fungi. Fungal Diversity 130: 1–261.
https://doi.org/10.1007/s13225-024-00541-y

Mao X, Wu Z, Bi C, Wang J, Zhao F, Gao J, Hou Y, Zhou M (2020) Molecular and biochemical characterization of pydiflumetofen-resistant mutants of *Didymella bryoniae*. Journal of Agricultural and Food Chemistry 68: 9120–9130.
https://doi.org/10.1021/acs.jafc.0c03690

Marin-Felix Y, Hernández-Restrepo M, Iturrieta-González I, García D, Gené J, Groenewald JZ, Cai L, Chen Q, Quaedvlieg W, Schumacher RK, Taylor PW, Ambers C, Bonthond G, Edwards J, Krueger-Hadfield SA et al. (2019a) Genera of phytopathogenic fungi: GOPHY 3. Studies in Mycology 94: 1–124.
https://doi.org/10.1016/j.simyco.2019.05.001

Marin-Felix Y, Hernandez-Restrepo M, Wingfield MJ, Akulov A, Carnegie AJ, Cheewangkoon R, Gramaje D, Groenewald JZ, Guarnaccia V, Halleen F, Lombard L, Luangsa-ard J, Marincowitz S, Moslemi A, Mostert L et al. (2019b) Genera of phytopathogenic fungi: GOPHY 2. Studies in Mycology 92: 47–133.
https://doi.org/10.1016/j.simyco.2018.04.002

Marquez N, Giachero ML, Declerck S, Ducasse DA (2021) *Macrophomina phaseolina*: General characteristics of pathogenicity and methods of control. Frontiers in Plant Science 12: 634397.
https://doi.org/10.3389/fpls.2021.634397

Mason EW (1927) On species of the genus *Nigrospora zimmermann* recorded on monocotyledons. Transactions of the British Mycological Society 12: 152–165.
https://doi.org/10.1016/s0007-1536(27)80011-2

Mathre DE (1997) Compendium of barley diseases. American Phytopathological Society Press.

Matiello RR, dos Santos DDPM, de Jesus Coelho C, Dalla Pria M, Gardingo JR (2015) Damage in maize ears associated with methods of inoculation of *Stenocarpella maydis*. African Journal of Agricultural Research 10: 2711–2716.
https://doi.org/10.5897/ajar2014.9332

McAlpine D (1902) Fungus diseases of stone-fruit trees in Australia and their treatment. RS Brain, Government Printer.

McMillan RT Jr (1984) Oxycarboxin a new fungicide for control of frangipani rust in nursery and field. Proceedings of the Florida State Horticultural Society 97: 247–248.

McTaggart AR, Aime MC (2018) The species of *Coleosporium* (*Pucciniales*) on *Solidago* in North America. Fungal Biology 122: 800–809.
https://doi.org/10.1016/j.funbio.2018.04.007

McTaggart AR, Doungsa-Ard C, Geering AD, Aime MC, Shivas RG (2015) A co-evolutionary relationship exists between *Endoraecium* (*Pucciniales*) and its *Acacia* hosts in Australia. Persoonia 35: 50–62.
https://doi.org/10.3767/003158515x687588

Mehrabi M, Asgari B (2024) A new sexual morph for *Neosetophoma iranianum*, and a key to *Neosetophoma* species. Mycologia Iranica 11: 51–59.

Mehrlich FP, Fitzpatrick HM (1935) *Dichotomophthora portulacae*, a pathogen of *Portulaca oleracea*. Mycologia 27: 543–550.
https://doi.org/10.5962/p.418403

Mei SS, Wang ZY, Zhang J, Rong W (2019) First report of leaf blight on *Stenotaphrum secundatum* caused by *Nigrospora osmanthi* in China. Plant Disease 103: 1783.
https://doi.org/10.1094/pdis-02-19-0270-pdn

Mello JF, Brito ACQ, Vieira JCB, Câmara MPS, Michereff SJ, de Souza-Motta CM, Machado AR (2021) Identification and pathogenicity of *Botryosphaeriaceae* species associated with

root and stem rot of sweet potato in Brazil. Plant Pathology 70: 1601–1615. https://doi.org/10.1111/ppa.13395

Meredith DS (1961) Atmospheric content of *Nigrospora* spores in Jamaican banana plantations. Microbiology 26: 343–349. https://doi.org/10.1099/00221287-26-2-343

Mesterházy Á, Lemmens M, Reid LM (2012) Breeding for resistance to ear rots caused by *Fusarium spp*. in maize–a review. Plant Breeding 131: 1–19. https://doi.org/10.1111/j.1439-0523.2011.01936.x

Meteyer CU, Buckles EL, Blehert DS, Hicks AC, Green DE, Shearn-Bochsler V, Thomas NJ, Gargas A, Behr MJ (2009) Histopathologic criteria to confirm white-nose syndrome in bats. Journal of Veterinary Diagnostic Investigation 21: 411–414. https://doi.org/10.1177/104063870902100401

Miles LE (1925) A pyrenomycetous leaf spot of bur clover. Phytopathology 15: 677–690.

Miller MA, Pfeiffer W, Schwartz T (2017) Creating the CIPRES Science Gateway for inference of large phylogenetic trees. In: 2010 gateway computing environments workshop (GCE), 1–8. https://doi.org/10.1109/gce.2010.5676129

Miller P, Mcwhorter F (1948) A disease of cabbage and other crucifers due to *Cercosporella brassicae.* Phytopathology 38: 893–898.

Minnis AM, Lindner DL (2013) Phylogenetic evaluation of *Geomyces* and allies reveals no close relatives of *Pseudogymnoascus destructans*, comb. nov., in bat hibernacula of eastern North America. Fungal Biology 117: 638–649. https://doi.org/10.1016/j.funbio.2013.07.001

Minter DW, Rodriguez Hernandez M, Mena Portales J (2001) Fungi of the Caribbean: an annotated checklist. PDMS Publishing.

Mitchell J (1986) *Dichotomophthora portulacae* causing black stem rot on common Purslane in Texas. Plant Disease 70: 603. https://doi.org/10.1094/pd-70-603b

Mokrani L, Jawhar M, Shoaib A, Arabi MIE (2012) Characterization of *Pyrenophora graminea* markers associated with a locus conferring virulence on barley. Plant Pathology 28: 290–294. https://doi.org/10.5423/ppj.nt.11.2011.0217

Mondal SN, Timmer LW (2006) Greasy spot, a serious endemic problem for citrus production in the Caribbean Basin. Plant Disease 90: 532–538. https://doi.org/10.1094/pd-90-0532

Monkai J, Phookamsak R, Bhat DJ, Ei TS, Xu J, Lumyong S (2025) Novel endophytic pestalotioid species associated with Itea in Thailand. Frontiers in Cellular and Infection Microbiology 15: 1532712. https://doi.org/10.3389/fcimb.2025.1532712

Moslemi M, Ghaderi F, Karami S, Charehgano H (2023) Identification and pathogenicity of *Macrophomina* species in sesame fields from Iran. Tropical Plant Pathology 49: 241–256. https://doi.org/10.1007/s40858-023-00601-9

Mułenko W, Majewski T, Ruszkiewicz-Michalska M (2008) A preliminary checklist of micromycetes in Poland. Biodiversity of Poland 9: 752.

Murray TD (1996) Resistance to benzimidazole fungicides in the cereal eyespot pathogen, *Pseudocercosporella herpotrichoides*, in the Pacific Northwest 1984 to 1990. Plant Disease 80: 19–23. https://doi.org/10.1094/pd-80-0019

Murray TD, de la Peña RC, Yildirim A, Jones SS (1994) A new source of resistance to *Pseudocercosporella herpotrichoides*, cause of eyespot disease of wheat, located on chromosome 4V of *Dasypyrum villosum*. Plant Breeding 113: 281–286. https://doi.org/10.1111/j.1439-0523.1994.tb00737.x

Murtza T, You M, Barbetti M (2021) Canola growth stage at time of infection determines magnitude of white leaf spot (*Neopseudocercosporella capsellae*) impact. Plant Disease 105: 1515–1521. https://doi.org/10.1094/pdis-09-20-2036-re

Narasimhan MJ, Thirumalachar MJ (1961) *Ravenelia esculenta* an edible rust fungus. Journal of Phytopathology 41: 97–102. https://doi.org/10.1111/j.1439-0434.1961.tb01946.x

Ndiaye M, Sarr MP, Cisse N, Ndoye I (2015) Is the recently described *Macrophomina pseudophaseolina* pathogenically different from *Macrophomina phaseolina*? African Journal of Microbiology Research 9: 2232–2238. https://doi.org/10.5897/ajmr2015.7742

Nees von Esenbeck CGD (1817) Das system der pilze und schwämme: Ein versuch. In der Stahelschen buchhandlung. https://doi.org/10.5962/bhl.title.46990

Nelson S (2009) *Plumeria* rust. Cooperative Extension Service Publication no. PD-61. College of Tropical Agriculture and Human Resources. University of Hawai'i at Manoa.

Nguyen TH, Mathur SB, Neergaard P (1973) Seed-borne species of *Myrothecium* and their pathogenic potential. Transactions of the British Mycological Society 61: 347-IN16. https://doi.org/10.1016/s0007-1536(73)80156-1

Ni W, Zhao H, Xu W, Xu F, Huang S, Wang R, Wu D (2023) First report of root rot caused by *Pleiocarpon algeriense* on peony (*Paeonia suffruticosa*) in China. Plant Disease 107: 2858. https://doi.org/10.1094/pdis-03-23-0425-pdn

Norphanphoun C, Jayawardena RS, Chen Y, Wen TC, Meepol W, Hyde KD (2019) Morphological and phylogenetic characterization of novel pestalotioid species associated with mangroves in Thailand. Mycosphere 10: 531–578. https://doi.org/10.5943/mycosphere/10/1/9

Nouri MT, Lawrence DP, Kallsen CE, Trouillas FP (2020) *Macrophomina* crown and root rot of pistachio in California. Plants 9: 134. https://doi.org/10.3390/plants9020134

Nozawa S, Yamaguchi K, Van Hop D, Phay N, Ando K, Watanabe K (2017) Identification of two new species and a sexual morph from the genus *Pseudopestalotiopsis*. Mycoscience 58: 328–337. https://doi.org/10.1016/j.myc.2017.02.008

Nylander JAA (2004) MrModeltest v2. Program distributed by the author. Evolutionary Biology Centre, Uppsala University.

Odriozola E, Odeon A, Canton G, Clemente G, Escande A (2005) *Diplodia maydis*: a cause of death of cattle in Argentina. Veterinarian Journal 52: 160–161. https://doi.org/10.1080/00480169.2005.36496

Okane I, Ono Y (2018) Phylogenetic study of indigenous grapevine leaf rust fungi in North America and biological identity of an invasive grapevine leaf rust fungus in Brazil. Mycoscience 59: 99–104. https://doi.org/10.1016/j.myc.2017.07.005

Orina AS, Gavrilova OP, Gagkaeva TY (2025) First report of *Nigrospora humicola* (*Apiosporaceae*, *Xylariales*) on *Phragmites* plant from North Asia. Studies in Fungi 10: e005. https://doi.org/10.48130/sif-0025-0006

Owati A, Agindotan B, Burrows M (2019) First microsatellite markers developed and applied for the genetic diversity study

and population structure of *Didymella pisi* associated with ascochyta blight of dry pea in Montana. Fungal Biology 123: 384–392. https://doi.org/10.1016/j.funbio.2019.02.004

Ozkilinc H, Akamatsu H, Abang M, Thomas K, Chilvers MI, Peever TL (2011) Development, characterization and linkage analysis of microsatellite loci for the *Ascochyta* blight pathogen of faba bean, *Didymella fabae*. Journal of Microbiological Methods 87: 128–130. https://doi.org/10.1016/j.mimet.2011.07.020

Padamsee M, McKenzie EHC (2014) A new species of rust fungus on the New Zealand endemic plant, *Myosotidium*, from the isolated Chatham Islands. Phytotaxa 174: 223–230. https://doi.org/10.11646/phytotaxa.174.4.3

Palmateer AJ, McLean KS, Van Santen E, Morgan-Jones G (2003) Occurrence of Nigrospora lint rot caused by *Nigrospora oryzae* on cotton in Alabama. Plant Disease 87: 873. https://doi.org/10.1094/pdis.2003.87.7.873c

Pearce TL, Scott JB, Crous PW, Pethybridge SJ, Hay FS (2016) Tan spot of *Pyrethrum* is caused by a *Didymella* species complex. Plant Pathology 65: 1170–1184. https://doi.org/10.1111/ppa.12493

Pei MH (2005) A brief review of *Melampsora* rusts on *Salix*. In: Rust diseases of Willow and Poplar. Ed. by Pei MH, McCraken AR, Wallingford, UK: CABI Publishing. https://doi.org/10.1079/9780851999999.0011

Pei MH, Royle DJ, Hunter T (1993) Identity and host alternation of some willow rusts (*Melampsora* spp.) in England. Mycological Research 97: 845–851. https://doi.org/10.1016/s0953-7562(09)81160-x

Perron G, Nourani D (1990) *Pseuocercosporella capsellae* (et. Et ev) ou maladies des taches blanches du colza. La Defense des Vegetaux 44: 22–27.

Petrak F (1923) Mykologische Notizen. VI. Numbers 201–300. Annales Mycologici 21: 182–335.

Petrie G, Vanterpool T (1978) *Pseudocercosporella capsellae*, the cause of white leaf spot and grey stem of *Cruciferae* in Western Canada. Canadian Plant Disease Survey 58: 69–72.

Pfeiffer CM, Wheeler JE, Gilbertson RL (1989) First report of *Dichotomophthora indica* as a pathogen of *Myrtillocactus geometrizans* and *Gymnocalycium mihanovichii* var. *friedrichii* in Arizona. Plant Disease 73: 81. https://doi.org/10.1094/pd-73-0081e

Phengsintham P, Chukeatirote E, McKenzie EHC, Hyde KD, Braun U (2013) Monograph of cercosporoid fungi from Laos. Current Reseach in Environmental & Applied Mycology 3: 34–158. https://doi.org/10.5943/cream/3/1/2

Phookamsak R, Liu JK, Chukeatirote E, McKenzie EH, Hyde KD (2013) Phylogeny and morphology of *Leptosphaerulina saccharicola* sp. nov. and *Pleosphaerulina oryzae* and relationships with Pithomyces. Cryptogamie Mycologie 34: 303–319. https://doi.org/10.7872/crym.v34.iss4.2013.303

Phookamsak R, Liu JK, McKenzie EHC, Manamgoda DS, Ariyawansa H, Thambugala KM, Dai DQ, Camporesi E, Chukeatirote E, Wijayawardene NN, Bahkali AH, Mortimer PE, Xu JC, Hyde KD (2014) Revision of *Phaeosphaeriaceae*. Fungal Diversity 68: 159–238. https://doi.org/10.1007/s13225-014-0308-3

Phukhamsakda C, Ariyawansa HA, Phillips AJ, Wanasinghe DN, Bhat DJ, McKenzie EH, Singtripop C, Camporesi E, Hyde KD (2016) Additions to *Sporormiaceae*: Introducing two novel genera, *Sparticola* and *Forliomyces*, from *Spartium*. Cryptogamie Mycologie 37: 75–97. https://doi.org/10.7872/crym/v37.iss1.2016.75

Phukhamsakda C, Hyde KD, Samarakoon MC, Louangphan J, Navasit K, Al-Otibi F, Bhunjun CS (2025) Unveiling *Sordariomycetes* taxa associated with woody litter in Northern Thailand. MycoKeys 17: 155–185. https://doi.org/10.3897/mycokeys.115.145330

Phukhamsakda C, McKenzie EHC, Phillips AJL, Jones EBG, Jayarama Bhat D, Stadler M, Bhunjun CS, Wanasinghe DN, Thongbai B, Camporesi E, Ertz D, Jayawardena RS, Perera RH, Ekanayake AH, Tibpromma S et al. (2020) Microfungi associated with *Clematis* (*Ranunculaceae*) with an integrated approach to delimiting species boundaries. Fungal Diversity 102: 1–203. https://doi.org/10.1007/s13225-020-00448-4

Phukhamsakda C, Nilsson RH, Bhunjun CS, de Farias AR, Sun YR, Wijesinghe SN, Raza M, Bao DF, Lu L, Tibpromma S, Dong W, Tennakoon DS, Tian XG, Xiong YR, Karunarathna SC et al. (2022) The numbers of fungi: Contributions from traditional taxonomic studies and challenges of metabarcoding. Fungal Diversity 114: 327–386. https://doi.org/10.1007/s13225-022-00502-3

Pidoplichko NM, Kirilenko TS (1971) On the taxonomy of the genus *Myrothecium*. In: Pidoplichko NM (Ed.) Metabolites of soil micromycetes. Dumka, Naukova, Kiev, Ukrain.

Ploetz RC, Thomas JE, Slabaugh WR (2003) Diseases of banana and plantain. Diseases of Tropical Fruit Crops, 73–134. https://doi.org/10.1079/9780851993904.0073

Ponomarenko A, Goodwin SB, Kema GHJ (2011) *Septoria tritici* blotch (STB) of wheat. Plant Health Instructor.

Poudel B, Shivas RG, Adorada DL, Barbetti MJ, Bithell SL, Kelly LA, Moore N, Sparks AH, Tan YP, Thomas G, Leur JV, Vaghefi N (2021) Hidden diversity of *Macrophomina* associated with broadacre and horticultural crops in Australia. European Journal of Plant Pathology 161: 1–23. https://doi.org/10.1007/s10658-021-02300-0

Prescott JM, Burnett PA, Saari EE, Ranson J, Bowman JD, Milliano WD, Singh RP, Bekele G (2007) Wheat Disease and Pests: a guide for field identification. International Maize and Wheat Improvement Center.

Quaedvlieg W, Kema GH, Groenewald JZ, Verkley GJ, Seifbarghi S, Razavi M, Gohari AM, Mehrabi R, Crous PW (2011) *Zymoseptoria* gen. nov.: a new genus to accommodate Septoria-like species occurring on graminicolous hosts. Persoonia 26: 57–69. https://doi.org/10.3767/003158511x571841

Quaedvlieg W, Verkley GJM, Shin HD, Barretto RW, Alfenas AC, Swart WJ, Groenewald JZ, Crous PW (2013) Sizing up *Septoria*. Studies in Mycology 75: 307–390. https://doi.org/10.3114/sim0017

Quezado Duval AM, Henz GP, Paz-Lima ML, Medeiros AR, Miranda BE, Pfenning LH, Reis A (2010) New hosts of *Myrothecium* spp. in Brazil and a preliminary in vitro assay of fungicides. Brazilian Journal of Microbiology 41: 246–252. https://doi.org/10.1590/s1517-83822010000100034

Raabe RD, Conners IL, Martinez AP (1981) Checklist of plant diseases in Hawaii. College of Tropical Agriculture and Human Resources, University of Hawaii. Information Text Series No. 22. Hawaii Inst Trop Agric Human Resources.

Rader WE (1948) *Helminthosporium portulacae* A new pathogen of *Protulaca oleracea.* Mycologia 40: 342–346. https://doi.org/10.1080/00275514.1944.12017711

Rao PN (1966) A new species of *Dichotomophthora* on *Portulaca oleracea* from Hyderabad, India. Mycopathologia et Mycologia Applicata 28: 137–140. https://doi.org/10.1007/bf02276042

Rashmi M, Kushveer JS, Sarma VV (2019) A worldwide list of endophytic fungi with notes on ecology and diversity. Mycosphere 10: 798–1079. https://doi.org/10.5943/mycosphere/10/1/19

Ray RV, Crook MJ, Jenkinson P, Edwards SG (2006) Effect of eyespot caused by *Oculimacula yallundae* and *O. acuformis*, assessed visually and by competitive PCR, on stem strength associated with lodging resistance and yield of winter wheat. Journal of Experimental Botany 57: 2249–2257. https://doi.org/10.1093/jxb/erj192

Raza M, Zhang ZF, Hyde KD, Diao YZ, Cai L (2019) Culturable plant pathogenic fungi associated with sugarcane in southern China. Fungal Diversity 99: 1–104. https://doi.org/10.1007/s13225-019-00434-5

Razaghi P, Raza M, Han SL, Ma ZY, Cai L, Zhao P, Chen Q, Phurbu D, Liu F (2024) *Sporocadaceae* revisited. Studies in Mycology 109: 155–272. https://doi.org/10.3114/sim.2024.109.03

Rebentisch JF (1804) Prodromus Flora Neomarchicae, Schüppel, Berlin.

Ren Y, Li D, Zhao X, Wang Y, Bao X, Wang X, Wu X, Wang D, Song B, Chen Z (2019) Whole genome sequences of the tea leaf spot pathogen *Didymella segeticola*. Phytopathology 109: 1676–1678. https://doi.org/10.1094/phyto-02-19-0050-a

Reyes-Franco MC, Hernández-Delgado S, Beas-Fernández R, Medina-Fernandez M, Simpson J, Mayek-Pérez N (2006) Pathogenic and genetic variability within *Macrophomina phaseolina* from Mexico and other countries. Journal of Phytopathology 154: 447–453. https://doi.org/10.1111/j.1439-0434.2006.01127.x

Rice AV, Currah RS (2006) Two new species of *Pseudogymnoascus* with *Geomyces* anamorphs and their phylogenetic relationship with *Gymnostellatospora*. Mycologia 98: 307–318. https://doi.org/10.1080/15572536.2006.11832703

Rodríguez-Gálvez E, Hilário S, Lopes A, Alves A (2020) Diversity and pathogenicity of *Lasiodiplodia* and *Neopestalotiopsis* species associated with stem blight and dieback of blueberry plants in Peru. European Journal of Plant Pathology 157: 89–102. https://doi.org/10.1007/s10658-020-01983-1

Romero Luna MP, Mueller D, Mengistu A, Singh AK, Hartman GL, Wise KA (2017) Advancing our understanding of charcoal rot in soybeans. Journal of Integrated Pest Management 8: 1–8. https://doi.org/10.1093/jipm/pmw020

Ronquist F, Huelsenbeck J (2003) MrBayes 3: Bayesian phylogenetic inference under mixed models. Bioinformatics 19: 1572–1574. https://doi.org/10.1093/bioinformatics/btg180

Root RPRP (1986) *Macrophomina phaseolina*. Plant Disease 70: 863.

Rossouw JD (2001) Genetics of resistance to *Stenocarpella maydis* ear rot of maize. Doctoral dissertation. University of the Free State.

Routien JB (1957) Fungi isolated from soils. Mycologia 49: 188–196. https://doi.org/10.1080/00275514.1957.12024632

Ruma K, Sunil K, Kini KR, Prakash HS (2015) Genetic diversity and antimicrobial activity of endophytic *Myrothecium* spp. isolated from *Calophyllum apetalum* and *Garcinia morella*. Molecular Biology Reports 42: 1533–1543. https://doi.org/10.1007/s11033-015-3884-8

Rupe J, Sconyers L (2008) Soybean Rust. The Plant Health Instructor.

Rush TA, Golan J, McTaggart A, Kane C, Schneider RW, Aime MC (2019) Variation in the internal transcribed spacer region of *Phakopsora pachyrhizi* and implications for molecular diagnostic assays. Plant Disease 103: 2237–2245. https://doi.org/10.1094/pdis-08-18-1426-re

Sadyś M, West JS (2017) Intra-diurnal and daily changes in *Didymella* ascospore concentrations in the air of an urban site. Fungal Ecology 27: 87–95. https://doi.org/10.1016/j.funeco.2017.03.002

Salgado-Salazar C, Rossman AY, Chaverri P (2016) The genus *Thelonectria* (*Nectriaceae*, *Hypocreales*, *Ascomycota*) and closely related species with cylindrocarpon-like asexual states. Fungal Diversity 80: 411–455. https://doi.org/10.1007/s13225-016-0365-x

Samson RA (1972) Notes on *Pseudogymnoascus*, *Gymnoascus* and related genera. Acta Botanica Neerlandica 21: 517–527. https://doi.org/10.1111/j.1438-8677.1972.tb00804.x

Sanabria-Velazquez A, Cubilla A, Flores-Giubi M, Barua J, Romero-Rodríguez C, Enciso-Maldonado GA, Thiessen LD, Shew HD (2022) First report of *Macrophomina euphorbiicola* causing charcoal rot of *Stevia* in Paraguay. Plant Disease 107: 229. https://doi.org/10.1094/PDIS-06-21-1279-PDN

Sarr MP, Groenewald JZ, Crous PW (2014) Genetic diversity in *Macrophomina phaseolina*, the causal agent of charcoal rot. Phytopathologia Mediterranea 53: 250.

Scarpari M, Vitale S, Di Giambattista G, Luongo L, De Gregorio T, Schreiber G, Petrucci M, Belisario A, Voglmayr H (2020) *Didymella corylicola* sp. nov., a new fungus associated with hazelnut fruit development in Italy. Mycological Progress 19: 317–328. https://doi.org/10.1007/s11557-020-01562-y

Scholler M, Aime MC (2006) On some rust fungi (*Uredinales*) collected in an *Acacia koa-Metrosideros polymorpha* woodland, Mauna Loa Road, Big Island, Hawaii. Mycoscience 47: 159–165. https://doi.org/10.1007/s10267-006-0286-8

Schol-Schwarz MB (1968) *Rhinocladiella*, its synonym *Fonsecaea* and its relation to *Phialophora*. Antonie Van Leeuwenhoek 34: 119–152. https://doi.org/10.1007/bf02046424

Seidel D, Wurster S, Jenks JD, Sati H, Gangneux JP, Egger M, Alastruey-Izquierdo A, Ford NP, Chowdhary A, Sprute R, Cornely O (2024) Impact of climate change and natural disasters on fungal infections. The Lancet Microbe 5: e594–e605. https://doi.org/10.1016/S2666-5247(24)00039-9

Senanayake IC, Crous PW, Groenewald JZ, Maharachchikumbura SS, Jeewon R, Phillips AJ, Bhat JD, Perera RH, Li QR, Li WJ, Tangthirasunun N, Norphanphoun C, Karunarathna SC, Camporesi E, Manawasighe IS et al. (2017) Families of *Diaporthales* based on morphological and phylogenetic evidence. Studies in Mycology 86: 217–296. https://doi.org/10.1016/j.simyco.2017.07.003

Senanayake IC, Jeewon R, Chomnunti P, Wanasinghe DN, Norphanphoun C, Karunarathna A, Pem D, Perera RH,

Camporesi E, McKenzie EH, Hyde KD, Karunarathna SC (2018) Taxonomic circumscription of *Diaporthales* based on multigene phylogeny and morphology. Fungal Diversity 93: 241–443. https://doi.org/10.1007/s13225-018-0410-z

Shabeer A, Bockus WW (1988) Tan spot effects on yield and yield components relative to growth stage in winter wheat. Plant Disease 72: 599–602. https://doi.org/10.1094/pd-72-0599

Shahriar SA, Nur-Shakirah AO, Mohd MH (2022) *Neopestalotiopsis clavispora* and *Pseudopestalotiopsis camelliae-sinensis* causing grey blight disease of tea (*Camellia sinensis*) in Malaysia. European Journal of Plant Pathology 1: 1–6. https://doi.org/10.1007/s10658-021-02433-2

Sharma P, Meena PD, Chauhan JS (2013) First report of *Nigrospora oryzae* (Berk. & Broome) petch causing stem blight on *Brassica juncea* in India. Journal of Phytopathology 161: 439–441. https://doi.org/10.1111/jph.12081

Sheng YT, Yu XL, Mao TT, Zhang J, Guo XT, Song ZZ, Zhang HX (2022) Genome Sequence Data of *Leptosphaerulina arachidicola*, a Causal Agent of Peanut Scorch Spot in China. Plant Disease 106: 748–750. https://doi.org/10.1094/pdis-08-21-1824-a

Shin HD, Jeon CH, Choi WI, Lee CK (2019) First report of rust caused by *Coleosporium zanthoxyli* on *Zanthoxylum planispinum* in Korea. Plant Disease 103: 371. https://doi.org/10.1094/pdis-06-18-1029-pdn

Shinyama Y, Yamaoka Y (2012) Ecology of two heteroecious *Melampsora* species that parasitize willows and *Papaveraceae* plants. Japanese Journal of Mycology 53: 15–32.

Shirai M, Eulgem T (2023): Molecular interactions between the soilborne pathogenic fungus *Macrophomina phaseolina* and its host plants. Frontiers in Plant Science 14: 1264569. https://doi.org/10.3389/fpls.2023.1264569

Shu J, Yu Z, Sun W, Zhao J, Li Q, Tang L, Guo T, Huang S, Mo J, Hsiang T, Luo S (2020) Identification and characterization of pestalotioid fungi causing leaf spots on mango in southern China. Plant Disease 104: 1207–1213. https://doi.org/10.1094/pdis-03-19-0438-re

Shurtleff M, Fermanian TW, Randell R (1987) Controlling turfgrass pests. Prentice-Hall International, Inc, USA.

Sinclair WA, Lyon HH, Johnson WT (1987) Diseases of trees and shrubs. Ithaca, NY: Cornell University Press.

Singh R, Singh A, Kumar S, Upadhyaya PP, Castañeda-Ruíz RF (2014) Two new species of *Zasmidium* from northeastern Uttar Pradesh, India. Nova Hedwigia 98: 257–263. https://doi.org/10.1127/0029-5035/2013/0137

Siqueira CDS, Barrocas EN, Machado JC, Da Silva UA, Dias IE (2014) Effects of *Stenocarpella maydis* in seeds and in the initial development of corn. Journal of Seed Science 36: 79–86. https://doi.org/10.1590/s2317-15372014000100010

Šišić A, Oberhänsli T, Baćanović-Šišić J, Hohmann P, Finckh MR (2021) A novel real time PCR method for the detection and quantification of *Didymella pinodella* in symptomatic and asymptomatic plant hosts. Journal of Fungi 8: 41. https://doi.org/10.3390/jof8010041

Smiley RW, Dernoeden PH, Clarke BB (1992) Compendium of turfgrass diseases. St. Paul, MN: APS Press. https://doi.org/10.2307/3792675

Smith D, Chilvers M, Dorrance A, Hughes T, Mueller D, Niblack T, Wise K (2014) Charcoal rot management in the north central region. University of Wisconsin Extension Bulletin.

Snyman LD, Kellerman TS, Viegaarr R, Flett BC, Basson KM, Schultz RA (2011) Diplonine, a neurotoxin isolates from cultures of the fungus *Stenocarpella maydis* (Berk.) Sacc. that induces diplodiosis. Journal of Agricultural and Food Chemistry 59: 9039–9044. https://doi.org/10.1021/jf202735e

Soares DJ, Nechet KL (2017) *Dichotomophthora* sp. causing leaf spot and foliar abscission on *Anredera cordifolia* in Brazil. Australas Plant Disease Notes 12: 51. https://doi.org/10.1007/s13314-017-0276-z

Solarte F, Muñoz CG, Maharachchikumbura SS, Álvarez E (2018) Diversity of *Neopestalotiopsis* and *Pestalotiopsis* spp., causal agents of guava scab in Colombia. Plant Disease 102: 49–59. https://doi.org/10.1094/pdis-01-17-0068-re

Stahel G (1937) The banana leaf speckle in Surinam caused by *Chloridium musae* nov. spec. and another related banana disease. Tropical Agriculture 14: 42–44.

Stamatakis A (2014) RAxML version 8: A tool for phylogenetic analysis and post-analysis of large phylogenies. Bioinformatics 30: 1312–1313. https://doi.org/10.1093/bioinformatics/btu033

Steyaert RL (1949) Contributions etude monographique de Pestalotia de Not. et Monochaetia Sacc. (*Truncatella* gen. nov. et *Pestalotiopsis* gen. nov.). Bull Jardin Botanique de l'EtatBruxelles 19: 285–354. https://doi.org/10.2307/3666710

Stone CL, Buitrago ML, Boore JL, Frederick RD (2010) Analysis of the complete mitochondrial genome sequences of the soybean rust pathogens *phakopsora pachyrhizi* and *P. meibomiae*. Mycologia102: 887–897. https://doi.org/10.3852/09-198

Stukenbrock EH, Banke S, Javan-Nikkhah M, McDonald BA (2007) Origin and domestication of the fungal wheat pathogen *Mycosphaerella graminicola* via sympatric speciation. Molecular Biology and Evolution 24: 398–411. https://doi.org/10.1093/molbev/msl169

Sun JE, Fu L, Norphanphoun C, Chen XJ, Yu LF, Hyde KD, McKenzie EH, Wang Y, Yang ZF, Liu FQ (2024) Study on the diversity of rust pathogens from different hosts in Guizhou Province, China. Mycosphere 15: 473–653. https://doi.org/10.5943/mycosphere/15/1/4

Sun X, Guo LD, Hyde KD (2011) Community composition of endophytic fungi in *Acer truncatum* and their role in decomposition. Fungal Diversity 47: 85–95. https://doi.org/10.1007/s13225-010-0086-5

Sun YR, Hyde KD, Liu NG, Jayawardena RS, Wijayawardene NN, Ma J, Zhang Q, Al-Otibi F, Wang Y (2025) Micro-fungi in southern China and northern Thailand: Emphasis on medicinal plants. Fungal Diversity 10: 1–201. https://doi.org/10.1007/s13225-024-00549-4

Sun YR, Jayawardena RS, Sun JE, Wang Y (2023) Pestalotioid species associated with medicinal plants in southwest China and Thailand. Microbiology Spectrum 11: e03987–22. https://doi.org/10.1128/spectrum.03987-22

Sundheim L, Wilcoxson RD (1965) *Leptosphaerulina briosiana* on alfalfa-infection and disease development host-parasite relationships ascospore germination and dissemination. Phytopathology 55: 546. https://doi.org/10.1094/phyto-64-243

Sutton BC (1977) Coelomycetes VI. Nomenclature of generic names proposed for coelomycetes. Mycological Papers 141:

1–253.
Sutton BC (1980) The coelomycetes. Fungi imperfecti with pycnidia, acervuli and stromata. Kew, UK.
Suzuki H, Hirose D, Yamaoka Y (2018) Species composition and distribution of *Coleosporium* species on the needles of *Pinus densiflora* at a semi-natural vegetation succession site in central Japan. Mycoscience 59: 424–432. https://doi.org/10.1016/j.myc.2018.04.001
Świderska-burek U (2020) A taxonomic revision of *Zasmidium* species occurring in Poland. Phytotaxa 437: 237–244. https://doi.org/10.11646/phytotaxa.437.4.5
Sydow H (1921) Novae fungorum species: XVII. Annales Mycologici 19: 304–309.
Sydow H, Sydow P (1917) Beitrag zur Kenntniss der Pilzflora der Philippinen-Inseln. Annales Mycologici 15: 165–268.
Tan YP, Bishop-Hurley SL, Shivas RG, Cowan DA, Maggs-Kölling G, Maharachchikumbura SS, Pinruan U, Bransgrove KL, De la Peña-Lastra S, Larsson E, Lebel T, Mahadevakumar S, Mateos A, Osieck ER, Rigueiro-Rodríguez A et al. (2022) Fungal Planet description sheets: 1436–1477. Persoonia 49: 261–350. https://doi.org/10.3767/persoonia.2022.49.08
Tehon LR, Stout GL (1928) An ascomycetous leaf spot of Cowpea. Phytopathology 18: 701–704.
Tennakoon DS, Thambugala KM, Wanasinghe DN, Gentekaki E, Promputtha I, Kuo CH, Hyde KD (2020) Additions to *Phaeosphaeriaceae* (*Pleosporales*): *Elongaticollum* gen. nov., *Ophiosphaerella taiwanensis* sp. nov., *Phaeosphaeriopsis beaucarneae* sp. nov. and a new host record of *Neosetophoma poaceicola* from *Musaceae*. MycoKeys 70: 59–88. https://doi.org/10.3897/mycokeys.70.53674
Thambugala KM, Camporesi E, Ariyawansa HA, Phookamsak R, Liu ZY, Hyde KD (2014) Phylogeny and morphology of *Phaeosphaeriopsis triseptata* sp nov and *Phaeosphaeriopsis glaucopunctata* Phytotaxa 176: 238-250. https://doi.org/10.11646/phytotaxa.176.1.23
Thambugala KM, Hyde KD, Zhang JF, Liu ZY (2018) *Didymella eriobotryae* sp. nov. (*Didymellaceae*) and *Arthrinium arundinis* (*Apiosporaceae*) from fruit of *Eriobotrya japonica* (loquat) in China. Phytotaxa 382: 136–147. https://doi.org/10.11646/phytotaxa.382.1.8
Toome M, Aime MC (2015) Reassessment of rust fungi on weeping willows in the Americas and description of *Melampsora ferrinii* sp. nov. Plant Pathology 64: 216–224. https://doi.org/10.1111/ppa.12237
Tsopelas P, Barnes I, Wingfield MJ, Xenopoulos S (2007) *Seiridium cardinale* on *Juniperus* species in Greece. Forest Pathology 37: 338–347. https://doi.org/10.1111/j.1439-0329.2007.00510.x
Tulloch M (1972) The genus *Myrothecium* Tode ex Fr. Commonwealth Mycological Institute.
Ukwatta KM, Lawrence JL, Wijayarathna CD (2019) The study of antimicrobial, anti-cancer, anti-inflammatory and α-glucosidase inhibitory activities of Nigronapthaphenyl, isolated from an extract of *Nigrospora sphaerica*. Mycology 10: 222–228. https://doi.org/10.1080/21501203.2019.1620892
Urbina J, Chestnut T, Allen JM, Levi T (2021) *Pseudogymnoascus destructans* growth in wood, soil and guano substrates. Scientific Reports 11: 1–11. https://doi.org/10.1038/s41598-020-80707-1
Vaghefi N, Kikkert JR, Pethybridge SJ (2016) Incidence and pathogenicity of *Didymella americana* on table beet in New York. Plant Health Progress 17: 270–272. https://doi.org/10.1094/php-br-16-0064
Vaidya G, Lohman DJ, Meier R (2011) SequenceMatrix: concatenation software for the fast assembly of multi-gene datasets with character set and codon information. Cladistics 27: 171–180. https://doi.org/10.1111/j.1096-0031.2010.00329.x
Valenzuela-Lopez N, Cano-Lira JF, Guarro J, Sutton DA, Wiederhold N, Crous PW, Stchigel AM (2018) Coelomycetous Dothideomycetes with emphasis on the families *Cucurbitariaceae* and *Didymellaceae*. Studies in Mycology 90: 1–69. https://doi.org/10.1016/j.simyco.2017.11.003
van Bruggen AH, Gamliel A, Finckh MR (2016) Plant disease management in organic farming systems. Pest Management Science 72: 30–44. https://doi.org/10.1002/ps.4145
van Niekerk JM, Calitz FJ, Halleen F, Fourie PH (2010) Temporal spore dispersal patterns of grapevine trunk pathogens in South Africa. European Journal of Plant Pathology 127: 375–390. https://doi.org/10.1007/s10658-010-9604-2
Veselská T, Homutová K, García Fraile P, Kubátová A, Martínková N, Pikula J, Kolařík M (2020) Comparative eco-physiology revealed extensive enzymatic curtailment, lipases production and strong conidial resilience of the bat pathogenic fungus *Pseudogymnoascus destructans*. Scientific Reports 10: 16530. https://doi.org/10.1038/s41598-020-73619-7
Vialle A, Feau N, Frey P, Bernier L, Hamelin RC (2013) Phylogenetic species recognition reveals host-specific lineages among poplar rust fungi. Molecular Phylogenetics and Evolution 66: 628–644. https://doi.org/10.1016/j.ympev.2012.10.021
Victoria AAD, Furtado BE, Holz MT, Romero-Arenas O, Dallagnol LJ (2020) First report of *Leptosphaerulina* leaf spot caused by *Leptosphaerulina trifolii* on *Trifolium repens* in Brazil. Plant Disease 104: 972. https://doi.org/10.1094/pdis-10-19-2151-pdn
Videira SIR, Groenewald JZ, Braun U, Shin HD, Crous PW (2016) All that glitters is not *Ramularia*. Studies in Mycology 83: 49–163. https://doi.org/10.1016/j.simyco.2016.06.001
Videira SIR, Groenewald JZ, Nakashima C, Braun U, Barreto RW, de Wit PJ, Crous PW (2017) *Mycosphaerellaceae*–chaos or clarity? Studies in Mycology 87: 257–421. https://doi.org/10.1016/j.simyco.2017.09.003
Villanueva P, Vásquez G, Gil-Durán C, Oliva V, Díaz A, Henríquez M, Álvarez E, Laich F, Chávez R, Vaca I (2021) Description of the first four species of the genus *Pseudogymnoascus* from Antarctica. Frontiers in Microbiology 12: 713189. https://doi.org/10.3389/fmicb.2021.713189
Vincelli P (1997) Ear rot of corn caused by *Stenocarpella maydis* (= *Diplodia maydis*). Cooperative extension service. University of Kentucky College of Agriculture 43: 3.
Vink SN, Elsas van JD (2017) Determining the pathogenicity of 13 fungal species with respect to their required containment measures. University of Groningen, Department of Microbial Ecology, Groningen Institute for Evolutionary Life Sciences (GELIFES).
Von Höhnel FV (1905) Über Myrothecium und Formverwandte Gattungen. Annales Mycologici 3: 559–560.
Wallwork H (1987) A *Tapesia* teleomorph for *Pseudocercosporella herpotrichoides*, the cause of eyespot of wheat. Australas

Plant Pathology 16: 92–93.
https://doi.org/10.1071/app9870092

Wanasinghe DN, Phukhamsakda C, Hyde KD, Jeewon R, Lee HB, Gareth Jones EB, Tibpromma S, Tennakoon DS, Dissanayake AJ, Jayasiri SC, Gafforov Y, Camporesi E, Bulgakov TS, Ekanayake AH, Hansika et R al. (2018) Fungal diversity notes 709–839: taxonomic and phylogenetic contributions to fungal taxa with an emphasis on fungi on Rosaceae. Fungal Diversity 89: 1–236.
https://doi.org/10.1007/s13225-018-0395-7

Wang B, Liang X, Gleason ML, Zhang R, Sun G (2017a) Genome sequence of the ectophytic fungus *Ramichloridium luteum* reveals unique evolutionary adaptations to plant surface niche. BMC Genomics 18: 729.
https://doi.org/10.1186/s12864-017-4118-3

Wang M, Liu F, Crous PW, Cai L (2017b) Phylogenetic reassessment of *Nigrospora*: ubiquitous endophytes, plant and human pathogens. Persoonia 39: 118–142.
https://doi.org/10.3767/persoonia.2017.39.06

Wang X, Wu X, Jiang S, Yin Q, Li D, Wang Y, Wang D, Chen Z (2021) Whole genome sequence and gene annotation resource for *Didymella bellidis* associated with tea leaf spot. Plant Disease 105: 1168–170.
https://doi.org/10.1094/pdis-05-20-0939-a

Wang Z, Binder M, Schoch CL, Johnston PR, Spatafora JW, Hibbett DS (2006) Evolution of helotialean fungi (*Leotiomycetes*, *Pezizomycotina*): a nuclear rDNA phylogeny. Molecular Phylogenetics and Evolution 41: 295–312.
https://doi.org/10.1016/j.ympev.2006.05.031

Ware SB, Verstappen ECP, Breeden J, Cavaletto JR, Goodwin SB, Waalwijk C, Crous PW, Kema GH (2007) Discovery of a functional *Mycosphaerella* teleomorph in the presumed asexual barley pathogen *Septoria passerinii*. Fungal Genetics and Biology 44: 389–397.
https://doi.org/10.1016/j.fgb.2006.12.005

Weaver MA, Hoagland RE, Boyette CD, Brown SP (2021) Taxonomic evaluation of a bioherbicidal isolate of *Albifimbria verrucaria*, formerly *Myrothecium verrucaria*. Journal of Fungi 7: 694.
https://doi.org/10.3390/jof7090694

Webster J (1952) Spore projection in the hyphomycete *Nigrospora sphaerica*. The New Phytologist 51: 229–235.
https://doi.org/10.1111/j.1469-8137.1952.tb06129.x

Weerasekara IT, Udayanga D, Manamgoda DS, Mapa MS, Sinniah GD, Castlebury LA (2024) Morphological and molecular reassessment of *Pseudopestalotiopsis* in the gray blight complex of tea with four new species from Sri Lanka. Mycological Progress 23: 72.
https://doi.org/10.1007/s11557-024-02010-x

Wehmeyer LE (1961) A world monograph of the genus *Pleospora* and its segregates, University of Michigan Press, Michigan.
https://doi.org/10.2307/3756425

Wei L, Muranty H, Zhang H (2011) Advances and prospects in wheat eyespot research: contributions from genetics and molecular tools. Journal of Phytopathology 159: 457–2470.
https://doi.org/10.1111/j.1439-0434.2011.01795.x

Weir J (1925) The genus *Coleosporium* in the northwestern United States. Mycologia 17: 225–239.
https://doi.org/10.1080/00275514.1925.12020478

Wicklow DT, Rogers KD, Dowd PF, Gloer JB (2011) Bioactive metabolites from *Stenocarpella maydis*, a stalk and ear rot pathogen of maize. Fungal Biology 115: 133–142.
https://doi.org/10.1016/j.funbio.2010.11.003

Widmer T, Castlebury L, Rossman A (2002) First report of *Phoma exigua* on *Centaurea solstitialis* (*Asteraceae*) in Russia. Plant Disease 86: 922.
https://doi.org/10.1094/pdis.2002.86.8.922a

Widmer TI, Kirk AL, Kirk GE, Guermache FA (2006) Foliar and cane rot of *Arundo donax* caused by *Nigrospora oryzae* in Europe. Plant Disease 90: 1107.
https://doi.org/10.1094/pd-90-1107a

Wijayawardene NN, Hyde KD, Dai DQ, Sánchez-García M, Goto BT, Saxena RK, Erdogdu M, Selcuk F, Rajeshkumar KC, Aptroot A, Blaszkowski J, Boonyuen N, da Silva GA, de Souza FA, Dong W et al. (2022) Outline of Fungi and fungus-like taxa: 2021. Mycosphere 13: 53–453.
https://doi.org/10.5943/mycosphere/11/1/8

Wijayawardene NN, Hyde KD, Al-Ani LKT, Tedersoo L, Haelewaters D, Rajeshkumar KC, Zhao RL, Aptroot A, Leontyev DV, Saxena RK, Tokarev YS, Dai DQ, Letcher PM, Stephenson SL, Ertz D et al. (2020) Outline of Fungi and fungus-like taxa. Mycosphere 11: 1060–1456.
https://doi.org/10.5943/mycosphere/11/1/8

Woudenberg JH, De Gruyter J, Crous PW, Zwiers LH (2012) Analysis of the mating-type loci of co-occurring and phylogenetically related species of *Ascochyta* and *Phoma*. Molecular Plant Pathology 13: 350–362.
https://doi.org/10.1111/j.1364-3703.2011.00751.x

Wright ER, Folgado M, Rivera MC, Crelier A et al. (2008) *Nigrospora sphaerica* causing leaf spot and twig and shoot blight on blueberry: a new host of the pathogen. Plant Disease 92: 171.
https://doi.org/10.1094/pdis-92-1-0171b

Wu B, Hussain M, Zhang W, Stadler M, Liu X, Xiang M (2019) Current insights into fungal species diversity and perspective on naming the environmental DNA sequences of fungi. Mycology 10: 127–140.
https://doi.org/10.1080/21501203.2019.1614106

Wu JB, Zhang CL, Mao PP, Qian YS, Wang HZ (2014a) First report of leaf spot caused by *Nigrospora oryzae* on *Dendrobium candidum* in China. Plant Disease 98: 996.
https://doi.org/10.1094/pdis-09-13-1006-pdn

Wu ML, Hanlin RT (1992) Host - parasite relationships between the fungus *Leptosphaerulina crassiasca* and peanut. Canadian Journal of Botany 70: 1724–1733.
https://doi.org/10.1139/b92-213

Wu YM, Wang HF, Zhang TY (2014b) Two new species of *Myrothecium* from Qinghai-Tibet Plateau Area, China. Mycotaxon 129: 403–406.
https://doi.org/10.5248/129.403

Yokoyama T, Tubaki K (1971) Cultural and taxonomical studies on the genus *Actinopelte*. Institute of Fermentation, Osaka, Research Communication 5: 43–77.

Yun HY, Kim YH (2018) *Tubakia subglobosa* causes leaf spots on ring-cupped oak trees in Korea. Plant Disease 102: 240.
https://doi.org/10.1094/pdis-04-17-0540-pdn

Yun HY, Kim YH, Hong SG, Lee KJ (2007) First Description of *Coleosporium plectranthi* causing *Perilla* rust in Korea. The Plant Pathology Journal 23: 7–12.
https://doi.org/10.5423/ppj.2007.23.1.007

Yun HY, Rossman AY (2011) *Tubakia seoraksanensis*, a new species from Korea. Mycotaxon 115: 369–373.
https://doi.org/10.5248/115.369

Yun YH, Ahn GR, Yoon SW, Kim HH, Son SY, Kim SH (2016) New rust disease of Korean Willow (*Salix koreensis*) caused by *Melampsora yezoensis*, unrecorded pathogen in Korea.

Mycobiology 44: 335–337.
https://doi.org/10.5941/myco.2016.44.4.335

Zeilinger S, Gupta VK, Dahms TE, Silva RN, Singh HB, Upadhyay RS, Gomes EV, Tsui CK, Nayak SC (2016) Friends or foes? Emerging insights from fungal interactions with plants. FEMS Microbiology Reviews 40: 182–207.
https://doi.org/10.1093/femsre/fuv045

Zhai LF, Liu J, Zhang MX, Hong N, Wang GP, Wang LP (2013) The first report of leaf spots in *Aloe vera* caused by *Nigrospora oryzae* in China. Plant Disease 97: 1256.
https://doi.org/10.1094/pdis-03-13-0314-pdn

Zhang G, Berbee ML (2001) *Pyrenophora* phylogenetics inferred from ITS and glyceradehyde-3phosphate dehydrogenase gene sequences. Mycologia 93, 1048–1063.
https://doi.org/10.1080/00275514.2001.12063240

Zhang LL, Li YZ (2021) First report of *Alfalfa* leaf spot caused by *Leptosphaerulina australis* in China. Plant Disease 105: 2254.
https://doi.org/10.1094/pdis-10-20-2136-pdn

Zhang LX, Li SS, Tan GJ, Shen JT, He T (2012a) First report of *Nigrospora oryzae* causing leaf spot of cotton in China. Plant Disease 96: 1379.
https://doi.org/10.1094/pdis-04-12-0349-pdn

Zhang W, Li Y, Lin L, Jia A, Fan X (2024) Updating the species diversity of pestalotioid fungi: Four new species of *Neopestalotiopsis* and *Pestalotiopsis*. Journal of Fungi 10: 475.
https://doi.org/10.3390/jof10070475

Zhang Y, Crous PW, Schoch CL, Hyde KD (2012b) *Pleosporales*. Fungal Diversity 53: 1–221.
https://doi.org/10.1007/s13225-011-0117-x

Zhang, Z, Dong C, Chen W, Mou Q, Lu X, Han Y, Huang J, Liang Z (2020) The enigmatic *Thelebolaceae* (*Thelebolales*, *Leotiomycetes*): one new genus *Solomyces* and five new species. Frontiers in Microbiology 11: 2618.
https://doi.org/10.3389/fmicb.2020.572596

Zhang Z, Mu T, Liu S, Liu R, Zhang X, Xia J (2021a) Morphological and phylogenetic analyses reveal a new genus and two new species of *Tubakiaceae* from China. MycoKeys 84: 185.
https://doi.org/10.3897/mycokeys.84.73940

Zhang ZY, Shao QY, Li X, Chen WH, Liang JD, Han YF, Huang JZ, Liang ZQ (2021b) Culturable fungi from urban soils in China I: description of 10 new taxa. Microbiology Spectrum 9: e00867–21.
https://doi.org/10.1128/spectrum.00867-21

Zhao L, Cai J, He W, Zhang Y (2019) *Macrophomina vaccinii* sp. nov. causing blueberry stem blight in China. MycoKeys 55: 1–14.
https://doi.org/10.3897/mycokeys.55.35015

Zhao P, Li Y, Li Y, Liu F, Liang J, Zhou X, Cai L (2023) Applying early divergent characters in higher rank taxonomy of *Melampsorineae* (*Basidiomycota*, *Pucciniales*), Mycology 14: 11–36.
https://doi.org/10.1080/21501203.2022.2089262

Zhao P, Tian CM, Yao YJ, Wang Q, Yamaoka Y, Kakishima M (2015a) Two new species and one new record of *Melampsora* on willows from China. Mycological Progress 14: 66.
https://doi.org/10.1007/s11557-015-1091-6

Zhao P, Wang QH, Tian CM, Kakishima M (2015b) Integrating a numerical taxonomic method and molecular phylogeny for species delimitation of *Melampsora* species (*Melampsoraceae*, *Pucciniales*) on willows in China. PLoS One 17: e0144883.
https://doi.org/10.1371/journal.pone.0144883

Zhao P, Wang QH, Tian CM, Wang Q, Yamaoka Y, Kakishima M (2015c) A morphological and molecular survey of Japanese *Melampsora* species on willows reveals a new species and two new records. Mycological Progress 14: 101.
https://doi.org/10.1007/s11557-015-1121-4

Zhao W, Hou Y, Bai J, Zhang W, Gao L, Zhang R, Gleason ML, Sun G (2016) A new species of *Zasmidium* associated with sooty blotch and flyspeck. Phytotaxa 258: 190–194.
https://doi.org/10.11646/phytotaxa.258.2.9

Zheng H, Yu ZF, Xu JP, Castañeda-Ruiz RF, Qiao M (2020) *Ramichloridium endophyticum* sp. nov., a novel species of endophytic fungus from *Potamogeton pectinatus*. International Journal of Systematic and Evolutionary Microbiology 70: 3433–3439.
https://doi.org/10.1099/ijsem.0.004190

Zheng W, Newcombe G, Hu D, Cao Z, Yu Z, Peng Z (2019) The first record of a North American Poplar leaf rust fungus, *Melampsora medusae*, in China. Forests 10: 182.
https://doi.org/10.3390/f10020182

Zhu YQ, Jiang N, Dou ZP, Xue H, Piao CG, Li Y (2022) Additions to the knowledge of *Tubakia* (*Tubakiaceae*, *Diaporthales*) in China. Journal of Fungi 8: 1143.
https://doi.org/10.3390/jof8111143

Zimmerman A (1902) Ueber einige an tropischen Kulturpflanzen beobachtete Pilze III. Zentralblatt für Bakteriologie, Parasitenkunde 8: 216–221.

Zlatković M, Sallmannshofer M, Schueler S, Cech TL, Djilas M, Hoch G, Lapin K, Ogris N, Piškur B, Schwanda K, Stojnić S, Westergren M, Orlović S (2024) *Tubakia* spp., *Didymella macrostoma* and *Apiognomonia errabunda* causing leaf spot and anthracnose of *Quercus robur* in the Mura-Drava-Danube Biosphere Reserve. Frontiers in Forests and Global Change 7: 1363141.
https://doi.org/10.3389/ffgc.2024.1363141

Zukal J, Berková H, Banďouchová H (2017) Bats and caves: Activity and ecology of Bats wintering. Cave investigation 12: 51.
https://doi.org/10.5772/intechopen.69267

Zuluaga C, Buriticá P, Marín M (2011) Phylogenetic analysis of rust fungi (*Uredinales*) from the Colombian Andean region using 28S ribosomal DNA sequences. Revista de Biologia Tropical 59: 517–54.